

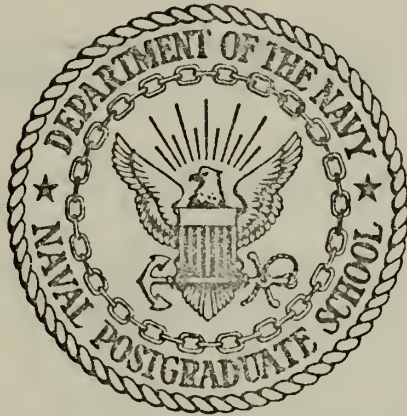
SOUND PHASE AND AMPLITUDE FLUCTUATIONS
IN AN ANISOTROPIC OCEAN

Charles Homer Alexander

Library
Naval Postgraduate School
Monterey, California 93940

NAVAL POSTGRADUATE SCHOOL

Monterey, California



THESIS

SOUND PHASE AND AMPLITUDE FLUCTUATIONS
IN AN ANISOTROPIC OCEAN

by

Charles Homer Alexander

Thesis Advisor:

H. Medwin

December 1972

T157770

Approved for public release; distribution unlimited.



Sound Phase and Amplitude Fluctuations
in an Anisotropic Ocean

by

Charles Homer Alexander
Lieutenant, United States Navy
B.S., Purdue University, 1964

Submitted in partial fulfillment of the
requirements of the degree of

MASTER OF SCIENCE ENGINEERING ACOUSTICS

from the
NAVAL POSTGRADUATE SCHOOL
December 1972

ABSTRACT

Sound of constant amplitude and frequency was transmitted simultaneously in three orthogonal beams over a distance of 1.5 meters in the upper ocean. Time records of the resulting phase and amplitude fluctuations of the sound beams were studied by means of auto and cross spectral analysis and correlation. The time lag between corresponding peaks of the phase fluctuation autocorrelation functions of vertical and horizontal beams indicate movement of inhomogeneities between the sound fields due to water particle motion caused by surface wave action. Envelope correlation times of the phase fluctuations are found to be approximately one-half as great in the mixed layer as in the thermocline, and are greater in the vertical than in the horizontal direction in the thermocline. Anisotropy in the thermocline is also indicated by the variance of phase fluctuation being greater for sound paths in the horizontal than in the vertical direction. The autocorrelation functions of amplitude and phase fluctuations in any one direction are similar.

TABLE OF CONTENTS

I.	INTRODUCTION-----	12
A.	BACKGROUND AND OBJECTIVES-----	12
B.	CAUSES OF FLUCTUATIONS-----	13
	1. Sound Amplitude Fluctuation-----	13
	2. Sound Phase Fluctuation-----	15
	3. Sound Amplitude and Phase Fluctuation---	15
II.	THE EXPERIMENT-----	17
A.	OBJECTIVE OF EXPERIMENT-----	17
B.	INSTRUMENTATION-----	17
	1. The Frame-----	17
	a. Construction-----	17
	b. Reflective Noise Considerations----	17
	c. Wire Tension Considerations-----	21
	2. Selection of Transducers (Sources)-----	21
	3. Selection of Hydrophones-----	22
	4. Circuit for Amplitude Fluctuation	
	Detection-----	22
	a. Wave Synthesizer-----	22
	b. Transducers-----	24
	c. Pre-Amplifiers-----	24
	d. Filters-----	24
	e. Envelope Detector-----	24
	f. Differential Amplifier-----	26
	g. Tape Recorder-----	27

5.	Circuit for Phase Fluctuation	
	Detection-----	27
C.	LOCATION OF EXPERIMENT-----	29
D.	INTERFERENCE FROM NEIGHBORING EXPERIMENT----	29
E.	ENVIRONMENTAL CONDITIONS-----	31
F.	CONDUCT OF EXPERIMENT-----	31
	1. Choice of Record Length-----	31
	2. Choice of Frequencies-----	34
	3. Bathythermographs-----	35
	4. Summary of Runs-----	35
III.	SIGNAL PROCESSING-----	38
A.	DIGITIZATION-----	38
B.	CONVERSION OF DATA-----	38
	1. Scaling of Data-----	39
	2. Clipping of Spikes-----	40
C.	ANALYSIS OF DATA-----	41
	1. Analysis Scheme-----	41
	a. Mean Removal and De-Trending-----	41
	b. Autocovariance Function-----	41
	c. Power Spectral Density-----	44
	d. Cross-Covariance Function-----	44
	e. Cross-Spectral Density-----	45
	f. Display of Results-----	45
	2. Parameters of Analysis-----	46
	a. Sampling Interval-----	46
	b. Resolution-----	47
	c. Degrees of Freedom-----	47

IV.	ANALYSIS RESULTS-----	48
A.	RESOLUTION BANDWIDTH AND DEGREES OF FREEDOM-----	48
B.	OVERVIEW OF ANALYSIS RESULTS-----	48
C.	INITIAL OBSERVATIONS AND INTERPRETATION OF SPECTRAL ANALYSIS-----	49
1.	Autocorrelation Function-----	55
a.	Frequency Content-----	55
(1)	Low Frequency-----	55
(2)	Surface Wave Frequency-----	55
(3)	High Frequencies-----	56
b.	Initial Drop in Autocorrelation Function-----	56
2.	Power Spectrum Levels-----	56
3.	Cross-Correlation Function-----	57
4.	Coherence-----	57
5.	Cross-Spectral Phase Angle-----	58
D.	CORRELATION TIME AS A FUNCTION OF THE SOUND FIELD'S SPATIAL RELATIONSHIP TO THE THERMO- CLINE-----	50
E.	Z-DIRECTION CORRELATION TIME VERSUS Y- DIRECTION CORRELATION TIME-----	78
F.	Y-DIRECTION VARIANCE VERSUS Z-DIRECTION VARIANCE-----	80
G.	CORRELATION OF PHASE AND AMPLITUDE FLUCTUATIONS-----	83

V.	CONCLUSIONS-----	96
VI.	RECOMMENDATIONS FOR FUTURE EXPERIMENTS-----	98
	APPENDIX A ANALYSIS RESULTS FOR VARIOUS RUNS-----	100
	COMPUTER PROGRAM CONVERT-----	234
	COMPUTER PROGRAM ANALYSIS-----	241
	LIST OF REFERENCES-----	253
	INITIAL DISTRIBUTION LIST-----	254
	FORM DD 1473-----	256

LIST OF FIGURES

1.	PHOTOGRAPH OF MODEL OF FRAME-----	18
2.	SCHEMATIC DRAWING OF FRAME, SHOWING SOUND FIELDS--	19
3.	PHOTOGRAPH OF FRAME ON TOWER-----	20
4.	BLOCK DIAGRAM OF AMP AND PHASE FLUC. DETECTION CKT.-----	23
5.	SCHEMATIC DRAWING OF ENVELOPE DETECTOR CKT-----	25
6.	PROGRESS OF INCOMING SIGNAL-----	28
7.	PHOTOGRAPH OF NUC TOWER-----	30
8.	CLIPPED AND NON-CLIPPED WAVE FORM PH-8, Z-PHASE---	42
9.	CLIPPED AND NON-CLIPPED WAVE FORM, PH-8 Z-AMP-----	43
10.	TIME RECORDS, PH-4, Y, Z PHASE FLUC.-----	50
11.	AUTOCORRELATION FUNCTION, PH-4, Y, Z PHASE FLUC.--	51
12.	AUTOSPECTRUM, PH-4, Y, Z PHASE FLUC.-----	52
13.	CROSS-CORRELATION FUNCTION, PH-4, Y, Z PHASE FLUC.-----	53
14.	COHERENCE, PHASE ANGLE, PH-4, Y, Z PHASE FLUC.----	54
15.	TEMPERATURE STRUCTURE, PH-2-----	63
16.	TEMPERATURE STRUCTURE, PH-3-----	64
17.	TEMPERATURE STRUCTURE, PH-4-----	65
18.	TEMPERATURE STRUCTURE, PH-5-----	66
19.	TIME RECORDS, PH-2 Y, Z, PHASE FLUC.-----	68
20.	TIME RECORDS, PH-3, Y, Z PHASE FLUC.-----	69
21.	TIME RECORDS, PH-4, Y, Z PHASE FLUC.-----	70
22.	TIME RECORDS, PH-5, Y, Z PHASE FLUC.-----	71

23.	AUTOCORRELATION FUNCTION, PH-2, Y, Z PHASE FLUC.-----	72
24.	AUTOCORRELATION FUNCTION, PH-3, Y, Z PHASE FLUC.-----	73
25.	AUTOCORRELATION FUNCTION, PH-4, Y, Z PHASE FLUC.-----	74
26.	AUTOCORRELATION FUNCTION, PH-5, Y, Z PHASE FLUC.-----	75
27.	GRAPH OF CORRELATION TIME VS DEPTH AND DISTANCE FROM Y-AXIS TO MIXED LAYER BOUNDARY-----	77
28.	GRAPH OF VARIANCE VS DEPTH OF Y-AXIS-----	81
29.	AUTOCORRELATION FUNCTION, PH-8, Z-PHASE FLUC. Z-AMP, FLUC.-----	85
30.	CORRECTED AUTOCORRELATION FUNCTION, PH-8, Z-PHASE, Z-AMP, FLUC.-----	86
31.	AUTOCORRELATION FUNCTION, PH-7, X-PHASE, X-AMP. FLUC.-----	87
32.	CORRECTED AUTOCORRELATION FUNCTION, PH-7, X-PHASE, X-AMP. FLUC.-----	88
33.	AUTOCORRELATION FUNCTION, PH-3, Y-PHASE, Y-AMP. FLUC.-----	90
34.	AUTOCORRELATION FUNCTION, PH-2, Y-PHASE, Y-AMP. FLUC.-----	91
35.	AUTOCORRELATION FUNCTION, PH-5, Z-PHASE, Z-AMP. FLUC.-----	92
36.	AUTOCORRELATION FUNCTION, PH-5, X-PHASE, X-AMP. FLUC.-----	93

37.	AUTOCORRELATION FUNCTION, PH-4, Z-PHASE, Z-AMP.	
	FLUC.-----	94
38.	AUTOCORRELATION FUNCTION, PH-8, Y-PHASE, Y-AMP.	
	FLUC.-----	95

LIST OF TABLES

1.	TABLE I - NUC Research Tower Environmental Conditions, 8, 9 June 1972-----	32
2.	TABLE II - Summary of Runs-----	36
3.	TABLE III - Cross Spectral Phase Angle Summary-----	61

ACKNOWLEDGEMENTS

I wish to express my sincere appreciation to my thesis advisor Dr. Herman Medwin for the guidance, motivation and resources which he provided for this work. Special thanks are also due Mr. William Smith, whose technical expertise in the fields of electronics, acoustics, and seamanship were invaluable in carrying out the experiment. I am also indebted to LCDR John Gossner and LCDR James Fitzgerald for their assistance in obtaining oceanographic and phase fluctuation data, to Mr. Dale Good of NUC, and the NUC Tower staff who so very ably assisted in the experiment, and to Dr. John Calhoun, who generously gave of his time in the early stages of computer program de-bugging.

This thesis serves as a technical report to Naval Ship Systems Command (Code PMS 302) which provided the major part of the financial support for the facilities, technician, and computer services required for this research. Partial support from the Office of Naval Research, Ocean Sciences and Technology Division is also acknowledged.

I. INTRODUCTION

A. BACKGROUND AND OBJECTIVES

When a sound wave is propagated in the upper layers of the ocean, both its amplitude and phase fluctuate. These fluctuations result from the motion of the medium inhomogeneities in the sound path, and motion of the medium itself. Relatively little study has been done in the relationship between the ocean microstructure and sonic fluctuations. This situation exists because early research on the interaction of sound and the ocean medium concentrated on the effect of the ocean medium on the sound wave's intensity only; it wasn't felt necessary to inquire about how the sound beam's amplitude and phase responded to the medium. However, a knowledge of how the ocean medium effects the phase and amplitude of a sound beam would now be useful from two standpoints. Devices are being developed for use in the ocean that utilize sound amplitude and phase information (acoustic imaging devices, underwater communication devices etc.) A knowledge of the effects of the ocean medium on the sound amplitude and phase is therefore mandatory. A knowledge of the relationship between the nature of the ocean's microstructure and the amplitude and phase fluctuation of a sound beam passing through that medium could enable one to derive information about the ocean microstructure by measuring such fluctuations.

The objective of this thesis was to take in-situ acoustical measurements over a range of approximately 1.5 meters in the near surface region of the ocean in order to study the relationship between sound phase and amplitude fluctuations and the nature of the medium. To do this, a constant frequency, constant amplitude sound beam was transmitted in each of three orthogonal directions simultaneously. Measurements of the position of the thermocline, swell magnitude and direction, and other environmental parameters were made. Spectral analysis and cross-spectral analysis are performed on the resulting phase and amplitude fluctuation records, and the sound phase and amplitude fluctuations are related to the behavior of the medium.

B. CAUSES OF FLUCTUATIONS

When a continuous sound beam of constant frequency and constant amplitude is transmitted through a volume of ocean, it is found that the sound beam arriving at a receiver placed some distance from the transmitter will have a fluctuating amplitude and a fluctuating phase. The causes of these fluctuations are described below.

1. Sound Amplitude Fluctuations

A sound beam traveling through an ocean medium encounters temperature and salinity inhomogeneities and "patches" of small bubbles of various sizes. The inhomogeneities and patches vary spatially with the motion of the medium (Medwin, 1970). The inhomogeneities present

a change in acoustic impedance, $\rho \cdot C$, to the sound beam, and the beam is partially reflected from the inhomogeneity, and partially transmitted through the inhomogeneity at some refraction angle. If a sound beam traveled through an ocean volume in which the inhomogeneities and bubble patches were "frozen" in place, reflection and refraction would still take place, but the received sound beam would have a constant amplitude. However, when the "frozen" inhomogeneities are allowed to move about, to move into and out of the sound beam's path, then the reflection and refraction of the sound beam changes with time, and hence the received sound amplitude will fluctuate accordingly. The motion of temperature and salinity inhomogeneities and bubble patches into and out of the sound beam's path causes sound amplitude fluctuation, due to the sound beam being both reflected and refracted by the changing acoustic impedance of the medium. The extent of the fluctuations depend upon the impedance mismatch between the medium and the inhomogeneities, size and shape of the inhomogeneities or patches, and the frequency with which they move into and out of the beam's path.

The bubbles mentioned above can have another effect on the sound beam. If the moving bubbles have a resonant frequency at or near the frequency of the sound beam, then the bubbles will resonate, absorb and scatter the incident sound beam. This reduces the sound beam's intensity, and causes the amplitude to fluctuate with time.

2. Sound Phase Fluctuation

A fluctuation in phase of the received sound beam results from a change in the integrated speed of sound propagation, C , between the source and the receiver. Such a change in C in the ocean results from the following:

a. A change in temperature, salinity, and/or the resonant bubble population in the volume of water through which the sound beam is traveling will effect the speed C . This will occur when temperature or salinity inhomogeneities and/or resonant bubbles move into or out of the path of the sound beam.

b. Motion of the medium with a vector component in the direction of sound propagation will add to or subtract from C (doppler shift). The entire ocean is in constant motion; the predominant motion encountered in the surface layers of the ocean is generally orbital motion due to surface wave action.

3. Sound Amplitude and Phase Fluctuation

The cause and effect relationship of the ocean medium and sound amplitude and phase fluctuations can be summarized as follows:

If a sound source and receiver are positioned in the upper layer of the ocean, the orbital motion of the volume of water between the source and receiver (in response to the surface wave action) carries temperature and salinity inhomogeneities and varying bubble populations into and out of the sound beam's path. Amplitude fluctuation

results due to scattering and refraction of the sound beam as it encounters the differing acoustic impedance of the inhomogeneities and bubble patches. Phase fluctuation occurs due to a change in the integrated speed of sound between the source and the receiver, and also due to the medium velocity component in the direction of sound propagation.

II. THE EXPERIMENT

A. OBJECTIVE OF THE EXPERIMENT

The objective of the experiment was to propagate constant amplitude, constant frequency acoustic signals in three orthogonal directions simultaneously at various depths in the upper layer of the ocean, and to record the resulting amplitude and phase fluctuations. Frequencies used in the experiment were 65 kHz, and 105 kHz.

B. INSTRUMENTATION

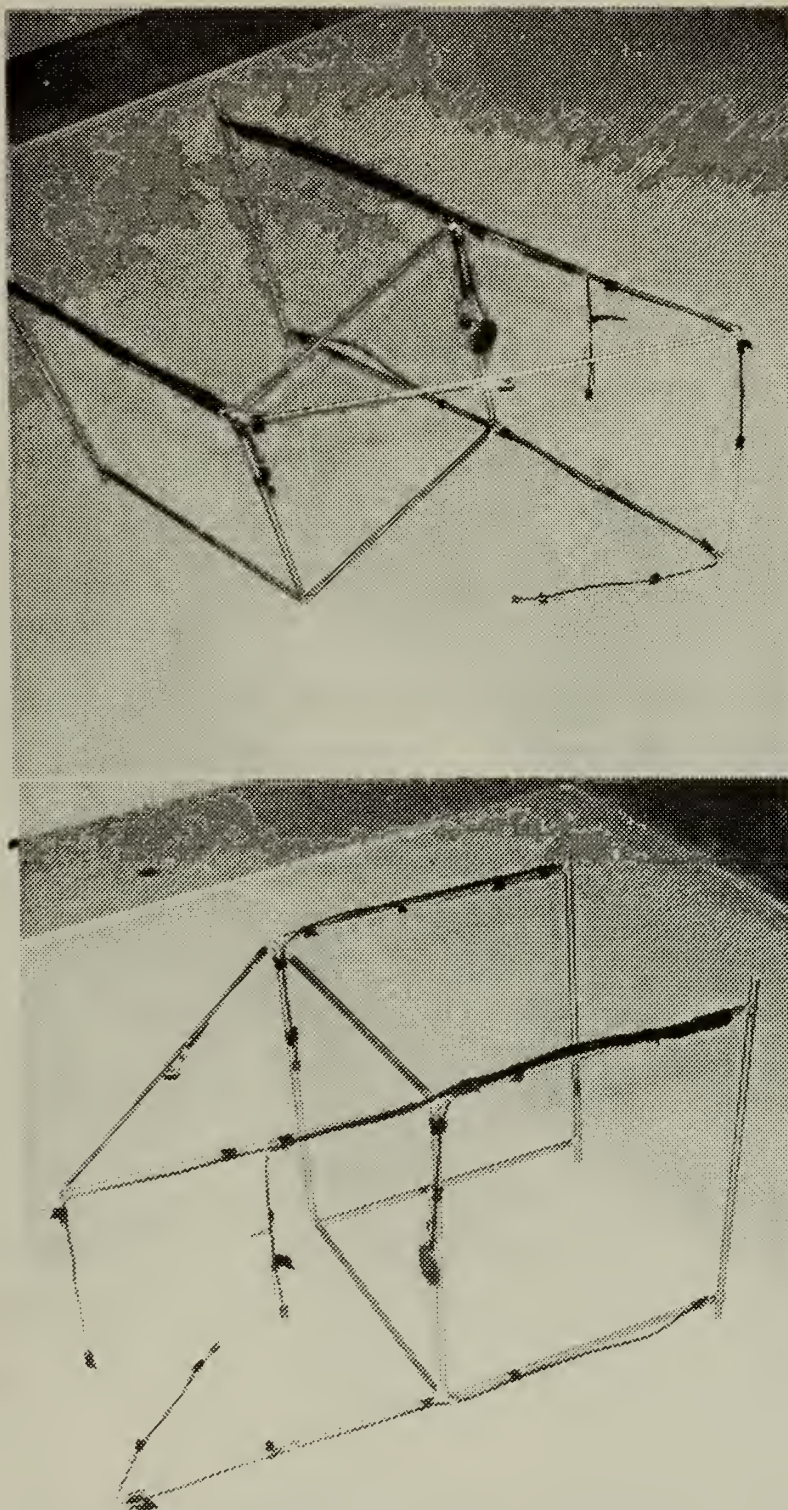
1. The Frame

a. Construction

A rigid frame was constructed in order to mount the transducers and hydrophones in a 3-dimensional configuration. Figure 1 is a photograph of a model of the frame, showing the orientation of the X, Y, and Z directions. Figure 2 is a schematic drawing of the sound fields. Figure 3 is a photograph of the actual frame in position at the experiment site. The frame was constructed of aluminum pipe with steel joints. The frame was designed to be disassembled for portability. The fully assembled frame, less instrumentation, weighed approximately 300 lb.

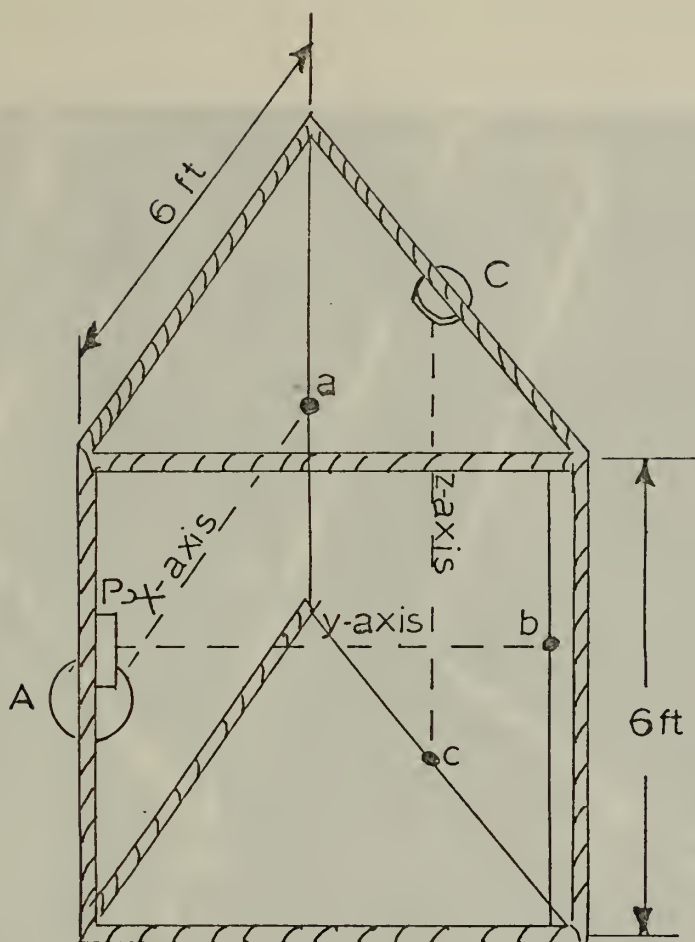
b. Reflective Noise Considerations

Since it was the objective of the experiment to measure the phase and amplitude fluctuation of a sound



PHOTOGRAPH OF MODEL OF FRAME

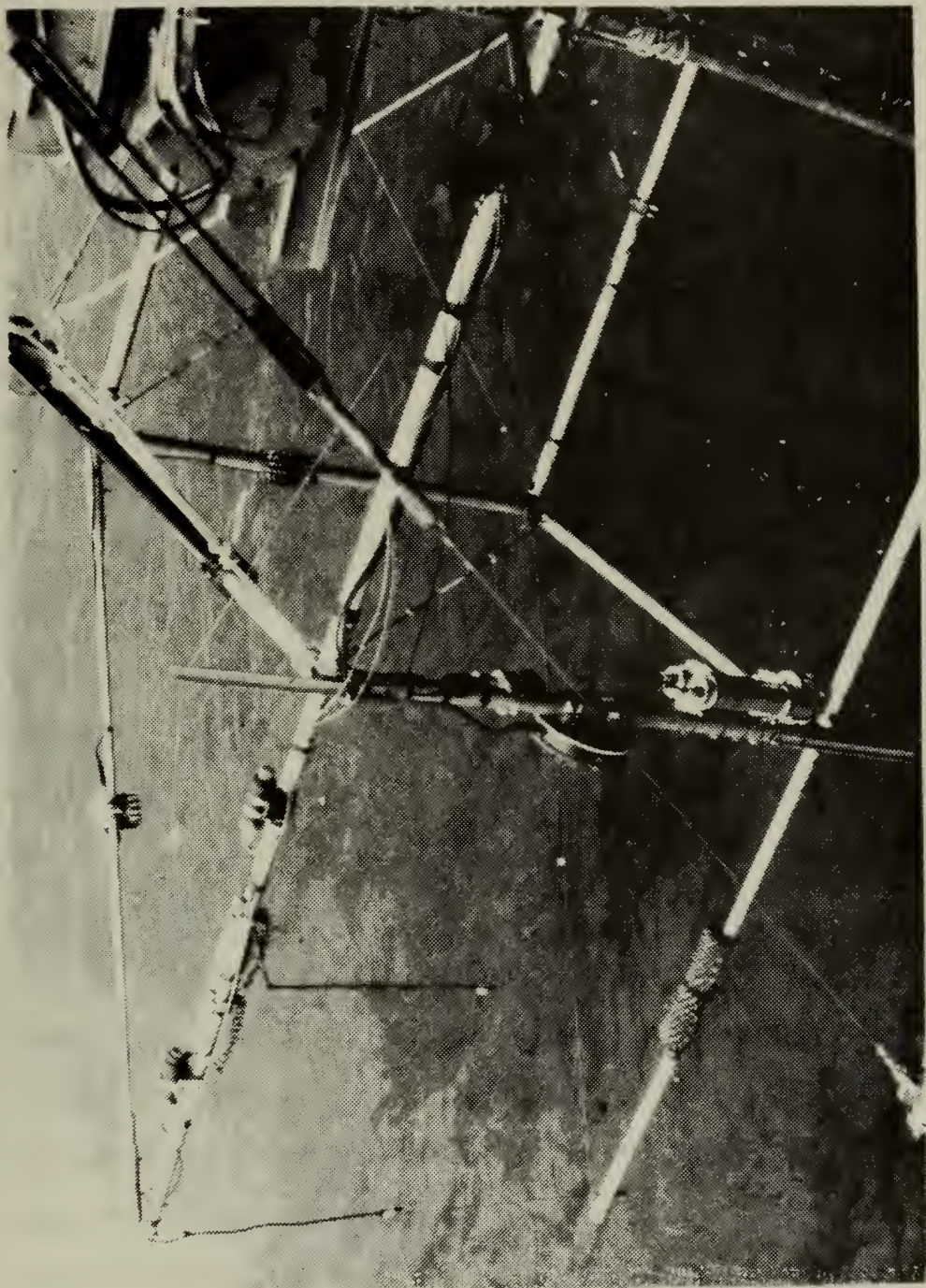
FIGURE 1



	SOURCE	RCVR	PATH LENGTH
X-DIRECTION	A:F-33	a:LC-10	1.35 m.
Y-DIRECTION	B:F-41	b:LC-10	1.50 m.
Z-DIRECTION	C:F-41	c:LC-10	1.65 m.

SCHEMATIC DRAWING OF FRAME, SHOWING
LOCATION OF SOUND AXES

FIGURE 2



PHOTOGRAPH OF FRAME ON NUC TOWER

FIGURE 3

beam traveling a direct path between the transducer and the hydrophone, it was necessary to eliminate any reflected sound. Pulse-echo testing of the frame configuration revealed points of specular reflection on the frame; acoustic absorbant rubber was affixed to the frame at these points, and all such reflections were reduced to at least 30 dB below the direct signal level.

c. Wire Tension Considerations

Scattering interference considerations necessitated mounting the hydrophones on small diameter wire. Such mounting caused vibration problems, however, which arose from Karman-vortex shedding as water flowed past the wires. Vibration of the mounting wire could cause an accelerometer effect in the hydrophone response, and more importantly, it could cause a false fluctuation in the received signal. This problem was decreased by maximizing the tension of the wires.

2. Selection of Transducers (Sources)

Since the experiment was to be performed in a frequency range from 65kHz to 105 kHz, a transducer with a well documented transmit-response in this range, and a reasonable degree of directivity was needed. One USRD type F-33 transducer and two USRD type F-41 transducers were chosen. Transmit responses for these transducers are:

<u>TRANSDUCER</u>	<u>65 kHz</u>	<u>105 kHz</u>
F-33	37dB	48dB
F-41	37dB	49dB

dB reference 1 microbar/volt at 1 meter

3. Selection of Hydrophones

A hydrophone with a flat receiving sensitivity in the frequency range of interest was the LC-10. Its measured sensitivity was:

<u>65 kHz</u>	<u>105kHz</u>
-109dB	-110dB

dB reference 1 volt/microbar

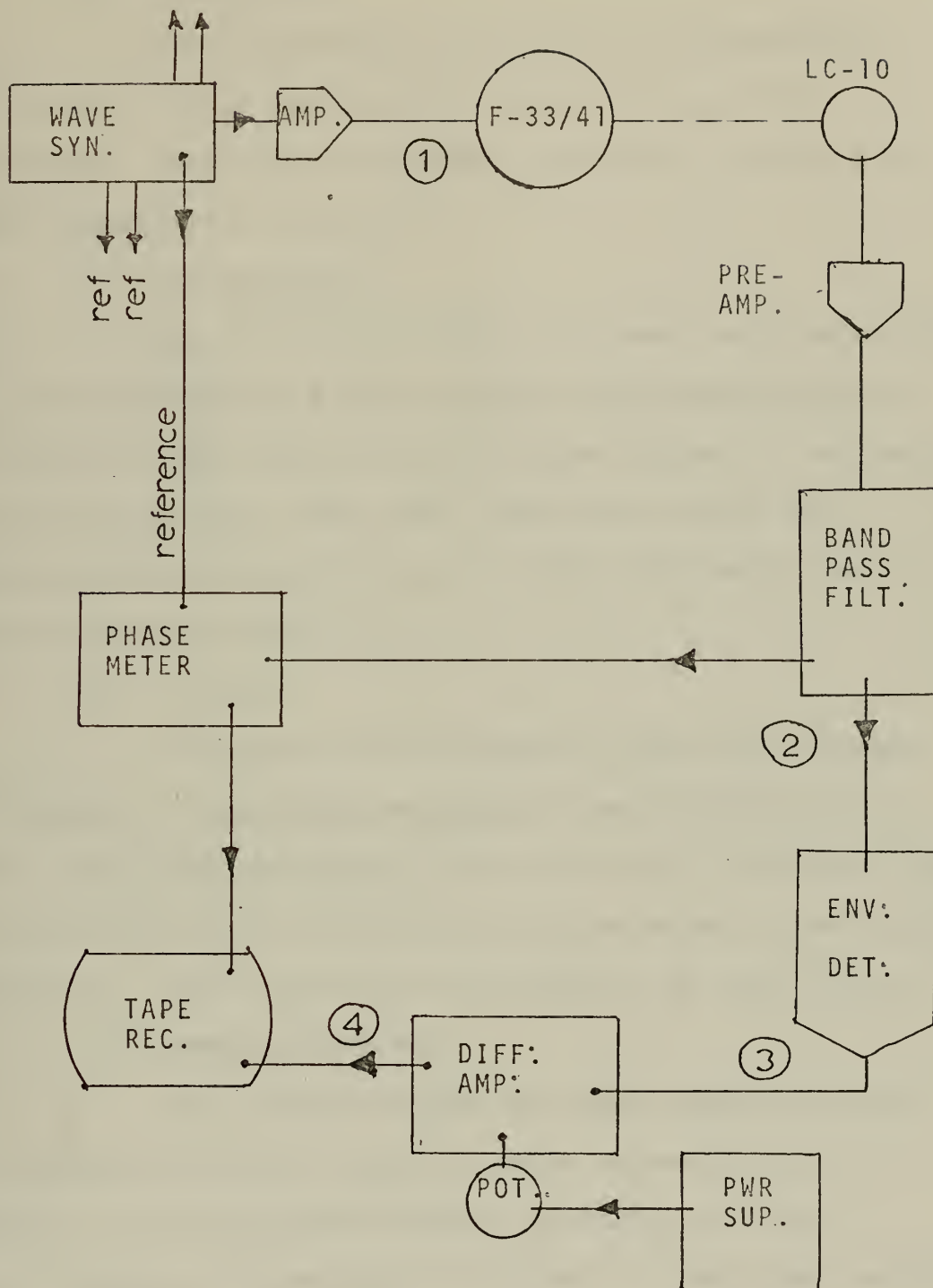
4. Circuit for Amplitude Fluctuation Detection

Figure 4 is a block diagram of the instrumentation used to measure amplitude and phase fluctuation. The phase fluctuation detection circuit is described in section II B-5. Amplitude fluctuation detection is described in the following.

a. Wave Synthesizer

A General Radio Wave Synthesizer, model 1162-A was used to generate a constant frequency, constant amplitude signal. The output of the synthesizer was divided, part of it going to a Hewlett/Packard amplifier, model 467A and then to the transducer, and part going to the phase meter as a reference signal for the phase fluctuation measurement. (section 5)

to other channels



ONE CHANNEL OF PHASE/AMPLITUDE
FLUCTUATION MEASUREMENT CIRCUIT

FIGURE 4

b. Transducers

The transducers (F-33 or F-41) transmitted an acoustic signal through the medium to the LC-10 hydrophone. One LC-10 hydrophone was used in each of the three channels, X, Y, and Z.

c. Pre-amplifier

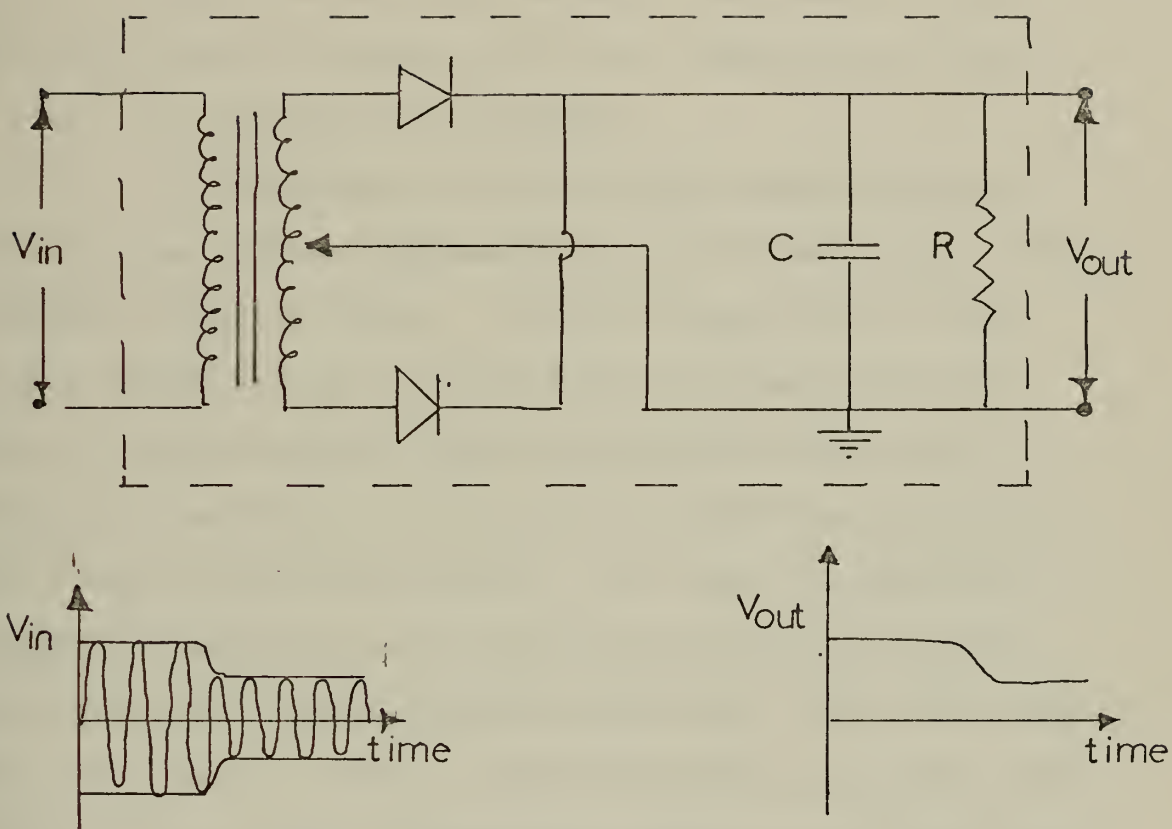
The LC-10 generated a low level voltage which was pre-amplified by a NUS constant gain pre-amplifier. One NUS pre-amplifier was used in each channel. Two models of the NUS pre-amp. were used, model 2010 which had a gain of approximately 30 dB, and model 2030 which had a gain of approximately 20 dB.

d. Filters

The signal was filtered by means of a Krohn-Hite filter. One filter was used in each channel; two model 3322's and one model 3342 were used. The signal was band-pass filtered at ± 300 Hz on either side of the carrier frequency. The filter has a +20 and +40 dB gain option.

e. Envelope Detector

The filtered signal was then passed through an envelope detector, which is shown schematically in figure 5. The envelope detector provided full wave rectification and low-pass filtering to remove the carrier signal. The response of this envelope detector was non-linear at low input voltages levels. That is, the output of the envelope detector was not proportional to the envelope of the modulated input voltage at low input



$C = .068$ microfarrads

$R = 50$ K ohms

DIODES - Switching Type 1N277

TRANSFORMER - TA-38

SCHEMATIC DRAWING OF ENVELOPE DETECTOR
CIRCUIT

FIGURE 5

voltage levels. With the aid of a computer, a 5th order polynomial curve was fitted to the empirically determined response of the envelope detector. This curve related input AC voltage, measured in volts peak-to-peak, to output DC volts. One envelope detector was used in each direction, and a response curve was computed for each.

f. Differential Amplifier

The output of the envelope detector was a fluctuating voltage representing the fluctuations of the incoming acoustic signal. This envelope had a DC component which had to be removed prior to amplification. This DC voltage removal was accomplished with a differential amplifier, which took the difference of two input voltages and amplified it. One input to the differential amplifier was a DC voltage equal to the DC voltage to be removed from the envelope. The other input was the envelope itself. One differential amplifier was used in each channel. Two of the differential amplifiers were Princeton Applied Research Amplifiers, model TM-113, which has a variable output gain control, and a band-pass filter option. Maximum input voltage to the PAR amplifier is 0.5 volts. The other differential amplifier was a Hewlett/Packard model 2470A, which has a variable output gain control. Maximum input voltage to the Hewlett/Packard amplifier is 20 volts. The constant DC input voltage was supplied by a Hewlett/Packard model 721A power supply. A "Heli-pot" potentiometer was used to achieve accurate and

stable DC voltages. A X10 gain was applied to the output of all three channels by the variable gain of the differential amplifiers.

g. Tape Recorder

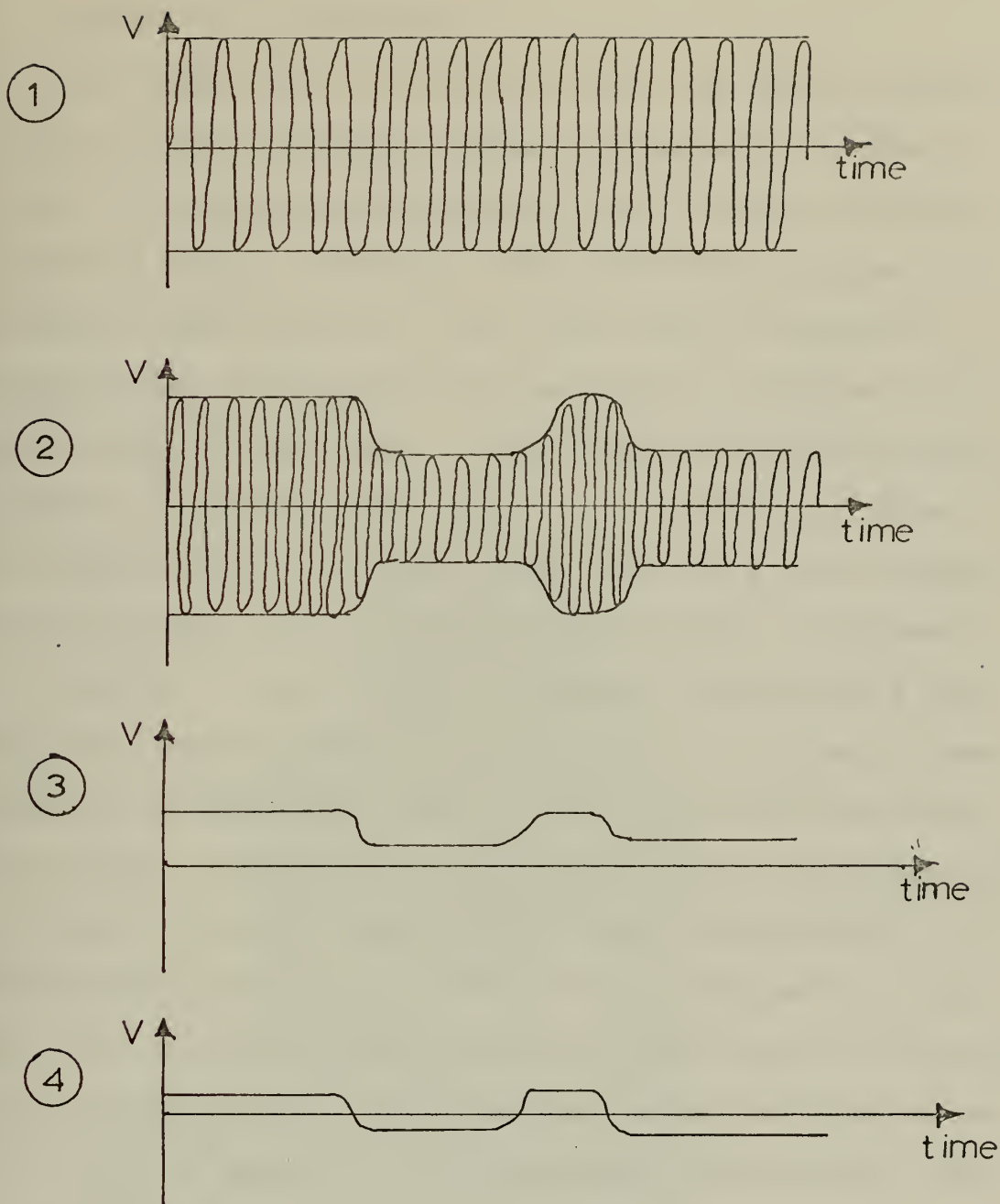
The amplified envelope was then recorded on a Precision Instrument model PI-6200 8-track magnetic tape recorder.

Figure 6 illustrates the progress of an incoming signal from the wave synthesizer to the tape recorder.

5. Circuit for Phase Fluctuation Detection

a. Phase Meter

After the signal was band-pass filtered, it was divided, and part of the signal was fed into a phase-meter. One phase-meter was used in each channel. Three different types of phase meter were used: Dranetz Phase-Meter Model 305-PA-3001, Dranetz Phase-Meter Model 305-PA-3002, and a Wiltron Phase-Meter. The phase-meter detected the phase difference between an input signal and a reference signal of the same frequency. The reference signal used was the input signal from the wave synthesizer. The output voltage of the phase-meter was proportional to the phase difference between the input and the reference signal. One degree of phase difference equals ten millivolts. The phase meter's output voltage was recorded on the 8-track tape recorder.



PROGRESS OF A SIGNAL PASSING THROUGH AMPLITUDE
FLUCTUATION DETECTION CIRCUIT.(SEE FIG. 4)

FIGURE 6

C. LOCATION OF EXPERIMENT

The experiment was carried out at the Naval Undersea Research and Development Center Oceanographic Research Tower, located approximately one mile off Mission Beach, near San Diego, California. The NUC Tower provided a rigidly fixed platform in the ocean which allowed continuous data accumulation and monitoring. Figure 7 is a photograph of the tower. It is fixed by supporting pins driven 63 feet into the ocean floor. Electrical power is supplied from the shore, thus insuring a power supply of relatively stable voltages and frequency. The tower is located in approximately 60 feet of water over a sand bottom. The instrumentation frame shown in Figure 2 was mounted on a six foot cube box standoff which was fixed to a sled. Figure 3 is a photograph of the frame mounted on the sled on the tower. The X axis was oriented in a due westerly direction. The sled was attached to a set of rails which extended from the working area of the tower to the ocean floor. The frame was raised and lowered on the rails by means of an electrically driven winch, and could be positioned at any depth.

D. INTERFERENCE FROM NEIGHBORING EXPERIMENT

A separate experiment was being carried out at the NUC tower in the proximity of this experiment. The neighboring experiment generated acoustic impulses every second from a transducer positioned near the bottom beneath the tower.



PHOTOGRAPH OF NUC OCEANOGRAPHIC TOWER

FIGURE 7

These acoustic impulses were detected by the LC-10 hydrophones of this experiment. The means of reducing this noise effect is described in section IIIb.2.

E. ENVIRONMENTAL CONDITIONS

The experiment was performed on the 8th and 9th of June, 1972. The prevailing environmental conditions are listed in Table I. Of particular note was the presence of swell waves and internal waves. The swell waves were approximately 4 ft, peak to trough, from the southwest, and with a period of approximately 15 seconds. The swell waves persisted throughout the experiment. The presence of internal waves was noted in the long term temperature fluctuations which were observed at various depths from 6 June to 9 June. These long term temperature fluctuations had a period of approximately 6 - 12 minutes. The presence of internal waves was also implied by the varying depth of the thermocline during the experiment.

Tuna and other fish were noted in the vicinity of the tower during the experiment.

F. CONDUCT OF THE EXPERIMENT

1. Choice of Record Length

A "run" consisted of radiating constant amplitude, constant frequency sound in three orthogonal directions simultaneously for approximately 20 minutes. The 20 minute run time interval was decided upon for the following reasons. Preliminary tests had shown that the sound amplitude and

TABLE I

NUC RESEARCH TOWER ENVIRONMENTAL CONDITIONS, 8, 9 JUNE 1972

RUN NO.	FREQ. kHz	START TIME	OBSERVED WEATHER					
			AIR TEMP °C	SURF. TEMP. °C	WIND DIR. DEG.	WIND SPD KTS	CLOUD COVER %	SWELL DIR.
PH-1A, B	65/105	1600.	19.6	18.95	240	8	100	W
PH-2	65	1654	19.2	18.20	240	9	100	WSW
PH-3	65	1800	18.7	19.1	225	6	100	SW
PH-4	65	1830	18.2	18.94	223	7	100	SW
PH-5	65	1922	17.9	18.77	235	4	100	SW
PH-6	105	0837	17.3	18.65	240	4	100	WSW
PH-7	105	0935	17.50	18.50	245	8	100	SW
PH-8	105	1000	18.8	18.5	240	4	60	SW

TABLE I (CONT.)

RUN NO.	BT DATA				BOTTOM TEMP. (DEPTH = 60FT) °F
	SURF. TEMP. °F	1ST LAYER TEMP/DEPTH °F FT	2ND LAYER TEMP/DEPTH °F FT		
PH-1A, B	72.5	72/10	68/42 63/52		62
PH-2	74	74/20	71/30 69/54		65
PH-3	70	70/16	67/22 65/58		62
PH-4	72	71/18	63/36 66/56		65
PH-5	68	68/19	61/50		61
PH-6	71	61/28			61
PH-7	71	61/31			61
PH-8	71	61/30			61

phase fluctuations had a strong component frequency of approximately .06 HZ (corresponding to a period of about 15 seconds). Also, evidence of internal waves was observed in the preliminary fluctuation records in the form of long term amplitude and phase fluctuation; these long term fluctuations had periods of approximately 6-12 minutes. A run length long enough to record the internal wave effect would have to include several cycles, minimally 30-40 minutes. However, experiment time constraints and computer processing limitations made it necessary to limit runs to 20 minutes. This record length would allow resolution of the 15 second surface wave effect, and identification of the long period internal wave effect. However, little analytical information could be derived concerning the latter.

2. Choice of Frequencies

Two Frequencies were chosen for this experiment, 65 kHz, and 105 kHz. It has been found by Medwin (1970) that the bubble population in the upper ocean contains a large number of bubbles that are resonant at frequencies around 60 kHz. In previous experiments by Rautmann (1971), it was found that a peak dispersion of the sound speed occurs around 65 kHz; this dispersion was attributed to the presence (and resonance) of bubbles in the medium. This dispersive effect results in speeds that may be as much as 8 or 10 meters/second above or below the empirically predicted or velocimeter measured values. Near this

frequency the variance of the phase fluctuation is also very large. At 105 kHz, this dispersive effect and the large variance of the phase fluctuation is negligible.

It was decided to run the experiment at 65 kHz and 105 kHz in order to observe amplitude and phase fluctuations in a bubble affected and a non-bubble affected region.

3. Bathythermograph

A bathythermograph was taken during each run to obtain a representative gross temperature structure of the medium. The BT drop was made from the tower, approximately 40 feet from the frame.

4. Summary of Runs

Runs were performed at several depths between the surface and the bottom, at the two frequencies, 65 kHz and 105 kHz. These runs were performed during the afternoon and evening of 8 June and the morning of 9 June.

Table II is a summary of the runs.

TABLE II

SUMMARY OF RUNS

RUN	DEPTH OF Y-AXIS (ft.)	FREQ (kHz)	RUN LENGTH (MIN.)	DEG. OF FRDM	CHAN. OF GOOD DATA AXIS PHASE ON AMP	COMMENTS
PH-1A	38	65	17.7	26	X-A Y-A X-P Y-P	
PH-1B	38	105	9.5	14		All channels too noisy for analysis
PH-2	31	65	17.7	26	Y-A Y-P Z-P	
PH-3	25	65	17.7	26	Y-A Z-A Y-P Z-P	Y-A noisy Z-A noisy
PH-4	18.8	65	15	22	Y-A Z-A Y-P Z-P	

TABLE II (cont.)

RUN	DEPTH OF Y-AXIS (ft.)	FREQ. (kHz)	RUN LENGTH (min.)	DEG. OF FRDM	CHAN. OF GOOD DATA AXIS PHASE ON AMP	COMMENTS
PH-5	7	65	17.7	26	X-A Z-A X-P Y-P Z-P	
PH-6	11.3	105	13.6	20	X-A X-P Y-P Z-P	
PH-7	44.2	105	17.7	26	X-A Y-A X-P Y-P	Y-A noisy X-A noisy X-P noisy
PH-8	26.8	105	17.7	26	Z-A Y-P Z-P	

III. SIGNAL PROCESSING

The data gathered during the experiment were in the form of varying analog voltage records recorded on six channels of 1/4 inch magnetic tape (X,Y, and Z direction phase fluctuations, and X, Y, and Z direction amplitude fluctuations).

A. DIGITIZATION

The data were digitized using a COMCOR 5000 - SDS - 9300 hybrid computer system of the Electrical Engineering Department, Naval Postgraduate School. It was observed from the time records that the data were generally band-limited to less than 4 HZ. A sampling rate of 50 HZ was used in the digitization process to minimize aliasing. At no time were the fluctuation records low-pass filtered. Such filtering was avoided to prevent non-linear phase shifting of the signal's component frequencies, which could result in errors in the cross-spectral analysis. A sampling pulse width of 0.1 millisecond was used, and the digitized data were blocked in records of 512 samples each. The digitization process produced a 7-track magnetic tape in octal notation, with the six channels multiplexed.

B. CONVERSION OF DATA

In order to process the digitized data on the Naval Postgraduate School's IBM 360 computer, the 7-track octal

notation tape was converted to 9-track, hexadecimal format, demultiplexed tape. In this process of conversion, scaling and "clipping" were also accomplished. The conversion program is listed on page 234.

1. Scaling of Data

During the conversion process, it was necessary to scale all of the channels. The X, Y, and Z direction phase fluctuation channels were scaled by 0.1 to compensate for the gain of the digitization process and to convert from volts to degrees of phase difference. The scaling applied to the X, Y, and Z direction amplitude fluctuations was more involved. The aim in this case was to convert the voltage records to acoustic pressures at the hydrophones for each channel. This was accomplished by computing a channel gain for each channel, based on the gain of each of the equipments. The polynomial curves described in Section IIa4.e, were employed here to describe the response of the envelope detectors. A channel was scaled as follows: for a particular channel, the DC nulling voltage (which was removed by the differential amplifier) was added to the signal; the channel gain is then applied. It was also desired to normalize all three channels of amplitude fluctuation to a common source level and a common transducer separation distance so that comparison of channels would be more meaningful. The above scaling - channel gain, source level normalization, separation distance normalization - was combined into one overall gain factor which was

applied to the X, Y, and Z amplitude fluctuation channels. This gain factor was different for each channel and for each run.

When the analysis was completed, it became evident that the scaling was in error, and unfortunately the actual values of the pressure levels at the hydrophones were unrecoverable from the data.

2. Clipping of Spikes

In many of the amplitude fluctuation records there were numerous voltage "spikes", caused by radiation from the research project mentioned in Section IID which was being conducted in the proximity of this experiment. In addition to this source of noise, there were extraneous voltage spikes which either originated in the electronics of the equipment, or resulted from a physical impulse shock to the system. Many of these spikes were removed from the time records during the digitization process. Many of those which remained in the digitized time records were removed by means of a simple "clipper" routine in the CONVERT program. When an extraneous spike was encountered in the data, the previous non-spike value was substituted for it. A threshold spike detection level had to be established for the routine; the level had to be low enough to detect the presence of a spike, but large enough so that actual data would not be interpreted as spikes. It was therefore impossible to remove all of the spikes from the time records. Samples of the time signals showing

the "raw" data and the "clipped" data are shown in Figures 8 and 9. (Note different ordinate scales)

C. ANALYSIS OF DATA

1. Analysis Scheme

Spectral and cross-spectral analysis of the fluctuation records was carried out as follows:

a. Mean Removal and De-trending

The first operations performed on each time record were removal of the mean value of the record and the removal of any linear trend of the record. The mean value (DC value) was removed so that in the succeeding analysis, the fluctuations of the signal alone would determine the nature of the results, and so that comparison of two different records would be meaningful. Removal of the linear trend of a record was accomplished by subtracting from the time record the least-mean-square fit of the record. This was done to remove any long term linear change of the signal. Such a change would have resulted not from the effects of the medium, but from instabilities in the electronics of the detecting circuits. The mean removal and the de-trending were accomplished by subroutine AVERAGE, and TREND in the analysis package.

b. Autocovariance Function

An autocovariance function was computed from a time record by a "multiply and add" process described by:

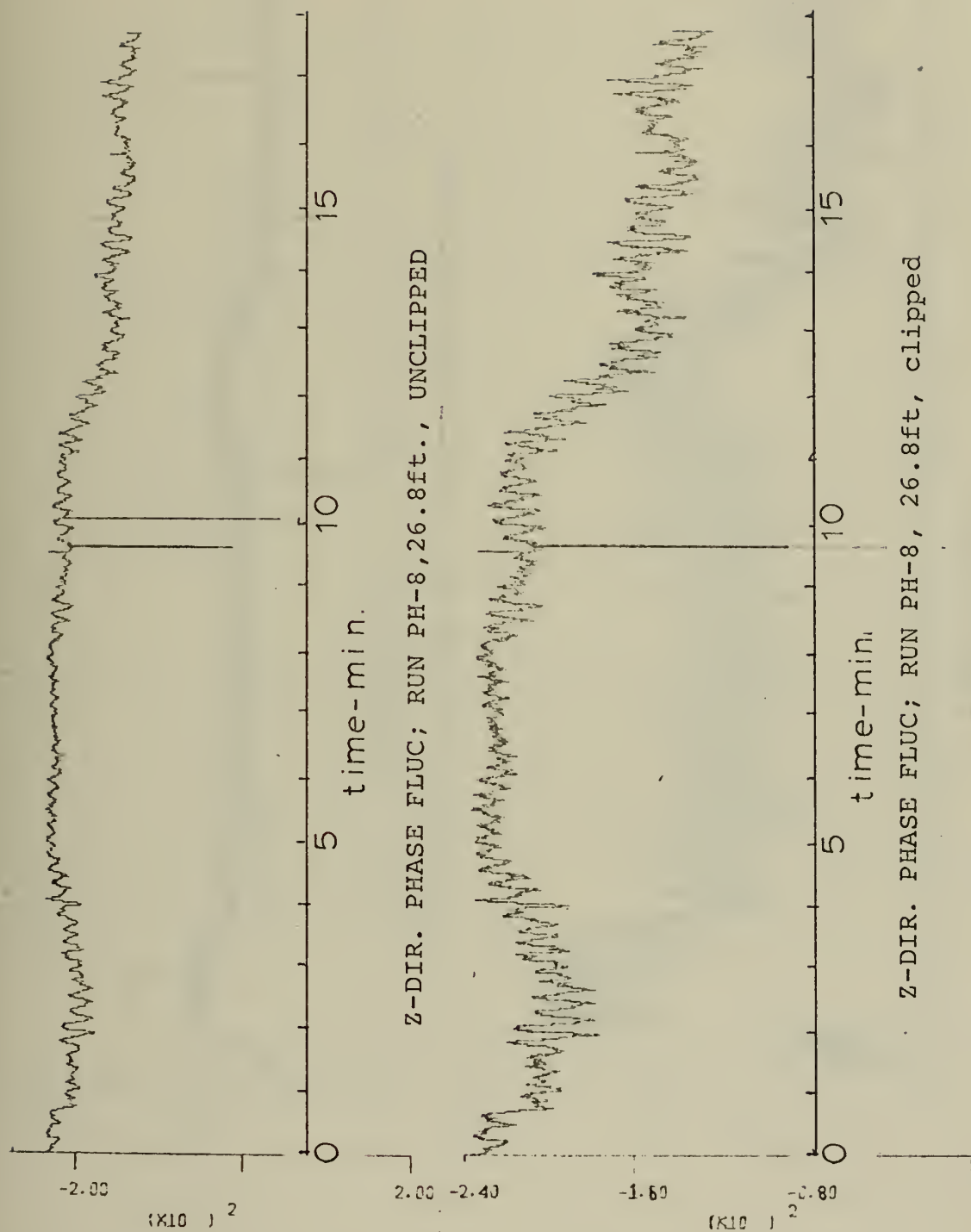


FIGURE 8

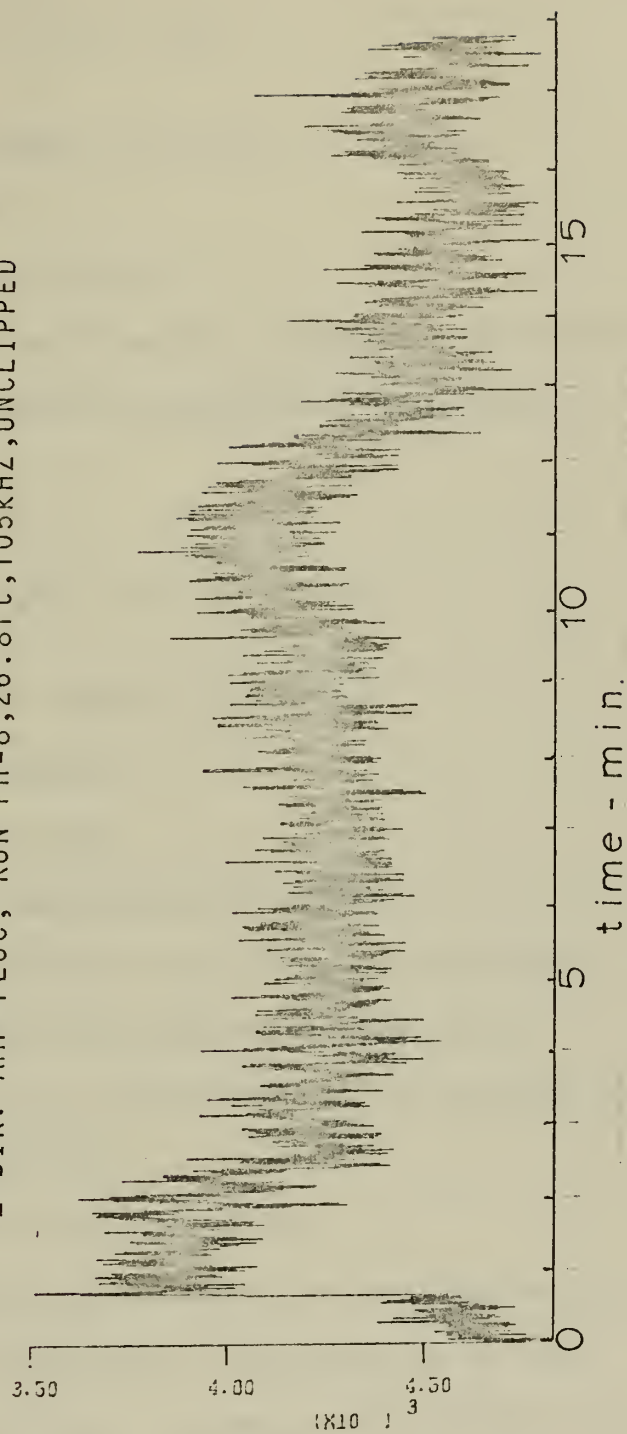
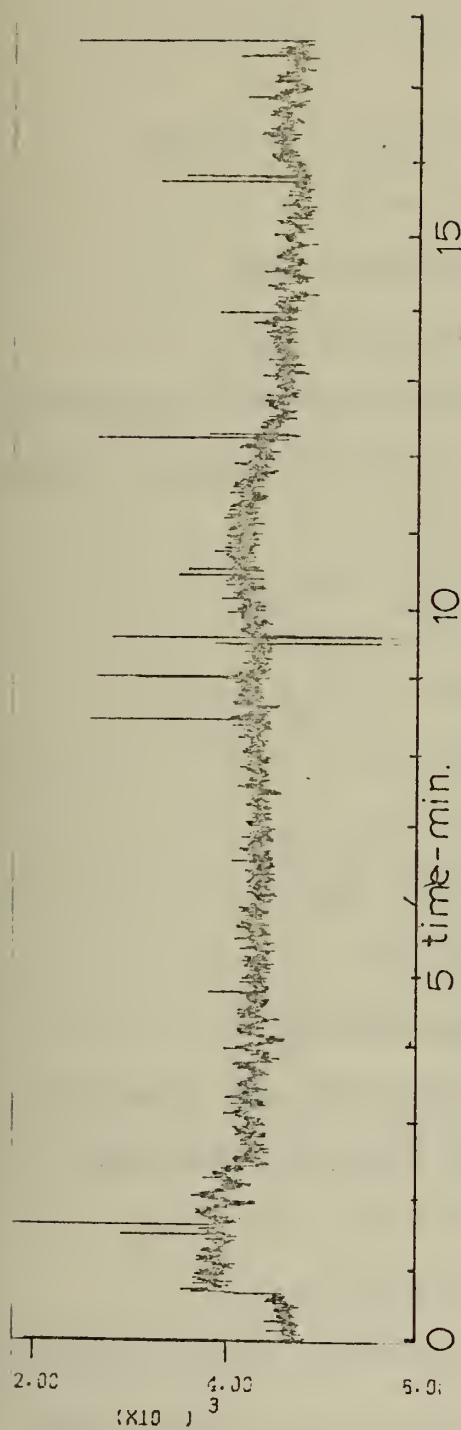


FIGURE 9

$$R_x(\uparrow) = \frac{1}{N-\uparrow} \sum_{i=1}^{N-\uparrow} x_i x_{i+\uparrow}$$

where N = total number of points in record

\uparrow = time lag

c. Power Spectral Density

Using the Wiener-Khinchine relation, the autocovariance function was Fourier transformed to produce a power spectral density

$$G_x(f) = 4 \int_0^L R_x(\uparrow) \cos(2\pi f\uparrow) d\uparrow$$

where $G_x(f)$ = Power Spectral Density

f = frequency

\uparrow = time lag

$R(\uparrow)$ = Autocovariance Function

L = Total time lag of Autocovariance

A Parzen window was applied to the autocovariance function prior to transformation for smoothing of the power spectral densities.

d. The Cross-Covariance Function

A cross-covariance function of two channels of interest (e.g. phase and amplitude fluctuations in the same direction for the same run, or phase fluctuation in two different directions for the same run) was computed. Since $R_{xy}(\uparrow) = R_{xy}(-\uparrow)$, the two parts of the cross-covariance function were computed for positive time delays:

$$R_{xy}(\tau) = \frac{1}{N-\tau} \sum_{i=1}^{N-\tau} X_i Y_{i+\tau}$$

$$R_{yx}(\tau) = \frac{1}{N-\tau} \sum_{i=1}^{N-\tau} Y_i X_{i+\tau}$$

e. The Cross-Spectral Density

The cross-spectral density was then computed by computing the cospectral density C_{xy} and the quad-spectral density Q_{xy} as follows:

$$C_{xy}(f) = 2 \int_0^L [R_{xy}(\tau) + R_{xy}(-\tau)] \cos(2\pi f\tau) d\tau$$

$$Q_{xy}(f) = 2 \int_0^L [R_{xy}(\tau) - R_{xy}(-\tau)] \sin(2\pi f\tau) d\tau$$

A Parzen window was applied to the cross-covariance function prior to transformation for smoothing of the resulting spectral densities. The cospectral density and the quad-spectral density were combined to form the cross-spectral coherence function, and the cross-spectral phase angle:

$$\text{Coherence} = \frac{C_{xy}^2(f) + Q_{xy}^2(f)}{G_x(f) G_y(f)}$$

$$\text{Phase Angle} = \tan^{-1} \frac{Q_{xy}(f)}{C_{xy}(f)}$$

f. Display of Results

The computer program used to make the above described computations is listed on pages 234 through 252. Various functions are plotted by this program:

Autocorrelation Function - The autocovariance function normalized with respect to the $\tau = 0$ value

Cross-Correlation Function - The cross-covariance function normalized with respect to the square root of the product of the $\tau = 0$ value of the component autocovariance functions

Auto-Spectrum Level - $10\log_{10}$ (power spectral density), in units of dB, reference degrees for phase fluctuation record. Relative dB are used for amplitude fluctuation records.

Coherence Function - as described in Section d. above

Cross-Spectral Phase Angle - as described in Section d. above

2. Parameters of Analysis

a. Sampling Interval

The analog voltage signals were sampled at 50 HZ when digitized. This sampling rate was chosen to insure that no aliasing of high frequencies occurred. A trial spectral analysis of a typical amplitude fluctuation record revealed that the majority of the energy of the spectrum was at frequencies less than 2 HZ. In order to reduce the amount of computer core requirements and computer time, the 50 HZ digitized data were sampled at every 8th point. This process effectively sampled the original time

signal at 6.125 HZ, with a sampling interval of 0.16 seconds.

b. Resolution

The resolution bandwidth of the power spectra is related to the autocovariance lag time and sampling interval by:

$$\Delta f = \frac{1}{(NLAG) \Delta t}$$

where NLAG = maximum number of time lags

Δt = sampling interval

c. Degrees of Freedom

The number of degrees of freedom of the power spectra is defined as

$$n = \frac{2N}{NLAG} , N = \text{sample size}$$

Degrees of freedom are an indication of the normalized standard error in the variance

$$\text{error} = \sqrt{\frac{2}{N}}$$

IV. ANALYSIS OF DATA

A. RESOLUTION BANDWIDTH AND DEGREES OF FREEDOM

In computing each of the autocovariance functions, 256 time lags were taken, each lag increment being .16 seconds. Total lag time was therefore equal to $256 \times .16 = 81.96$ seconds. Therefore, the resolution bandwidth of each power spectrum was

$$f = \frac{1}{(\text{NLAG})(\Delta t)} = \frac{1}{(512)(.16)} = .0122 \text{ HZ}$$

The sample size of the time record for the majority of runs was 6656 points, $\Delta t = 0.16$ seconds. This represented approximately 17 minutes of record. The number of degrees of freedom of runs of this length was

$$n = \frac{2N}{\text{NLAG}} = \frac{2(6656)}{512} = 26$$

and the normalized standard error for the variance was

$$\frac{2}{N} = \sqrt{.077} = .278$$

Runs that were shorter than 6656 samples had correspondingly smaller degrees of freedom, and are so noted in the Summary of Runs, Table II.

B. OVERVIEW OF ANALYSIS RESULTS

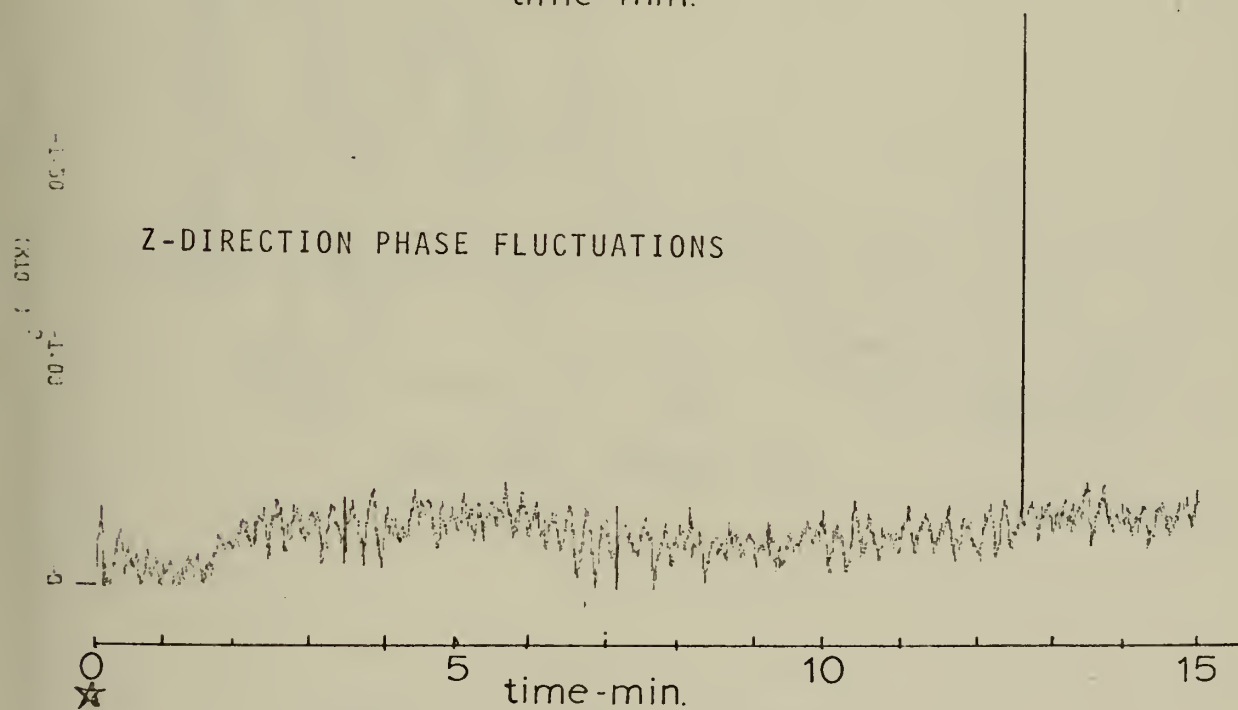
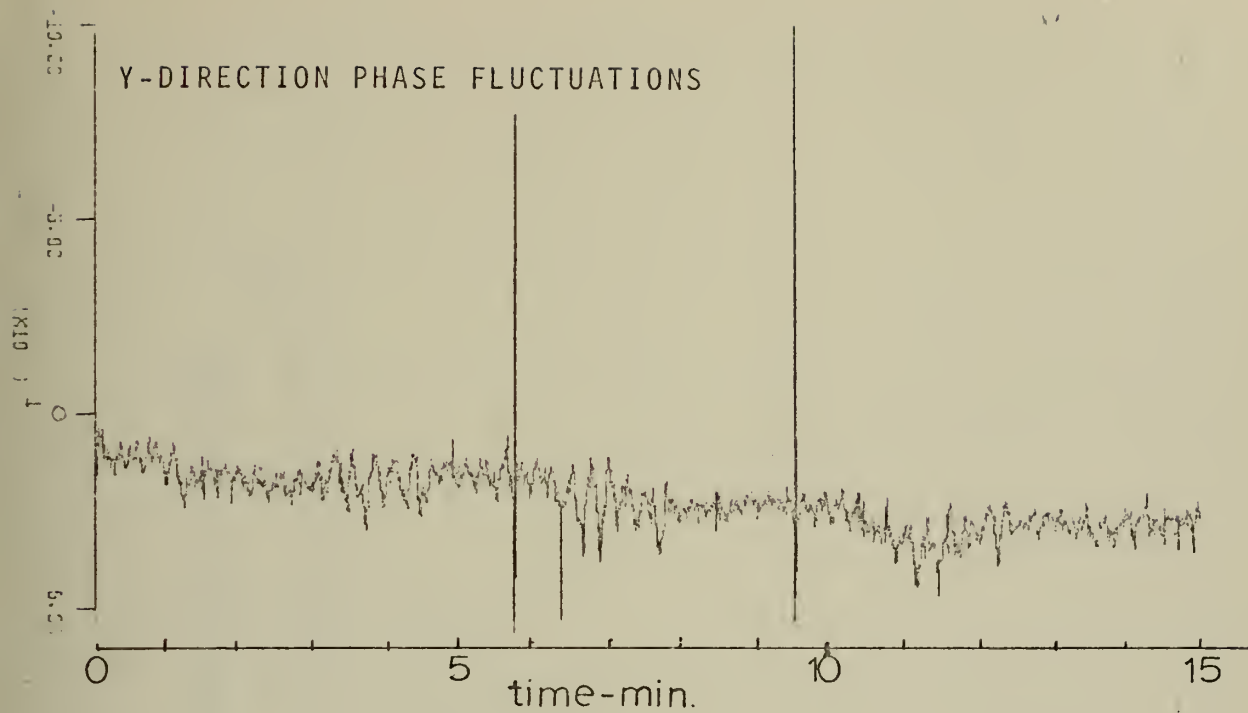
Six channels of data (X, Y, and Z phase fluctuations, and X, Y, and Z amplitude fluctuations) were recorded for

5 depths at frequency 65 kHz, and 4 depths at 105 kHz. For various reasons, the data of several of the channels were of poor quality or were non-existent when played back. These bad channels were due to the presence of high background noise, and equipment/operator malfunction. The interpretations set forth in the following sections are based on fluctuation records which were relatively free of noise, and, in the experimenter's best judgment, reflected the effect of the medium on the sound beam.

One can see from Table II that a large quantity of data were gathered during this experiment. Time limitations prevented examination of many of the different aspects and implications of this data. Some of the more obvious features of the data are discussed in the following sections. This coverage is by no means extensive, but it is adequate to point out that much information about the medium can be derived from a statistical study of sound amplitude and phase fluctuations.

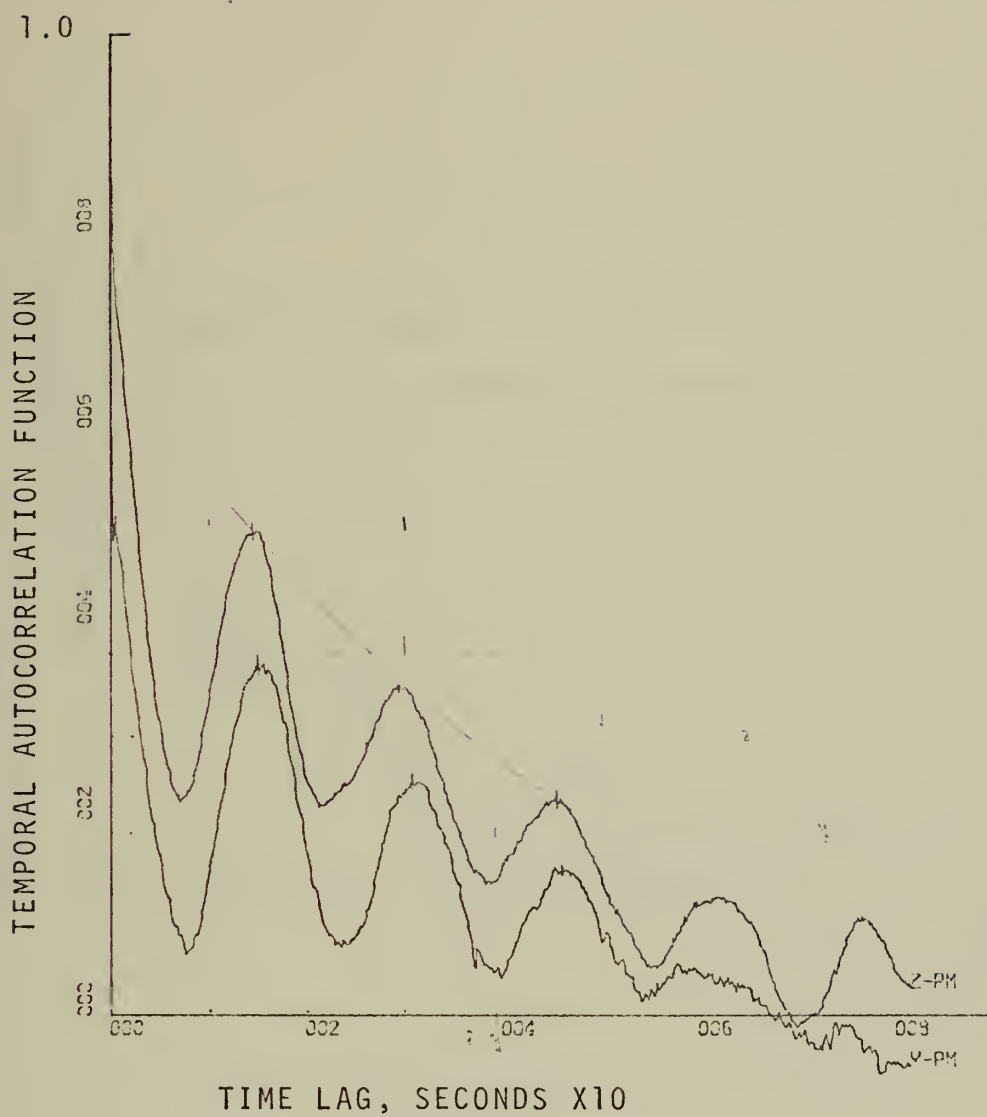
C. INITIAL OBSERVATIONS AND INTERPRETATION OF SPECTRAL ANALYSIS

The time records and the results of analysis of a typical pair of phase fluctuation channels are presented as figures 10 - 14. The two channels analyzed are the phase fluctuations in the Y and Z direction of run PH-4 at a depth of 18.8 feet, with a transmission frequency of 65 kHz.



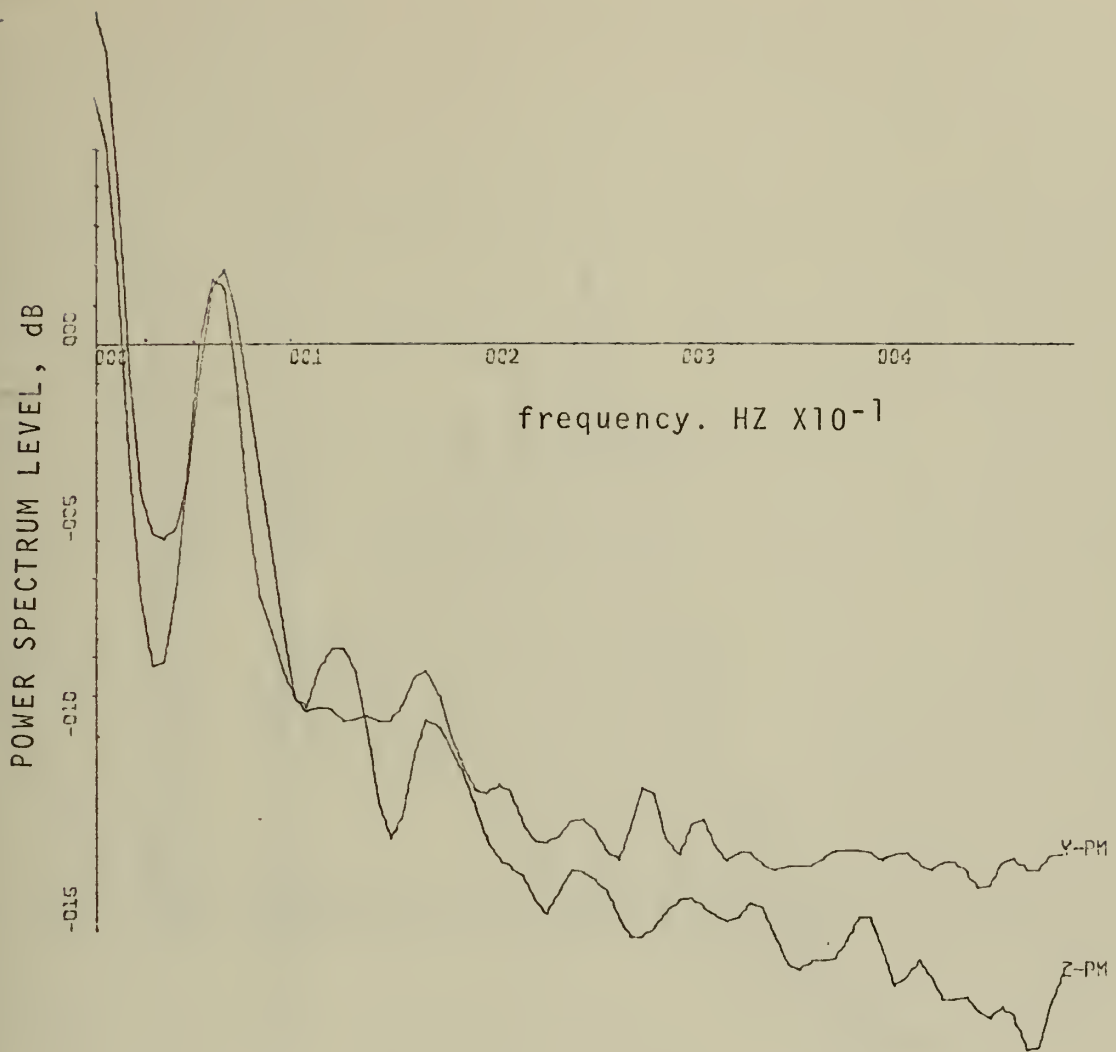
RUN PH-4, FREQ.=65KHZ, Y-AXIS DEPTH=18.8 ft.

FIGURE 10



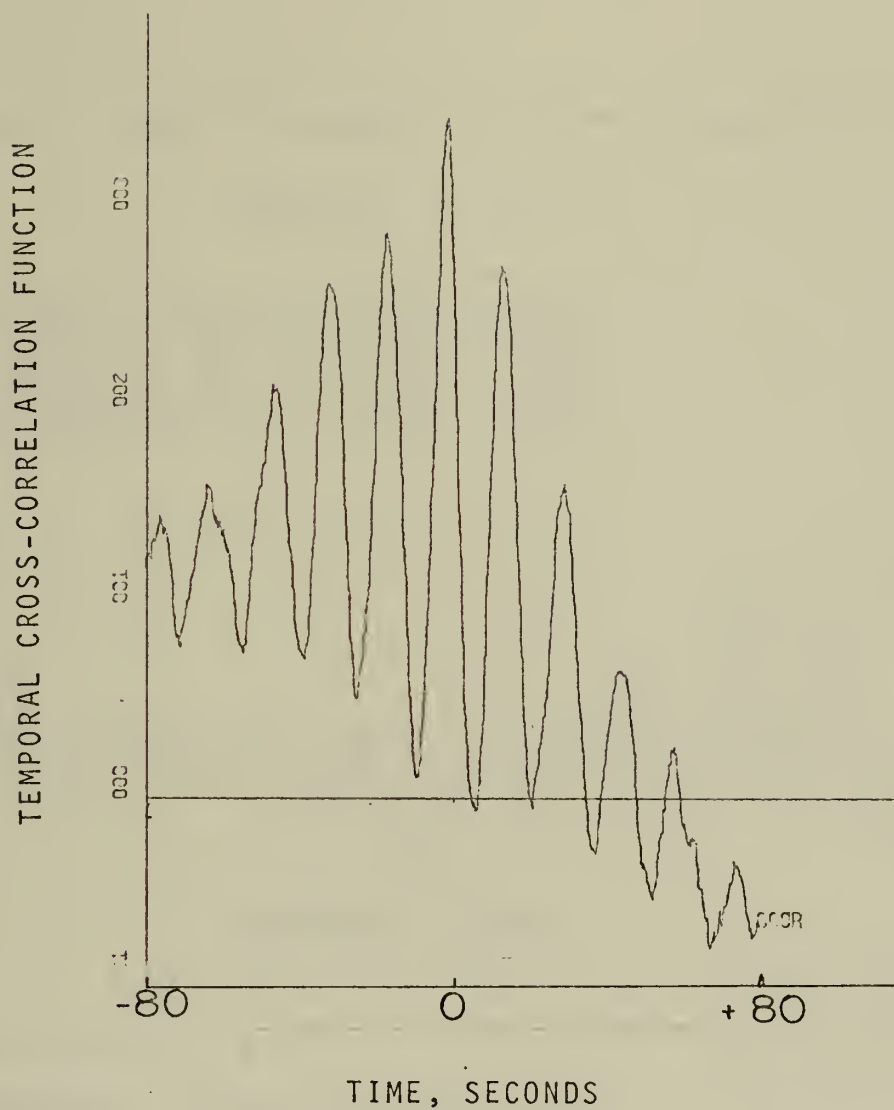
RUN PH-4, Y-PHASE, Z-PHASE
 FREQ.=65KHZ, Y-AXIS DEPTH=18.8 ft.

FIGURE 11



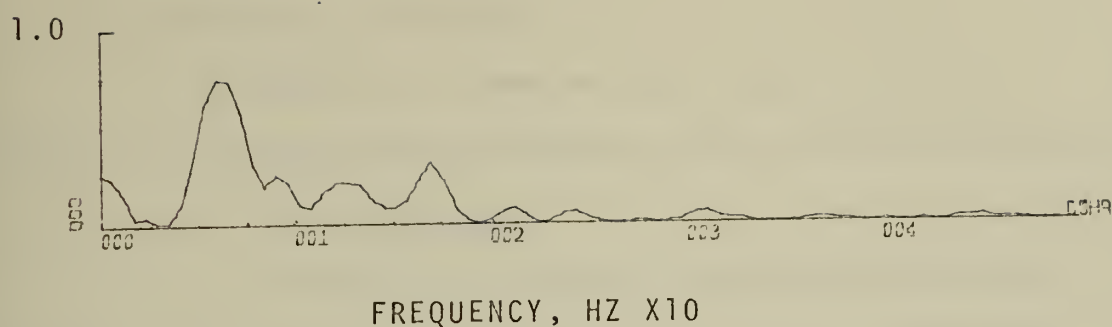
RUN PH-4, Y-PHASE, Z-PHASE
FREQ.=65 KHZ, Y-AXIS DEPTH = 18.8 ft.

FIGURE 12

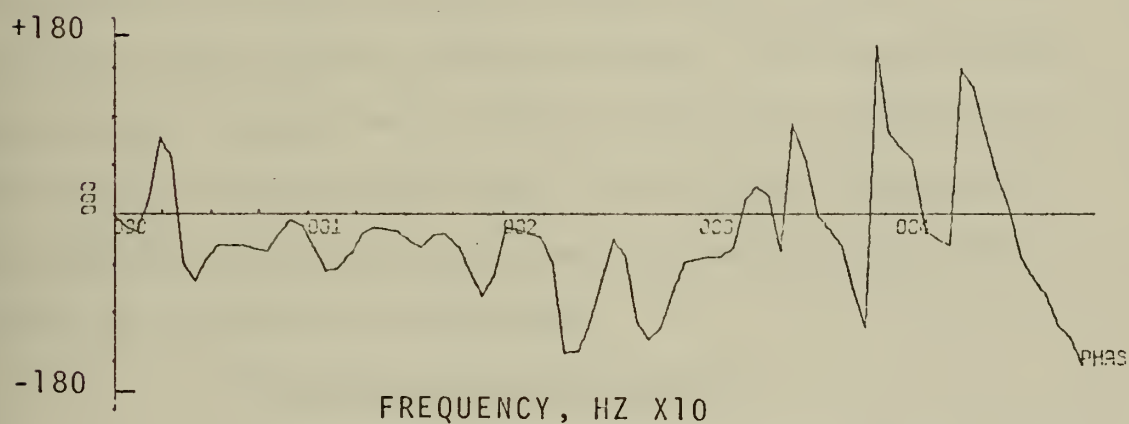


RUN PH-4, Y-PHASE, Z-PHASE
FREQ.=65KHZ, Y-AXIS DEPTH=18.8 ft.

FIGURE 13



X-SCALE=1.00E-01 UNITS INCH.
 Y-SCALE=1.00E+00 UNITS INCH.
 COHERENCE FUNCTION



X-SCALE=1.00E-01 UNITS INCH.
 Y-SCALE=2.00E+02 UNITS INCH.
 CROSS SPECTRAL PHASE ANGLE,

RUN PH-4 Y-PHASE, Z-PHASE
 Y-AXIS DEPTH=18.8 ft, FREQ.=65KHZ

FIGURE 14

1. Autocorrelation Function

a. Frequency Content

In Figure 11, observe that there are three predominant periodicities in these autocorrelation functions.

(1) Low Frequency

A very low frequency periodicity can be observed: only about one quarter of a cycle is included in the 81 second lag time. The period of this long term fluctuation which is approximately 6 minutes is substantiated by Figure 13. It is believed that this long term fluctuation is the response of the sound phase to temperature changes due to internal waves. One can also observe this internal wave effect in the time records. As the medium's mean temperature fluctuates in response to the passage of an internal wave, the sound speed, and hence the phase also fluctuates.

(2) Surface Wave Frequency

The most obvious periodicity of the autocorrelation function is the one which recurs approximately every 16 seconds. This 16 second periodicity appears in both autocorrelation functions of Figure 11, indeed, it appears in all autocorrelation functions of this experiment. As stated before, the observed periods of the surface swell waves was also about 16 seconds. It is believed that orbital motion of the medium, in direct response to the surface wave action, caused temperature and salinity inhomogeneities and bubble patches to pass into and out

of the sound field in a periodic manner. This movement causes the phase and amplitude of the sound beam to fluctuate, as explained in Section I.B.

(3) High Frequencies

There is an unsteady, low level 2 to 8 HZ fluctuation superimposed on the autocorrelation function. This may be the result of fine structure of the medium inhomogeneities or partly due to random motion of the medium, or system noise.

b. Initial Drop in Autocorrelation Function

There is a sharp drop in the autocorrelation function at the first or second time lag. This initial drop is due to the presence of intermittent noise spikes in the corresponding time records which are spaced more than 81 seconds apart (the maximum time lag of the correlation products). At the $\tau = 0$ value of the autocorrelation function all spikes in the time record are multiplied by themselves and added to the autocorrelation sum. For any other time lag, the spikes will not "line up" again, and the effect of the spikes will be distributed over the entire autocorrelation function.

2. Power Spectrum Levels

Figure 12 shows the power spectrum levels which were obtained by Fourier transforming the autocovariance function, and then applying the operation of 10Log_{10} to the transform. The 6 minute period (.003 HZ) component is less than our resolution (.01 HZ). Its effect appears

but is unresolvable in the frequency range 0 - 0.015 HZ. The strong frequency component due to surface swell is observed at approximately .065 HZ in the spectra for both the Y and Z directions. Components at higher frequencies are at least 10 dB down from the spectrum level of the $f = .065$ HZ component, and probably represent the effect of other sea surface components, and noise of the system.

3. Cross Correlation Function

The cross-correlation function shows a strong cross-correlation between the two signals at about 16 second intervals. The envelope of the 16 second periodicities suggests that a 6 minute cross-correlation periodicity also exists. However, this cannot be verified due to the relatively short lag time.

4. Coherence

If the Y direction phase fluctuation and the Z direction fluctuations were completely unrelated, the coherence function would be equal to zero. If the coherence function equals 1, the two channels are completely correlated and are linearly related. In general, if the coherence function is greater than zero but less than unity, one or more of the following three situations exists:

a. Extraneous noise is present in the measurements of either or both channels.

b. The relationship between the Z phase fluctuation and the Y phase fluctuation is not linear.

c. There are inhomogeneities or bubble patches affecting one channel which do not effect the other channel; that is, the propogation is not isotropic.

The coherence function shown in Figure 14 ranges from 0 to 0.75; no coherence function computed in this experiment exceeded 0.8. Of the three situations listed above, situation C is the one most likely to have caused the coherence to be less than unity.

As might be expected from observing the similarities of the autocorrelation functions, the coherence function has a relative maximum value at frequencies of approximately .005, .065, .085, .125, and .170 HZ, the strongest maximum being at .065 HZ. These frequencies correspond to frequencies which are common to the two channels, the .065 HZ frequency being the strongest common frequency.

5. Cross-Spectral Phase Angle

The cross-spectral phase angle function has significance only at frequencies for which the coherence is greater than zero. For example, at .065 HZ, where the coherence equals .75, the phase angle equals -30° . This measurement can be explained in the following way: Observe the alignment of the 16 second peaks of the two autocorrelation functions, Figure 11. Careful measurement of the time lag value associated with corresponding peaks shows that the Z peak always precedes the Y peak by 1 to 1.5 seconds. In other words, the correlation peaks of the

Z phase fluctuation channel leads the correlation peaks of the Y fluctuation channel by 1 to 1.5 seconds. Essentially the same changes of medium took place in the Y and Z directions but they are happening 1 to 1.5 seconds sooner in the Z direction. The frequency of this fluctuation is about .065 HZ; at this frequency, 1.5 seconds corresponds to approximately 30° . Therefore the cross-spectral phase angle is a measure of the phase difference between the two channels in question, at a particular fluctuation frequency.

The fact that there is a phase difference in the occurrence of the phase fluctuation of the sound beam in the Y and Z directions as shown by the cross-spectral phase angle, or by direct measurement of the time lag between peaks of the autocorrelation functions, indicates that moving inhomogeneities are causing the 16 second period fluctuations. It is suggested that it takes a particular patch of water on the order of 1 or 1.5 seconds to move from the axis of the Y direction sound field into the axis of the Z direction sound field, a distance of approximately one meter; this implies a speed of approximately 65 to 100 centimeters per second. Fringe field interaction would occur at about one-half meter at half this speed. From the swell wave point of view, if the motion were solely orbital at frequency 0.065 HZ and amplitude of about 50 cm. (this was the amplitude of the observed

swell), the orbital velocity would be approximately 25 cm/second. The moving patch explanation appears to be quite reasonable.

It was found that a phase difference in the occurrence of the 16 second sound phase fluctuation between the Y and Z directions was common. Table III shows the cross-spectral phase angle of the fluctuations for several runs. There is consistency in the magnitude of the angle but not in the sign. This can be explained by the randomness of whether, for example, a hot patch starts from the Y axis field or the Z axis field position at the beginning of the run; this position is of course random, so that the sign of the phase would be random.

D. CORRELATION TIME AS A FUNCTION OF THE SOUND FIELD'S RELATION TO THE THERMOCLINE

For the purpose of this work, correlation time is defined as that time required for the envelope of the autocorrelation function to decay to $1/e$ of its initial value. In cases where there is an initial drop D at the first lag value, $t = .16$ seconds, the correlation time is taken to be that time required for the envelope of the autocorrelation function to decay to $(1-D)/e$. (See Section IV.C.1.b. for the explanation of the cause of steep initial drops in the autocorrelation function.)

It is assumed that the speed of sound in the upper ocean is primarily a function of temperature and bubbles

TABLE III

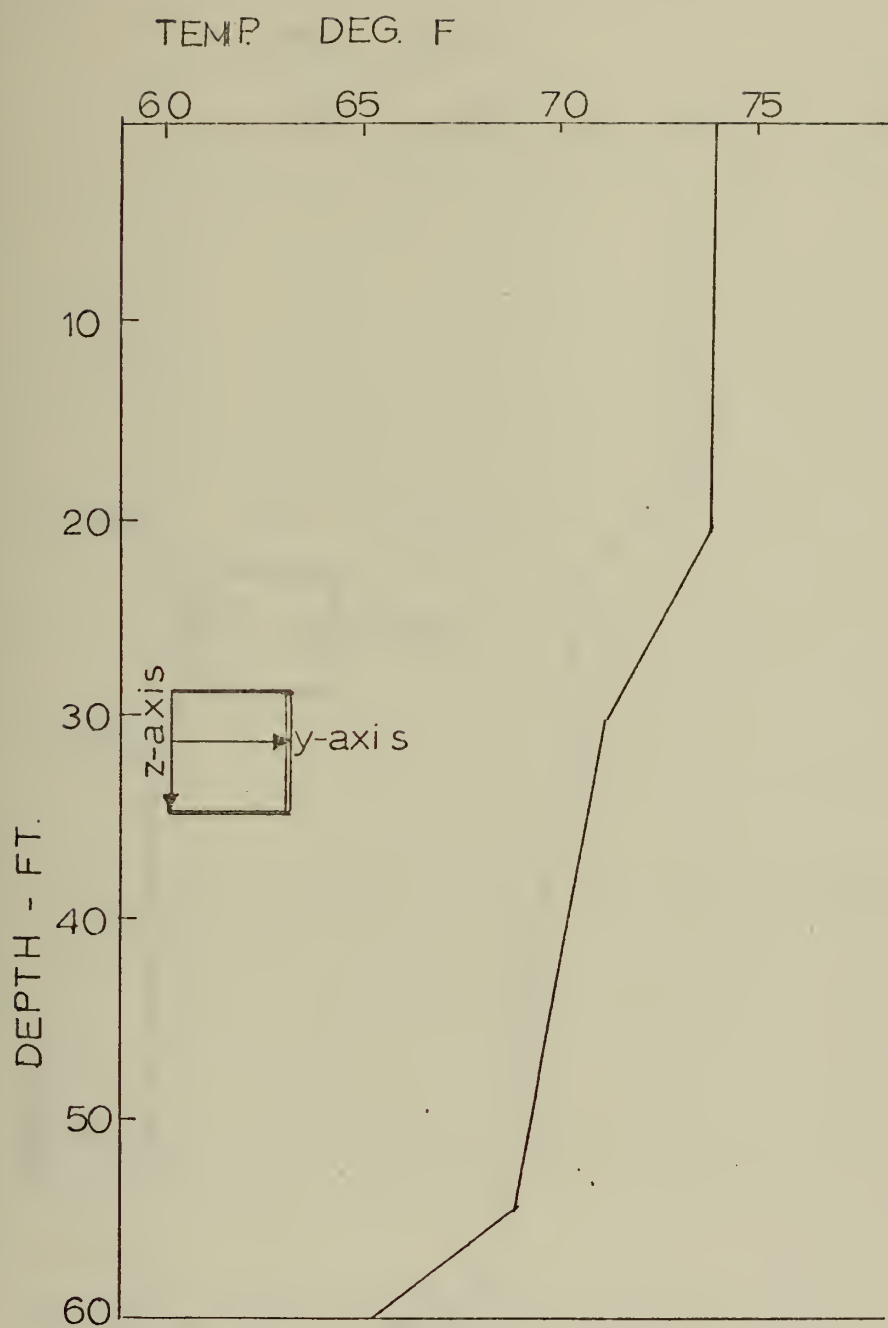
Cross Spectral Phase Angle of Y and Z direction Phase
Fluctuations at Fluctuation Frequency 0.06 HZ

RUN	DEPTH	FREQ	COH	CROSS-SPECTRAL
	FT.	KHZ		PHASE ANGLE
PH-6	11.3	105	.75	+30°
PH-4	18.8	65	.70	-35°
PH-3	25	65	.70	-25°
PH-8	26.8	105	.55	-30°
PH-2	31	65	.25	+25°

(Rautmann 1971). The periodic recurrence of a particular integrated speed of sound along a sound axis implies a stable (not changing with time) temperature microstructure. The correlation time of sound phase fluctuations is an indication of the periodic recurrence of the integrated speed of sound of the medium along the sound axis. A long correlation time indicates stability in the temperature structure of the medium in the vicinity of the sound field. In other words, a volume of water having a slowly changing (stable) temperature microstructure was moving through the sound field with periodic motion in response to surface wave action (orbital motion). Short correlation time indicates instability in the temperature microstructure; that is, the volume of water moving through the sound field periodically in response to surface wave action has a more rapidly changing temperature microstructure, resulting in a less periodic recurrence of an integrated speed of sound along the sound axis.

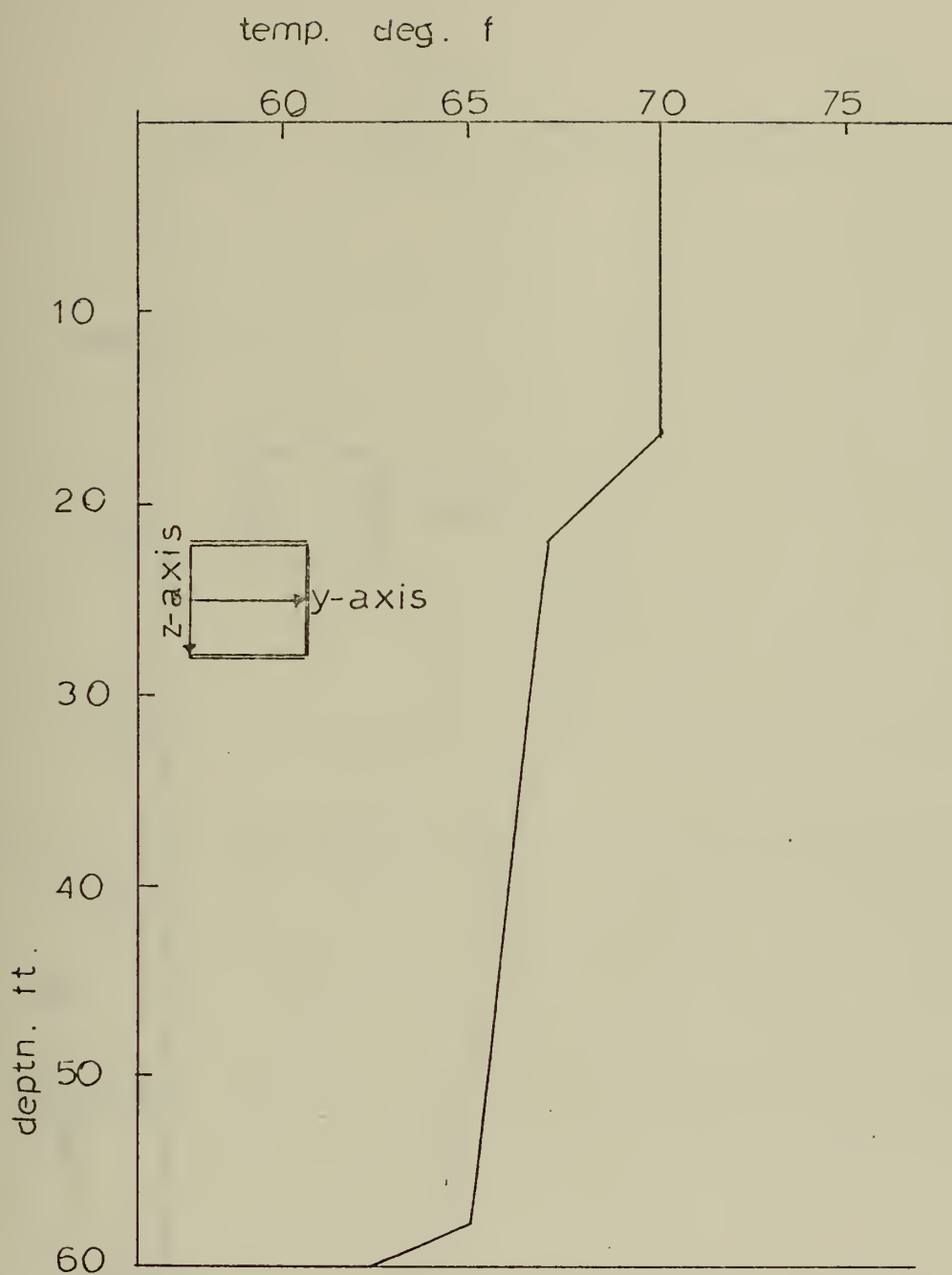
The behavior of the correlation times of phase fluctuations in the Y and Z directions have been examined. It is shown that the correlation times of the phase fluctuations in the Y and Z directions were greater (greater stability of the medium) when the sound field was in the thermocline, than when it was in the well mixed layer.

Figures 15 to 18 are diagrams of the temperature structure of the ocean in the vicinity of the tower during



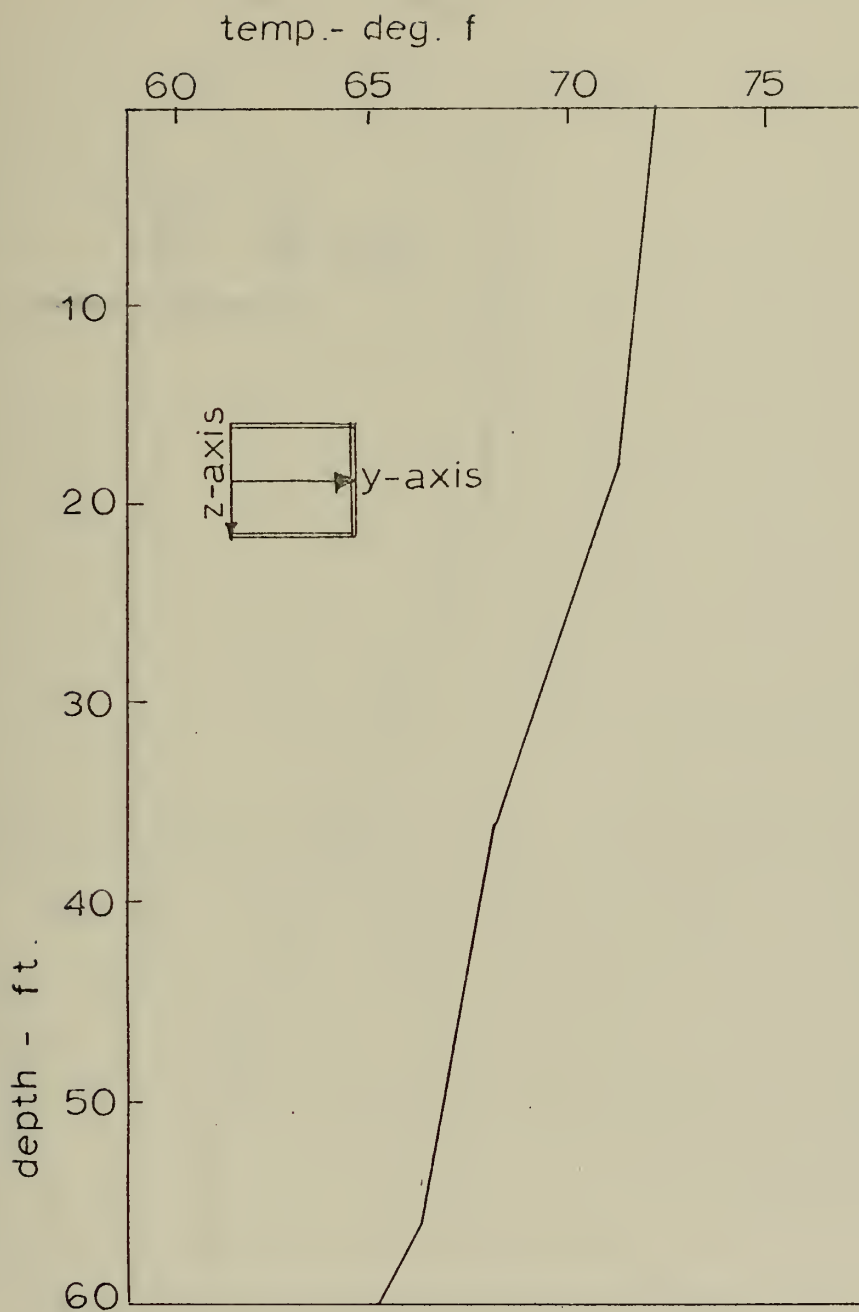
TEMPERATURE STRUCTURE, RUN PH-2
65 KHZ, Y-AXIS = 31 ft., TIME = 1655

FIGURE 15



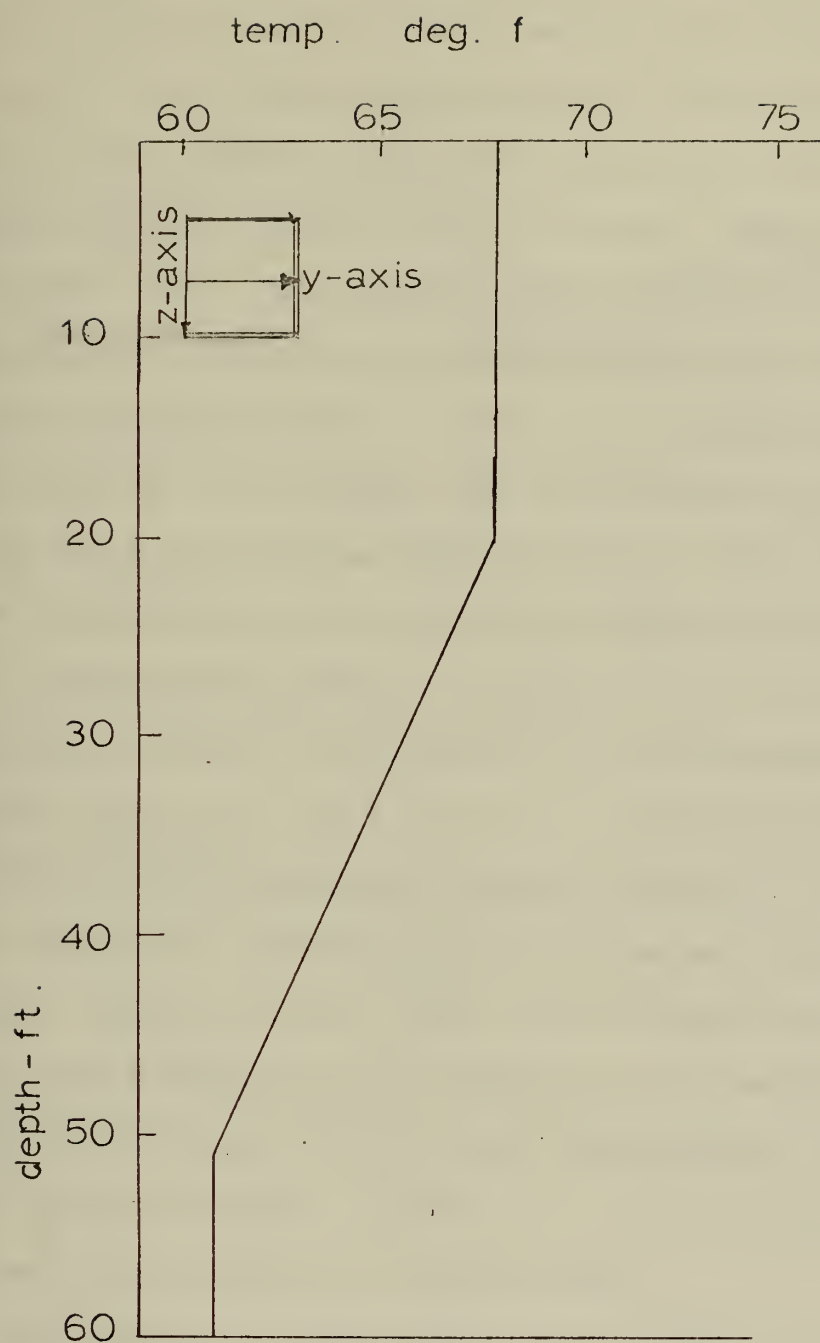
TEMPERATURE STRUCTURE, RUN PH-3
65 KHZ, Y-AXIS DEPTH = 25 ft., TIME=1756

FIGURE 16



TEMPERATURE STRUCTURE, RUN PH-4
65 KHZ, Y-AXIS DEPTH = 18.8 ft., TIME = 1830

FIGURE 17



TEMPERATURE STRUCTURE, RUN PH-5

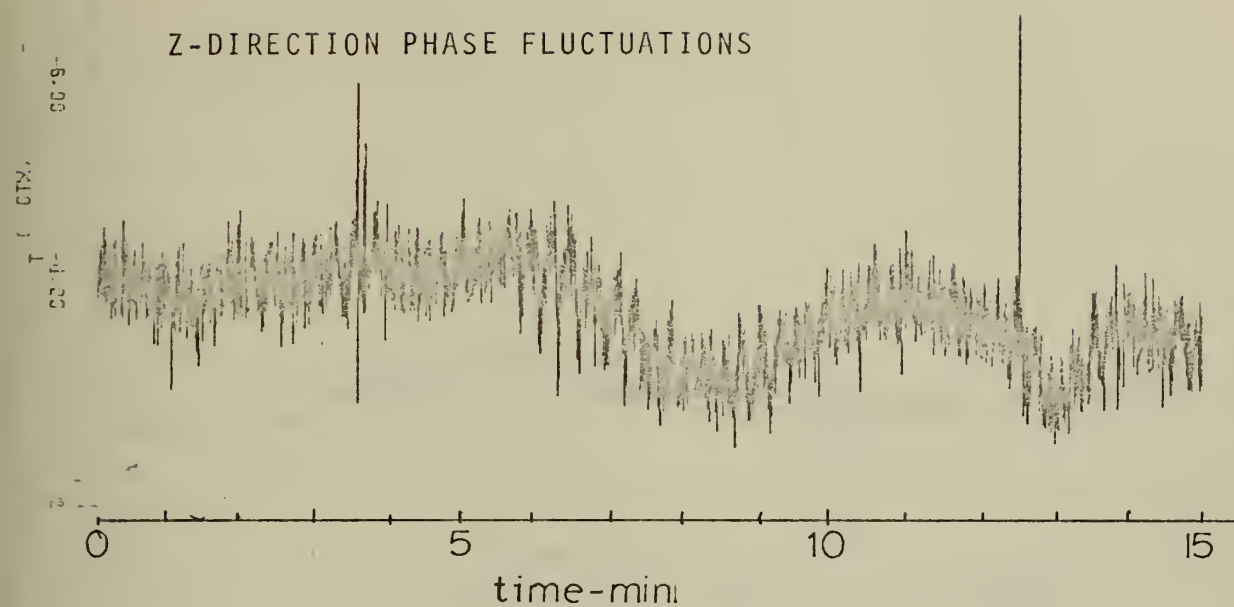
65 KHZ, Y-AXIS DEPTH=7 ft, TIME=1935

FIGURE 18

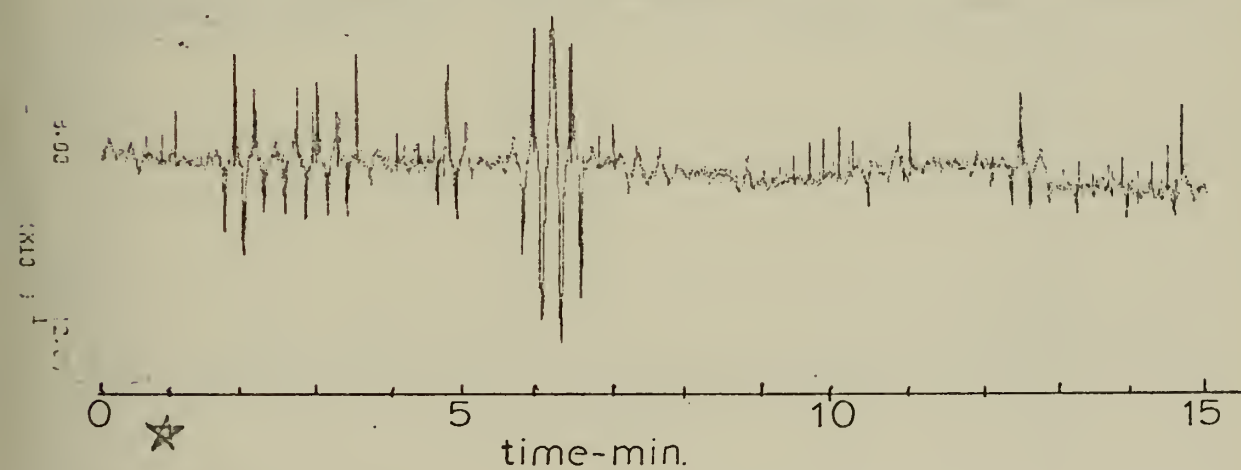
runs PH-2 (31 ft, 65 kHz), PH-3 (25 ft, 65 kHz), PH-4 (18.8 ft, 65 kHz), and PH-5 (7 ft, 65 kHz). The position of the Y and Z axes for each run is also indicated on the figures. This temperature structure varied during each run, as the thermocline moved up and down with the medium with a periodicity of 6 to 10 minutes. The temperature structure shown is probably fairly representative of the temperature that prevailed during the entire run, but is truly representative of the actual temperature structure only at the precise time at which it was taken. Since the run durations were 1 1/2 to 3 times the internal wave periodicity, data processing gives average results over the changing medium. Figures 19, 20, 21, and 22, are the 17 minute time records of the channels of interest of runs PH-2, 3, 4, and 5. A star on each time record marks the time the BT was taken. During run PH-5 (7 ft, 65 kHz), the Z axis was located well within the well mixed isothermal layer. During run PH-4 (18.8 ft, 65 kHz) and Y and Z axes were located in the vicinity of the boundary between the surface layer and the first thermocline. During run PH-3 (25 ft, 65 kHz), and PH-2 (31 ft, 65 kHz) the Y and Z axes were located in a thermocline.

The autocorrelation function of these runs are shown in Figures 23, 24, 25, and 26. The corrected correlation times are plotted as a function of depth, and as a function

Z-DIRECTION PHASE FLUCTUATIONS

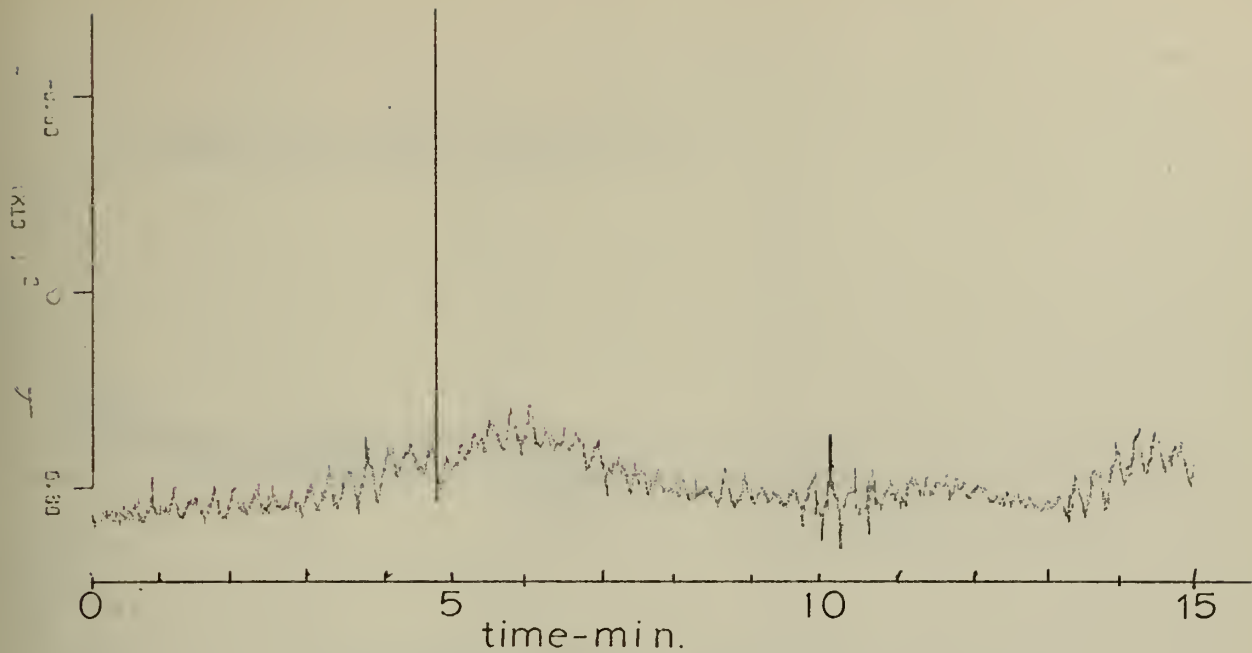


Y-DIRECTION PHASE FLUCTUATIONS

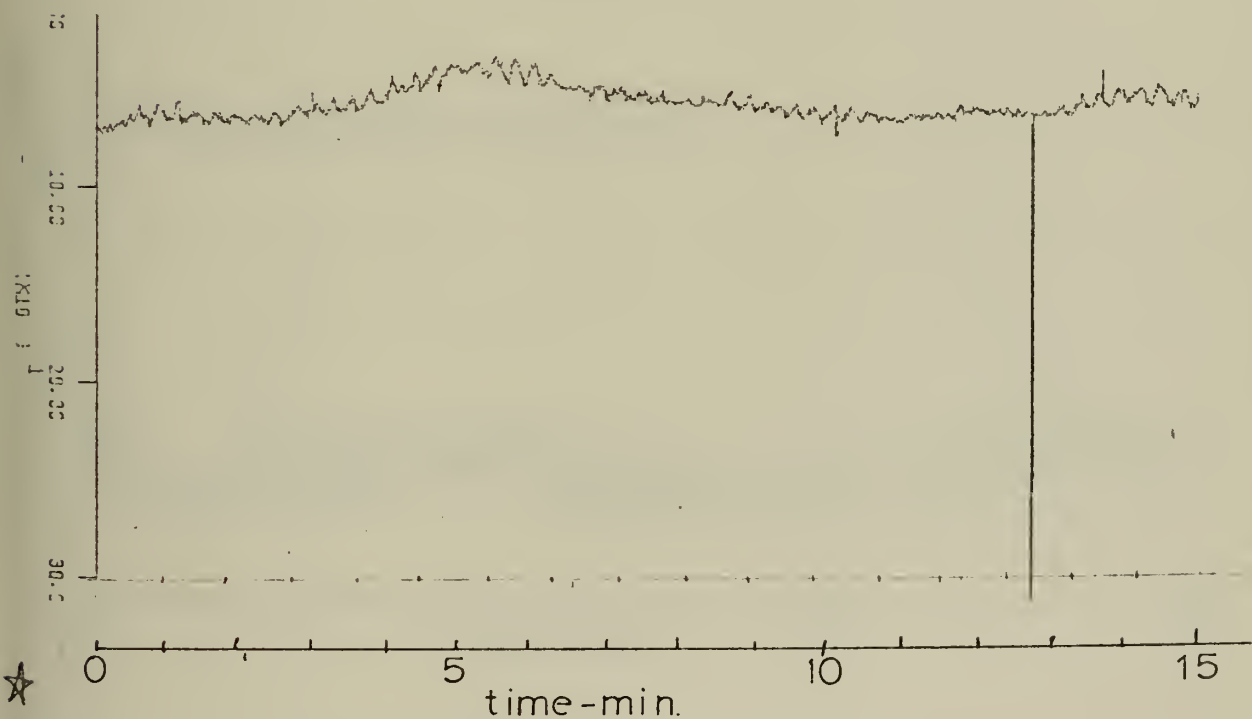


RUN PH-2, FREQ.=65KHZ, Y-AXIS DEPTH=31 ft.

FIGURE 19

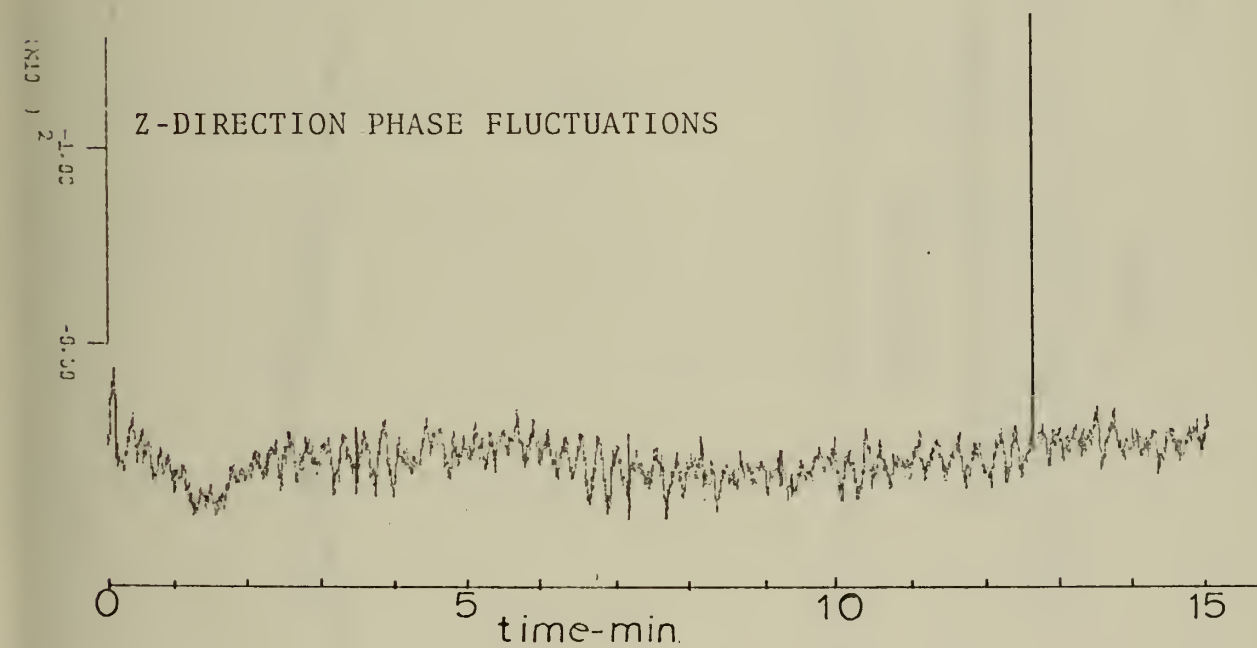
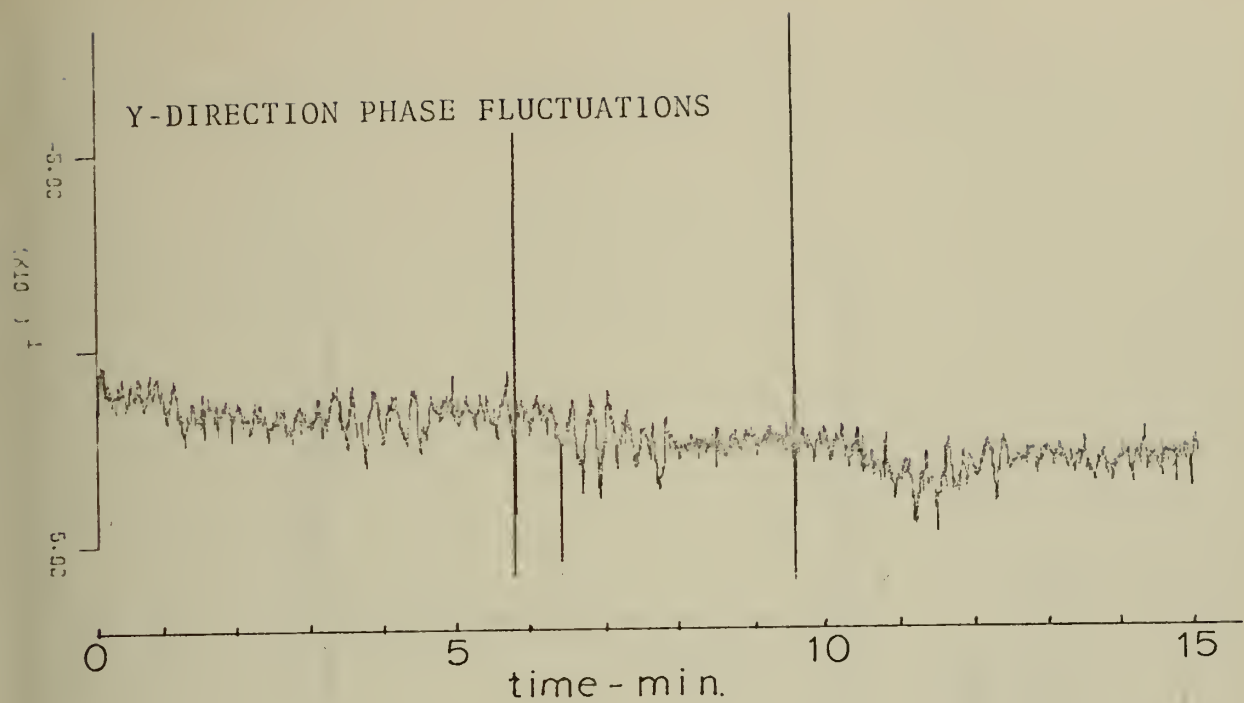


Y-DIR. PHASE FLUC; RUN PH-3, 25ft, 65kHz



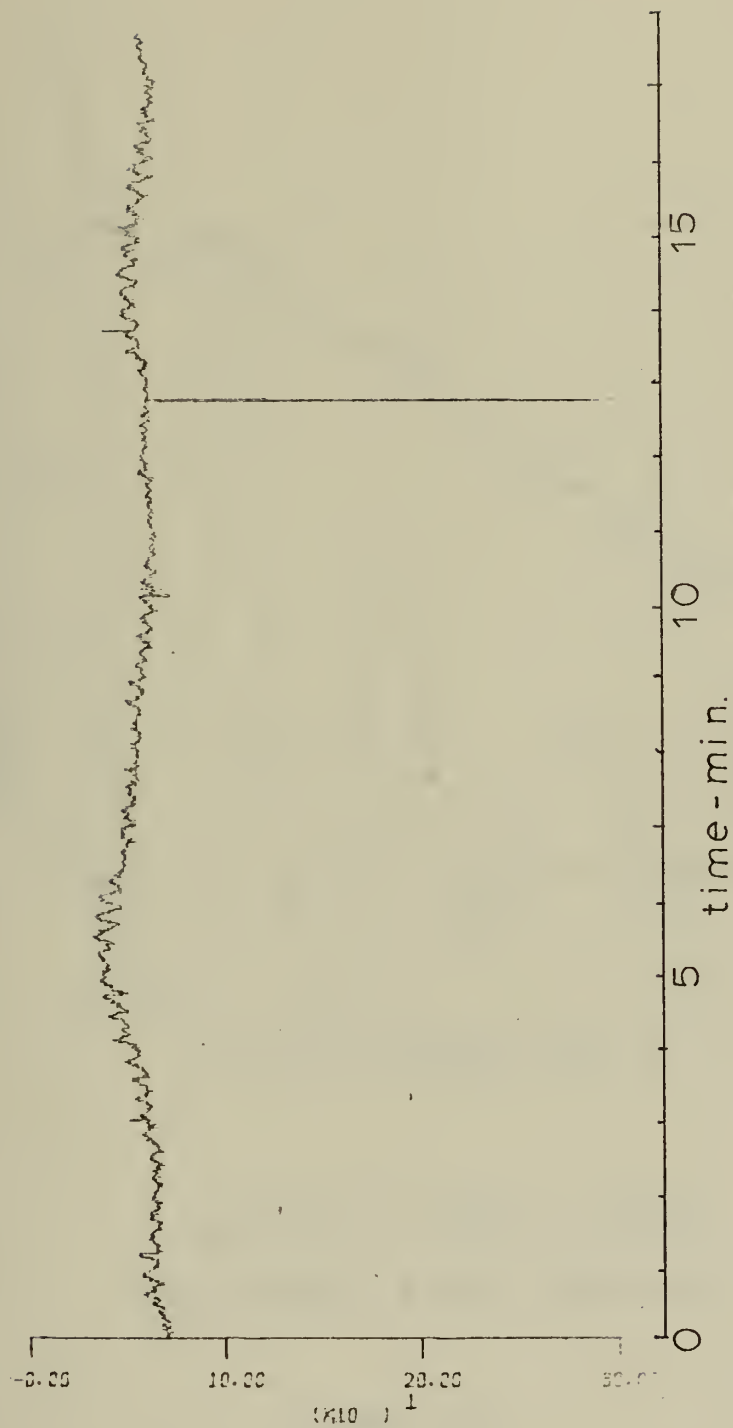
Z-DIR. PHASE FLUC; RUN PH-3, 25ft, 65kHz,

FIGURE 20



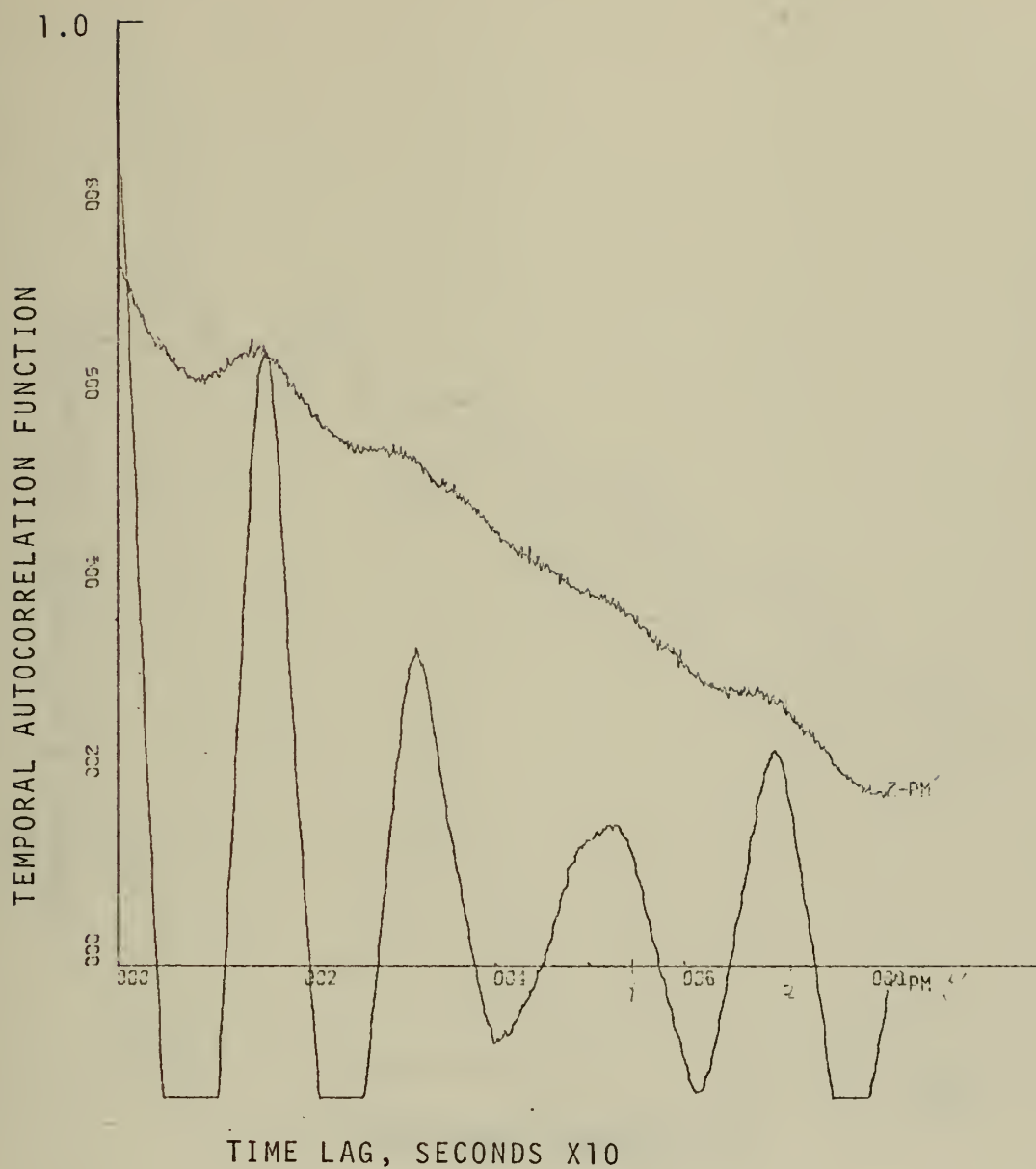
RUN PH-4, FREQ.=65KHZ, Y-AXIS DEPTH=18.8 ft.

FIGURE 21



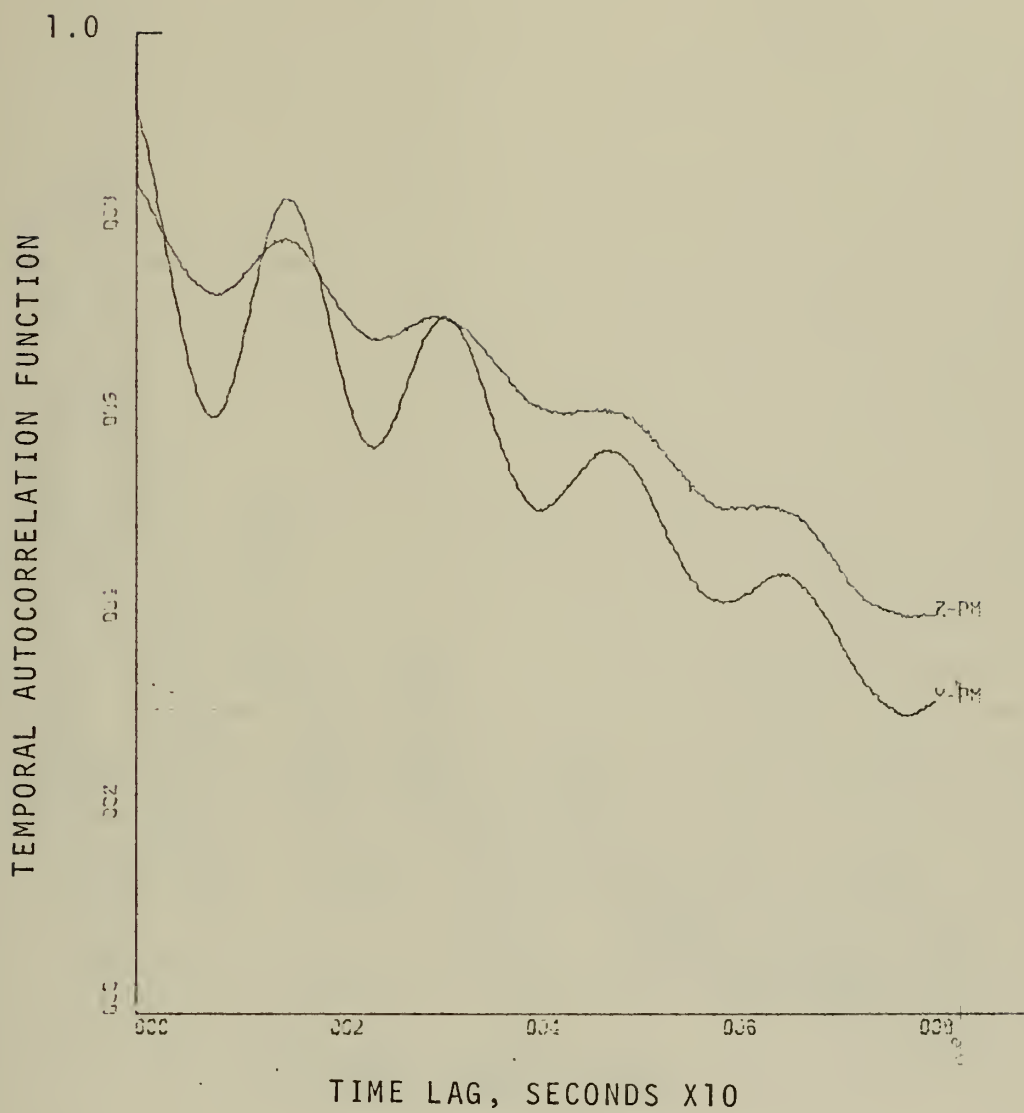
Z-DIRECTION PHASE FLUCTUATIONS
 RUN PH-5, FREQ.=65kHz, Y-AXIS DEPTH=7 ft.

FIGURE 22



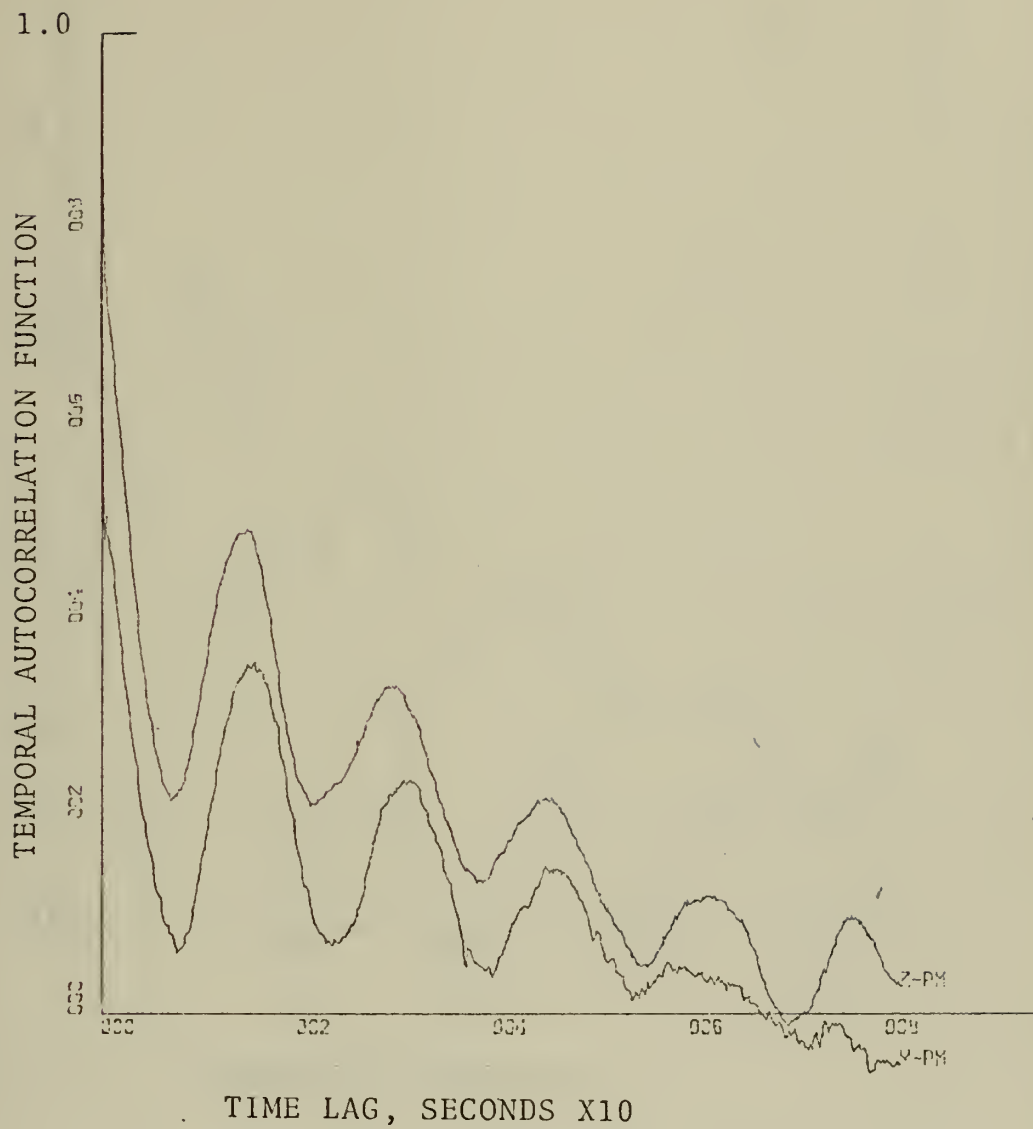
RUN PH-2, Y-PHASE, Z-PHASE
 FREQ.=65KHZ, Y-AXIS DEPTH=31ft.

FIGURE 23



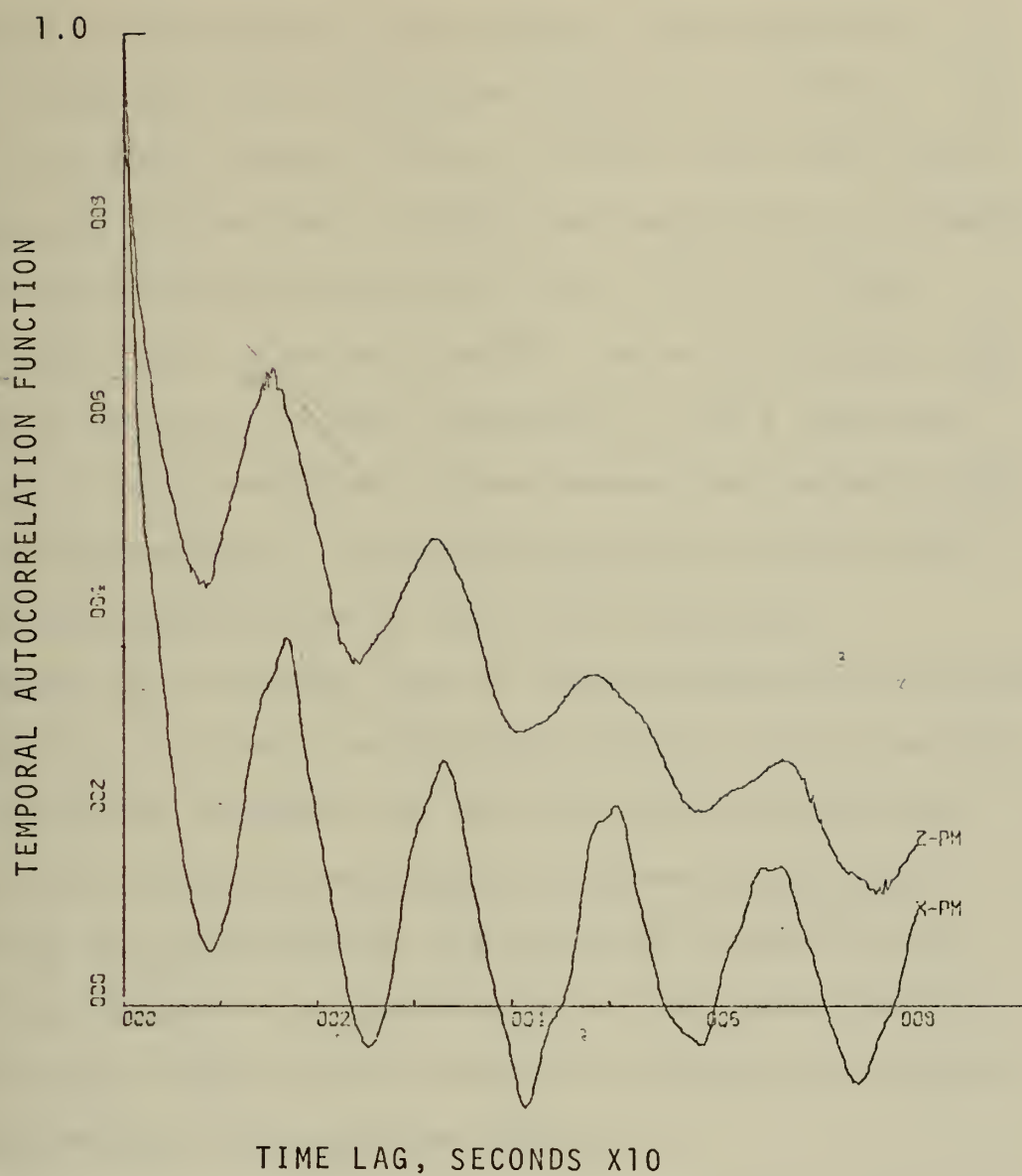
RUN PH-3, Y-PHASE, Z-PHASE
 FREQ.=65KHZ, Y-AXIS DEPTH=25 ft.

FIGURE 24



RUN PH-4, Y-PHASE, Z-PHASE
FREQ.=65KHZ, Y-AXIS DEPTH=18.8 ft.

FIGURE 25



RUN PH-5, X-PHASE, Z-PHASE
FREQ.=65kHz, Y-AXIS DEPTH=7 ft.

FIGURE 26

of the distance from the Y axis sound field to the lower boundary of the surface mixed layer. (See Figure 27) It can be seen that the correlation times of runs PH-2 (31 ft, 65 kHz) and PH-3 (25 ft, 65 kHz) where the Y and Z axes were located well within the thermocline, is greater than the correlation time of run PH-5 (7 ft, 65 kHz), where the Y and Z axes were within the surface layer, and run PH-4 (18.8 ft, 65 kHz), where the Y and Z axes were located in the transition region between the surface layer and the thermocline. It is believed that this behavior of the correlation time is due to the following.

Measuring the decay time of the autocorrelation function envelope to $(1-D)/e$, vice the decay time of the 16 second periodicities, measures the de-correlation of the long-term (6 to 10 minute periodicities) phase fluctuation. The long term fluctuations are believed to result from long term temperature fluctuations of the medium of the sound field, which reflect the medium movement in response to the passage of an internal wave.

In the surface mixed layer, the temperature, salinity and bubble microstructure is random; Skudrzyk (1963) describes this random distribution as "temperature patches" of varying sizes. On the other hand, since the work of Woods (1968), a picture of the more stable thermocline has evolved. The thermocline is said to consist of alternate sheets of high temperature gradients (order of cm. thick) and plates of low temperature gradient water

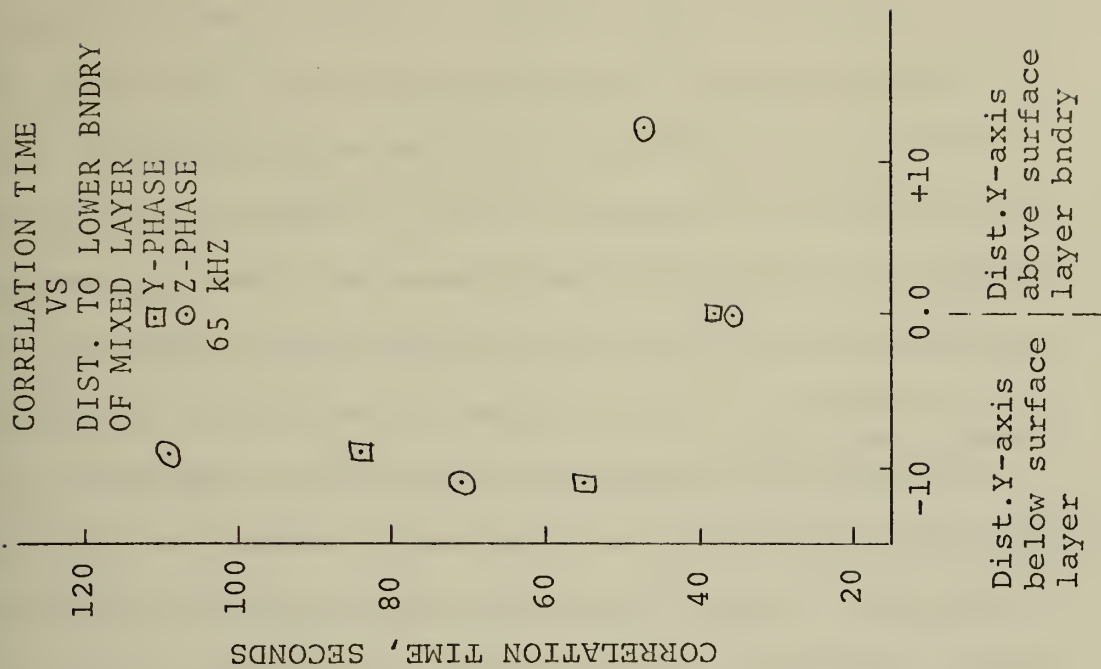
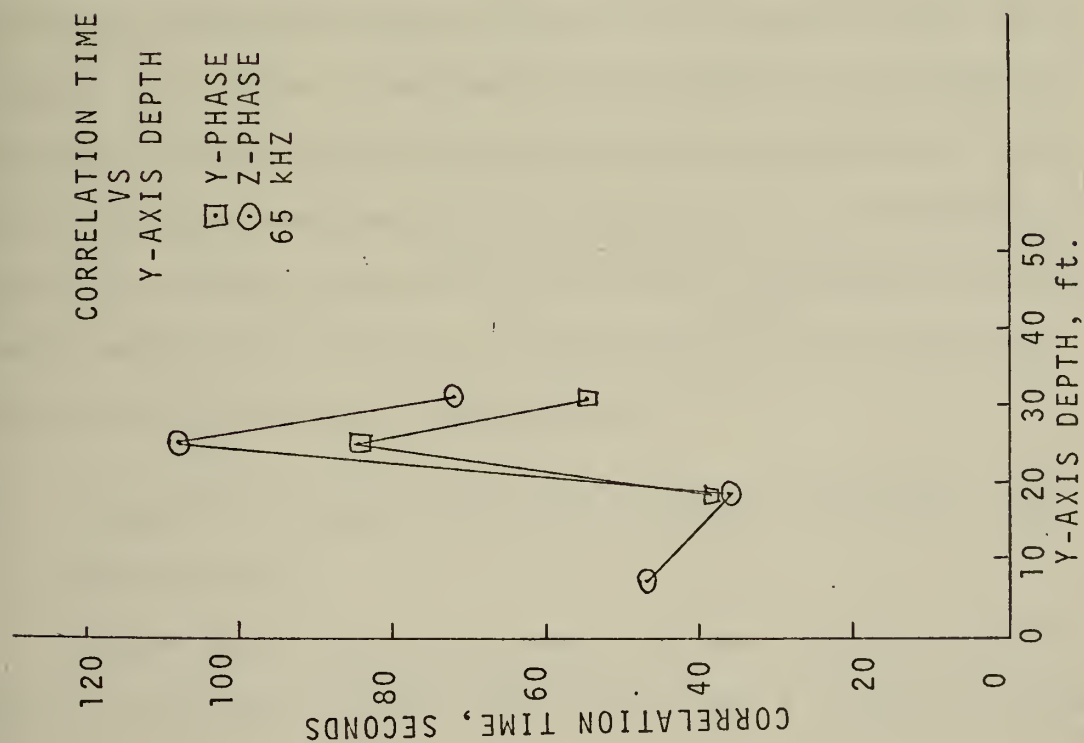


FIGURE 27

(order of a meter thick), both parallel to the sea surface. If a volume of this well structured thermocline water is moved vertically into and out of a sound field with an approximate periodicity, as in response to the passage of an internal wave, the sound speed fluctuation, and therefore the phase fluctuations should reflect the periodic recurrence of particular temperatures. In contrast to this, consider the surface layer where the temperature structure is random. There will be only random recurrence of particular temperature structures for the same long term medium movements since the motion of the well mixed layer has a superimposed random horizontal and vertical motion of the inhomogeneities. Hence, the long term (envelope) fluctuations of the autocorrelation function will decorrelate faster (will have a shorter correlation time) in the surface layer than in the thermocline. This behavior is in fact observed in the shorter correlation time of runs PH-5 which was located in the surface layer, and PH-4 which was located in the transition region between the surface layer and the first thermocline, and the longer correlation times of runs PH-3 and PH-2, both of which are located in a thermocline.

E. Z DIRECTION CORRELATION TIME VERSUS Y DIRECTION CORRELATION TIME

In runs PH-2 (31 ft, 65 kHz) and PH-3 (25 ft, 65 kHz) which took place in the thermocline, the Z direction phase

fluctuations have a longer correlation time than the Y direction phase fluctuation; while in run PH-4 (18.8 ft, 65 kHz) which took place in the mixed layer, the Y and Z direction phase fluctuations have approximately equal correlation times. This may well be due to the presence of stable layered patches of isothermal water in the thermocline, and isotropically random patches of isothermal water in the mixed layer. As stated in Section IV.D, by defining the correlation time to be the time associated with the envelope decay, a correlation time is a measure of the stability of the medium over long term changes; in this case changes resulting from internal waves. Long term periodicities of a phase fluctuation depend on a particular value of integrated sound speed recurring in the sound field at regular (long term) intervals. As previously mentioned, there is evidence that there are regions of thermocline "sheets" and "plates" parallel to the surface of isothermal water in the thermocline.

If the medium undergoes vertical movement, the extent of the periodicity of long term phase fluctuations in the Y direction will depend on a recurring isothermal plate at the Y axis, since the Y axis sound beam travels horizontally through the isothermal plate. In contrast, the Z axis sound beam travels vertically through horizontal plates of isothermal water. The integrated sound speed over the path is the average temperature of the horizontal plates. Long term periodicities of the phase fluctuation

in the Z direction depend on the recurrence of an average sound speed over one or more isothermal plates; such a periodicity in the Y direction depends on the recurrence of a particular isothermal plate.

Therefore, in a thermocline, where a fairly stable gradient prevails, long term phase fluctuations are more stable in the Z direction than in the Y direction because the orbital movement of the medium is less likely to cause deviations from a recurring average sound speed in the Z direction than in the Y direction.

Note that for run PH-4 (18 ft, 65 kHz) which was in the transition region between the thermocline and the mixed layer, the Y and Z correlation times are nearly equal. The mixed layer is composed of randomly distributed patches. It is therefore equally likely to have an integrated sound speed repeated in the Y direction as in the Z direction.

Thus, for the cases examined, sound phase correlation times are not isotropic in the thermocline, but are nearly isotropic in the mixed layer.

F. Y DIRECTION VARIANCE VERSUS Z DIRECTION VARIANCE

Figure 28 is a graph of the variance of Y and Z direction phase fluctuations for runs PH-2 (31 ft, 65 kHz), PH-3 (25 ft, 65 kHz), and PH-4 (18.8 ft, 65 kHz). The variance of a time record is defined as the zero lag value of the autocovariance function. Because of the sharp initial drop in many of the autocovariance functions due

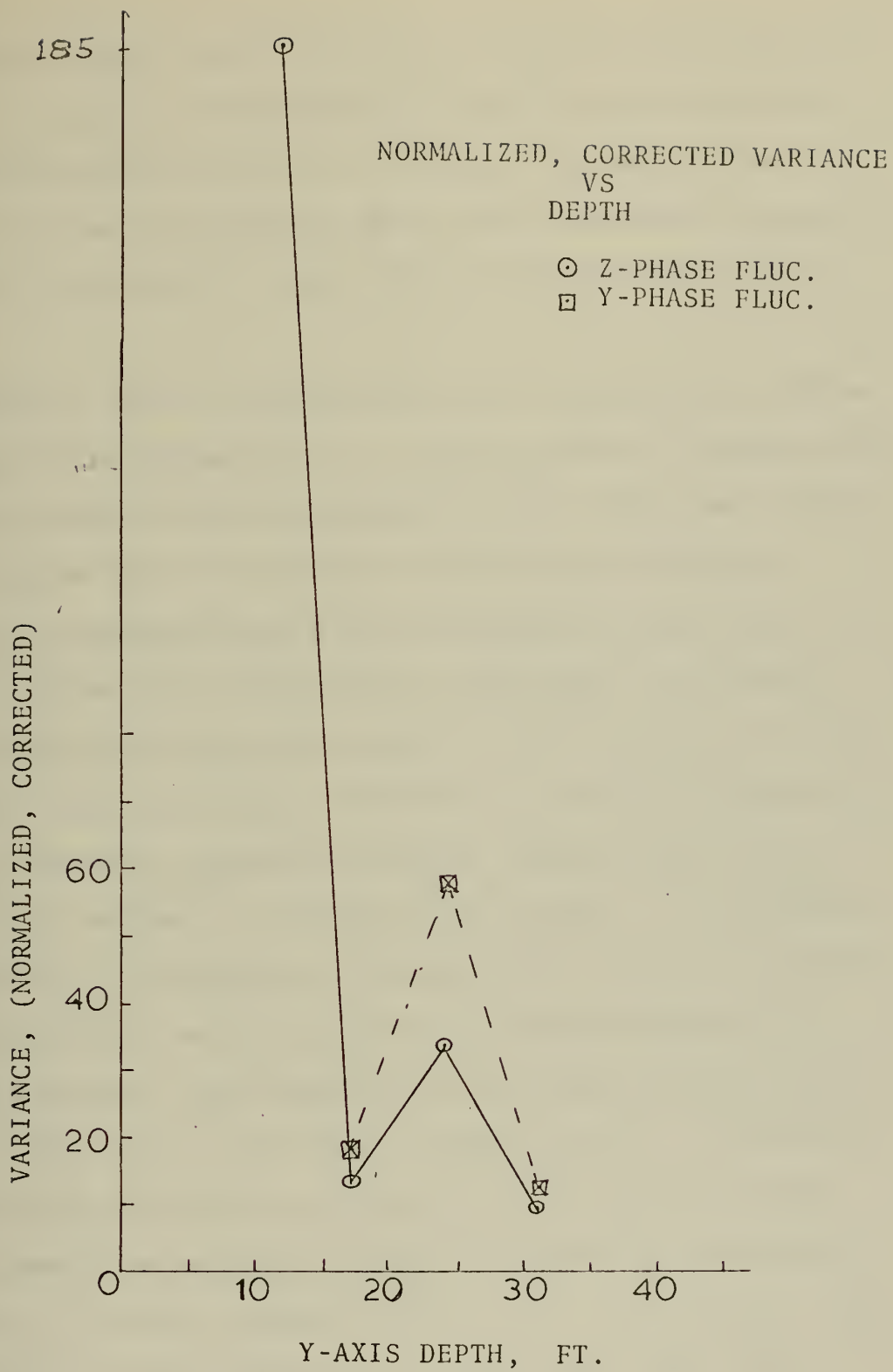


FIGURE 28

to noise spikes, the value of the autocovariance function at $\tau = 0.16$ or 0.32 seconds is a more accurate estimate of the variance than the $\tau = 0$ value. Therefore, in comparing the variances of the Y and Z direction fluctuations of runs PH-2,3, and 4, this corrected variance was used.

Chernov (1960) has shown that the variance of a phase or amplitude fluctuation in a random medium is proportional to the length of the transmission path. The Y and Z direction paths were of different lengths, and although Chernov's assumptions are not fulfilled in the thermocline, all variances were normalized to one meter by dividing each variance by its path length. The corrected and normalized variance versus run depth is plotted in Figure 28. The Y direction variance is always greater than the Z direction variance. This may also be due to the layered structure of the medium. If horizontal plates of various thicknesses are moving through the sound field due to orbital motion, the integrated phase fluctuations will be more sensitive to a vertical movement in the Y direction than in the Z direction, because the Y direction sound beam passes horizontally through a horizontal isothermal "plate". A small movement could shift a new "plate" and therefore a sharp temperature change into the Y axis, while the integrated speed and temperature over the Z direction would not be so greatly effected.

The Z direction variance of the phase fluctuations for run PH-5, which took place in the surface mixed layer, is much greater than the variances of runs PH-2, PH-3, and PH-4. This is an expected result due to two characteristics of the surface mixed layer: the random orientation of temperature patches and the presence of bubble populations which have been found to be resonant at 65 kHz. (Rautmann, 1971, Fitzgerald, 1972)

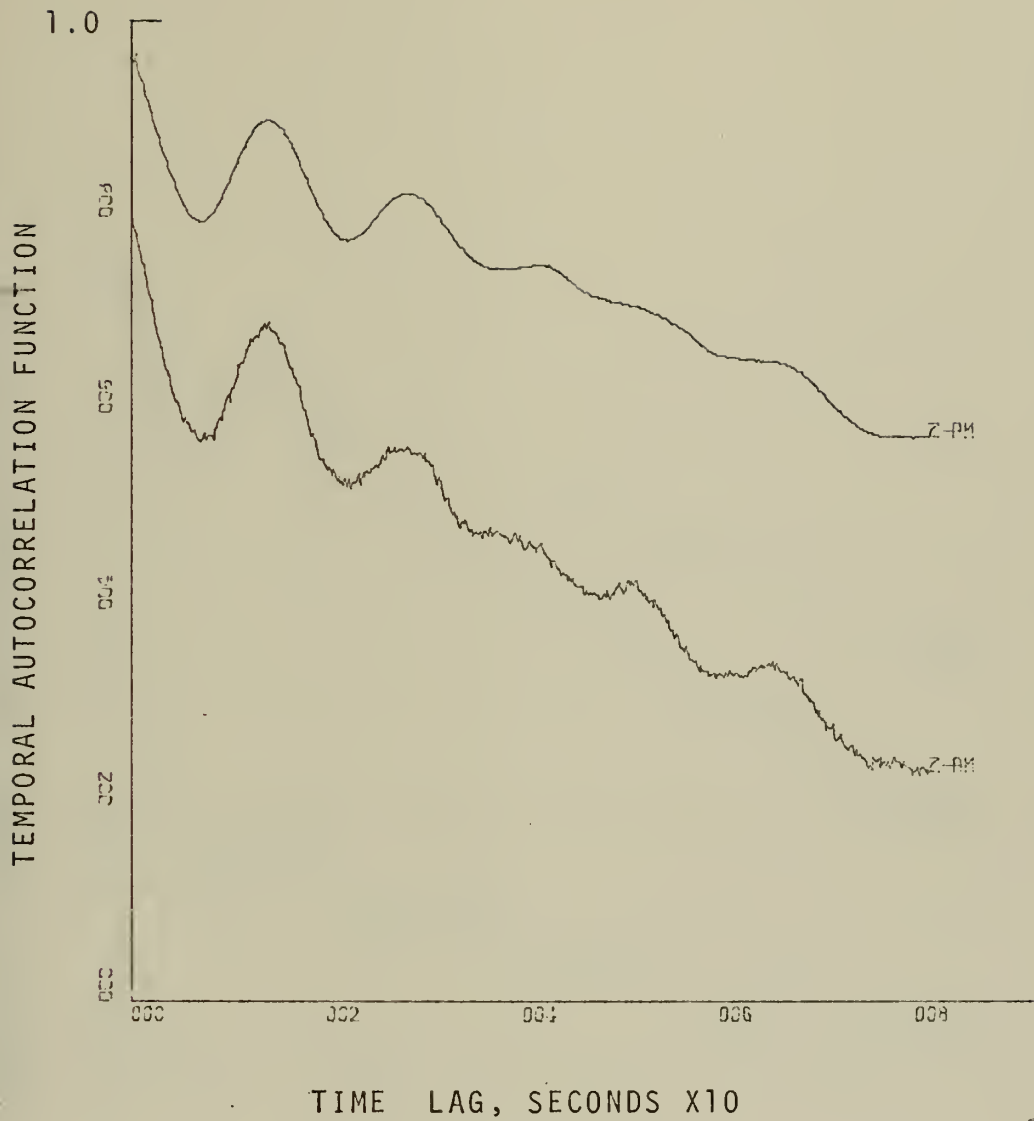
It is concluded that the variance of the phase fluctuation in the thermocline is not isotropic.

G. CORRELATION OF PHASE AND AMPLITUDE FLUCTUATIONS

Chernov (1950) has derived expressions for the temporal autocorrelation function of the phase and amplitude fluctuations of a sound beam in an isotropic, stationary random medium. He concludes that the temporal autocorrelation function of the phase fluctuations equals the temporal autocorrelation function of the amplitude fluctuations. The autocorrelation function of phase and amplitude fluctuations of this experiment can be compared to see how closely they approach the Chernov equality.

In examining the autocorrelation functions, it will be noted that in many cases the autocorrelation function has a very steep initial drop at $t = .6$ seconds after which it decays more normally. It is believed that this sharp initial drop is due to extraneous, widely spaced noise spikes, as explained in Section IV C.1.b. Therefore,

in comparing phase and amplitude fluctuations, the effects of the extraneous spikes should be removed from each function prior to comparison. This could be done by taking the 0.16 second or 0.32 second value of the autocovariance function as the normalizing factor in each case. This re-calculation of the autocovariance function was not done, for lack of time, but a roughly equivalent correction was made, that of merely subtracting the initial drop from each of the autocorrelation functions. Figure 29 shows the autocorrelation function of the Z direction phase and amplitude fluctuations from PH-8 for 65 kHz, 26.8 ft. depth. Figure 30 shows the same two autocorrelation functions with the initial drop subtracted from each function. It can be seen that the phase and amplitude fluctuation autocorrelation functions are very similar in this case. This is an example of excellent agreement between the phase and amplitude fluctuation autocorrelation functions. Figure 31 shows the X direction phase and amplitude autocorrelation functions from PH-7 for the 65kHz, 44.2 ft. depth run. In this case, the phase fluctuation is greatly affected by extraneous noise spikes, and by high frequency periodicities. The extraneous noise spikes cause the initial sharp drop at $\tau = .16$ or $.32$ seconds. The high frequency periodicity is either high frequency noise, or the effects of aliasing of high frequency noise. In either case, these high frequency signals are not caused by the effects of the ocean medium on the sound wave, as explained in



RUN PH-8, Z-PHASE, Z-AMP.
FREQ.=105KHZ, Y-AXIS DEPTH=26.8 ft.

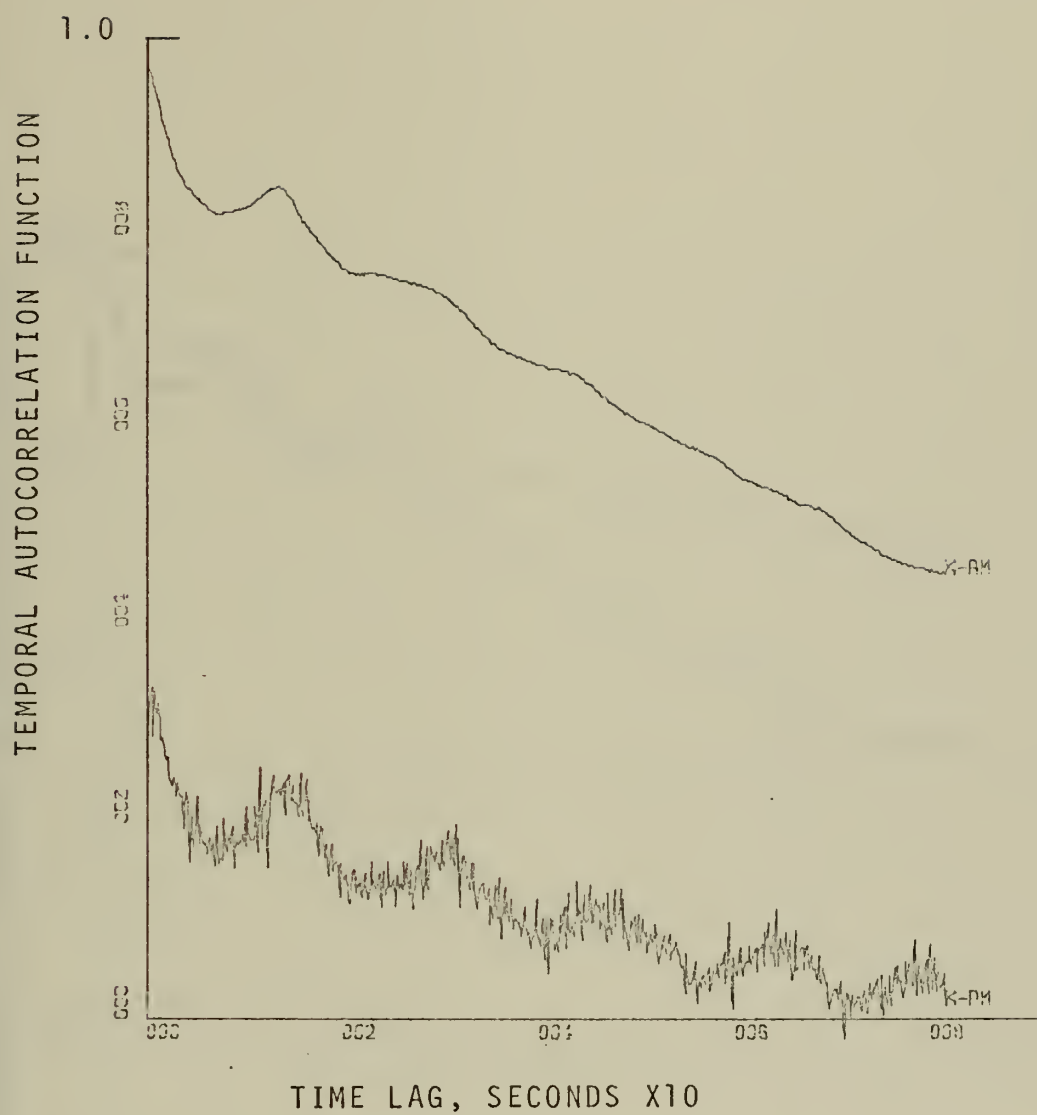
FIGURE 29



RUN PH-8, Z-PHASE, Z-AMP.

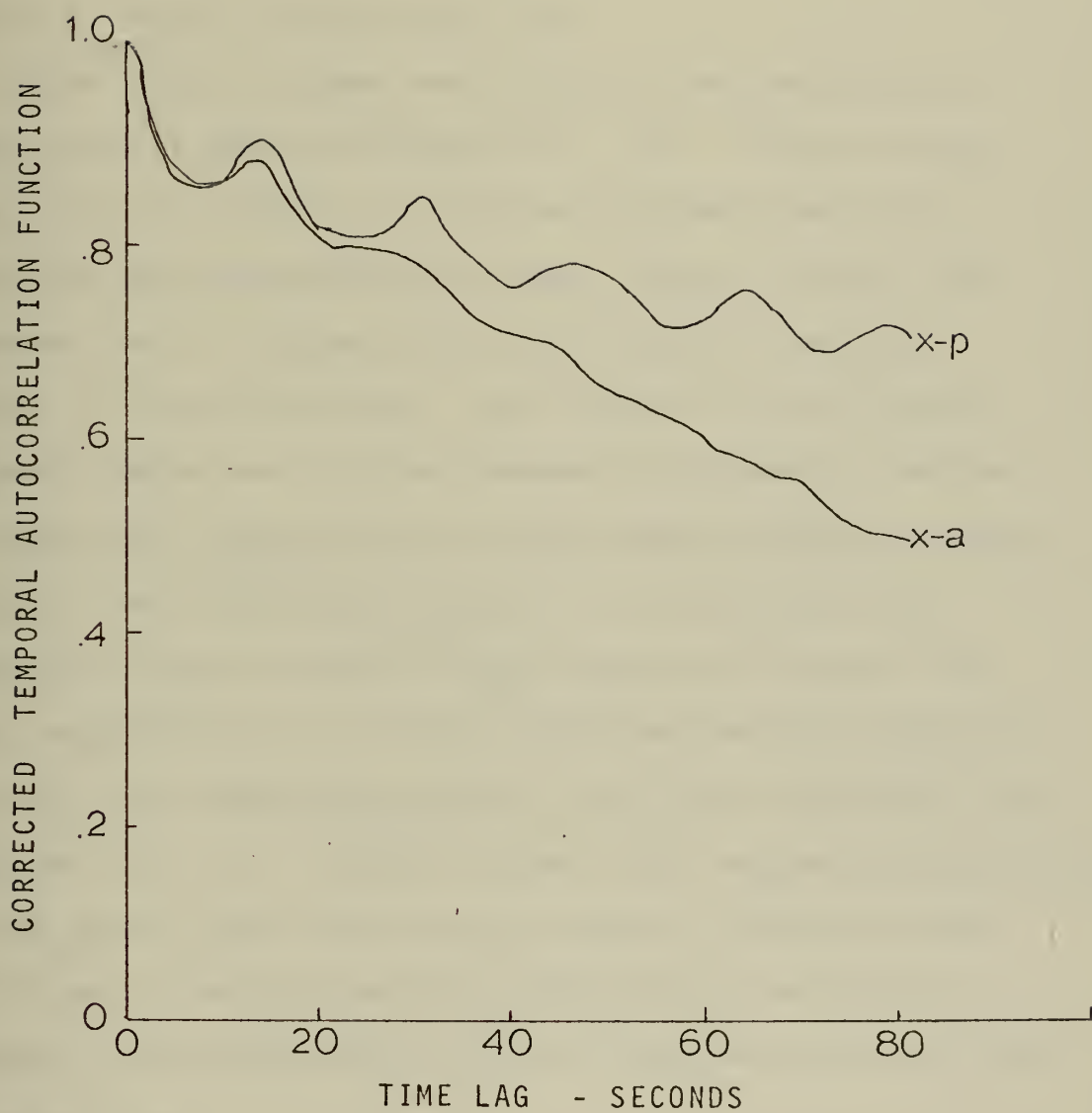
FREQ.=105kHz, Y-AXIS DEPTH=26.8 ft.

FIGURE 30



RUN PH-7, X-PHASE, X-AMP.
 FREQ.=105KHZ,Y-AXIS DEPTH=44.2 ft.

FIGURE 31



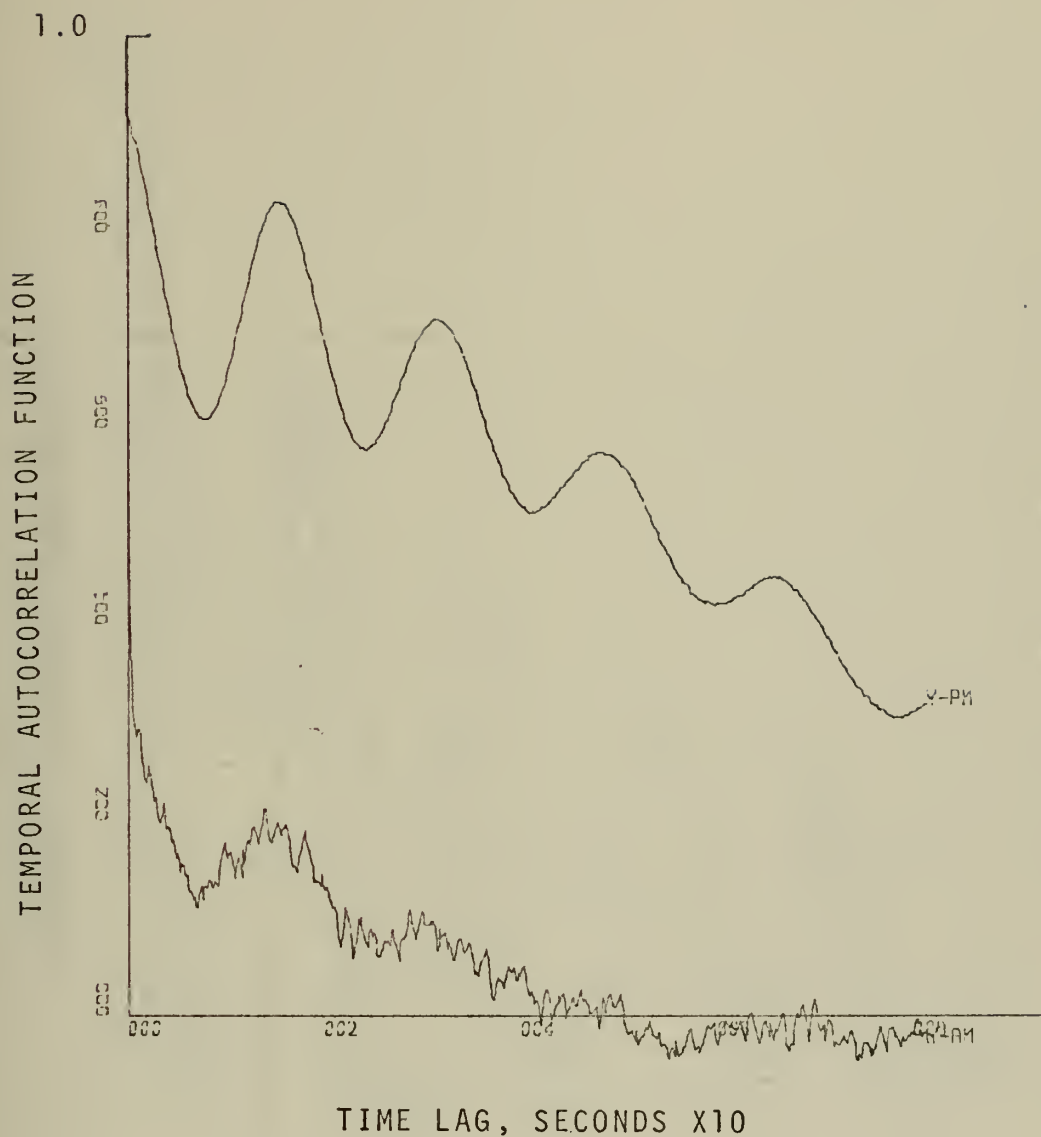
RUN PH-7, X-PHASE, X-AMP.

FREQ.=105KHZ, Y-AXIS DEPTH=44.2 ft.

FIGURE 32

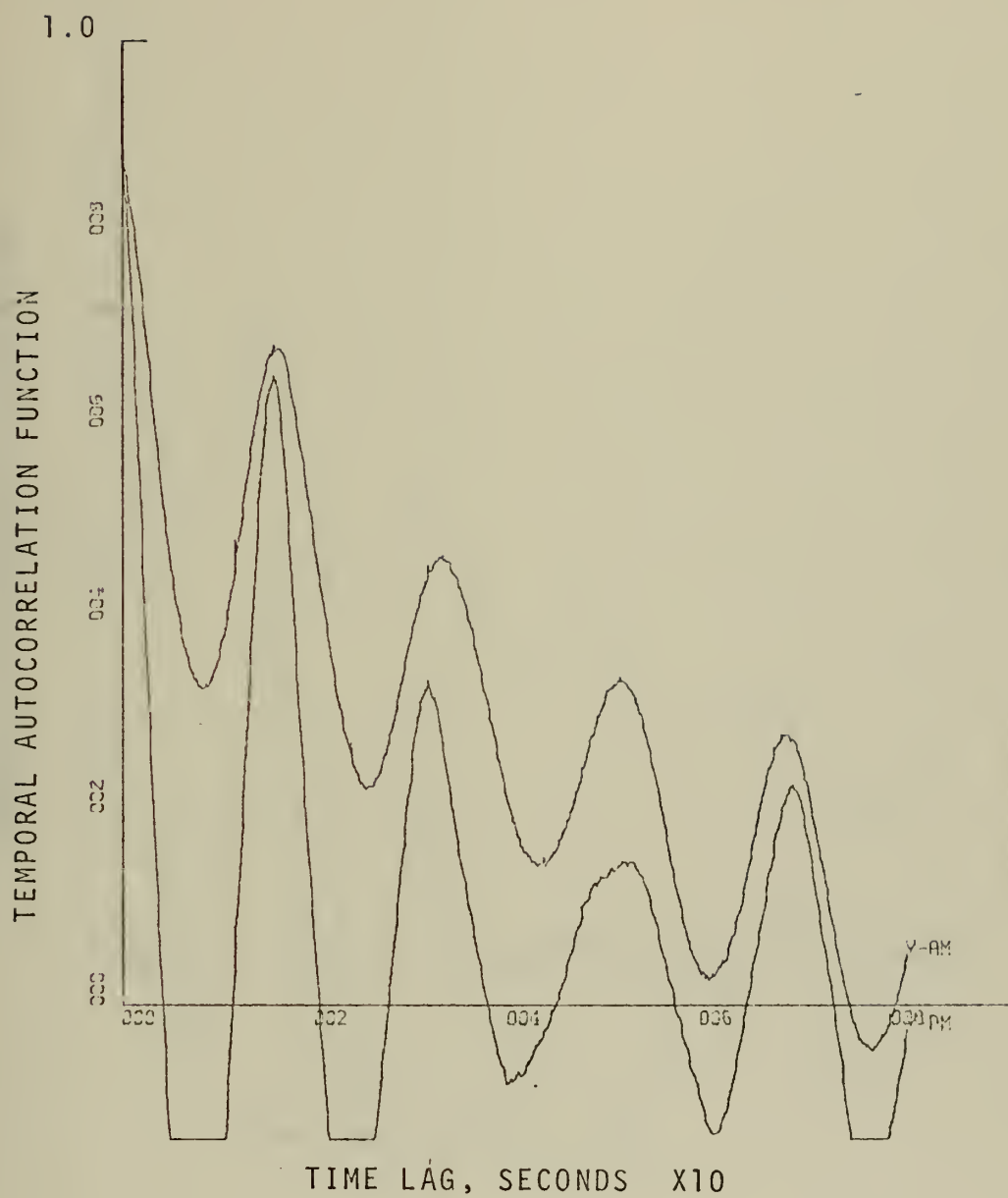
Section IV.C.1.b; hence, these high frequency effects are not considered in this analysis. In Figure 32, the extraneous noise spike effect has been removed, and the phase autocorrelation function has been smoothed. It can be seen that the phase and amplitude autocorrelation functions are still similar in appearance, and have relative maxima and minima at about the same lag times.

Other pairs of phase and amplitude autocorrelation functions are shown in Figures 33 - 38. If the initial sharp drop is ignored, it will be observed that their behaviors are essentially the same. Thus, for the case observed here, it appears that the Chernov statement holds, to varying degrees. The reasons why the Chernov equality fails are: 1) the presence of different amounts of extraneous noise spikes in each signal causing a sharp initial drop, and 2) the presence of extraneous high frequency signals in one of both channels (noise), and most importantly, 3) the phase fluctuations are sensitive to long term temperature changes while the amplitude fluctuations are not. Chernov assumed that random inhomogeneities in the sound field were the sole cause of fluctuations; he did not consider long term anisotropic temperature changes, such as those that result from the passage of an internal wave.



RUN PH-3, Y-PHASE, Y-AMP
 FREQ.=65KHZ, Y-AXIS DEPTH=25 ft.

FIGURE 33



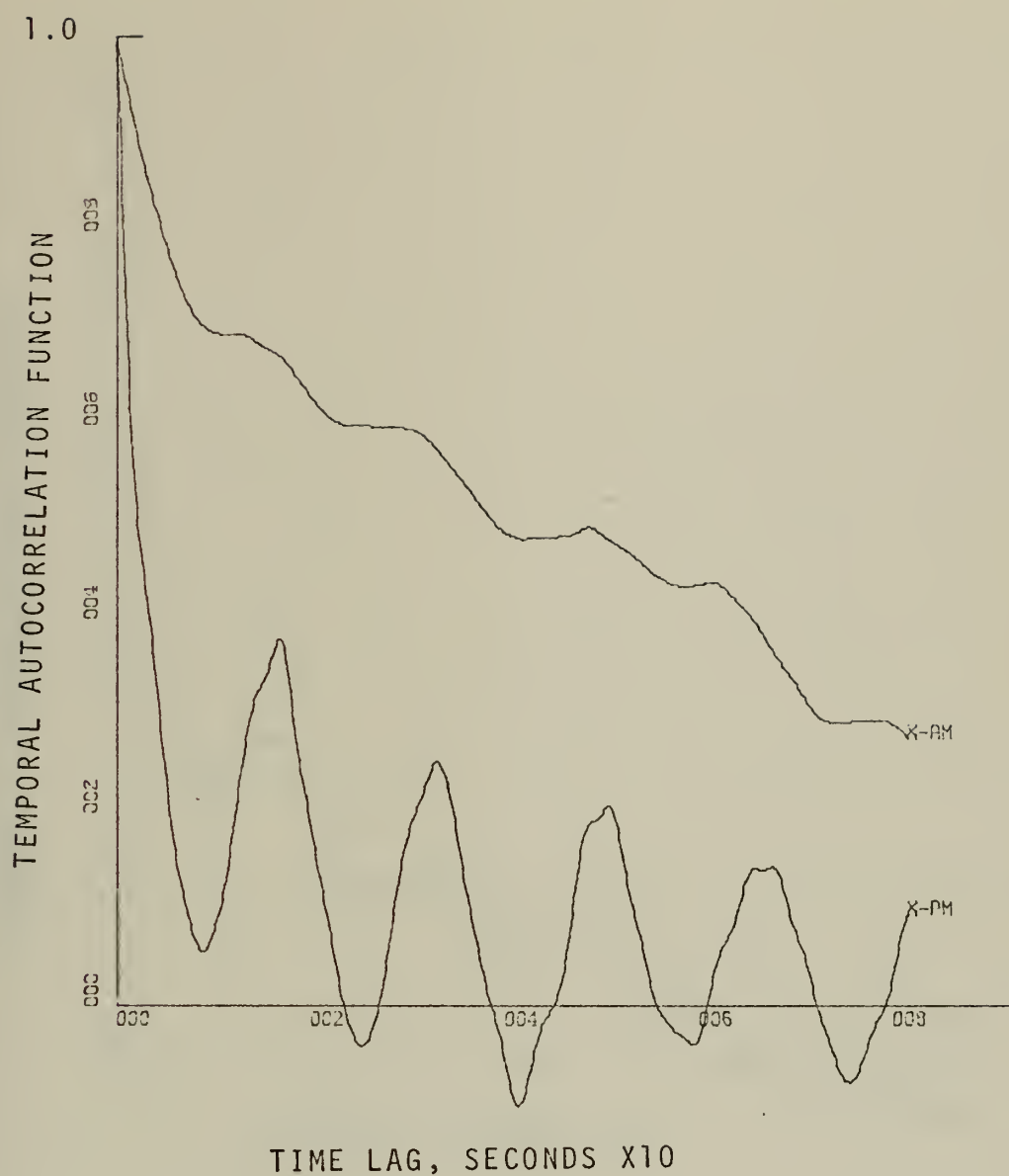
RUN PH-2, Y-PHASE, Y-AMP.
 FREQ.=65KHZ, Y-AXIS DEPTH=31 ft.

FIGURE 34



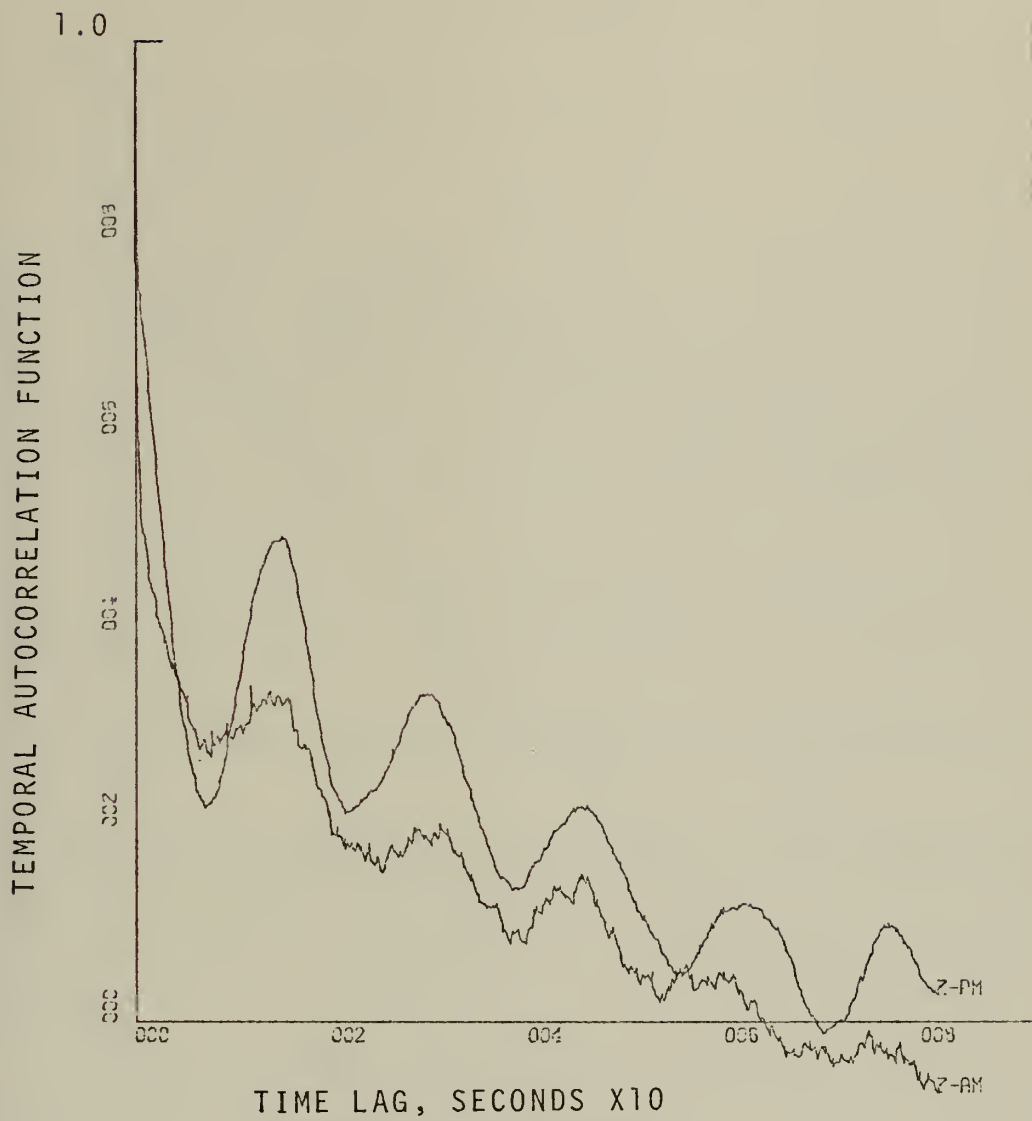
RUN PH-5, Z-PHASE, Z-AMP.
 FREQ.=65KHZ,Y-AXIS DEPTH=7 ft.

FIGURE 35



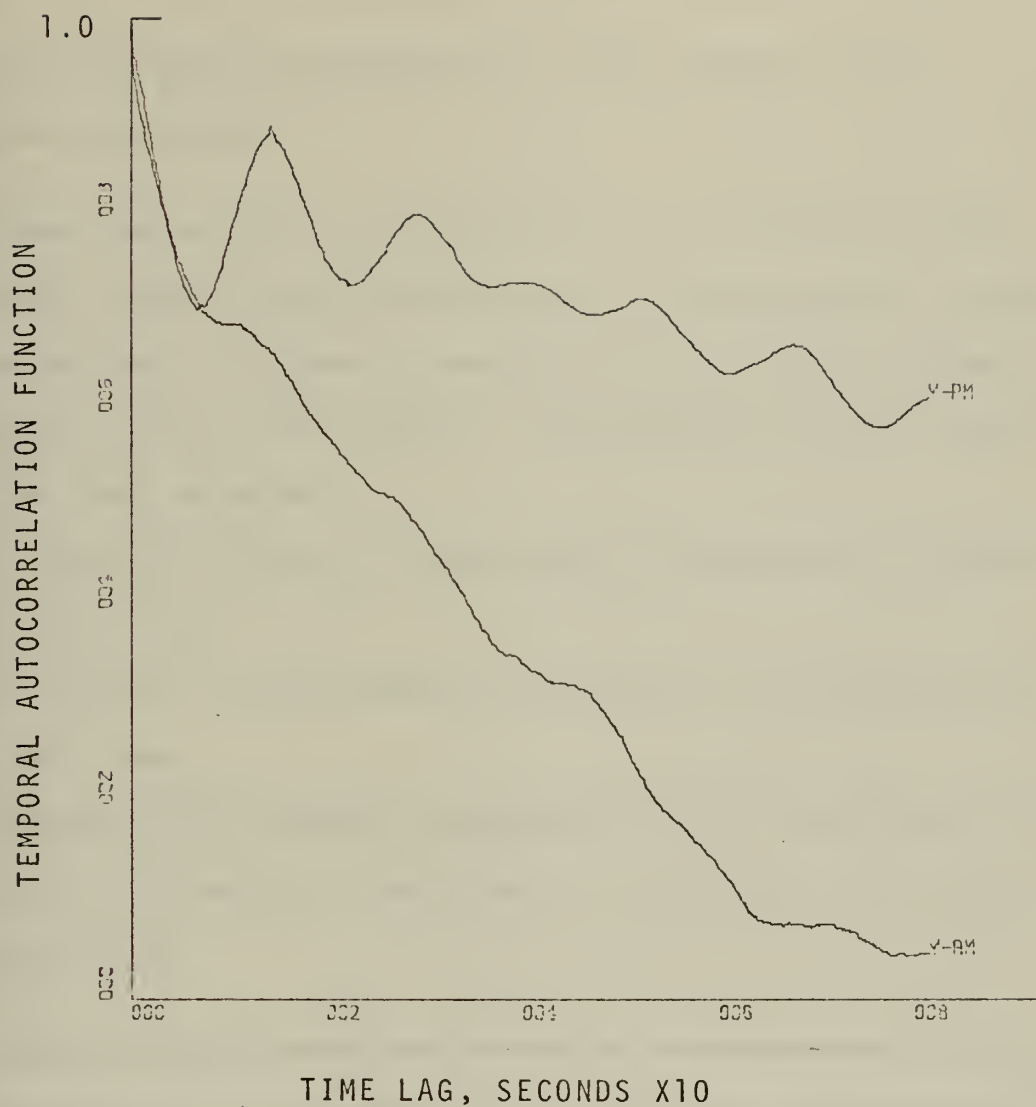
RUN PH-5, X-PHASE, X-AMP.
 FREQ.=65KHZ,Y-AXIS DEPTH=7 ft.

FIGURE 36



RUN PH-4, Z-PHASE, Z-AMP.
 FREQ.=65KHZ, Y-AXIS DEPTH=18.8 ft.

FIGURE 37



RUN PH-8, Y-PHASE, Y-AMP.
 FREQ.=105KHZ, Y-AXIS DEPTH=26.8 ft.

FIGURE 38

V. CONCLUSIONS

The following conclusions are drawn based on the preceeding analysis:

A. Phase and amplitude fluctuations of a 65 kHz and 105 kHz sound beam in the surface layer of the ocean are caused by the motion of medium inhomogeneities of varying acoustic impedance in the sound field. Inhomogeneity motion arises from two main sources:

1. Orbital motion of the medium in response to surface wave action, and
2. Motion of the medium in response to the passage of internal waves.

The dominant frequency components of the phase and amplitude fluctuations are those of the surface waves and internal waves.

B. The envelopes of the autocovariance functions of the phase fluctuations in a horizontal and a vertical sound beam of 65 kHz decorrelate (reduce to $1/e$ of their initial value) faster in the surface mixed layer than in the thermocline. It is believed that this is an indication of two characteristics of the mixed layer: the greater instability of the temperature structure in the mixed layer, versus that in the thermocline, and the presence of bubbles resonant at 65 kHz in the mixed layer.

C. In the thermocline, the autocovariance function of the phase fluctuations of a horizontal sound beam decorrelates faster than the autocovariance function of the phase fluctuations of a vertical sound beam. It is believed that this results from a layered "plate" temperature structure of the thermocline. Therefore, the correlation time in a thermocline is not isotropic.

D. In the thermocline, the variance of the phase fluctuation of a 65 kHz sound beam in the horizontal direction is greater than the variance of the phase fluctuations in the vertical direction. It is believed that this is a result of a layered "plate" temperature structure of the thermocline. Therefore, the variance in the thermocline is not isotropic.

E. From C. and D. above, it is concluded that the medium in the thermocline is anisotropic.

F. The autocorrelation function of the phase fluctuation approximately equals the autocorrelation function of the amplitude fluctuations for a 65 kHz sound beam traveling through 1 meter of the surface layer of the ocean. This result reinforces and extends the theoretical work of Chernov (1950) which predicted that the autocorrelation functions of the phase and amplitude fluctuations of a sound beam traveling through a random, stationary isotropic medium would be equal.

VI. RECOMMENDATIONS FOR FUTURE EXPERIMENTS

A. EXPERIMENTAL TECHNIQUE

The results of this experiment demonstrate the feasibility of obtaining useful information about the micro-structure of a volume of ocean water by studying the sound phase and amplitude fluctuations of sound passing through the volume. It also points out some of the pitfalls in making such measurements. For those who repeat this experiment, or perform similar experiments in the future, the following recommendations are offered.

1. Use differential amplifiers that are not limited to a low input voltage. This will allow operation well above many of the noise levels of the system. The PAR 113 differential amplifier, although ideal from the point of view of internal electrical noise, was poorly suited for this purpose.

2. To obtain any variance information from the amplitude fluctuation records, the system gains must be known exactly (phase fluctuation measurements will not be effected by varying gains or voltage levels). Careful measurement of these gains, preferably before the experiment, is the only way to obtain such information. System gain measurements should be done with the detection circuit fully assembled, vice piecemeal.

B. AREAS FOR FUTURE INVESTIGATION

1. Much more information can be gleaned from the data of this experiment. Analysis results of runs not previously considered are included as Appendix A. It is felt that further analysis of these data would be fruitful.

2. Concurrent measurement of sound amplitude and phase fluctuation, particle velocity, and temperature in the sound field would shed more light on the relationship between medium motion and sound phase and amplitude fluctuation. By making such concurrent measurements of particle velocity, temperature, and sound phase and amplitude fluctuation, it should be possible to deduce the role of resonant bubbles in the acoustic fluctuations.

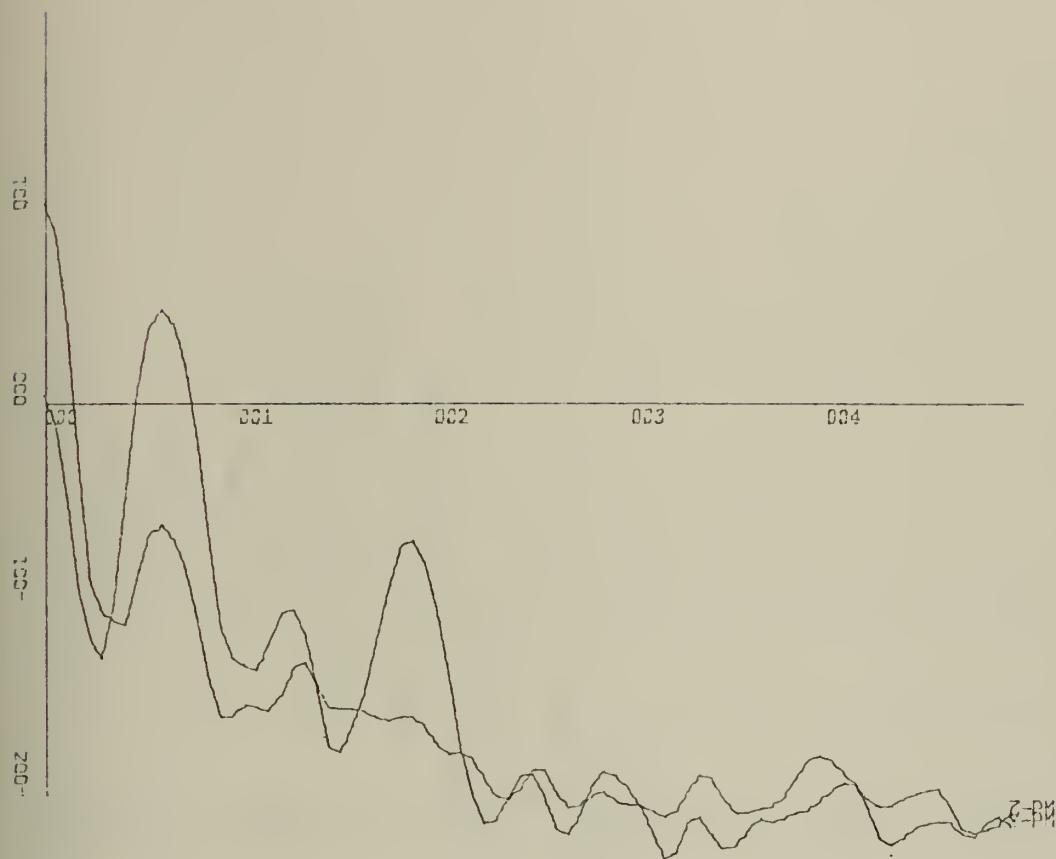
APPENDIX A

Analysis Results For Various Runs

Table II lists the experimental runs which were analyzed by the computer programs CONVERT and ANALYSIS. Various outputs of this analysis are displayed throughout the body of the thesis.

Appendix A contains the remainder of the analysis. This information is included to permit comparison with future studies in this field, and for further analysis of this data at some future time. A typical "set" of results for a given run are (1) Temporal Autocorrelation Function, (2) Power Spectrum Level, (3) Temporal Cross-Correlation Function, and (4) Coherence Function and Cross-Spectral Phase Angle. Some sets are not complete, as portions of them were displayed in the body of the thesis.

Interpretation of these outputs is explained in Section IV-C. The ordinates of the cross-correlation function graphs are labeled incorrectly; they should be labeled as in Figure 13.

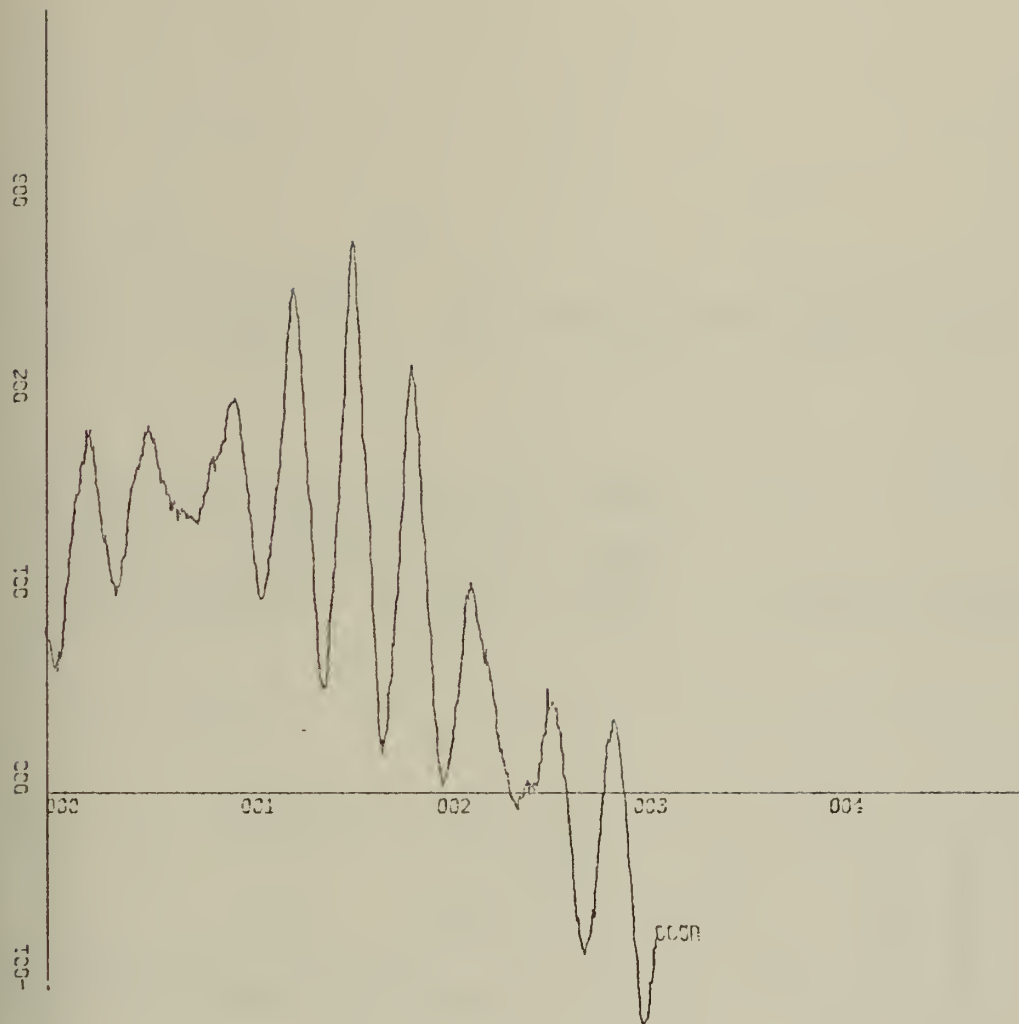


X-SCALE=1.00E-01 UNITS INCH.

Y-SCALE=1.00E+01 UNITS INCH.

POWER SPECTRUM LEVEL (DB) Y-PM, Z-PM

RUN PH-2, FILE 4 OF CON6



X-SCALE=1.00E+00 UNITS INCH.

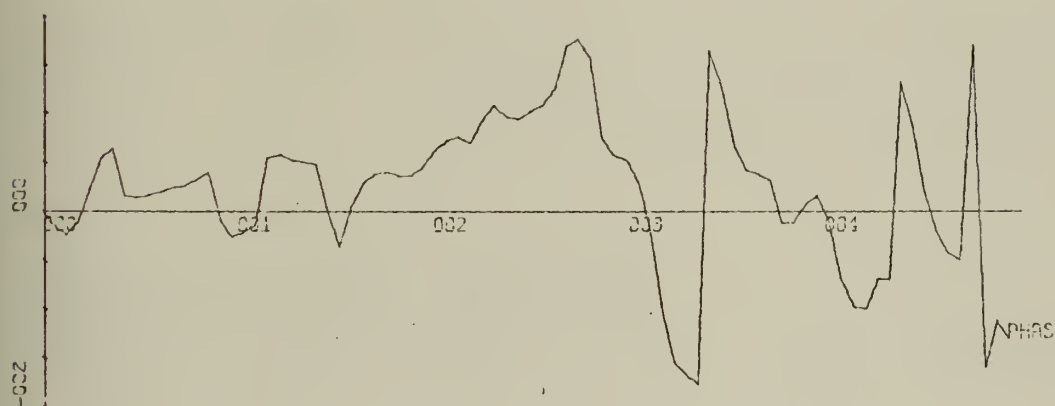
Y-SCALE=1.00E-01 UNITS INCH.

CROSS-CORRELATION FN, Y-PM, Z-PM

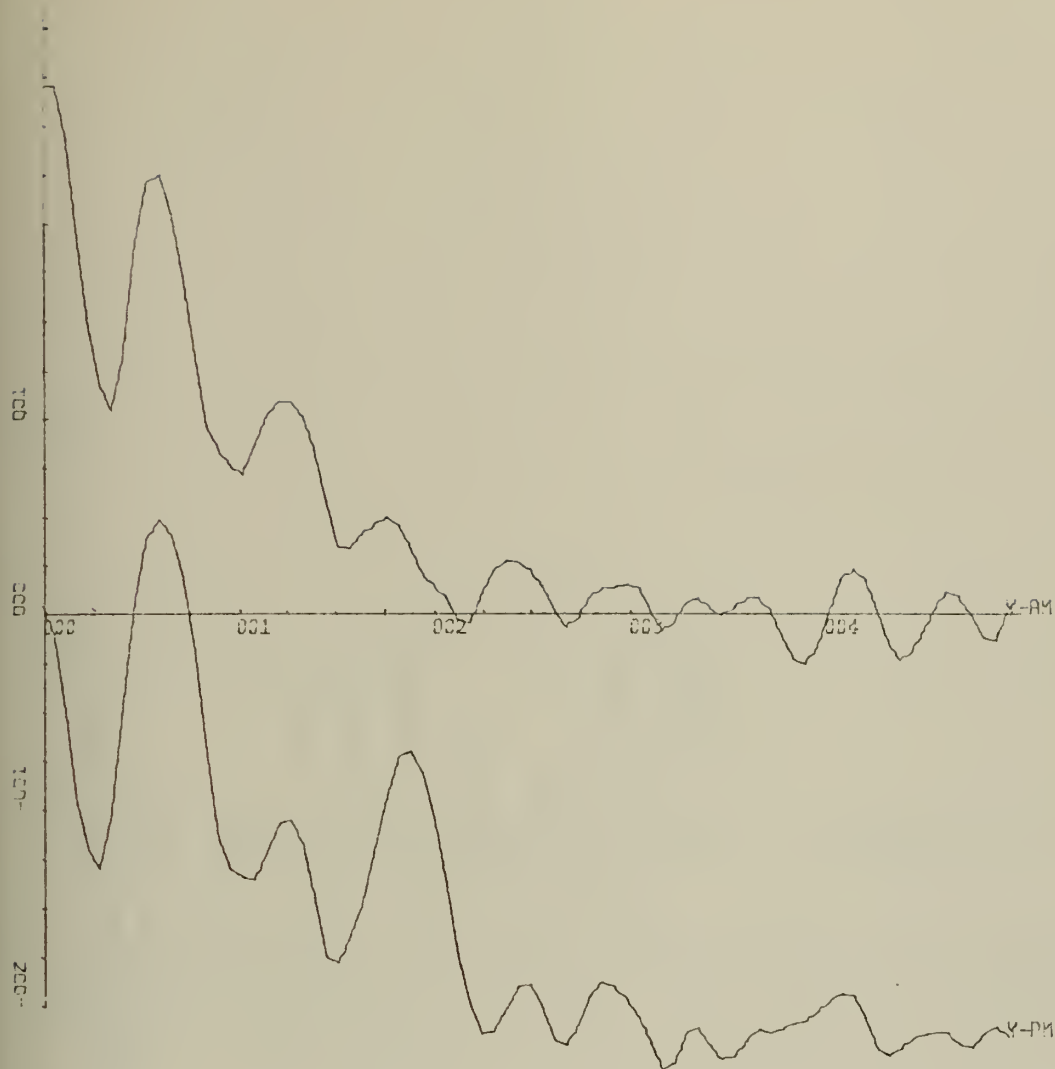
RUN PH-2, FILE 4 OF CON6



X-SCALE=1.00E-01 UNITS INCH.
 Y-SCALE=1.00E+00 UNITS INCH.
 COHERENCE FUNCTION Y-PM, Z-PM
 RUN PH-1



X-SCALE=1.00E-01 UNITS INCH.
 Y-SCALE=2.00E+02 UNITS INCH.
 CROSS SPECTRAL PHASE ANGLE Y-PM, Z-PM
 RUN PH-2

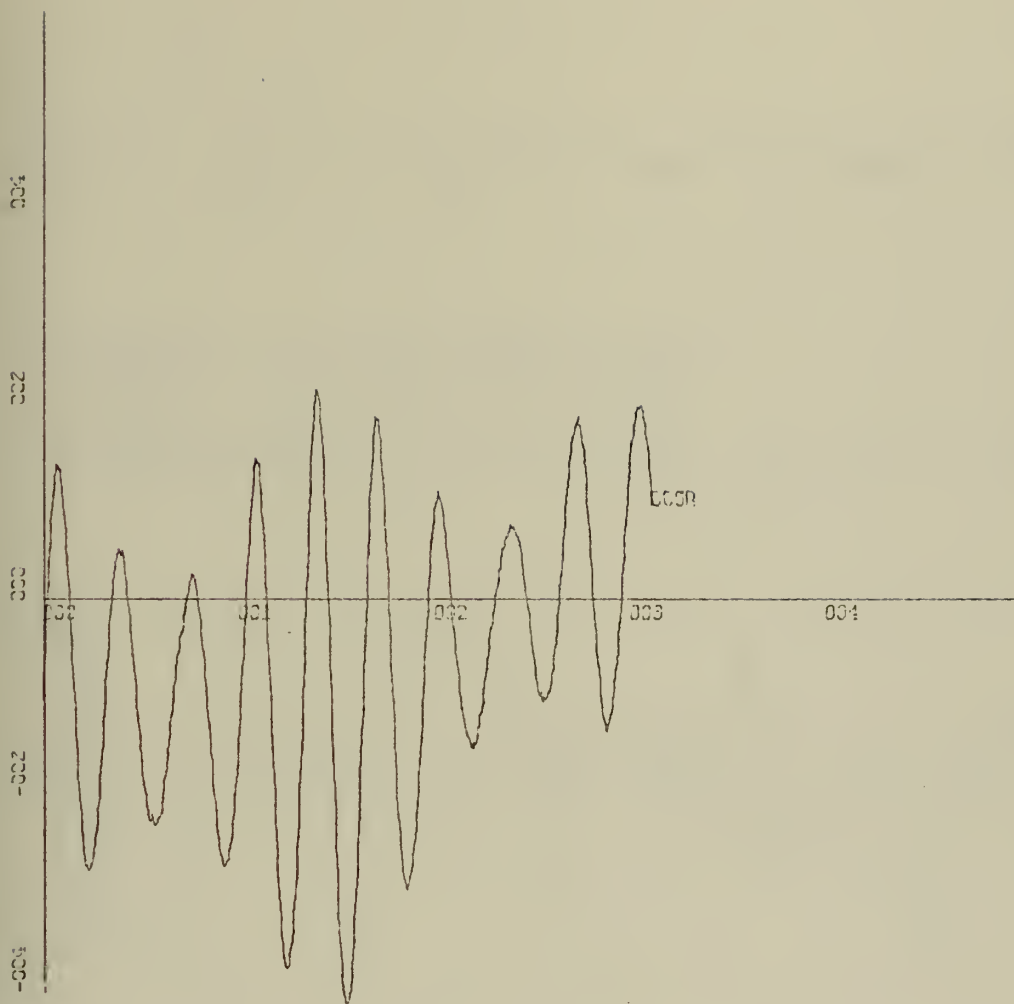


X-SCALE:-1.00E-01 UNITS INCH.

Y-SCALE:-1.00E+01 UNITS INCH.

POWER SPECTRUM LEVEL (DB) Y-PM, Y-AM

RUN PH-2, FILE 4 OF CON6

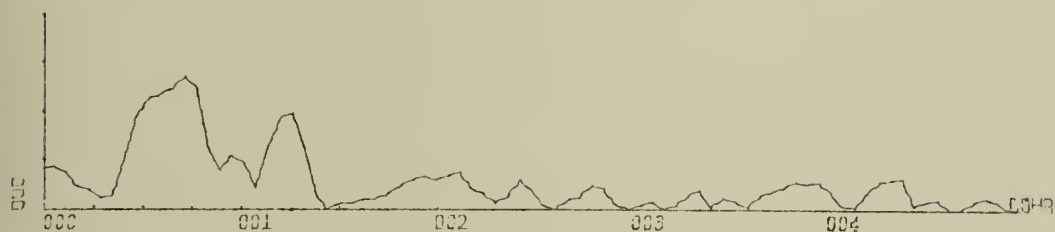


X-SCALE=-1.00E+00 UNITS INCH.

Y-SCALE=-2.00E-01 UNITS INCH.

CROSS-CORRELATION FN, Y-PM, Y-AM

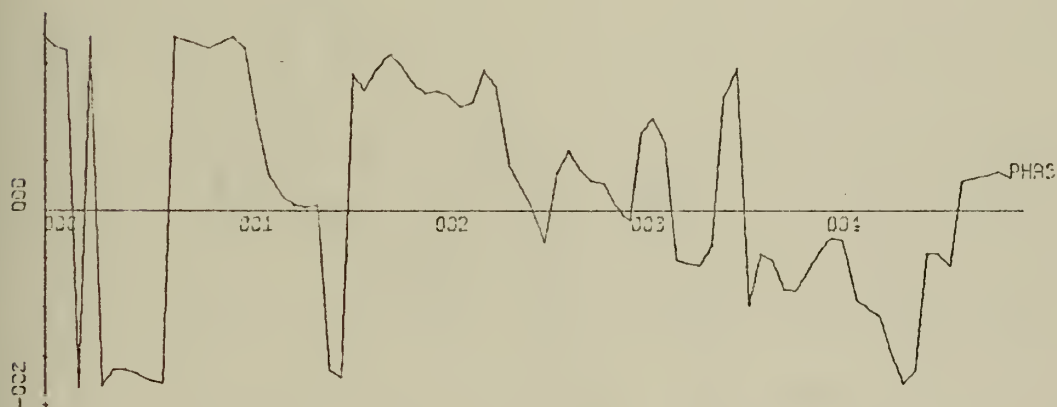
RUN PH-2, FILE 4 OF CON6



X-SCALE=1.00E-01 UNITS INCH.

Y-SCALE=1.00E+00 UNITS INCH.

COHERENCE FUNCTION Y-PM, Y-AM

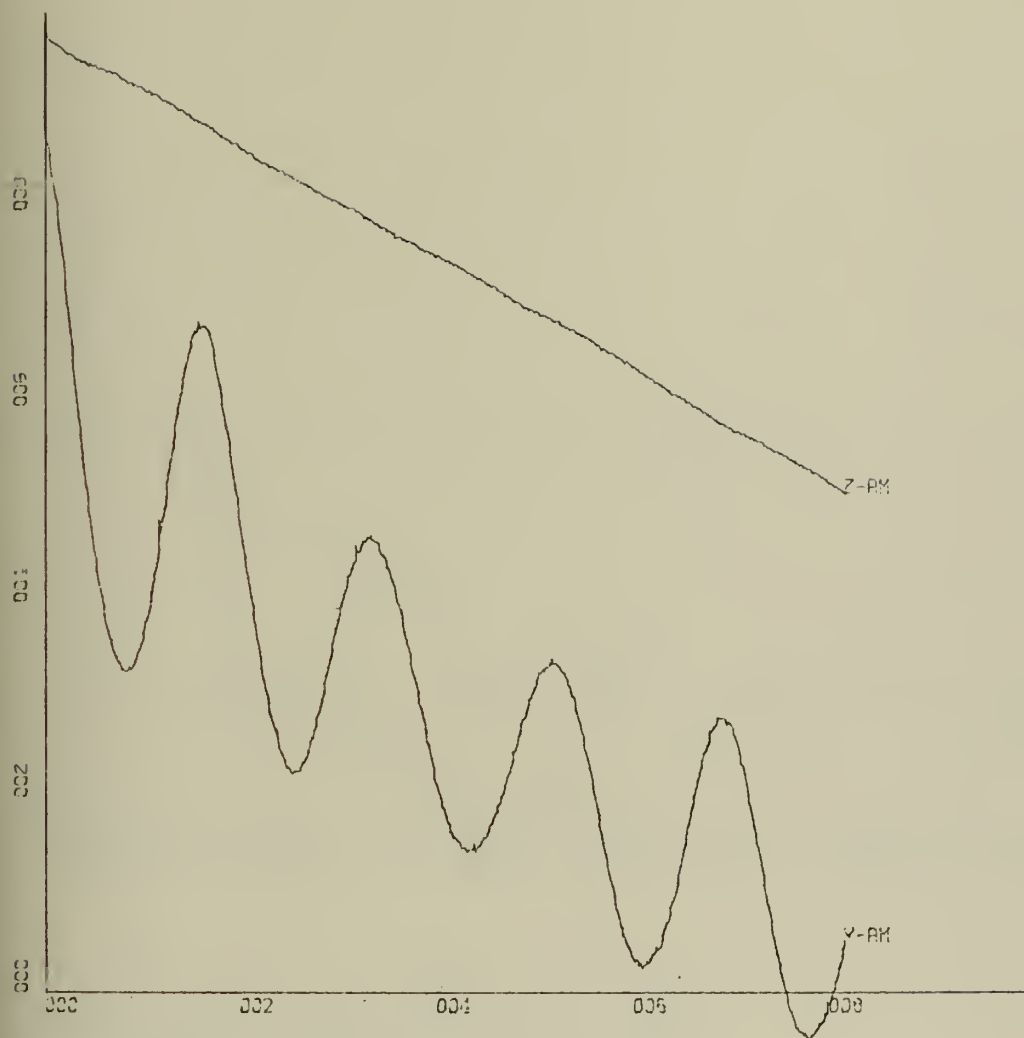


X-SCALE=1.00E-01 UNITS INCH.

Y-SCALE=2.00E+02 UNITS INCH.

CROSS SPECTRAL PHASE ANGLE Y-PM, Y-AM

RUN PH-2

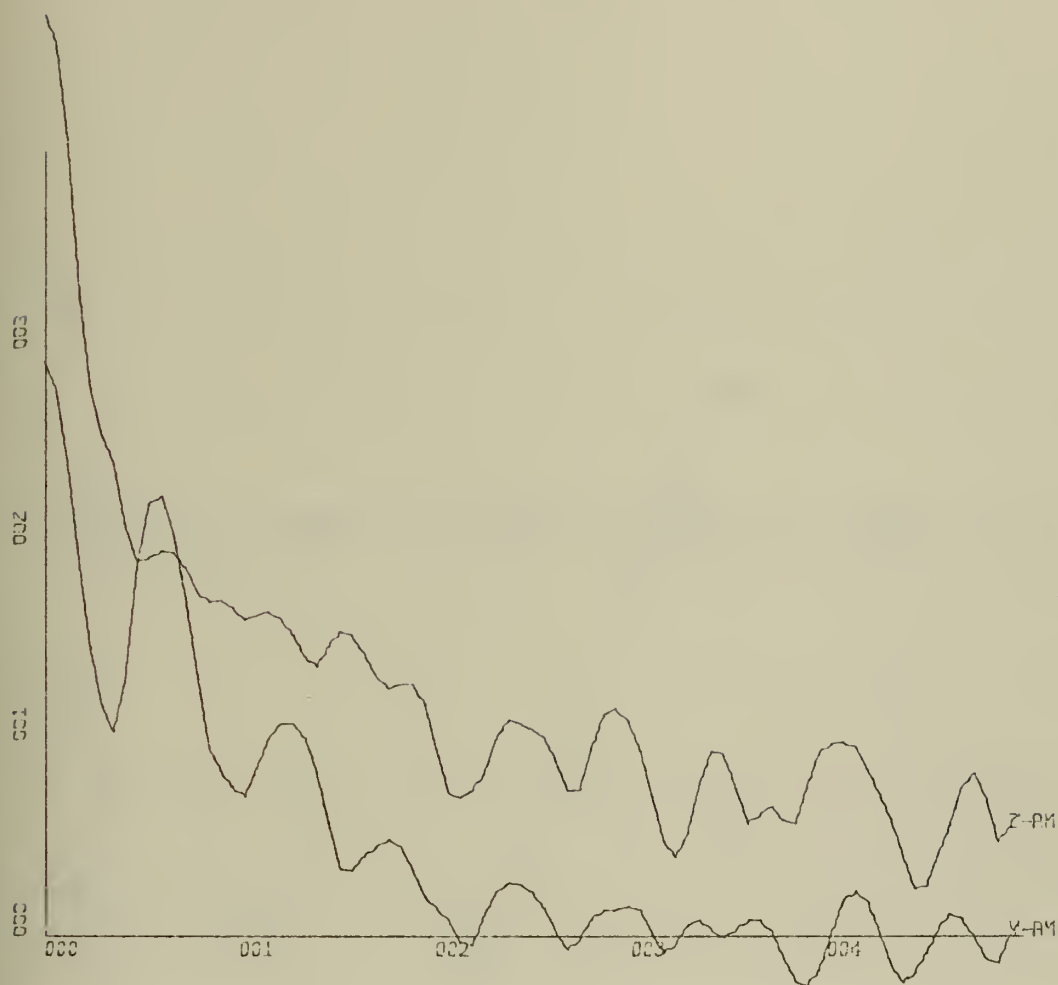


X-SCALE=2.00E+01 UNITS INCH.

Y-SCALE=2.00E-01 UNITS INCH.

TEMPORAL AUTOCORRELATION FN, Y-AM, Z-AM

RUN PH-2, FILE 4 OF CON6

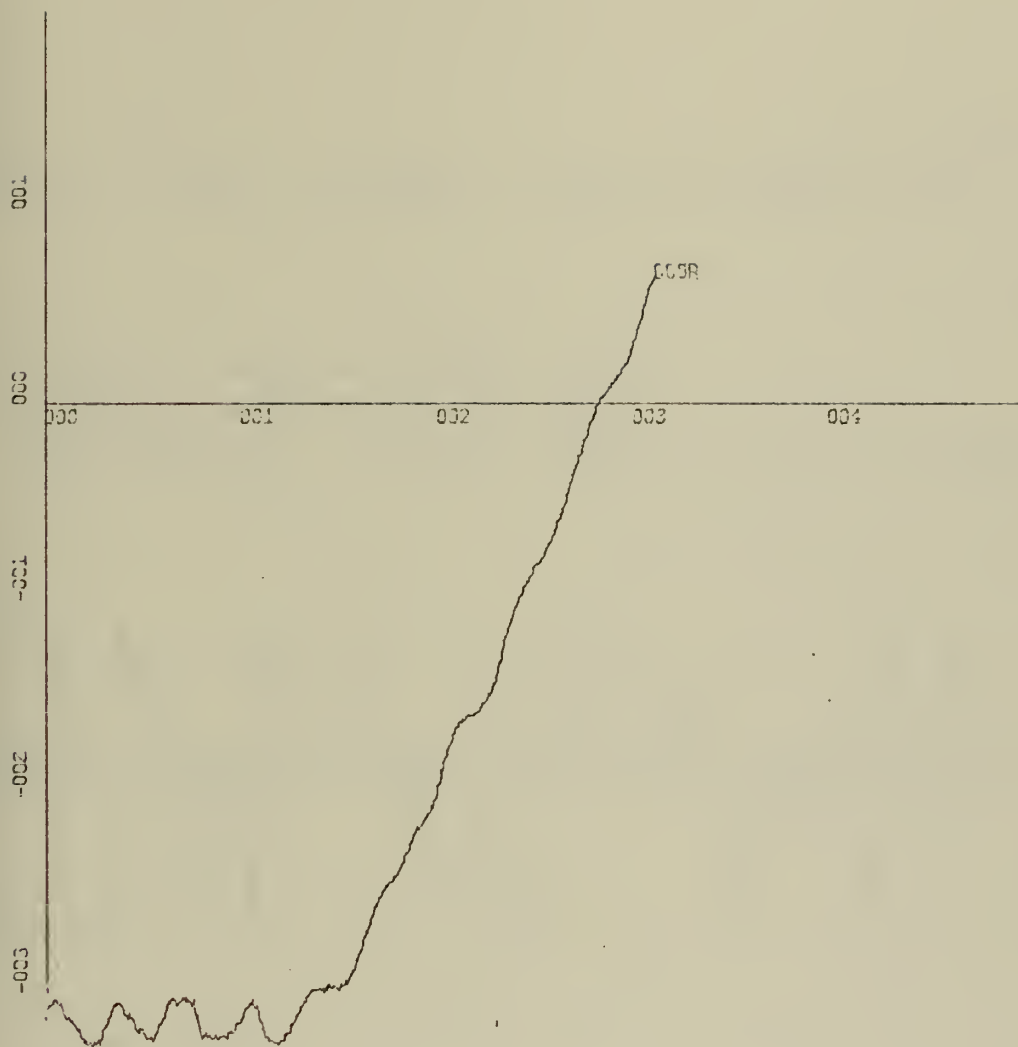


X-SCALE=1.00E-01 UNITS INCH.

Y-SCALE=1.00E+01 UNITS INCH.

POWER SPECTRUM LEVEL (DB) Y-AM, Z-AM

RUN PH-2, FILE 4 OF CON6

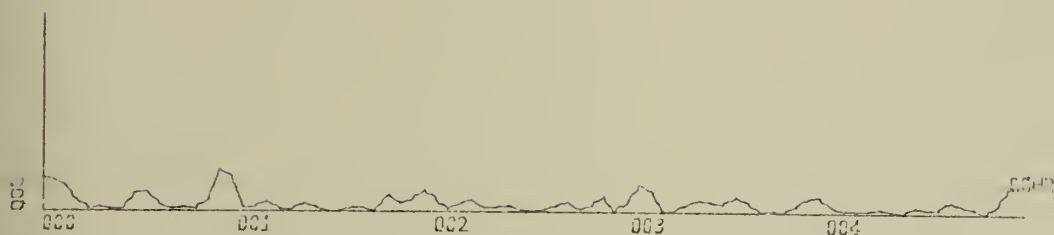


X-SCALE=1.00E+00 UNITS INCH.

Y-SCALE=1.00E-01 UNITS INCH.

CROSS-CORRELATION FN, Y-AM, Z-AM

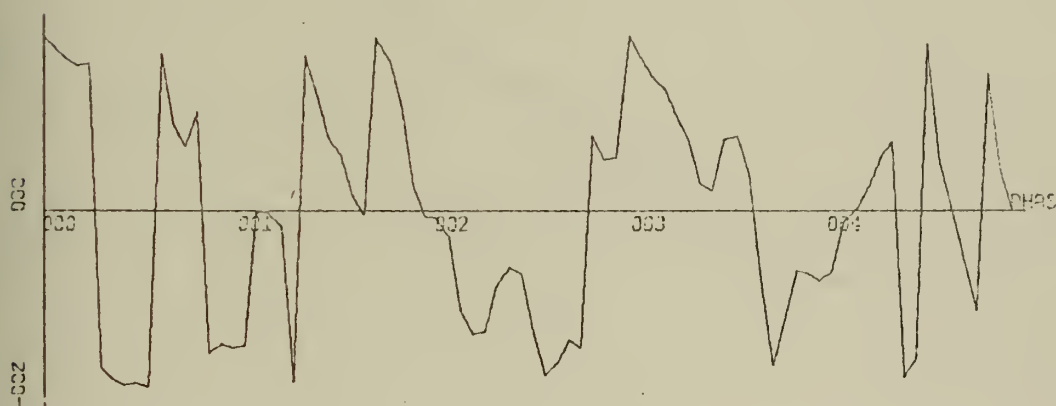
RUN PH-2, FILE 4 OF CON6



X-SCALE=1.00E-01 UNITS INCH.

Y-SCALE=1.00E+00 UNITS INCH.

COHERENCE FUNCTION Y-AM, Z-AM

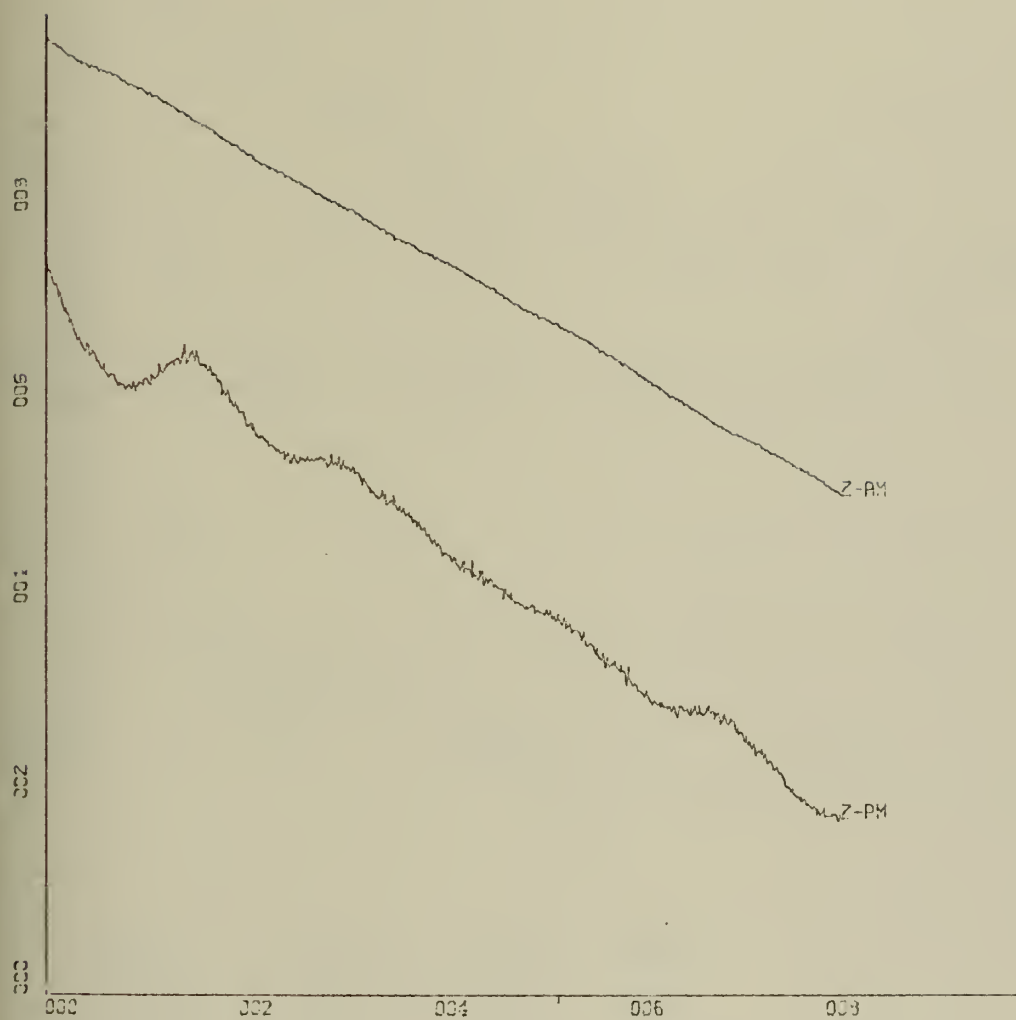


X-SCALE=1.00E-01 UNITS INCH.

Y-SCALE=2.00E+02 UNITS INCH.

CROSS SPECTRAL PHASE ANGLE Y-AM, Z-AM

RUN PH-2

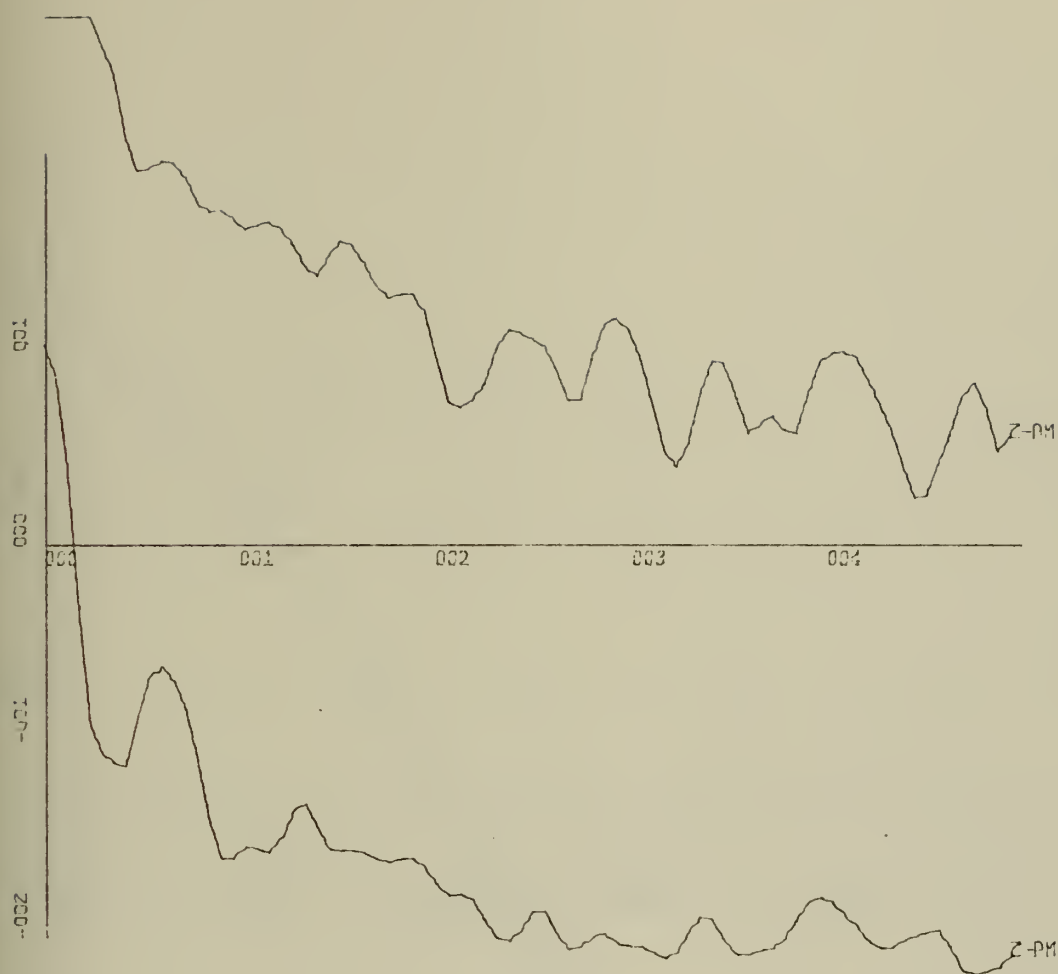


X-SCALE=2.00E+01 UNITS INCH.

Y-SCALE=2.00E-01 UNITS INCH.

TEMPORAL AUTOCORRELATION FN, Z-PM, Z-AM

RUN PH-2, FILE 4 OF CON6

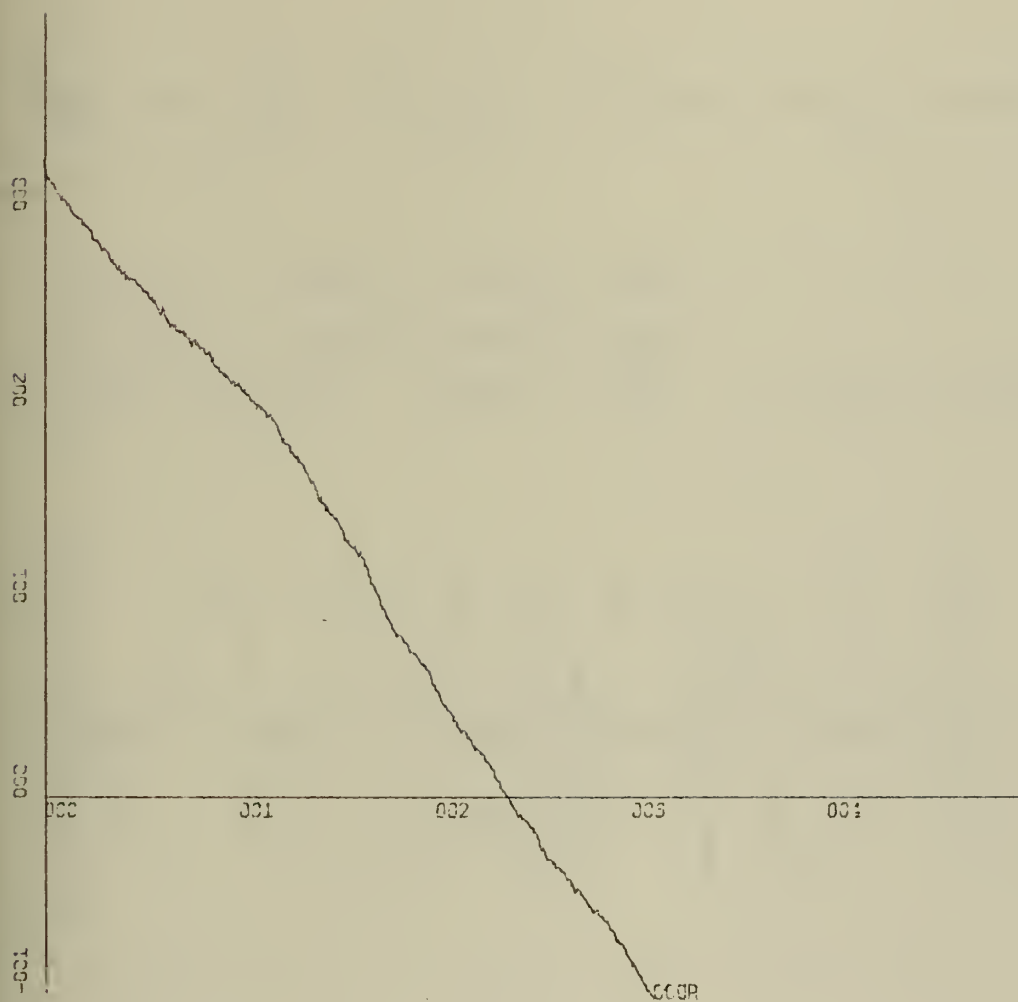


X-SCALE=1.00E-01 UNITS INCH.

Y-SCALE=1.00E+01 UNITS INCH.

POWER SPECTRUM LEVEL (DB) Z-PM, Z-AM

RUN PH-2, FILE 4 OF CON6

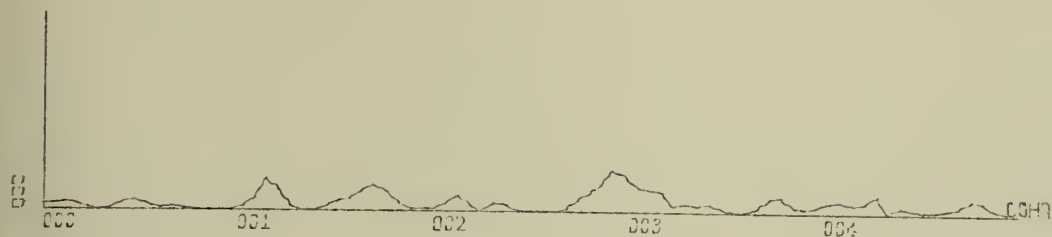


X-SCALE=1.00E+00 UNITS INCH.

Y-SCALE=1.00E-01 UNITS INCH.

CROSS-CORRELATION FN, Z-PM, Z-AM

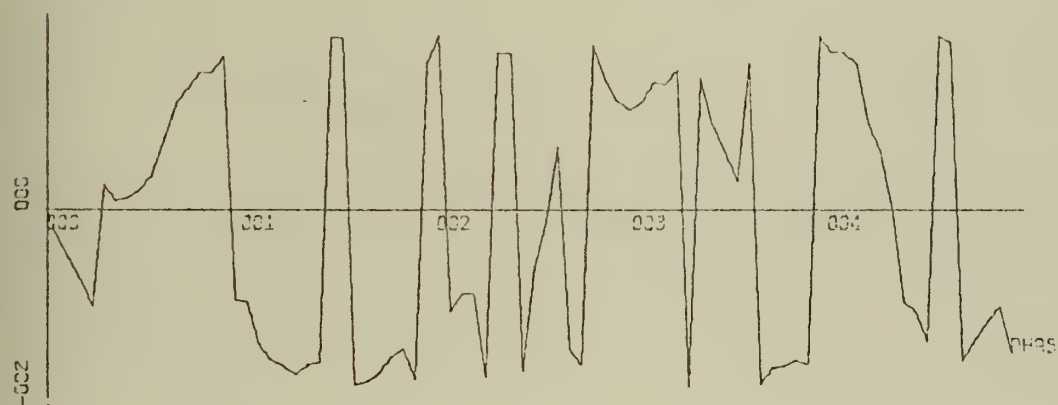
RUN PH-2, FILE 4 OF CON6



X-SCALE=1.00E-01 UNITS INCH.

Y-SCALE=1.00E+00 UNITS INCH.

COHERENCE FUNCTION Z-PM, Z-AM

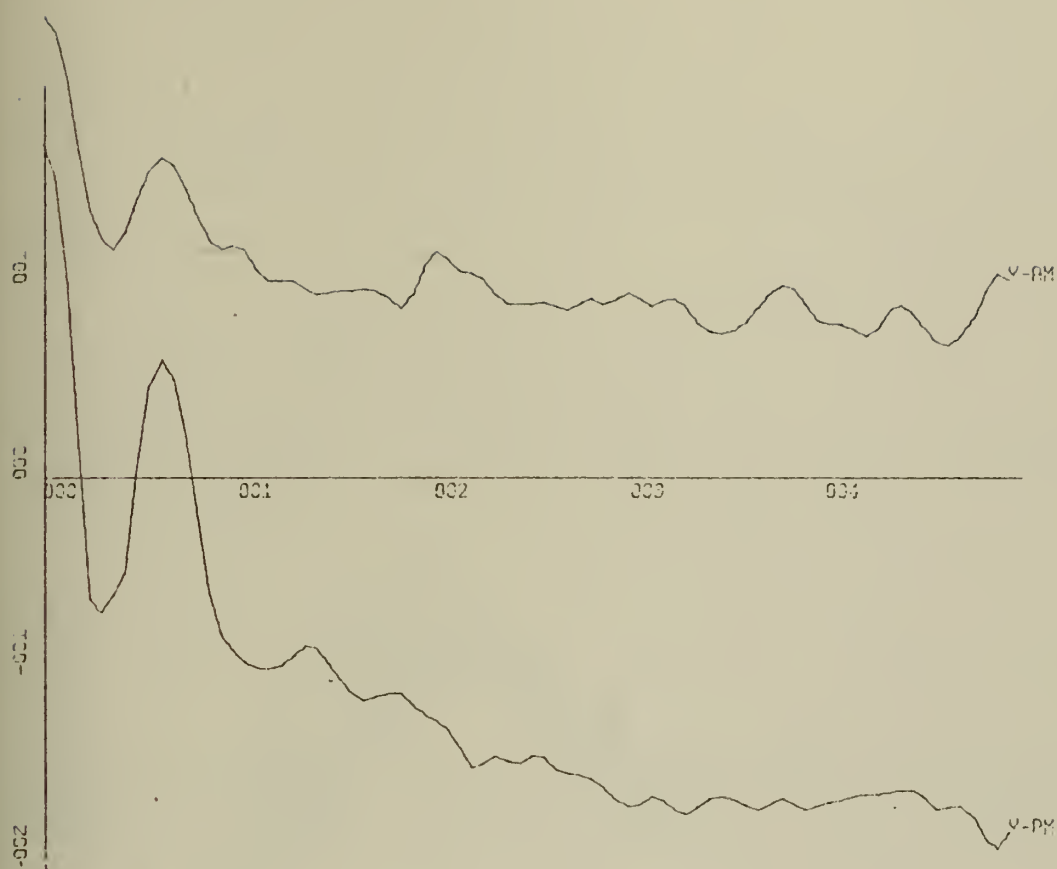


X-SCALE=1.00E-01 UNITS INCH.

Y-SCALE=2.00E+02 UNITS INCH.

CROSS SPECTRAL PHASE ANGLE Z-PM, Z-AM

RUN PH-2

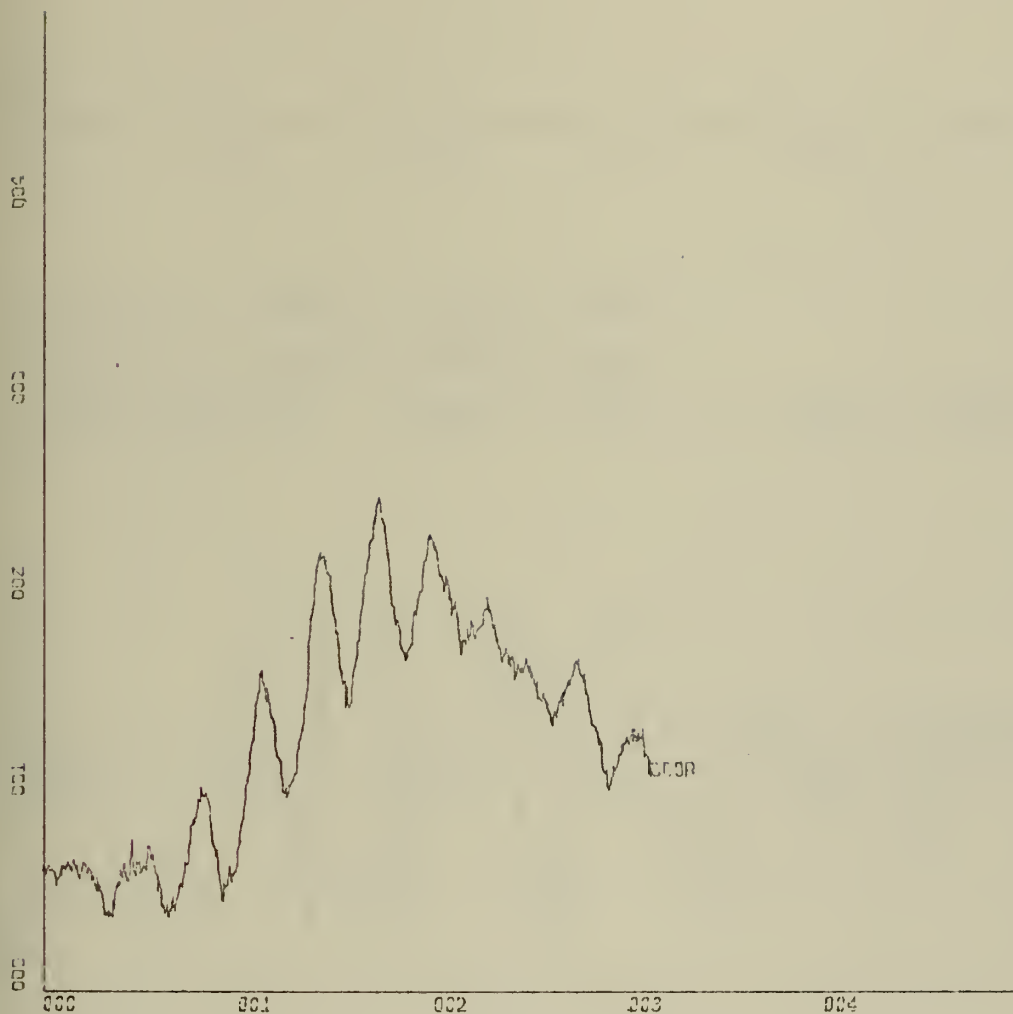


X-SCALE=1.00E-01 UNITS INCH.

Y-SCALE=1.00E+01 UNITS INCH.

POWER SPECTRUM LEVEL (DB) Y-PM, Y-AM

RUN PH-3, FILE 6 OF CON6

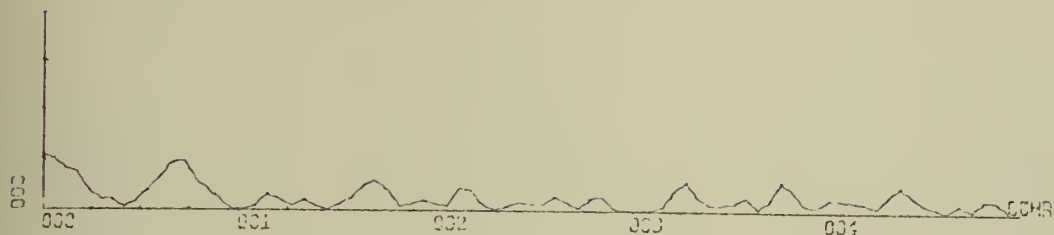


X-SCALE=1.00E+00 UNITS INCH.

Y-SCALE=1.00E-01 UNITS INCH.

CROSS-CORRELATION FN, Y-PM, Y-AM

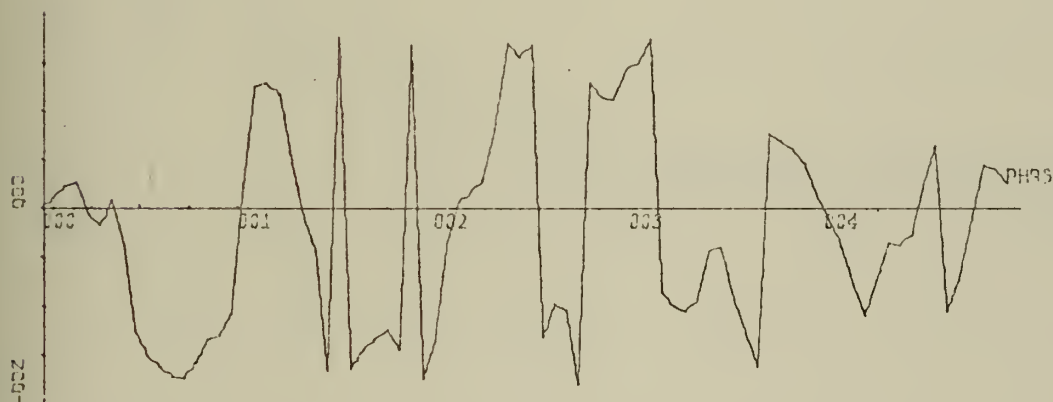
RUN PH-3, FILE 6 OF CCN6



X-SCALE=1.00E-01 UNITS INCH.

Y-SCALE=1.00E+00 UNITS INCH.

COHERENCE FUNCTION Y-PM, Y-AM

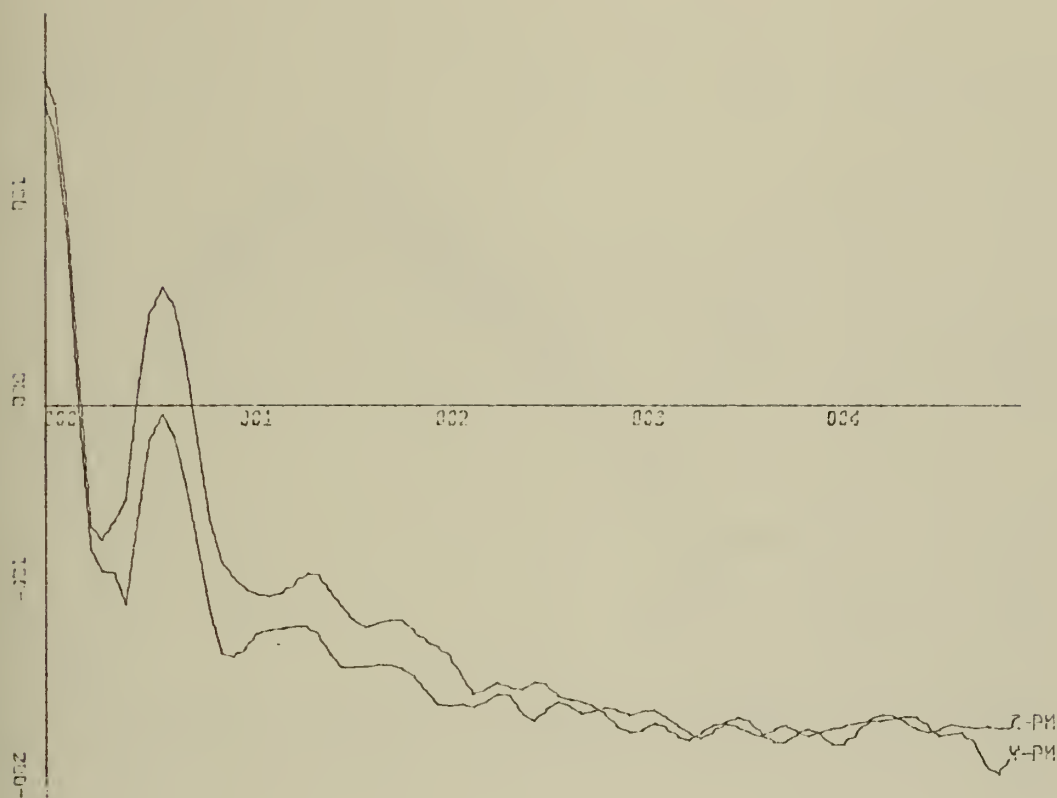


X-SCALE=1.00E-01 UNITS INCH.

Y-SCALE=2.00E+02 UNITS INCH.

CROSS SPECTRAL PHASE ANGLE Y-PM, Y-AM

RUN PH-3

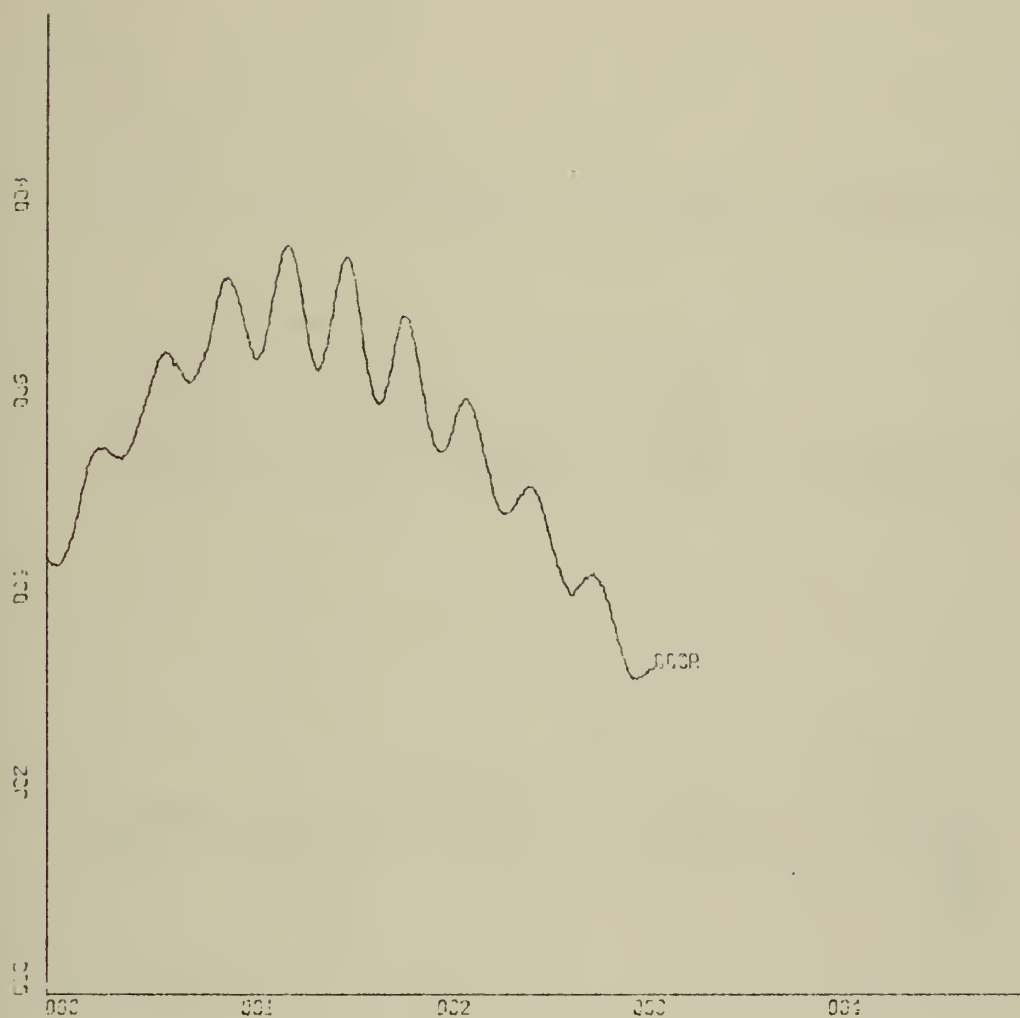


Y-SCALE=1.00E+01 UNITS INCH.

POWER SPECTRUM LEVEL (DB) Y-PM, Z-PM

RUN PH-3, FILE 6 OF CON6

M



X-SCALE:-1.00E+00 UNITS INCH.

Y-SCALE:-2.00E-01 UNITS INCH.

CROSS-CORRELATION FN, Y-PM, Z-PM

RUN PH-3, FILE 6 OF CON6

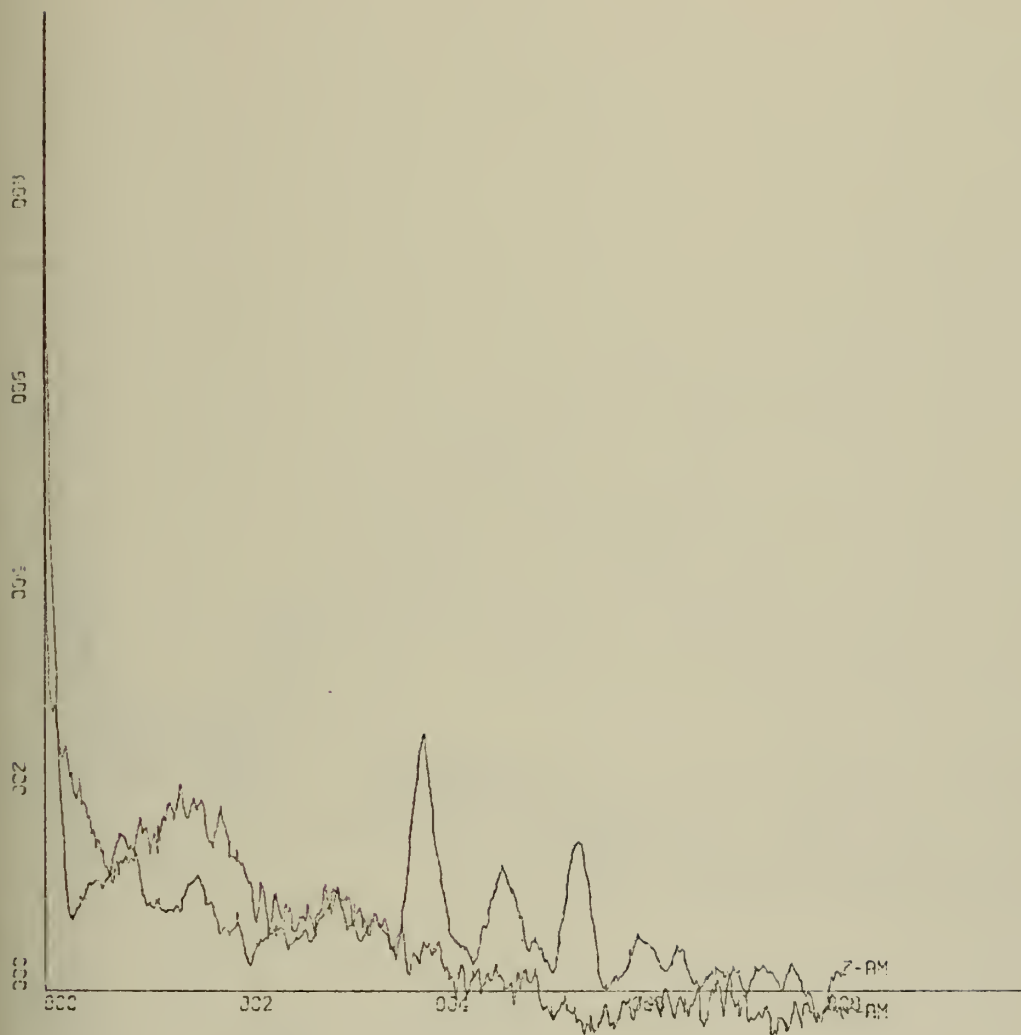


X-SCALE=1.00E-01 UNITS INCH.
 Y-SCALE=1.00E+00 UNITS INCH.
 COHERENCE FUNCTION, Y-PM, Z-PM



X-SCALE=1.00E-01 UNITS INCH.
 Y-SCALE=2.00E+02 UNITS INCH.
 CROSS SPECTRAL PHASE ANGLE Y-PM, Z-PM

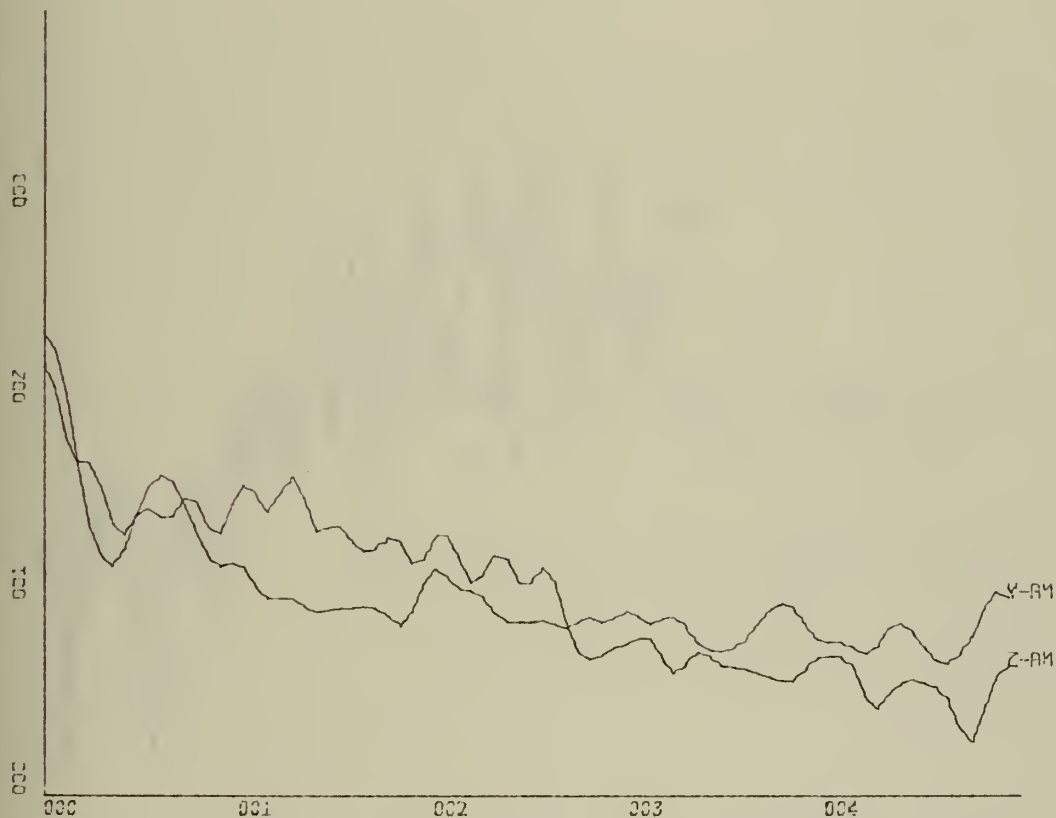
RUN PH-3



X-SCALE=2.00E+01 UNITS INCH.

Y-SCALE=2.00E-01 UNITS INCH.

TEMPORAL AUTOCORRELATION FN, Y-AM, Z-AM
RUN PH-3, FILE 6 OF CON6

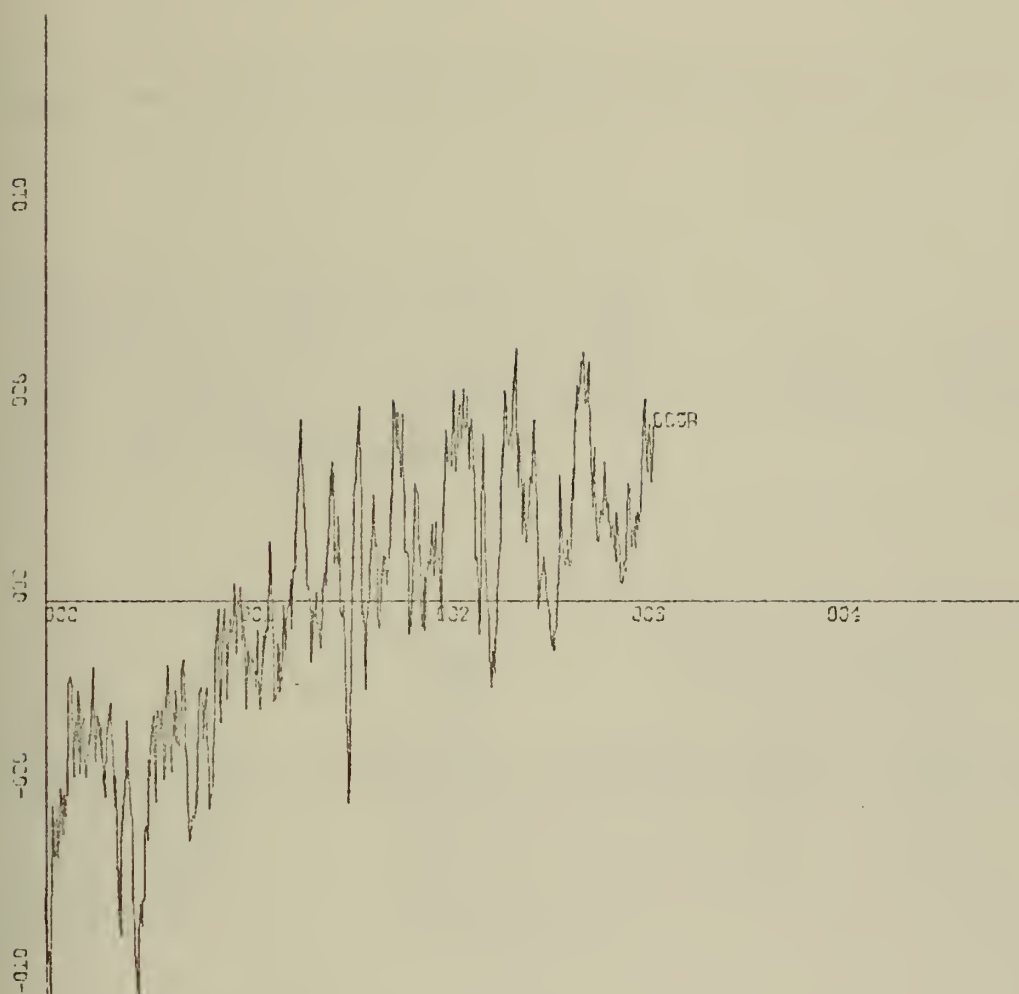


X-SCALE=1.00E-01 UNITS INCH.

Y-SCALE=1.00E+01 UNITS INCH.

POWER SPECTRUM LEVEL (DB) Y-AM, Z-AM

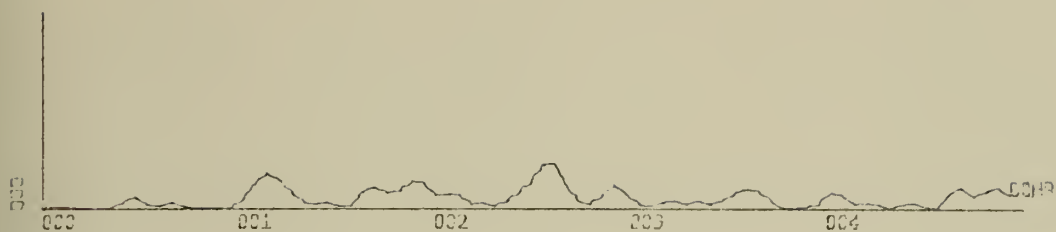
RUN PH-3, FILE 6 OF CON6



X-SCALE=1.00E+00 UNITS INCH.

Y-SCALE=5.00E-02 UNITS INCH.

CROSS-CORRELATION FN, Y-AM, Z-AM
RUN PH-3. FILE 6 OF CON6



X-SCALE=1.00E-01 UNITS INCH.

Y-SCALE=1.00E+00 UNITS INCH.

COHERENCE FUNCTION Y-AM, Z-AM

CH ALEXANDER



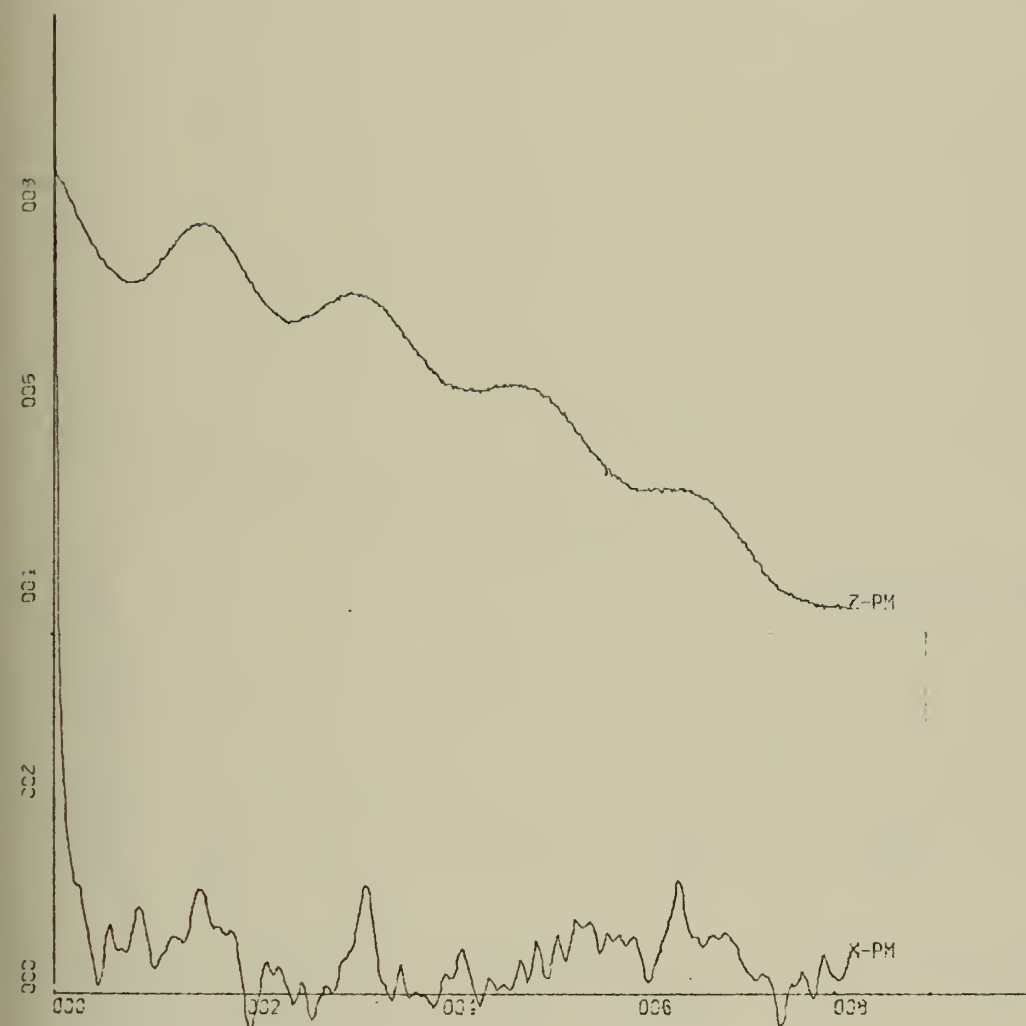
X-SCALE=1.00E-01 UNITS INCH.

Y-SCALE=2.00E+02 UNITS INCH.

CROSS SPECTRAL PHASE ANGLE Y-AM, Z-AM

CH ALEXANDER

RUN PH-3

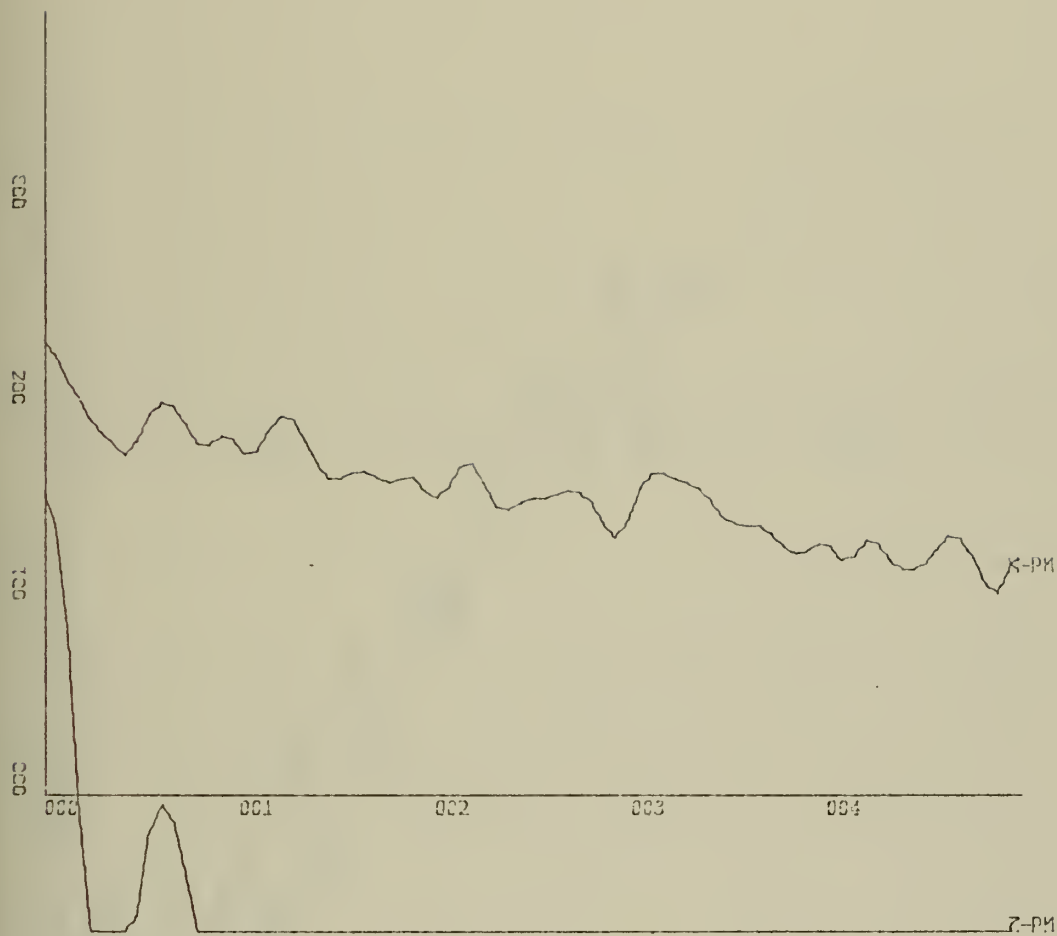


X-SCALE=2.00E+01 UNITS INCH.

Y-SCALE=2.00E-01 UNITS INCH.

TEMPORAL AUTOCORRELATION FN, X-PM, Z-PM

RUN PH-3, FILE 6 OF CON6

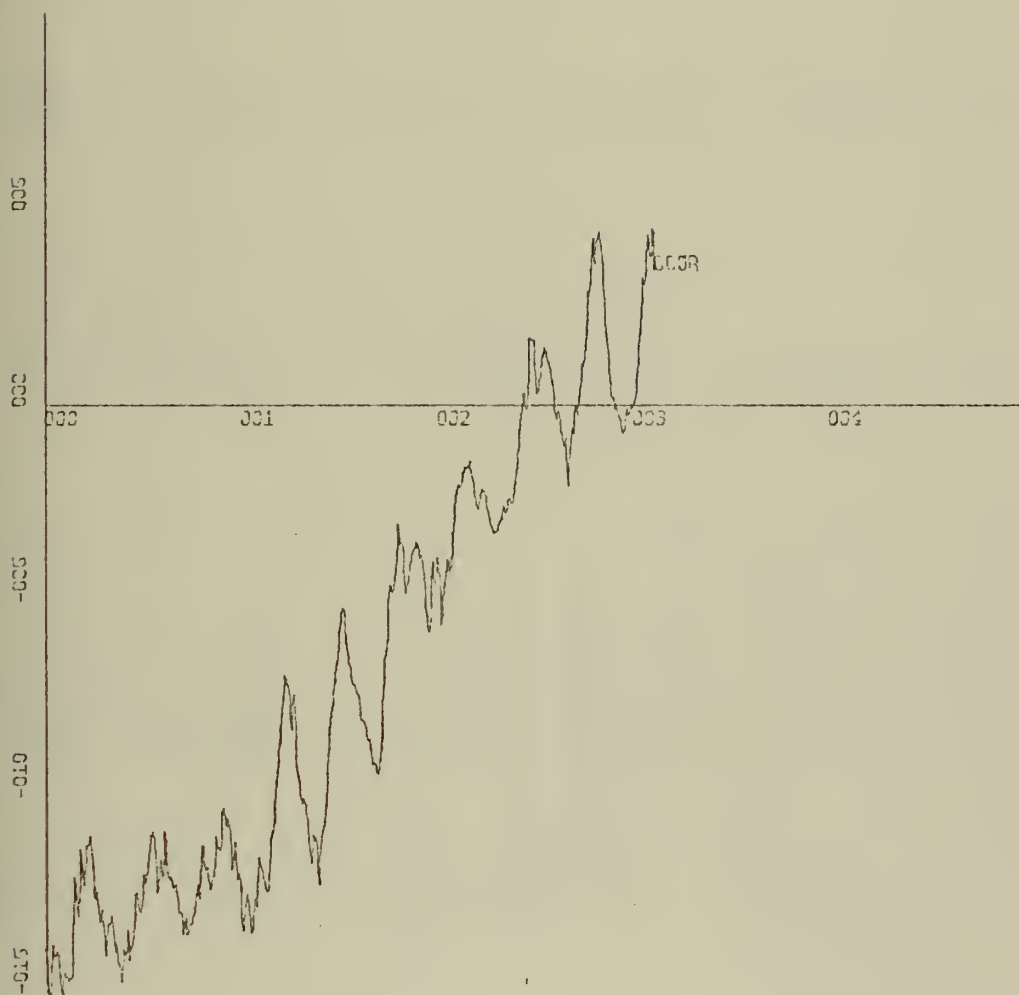


X-SCALE=1.00E-01 UNITS INCH.

Y-SCALE=1.00E+01 UNITS INCH.

POWER SPECTRUM LEVEL (DB) X-PM, Z-PM

RUN PH-3, FILE 6 OF CON6

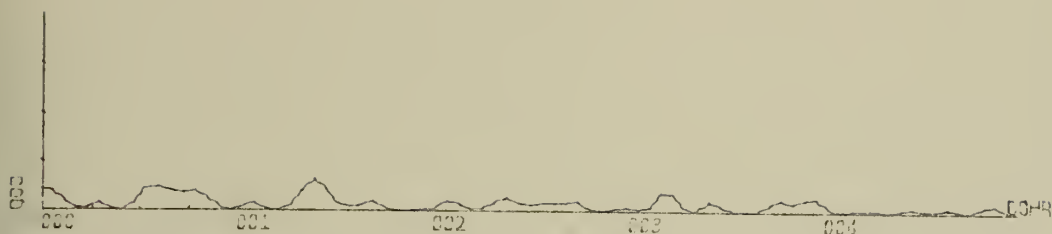


X-SCALE=1.00E+00 UNITS INCH.

Y-SCALE=5.00E-02 UNITS INCH.

CROSS-CORRELATION FN, X-PM, Z-PM

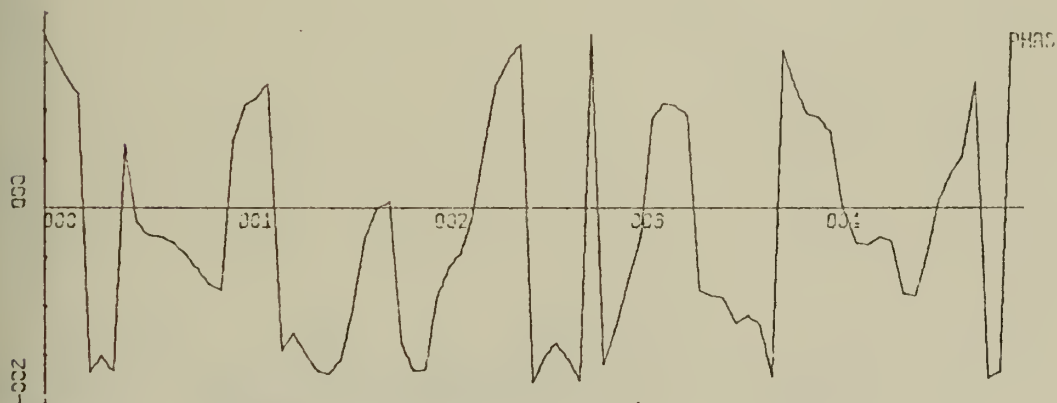
RUN PH-3, FILE 6 OF CON6



X-SCALE=1.00E-01 UNITS INCH.

Y-SCALE=1.00E+00 UNITS INCH.

COHERENCE FUNCTION X-PM, Z-PM

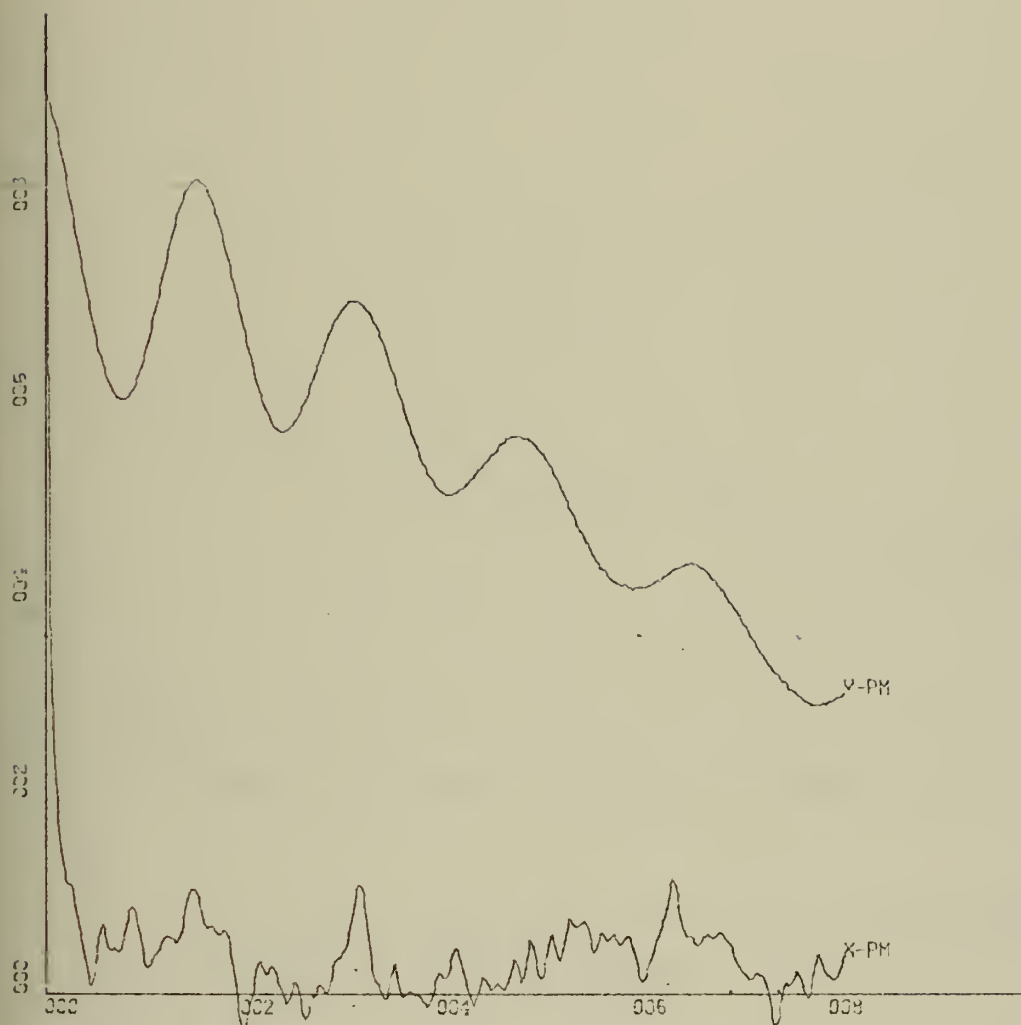


X-SCALE=1.00E-01 UNITS INCH.

Y-SCALE=2.00E+02 UNITS INCH.

CROSS SPECTRAL PHASE ANGLE X-PM, Z-PM

RUN PH-3

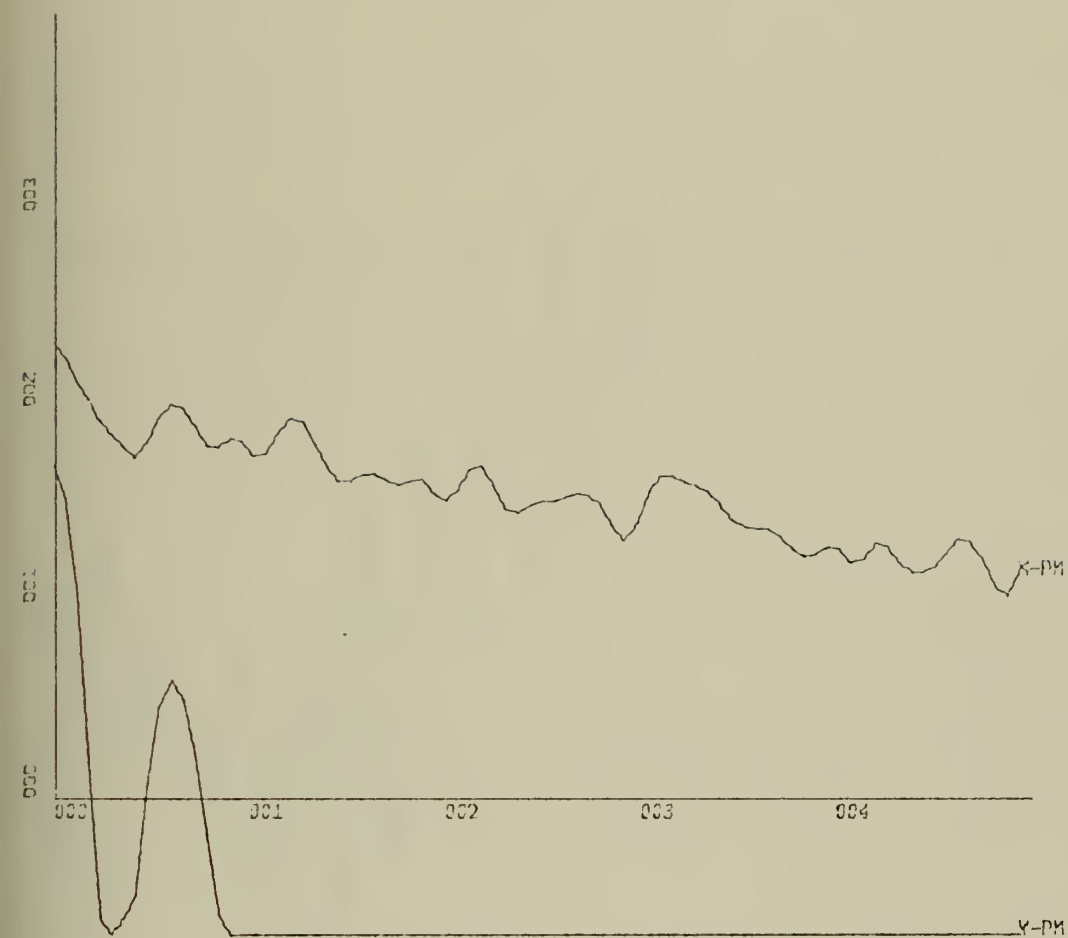


X-SCALE=2.00E+01 UNITS INCH.

Y-SCALE=2.00E-01 UNITS INCH.

TEMPORAL AUTOCORRELATION FN, X-PM, Y-PM

RUN PH-3, FILE 6 OF CON6

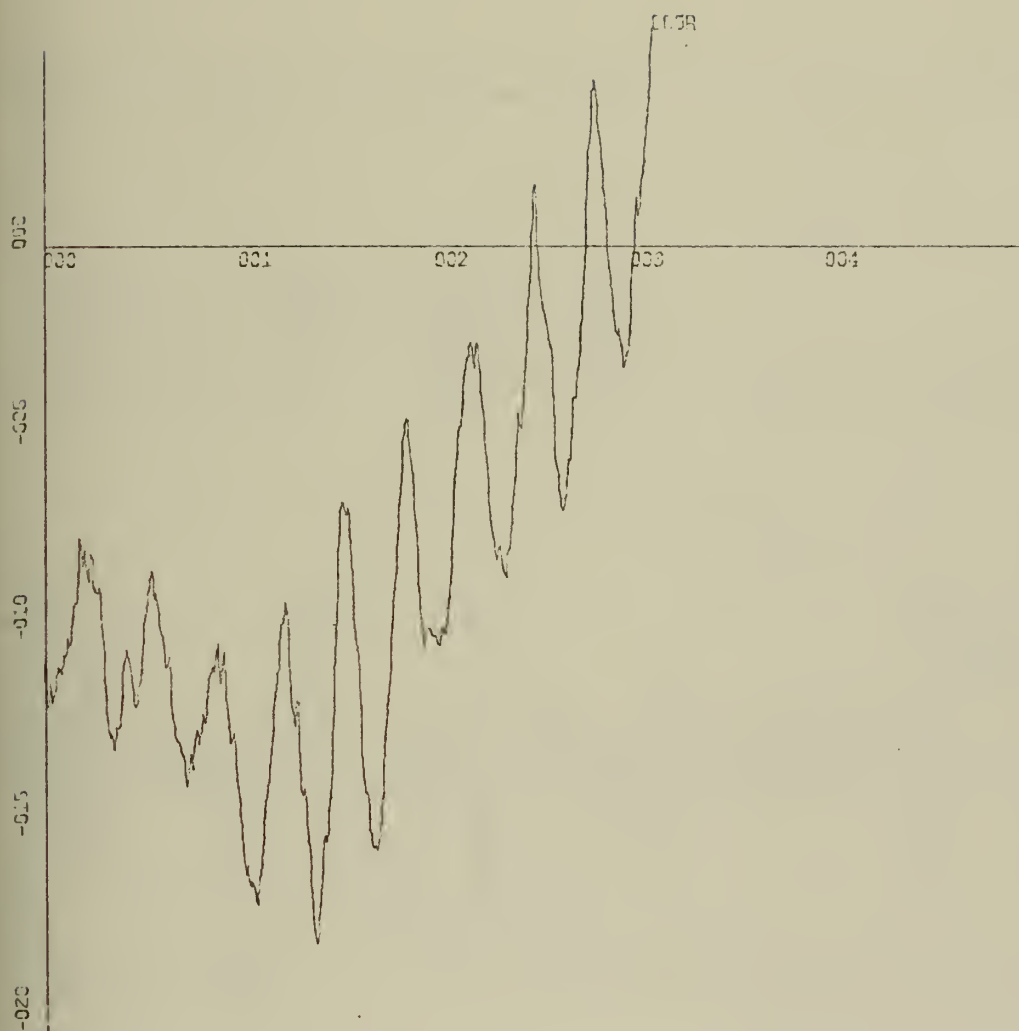


X-SCALE=1.00E-01 UNITS INCH.

Y-SCALE=1.00E+01 UNITS INCH.

POWER SPECTRUM LEVEL (DB) X-PM, Y-PM

RUN PH-3, FILE 6 OF CON6

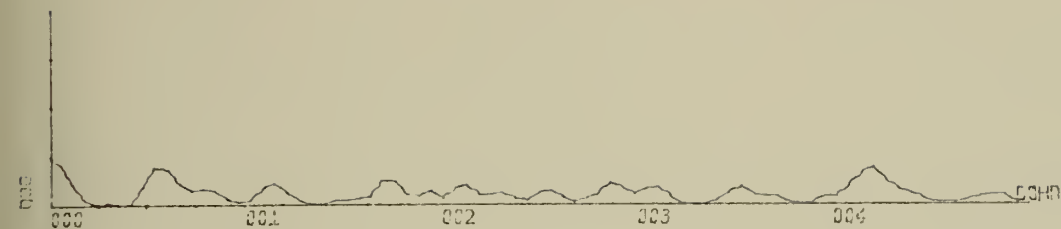


X-SCALE=1.00E+00 UNITS INCH.

Y-SCALE=5.00E-02 UNITS INCH.

CROSS-CORRELATION FN, X-PM, Y-PM

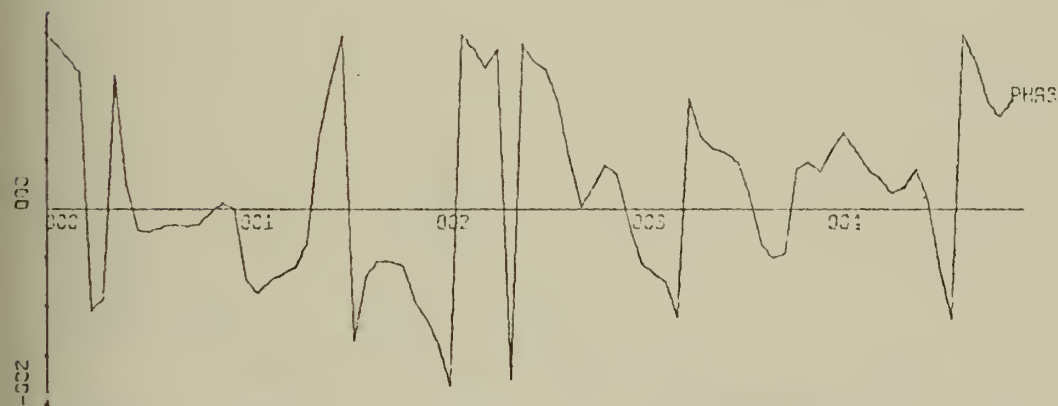
RUN PH-3, FILE 6 OF CON6



X-SCALE=1.00E-01 UNITS INCH.

Y-SCALE=1.00E+00 UNITS INCH.

COHERENCE FUNCTION X-PM, Y-PM

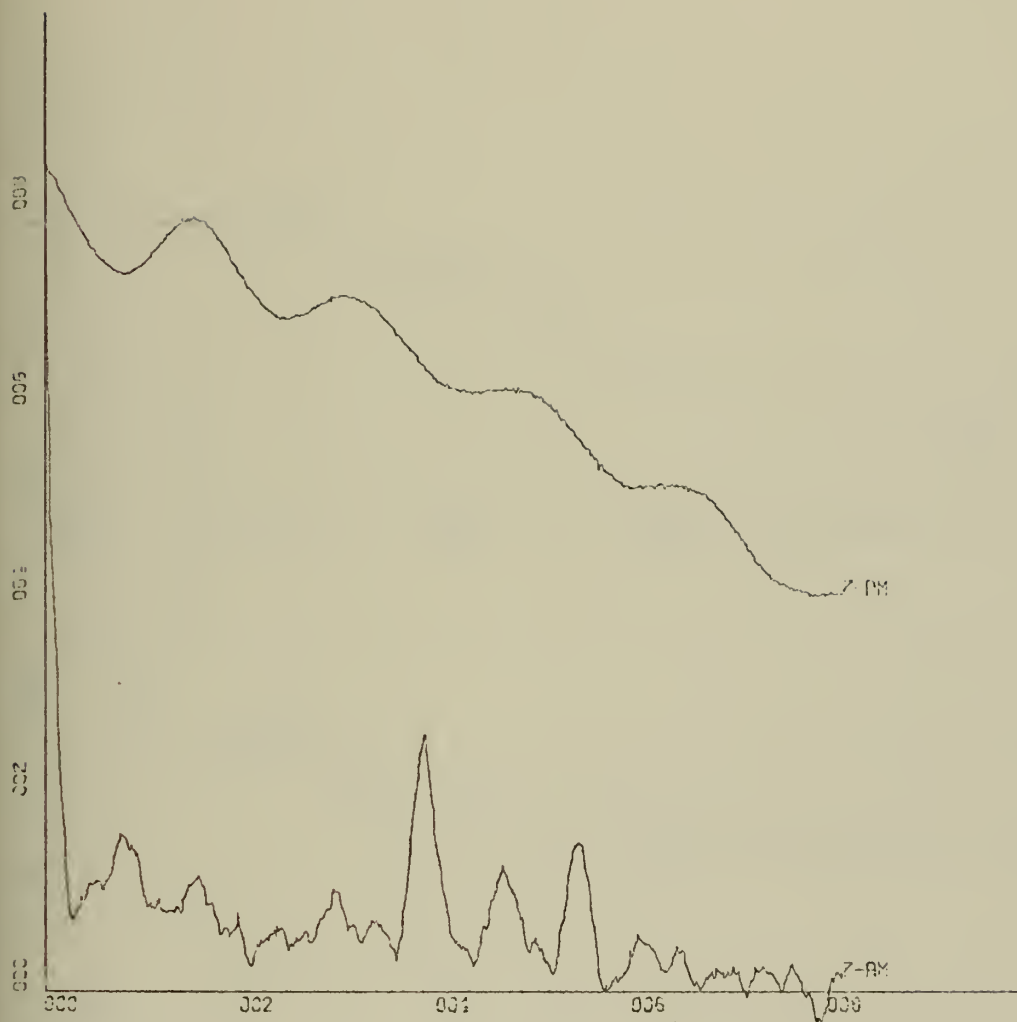


X-SCALE=1.00E-01 UNITS INCH.

Y-SCALE=2.00E+02 UNITS INCH.

CROSS SPECTRAL PHASE ANGLE X-PM, Y-PM

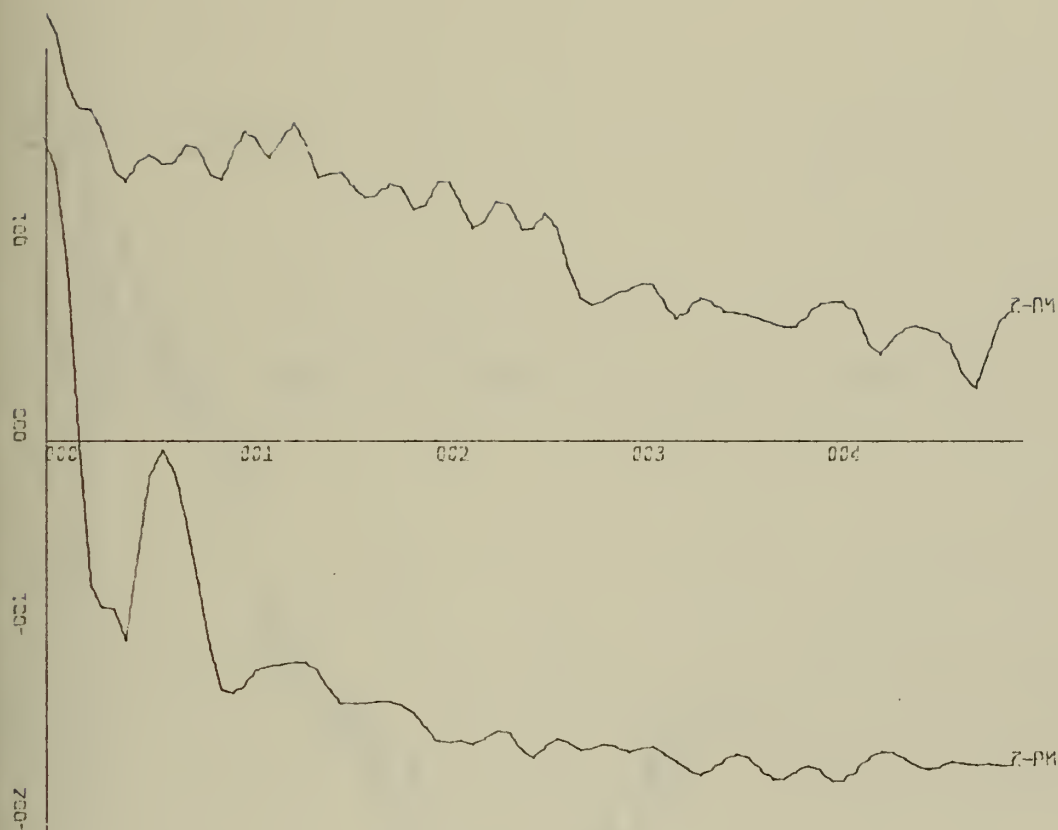
RUN PH-3



X-SCALE=2.00E+01 UNITS INCH.

Y-SCALE=2.00E-01 UNITS INCH.

TEMPORAL AUTOCORRELATION FN, Z-PM, Z-AM
 RUN PH-3, FILE 6 OF CON6

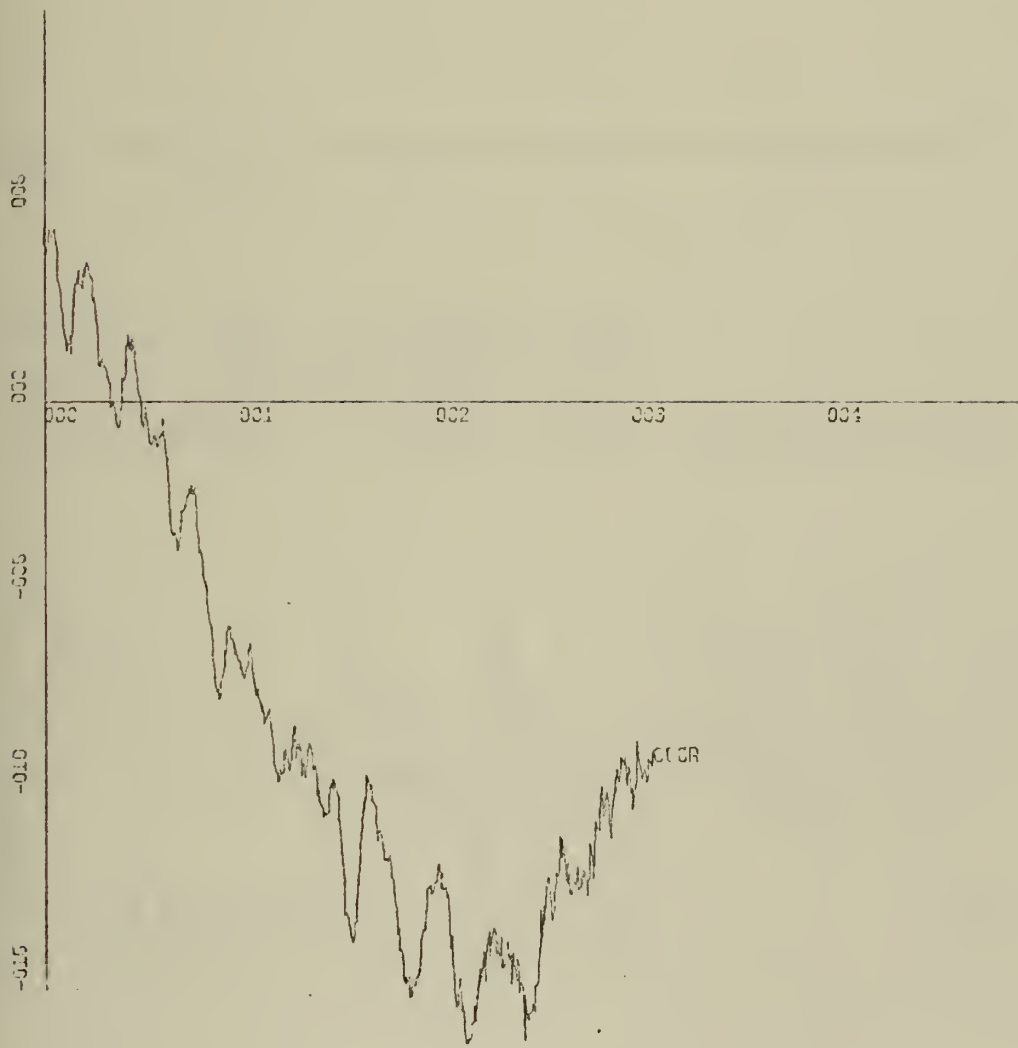


X-SCALE=1.00E-01 UNITS. INCH.

Y-SCALE=1.00E+01 UNITS INCH.

POWER SPECTRUM LEVEL (DB) Z-PM, Z-AM

RUN PH-3, FILE 6 OF CON6

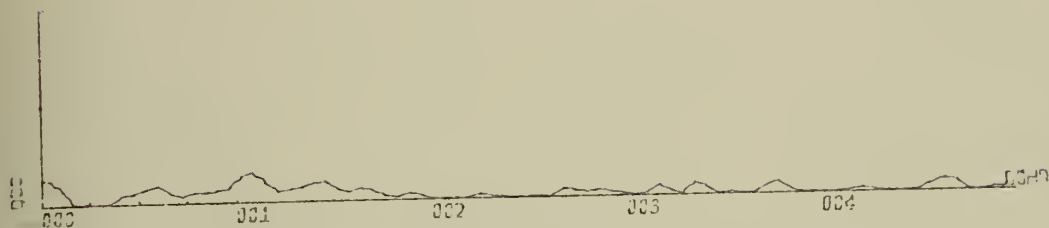


X-SCALE=1.00E+00 UNITS INCH.

Y-SCALE=5.00E-02 UNITS INCH.

CROSS-CORRELATION FN, Z-PM, Z-AM

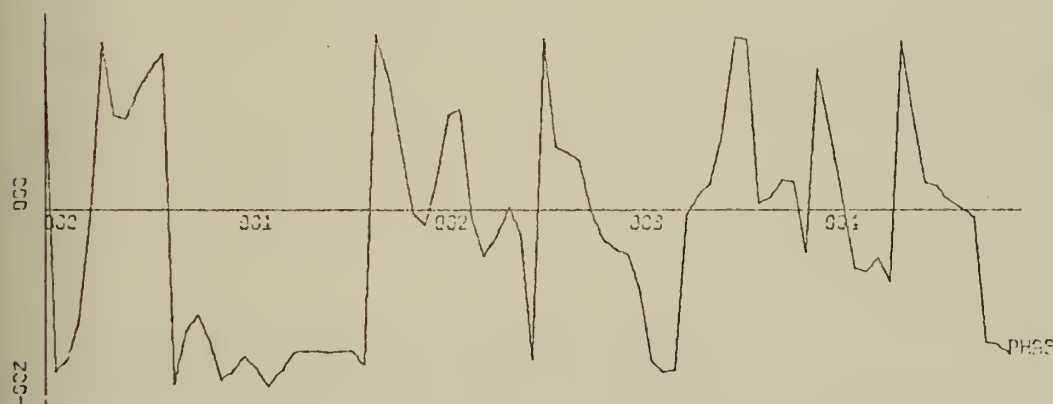
RUN PH-3, FILE 6 OF CON6



X-SCALE=1.00E-01 UNITS INCH.

Y-SCALE=1.00E+00 UNITS INCH.

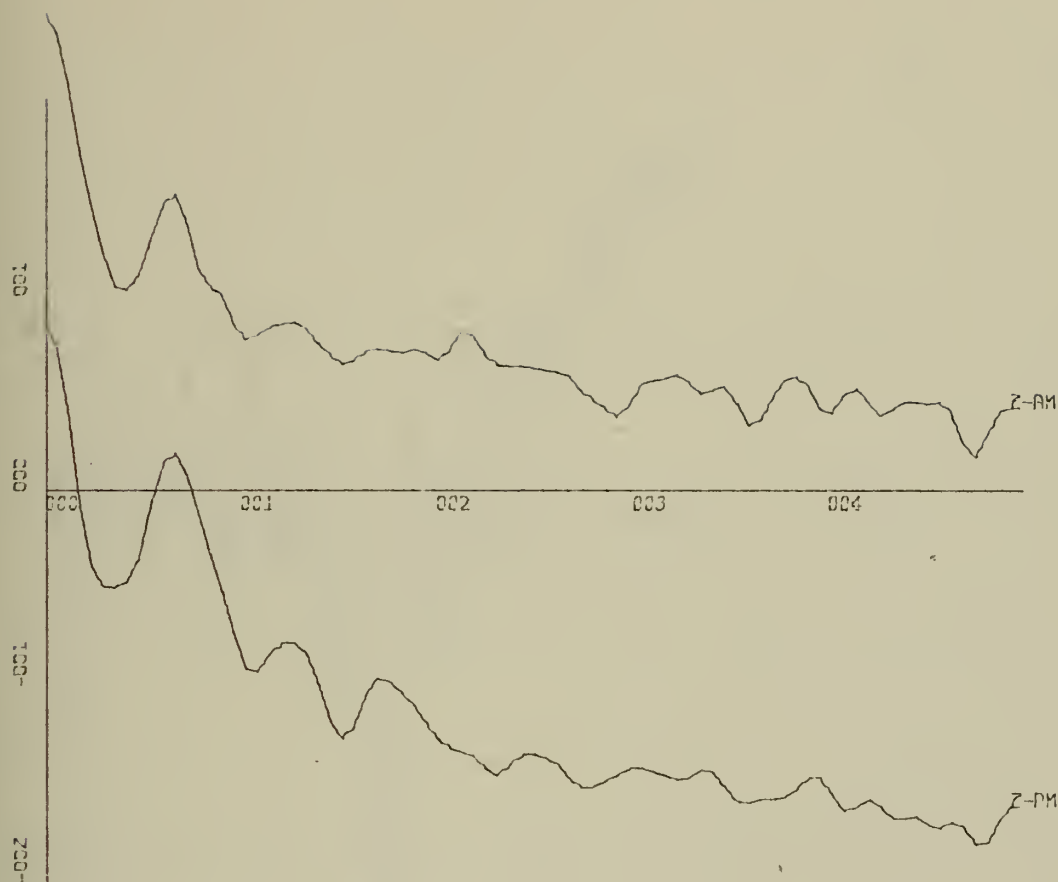
COHERENCE FUNCTION Z-PM, Z-AM



X-SCALE=1.00E-01 UNITS INCH.

Y-SCALE=2.00E+02 UNITS INCH.

CROSS SPECTRAL PHASE ANGLE Z-PM, Z-AM

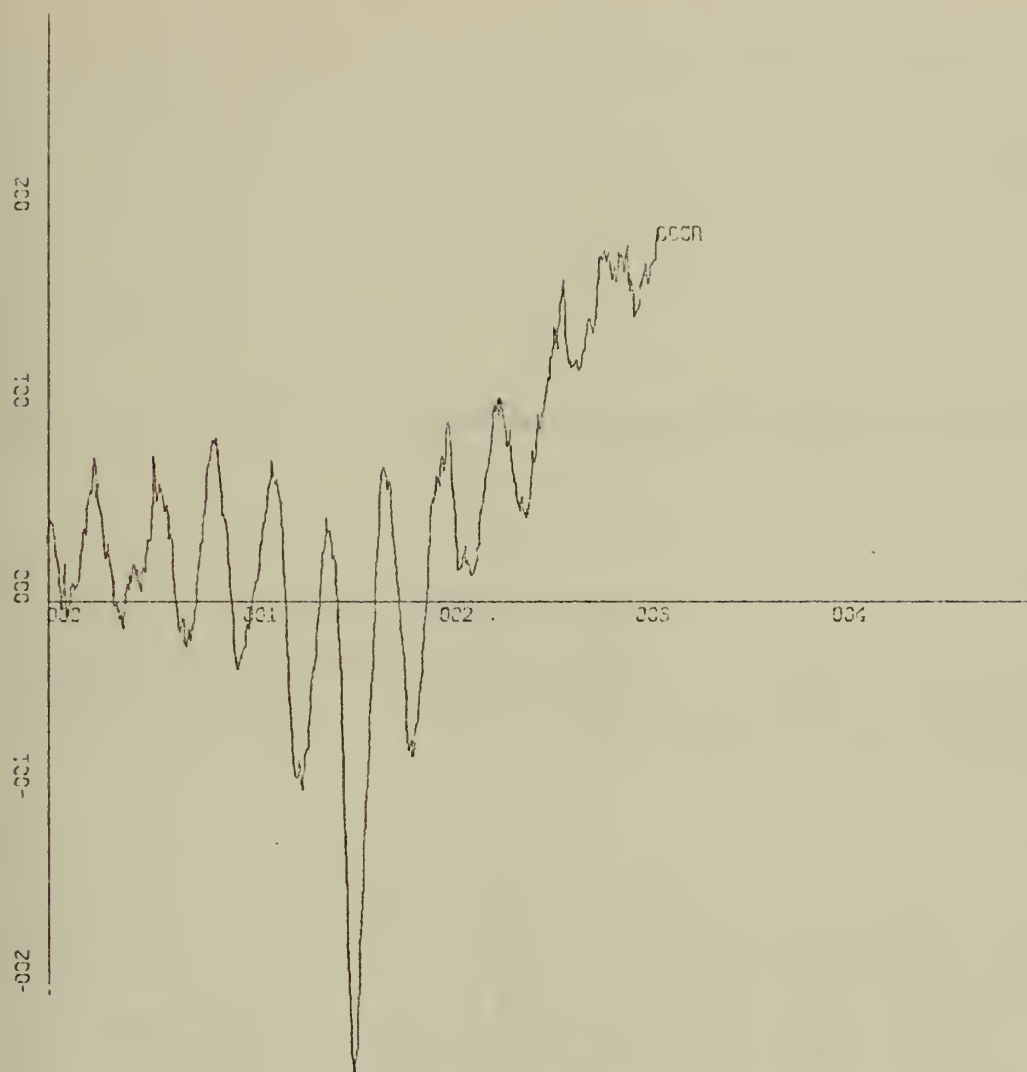


X-SCALE=1.00E-01 UNITS INCH.

Y-SCALE=1.00E+01 UNITS INCH.

POWER SPECTRUM LEVEL (DB) Z-PM, Z-AM

RUN PH-4, FILE 7 OF CON6

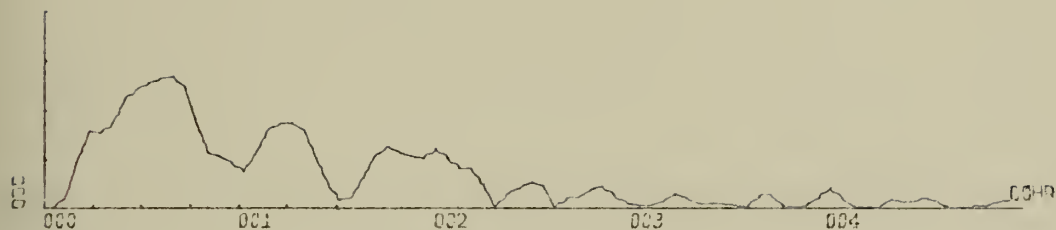


X-SCALE=1.00E+00 UNITS INCH.

Y-SCALE=1.00E-01 UNITS INCH.

CROSS-CORRELATION FN, Z-PM, Z-AM

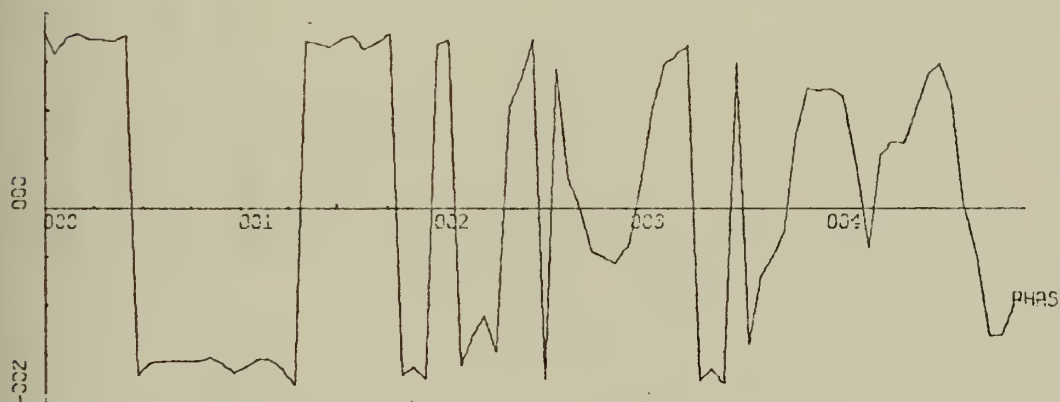
RUN PH-4, FILE 7 OF CON6



X-SCALE=1.00E-01 UNITS INCH.

Y-SCALE=1.00E+00 UNITS INCH.

COHERENCE FUNCTION Z-PM, Z-AM

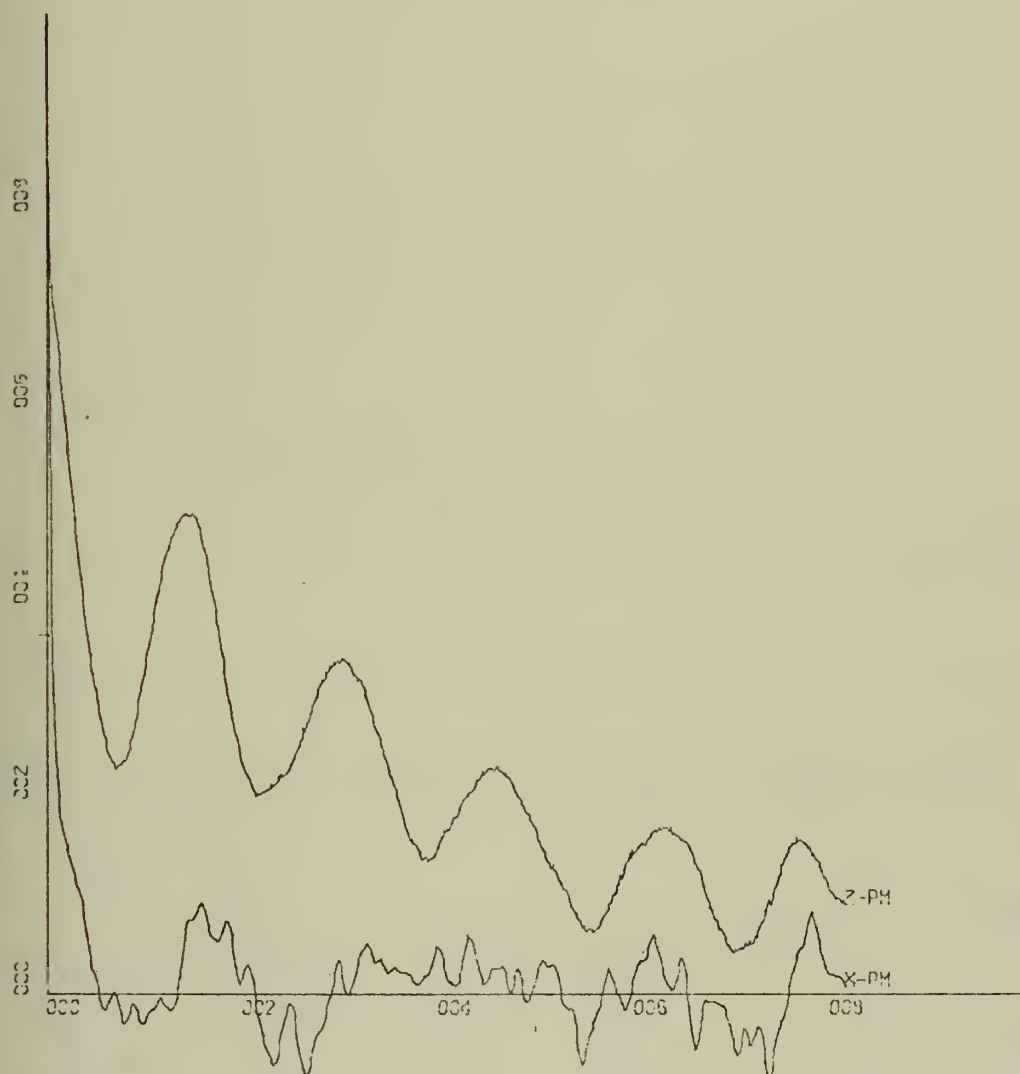


X-SCALE=1.00E-01 UNITS INCH.

Y-SCALE=2.00E+02 UNITS INCH.

CROSS SPECTRAL PHASE ANGLE, Z-PM, Z-AM

RUN PH-4

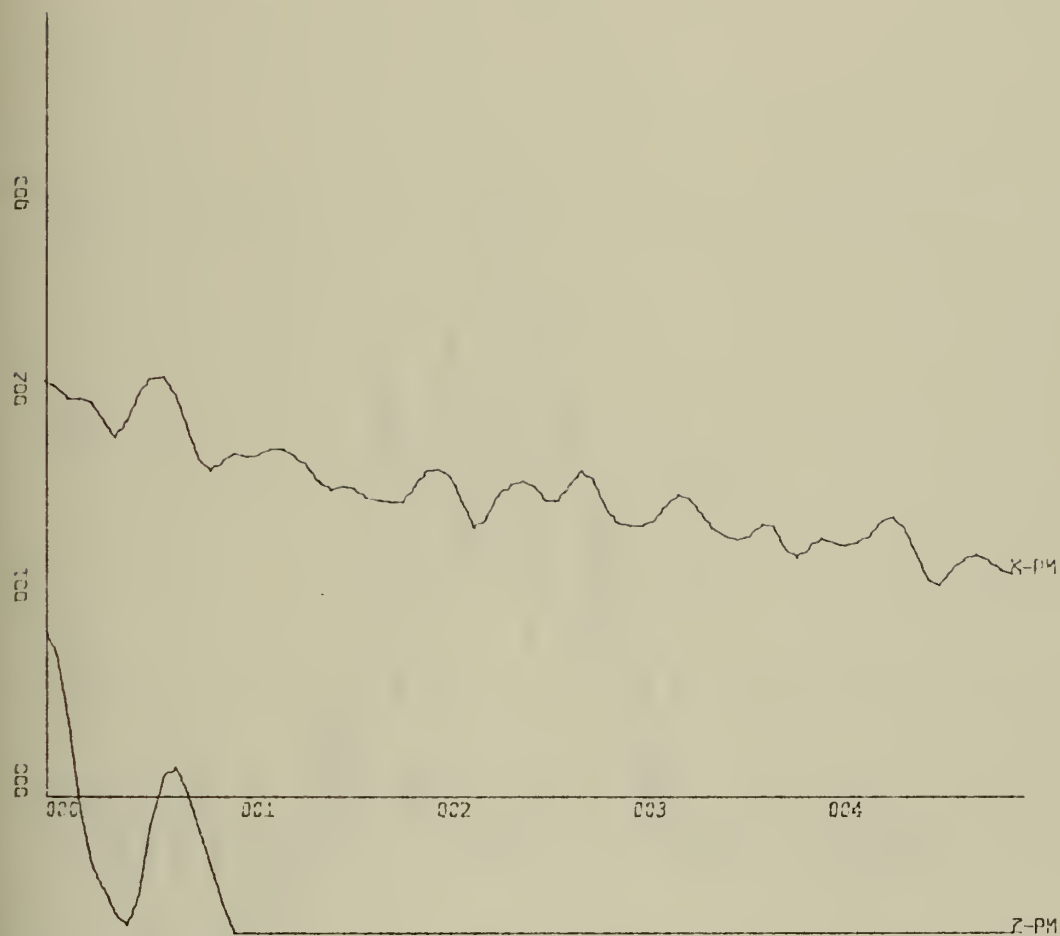


X-SCALE=2.00E+01 UNITS INCH.

Y-SCALE=2.00E-01 UNITS INCH.

TEMPORAL AUTOCORRELATION FN, X-PM, Z-PM

RUN PH-4, FILE 7 OF CON6

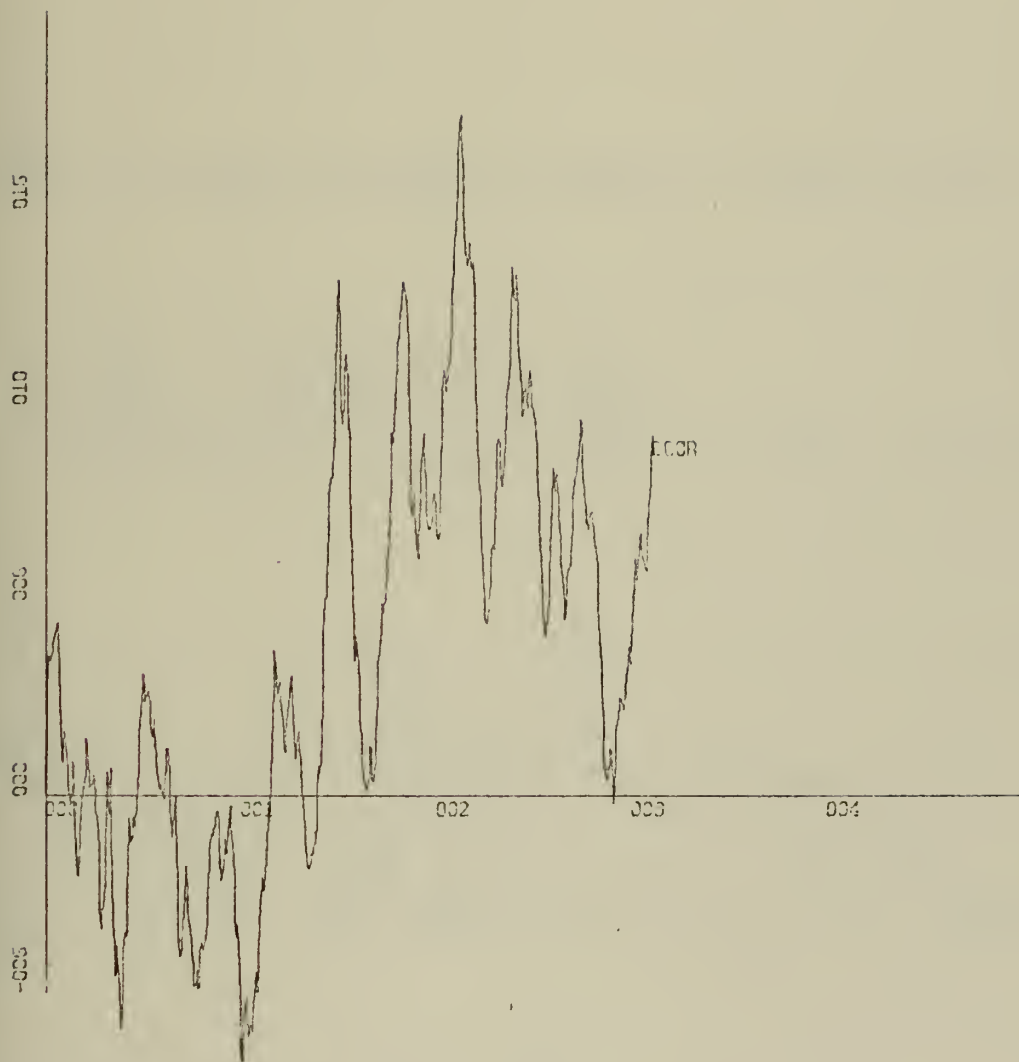


X-SCALE=1.00E-01 UNITS INCH.

Y-SCALE=1.00E+01 UNITS INCH.

POWER SPECTRUM LEVEL (DB) X-PM, Z-PM

RUN PH-4, FILE 7 OF CON6

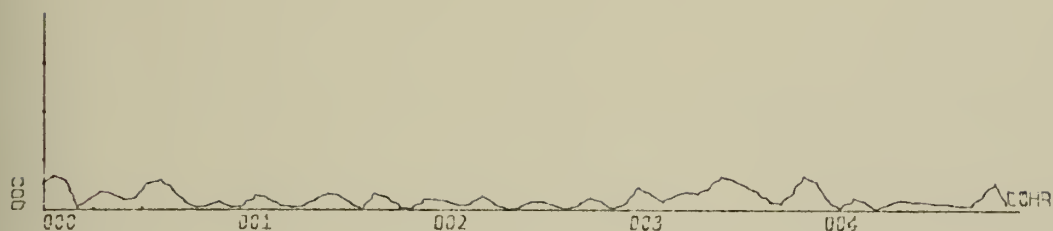


X-SCALE=1.00E+00 UNITS INCH.

Y-SCALE=5.00E-02 UNITS INCH.

CROSS-CORRELATION FN, X-PM, Z-PM

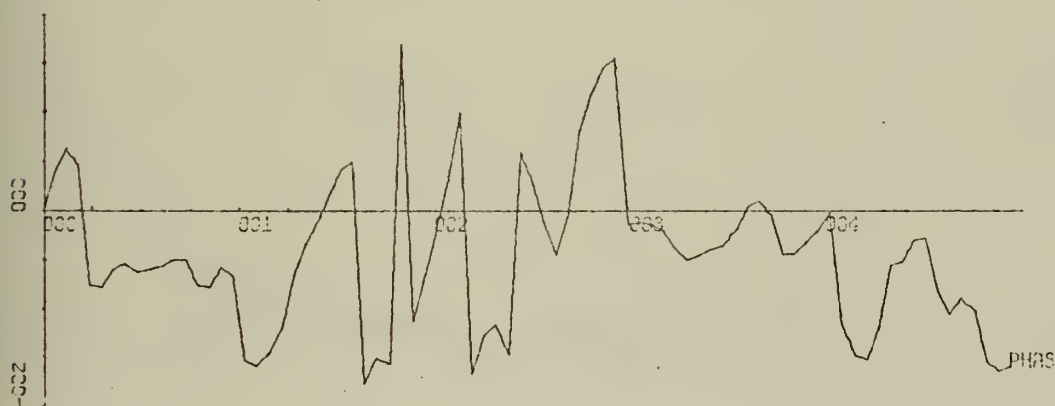
RUN PH-4, FILE 7 OF CON6



X-SCALE=1.00E-01 UNITS INCH.

Y-SCALE=1.00E+00 UNITS INCH.

COHERENCE FUNCTION X-PM, Z-PM

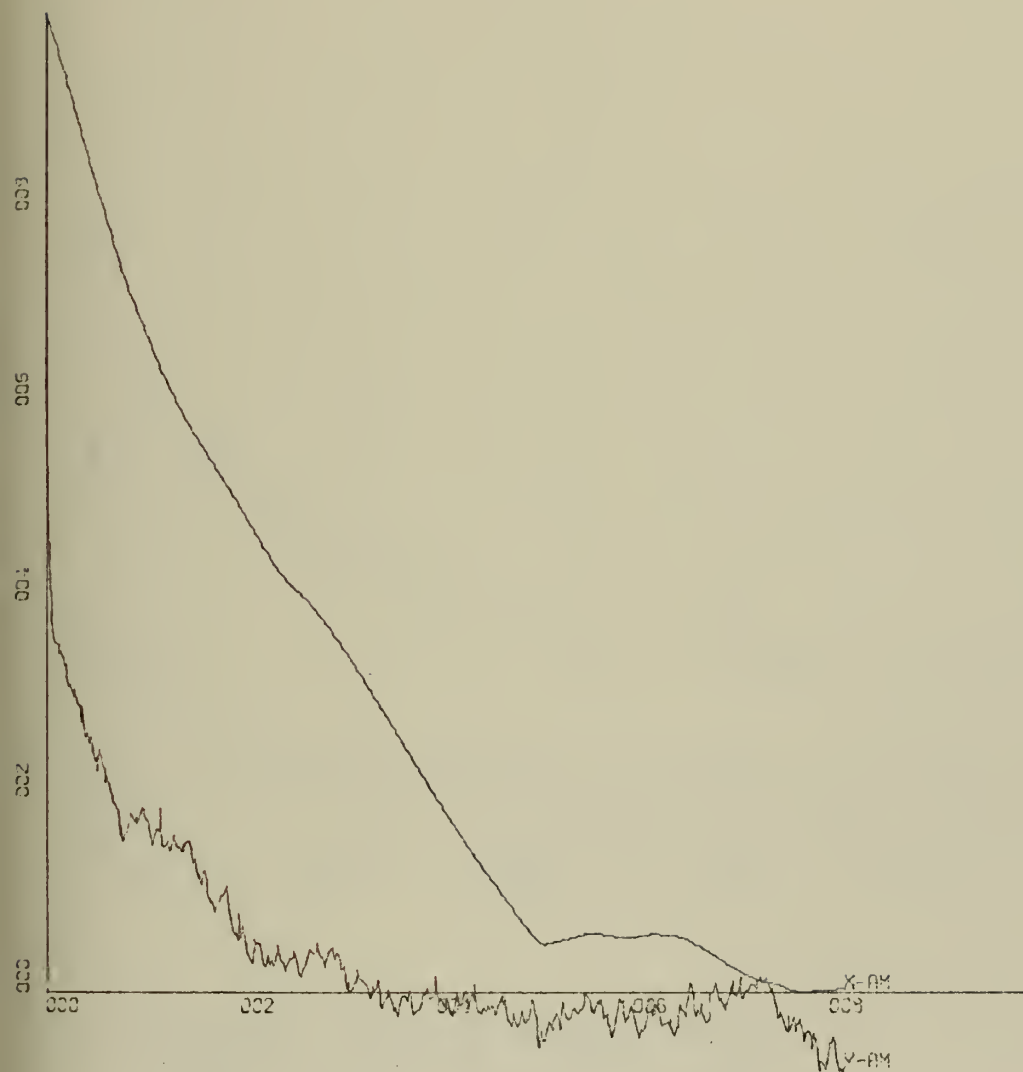


X-SCALE=1.00E-01 UNITS INCH.

Y-SCALE=2.00E+02 UNITS INCH.

CROSS SPECTRAL PHASE ANGLE, X-PM, Z-PM

RUN PH-4



X-SCALE=-2.00E+01 UNITS INCH.

Y-SCALE=-2.00E-01 UNITS INCH.

TEMPORAL AUTOCORRELATION FN, X-AM, Y-AM
 RUN PH-4, FILE 7 OF CON6

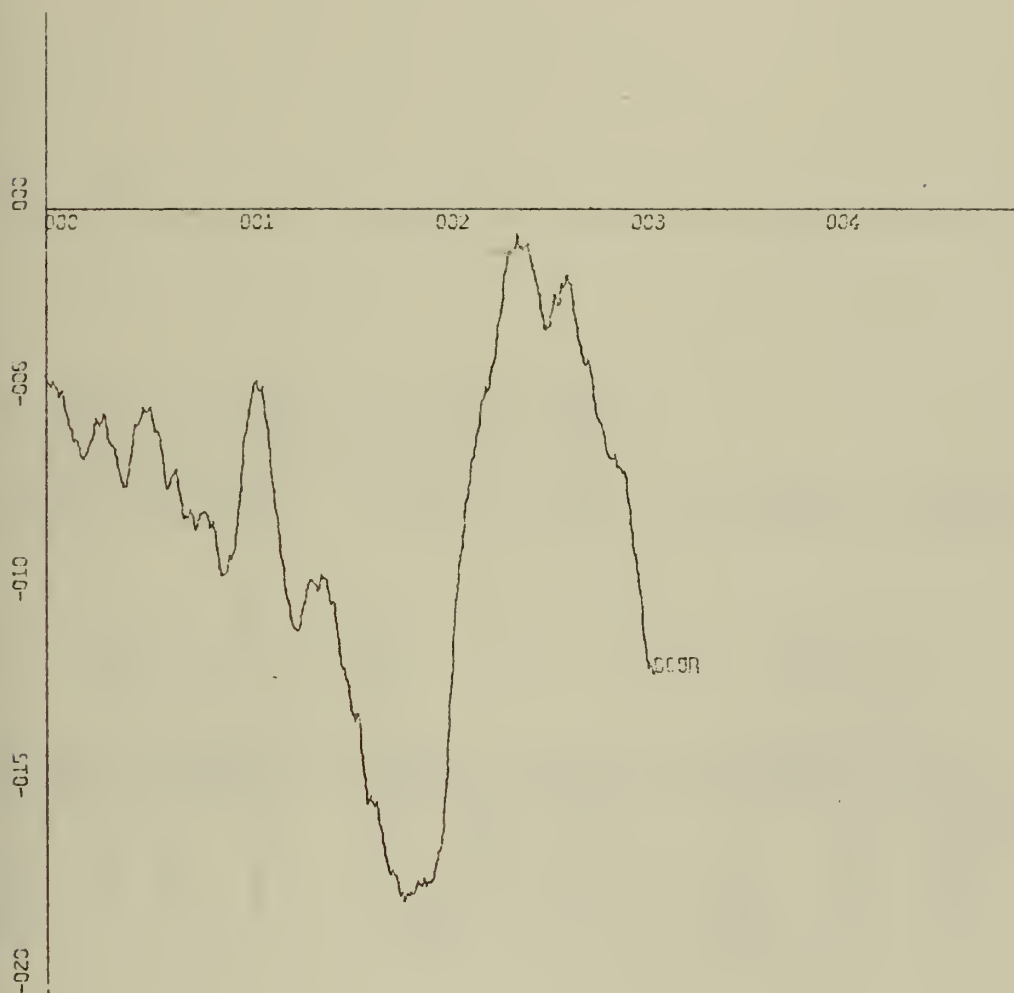


X-SCALE=1.00E-01 UNITS INCH.

Y-SCALE=2.00E+01 UNITS INCH.

POWER SPECTRUM LEVEL (DB) X-AM, Y-AM

RUN PH-4, FILE 7 OF CON6

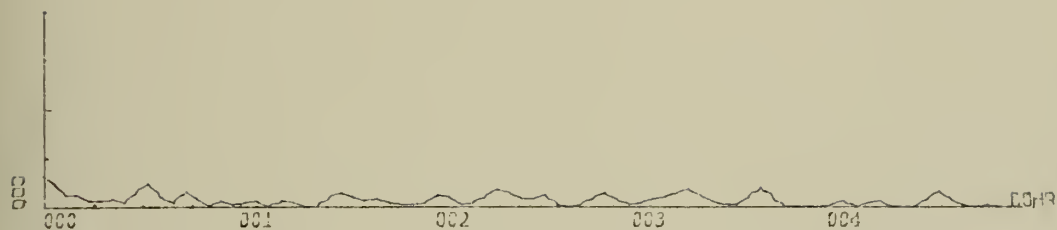


X-SCALE=1.00E+00 UNITS INCH.

Y-SCALE=5.00E-02 UNITS INCH.

CROSS-CORRELATION FN, X-AM, Y-AM

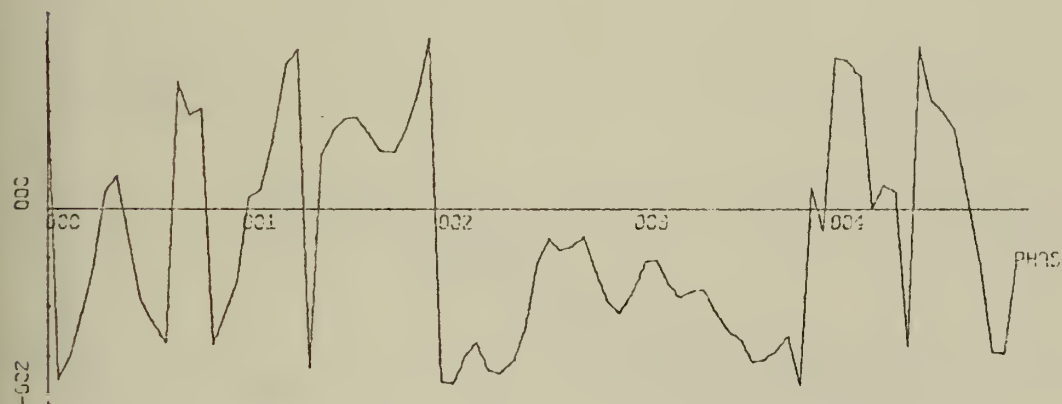
RUN PH-4, FILE 7 OF CON6



X-SCALE= $1.00E-01$ UNITS INCH.

Y-SCALE= $1.00E+00$ UNITS INCH.

COHERENCE FUNCTION X-AM, Y-AM

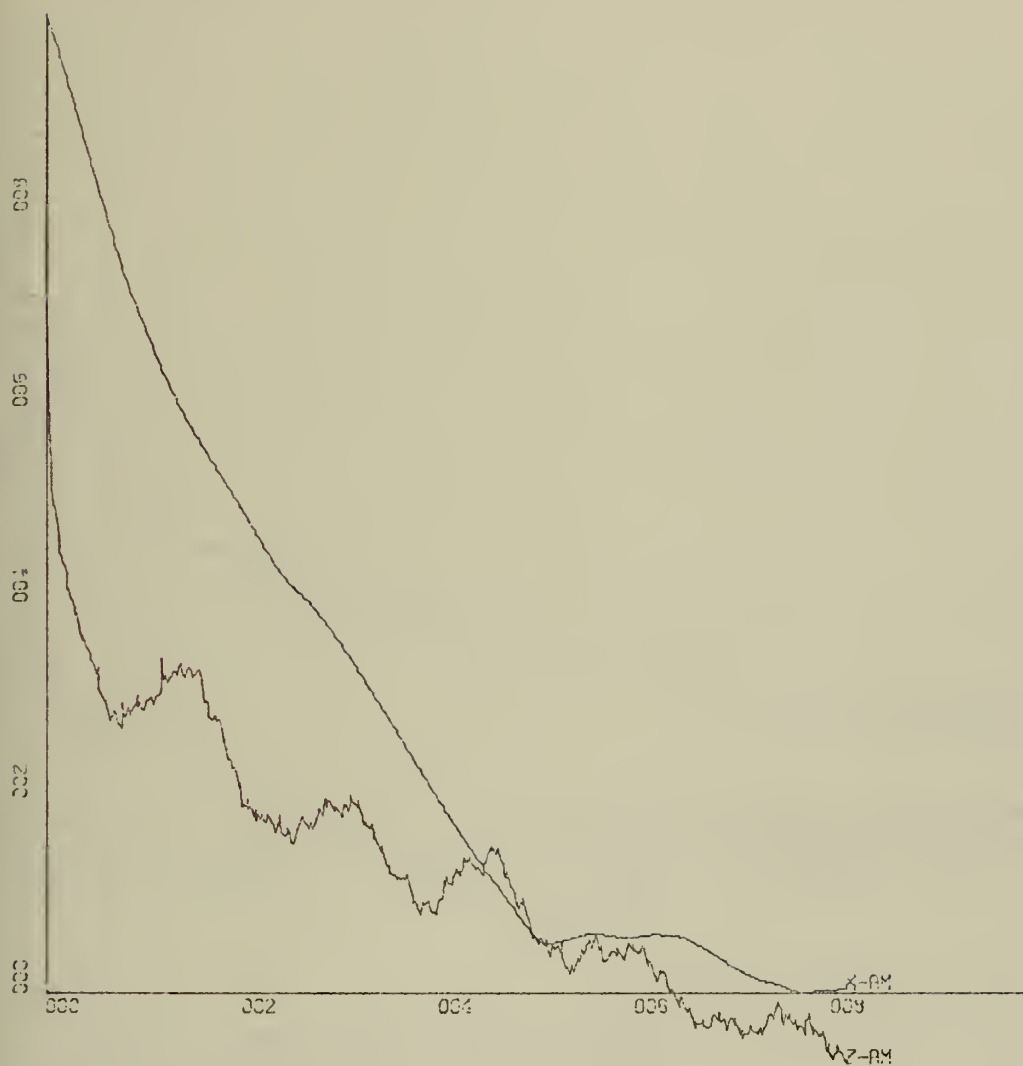


X-SCALE= $1.00E-01$ UNITS INCH.

Y-SCALE= $2.00E+02$ UNITS INCH.

CROSS SPECTRAL PHASE ANGLE, X-AM, Y-AM

RUN PH-4



X-SCALE:-2.00E+01 UNITS INCH.

Y-SCALE:-2.00E-01 UNITS INCH.

TEMPORAL AUTOCORRELATION FN, X-AM, Z-AM

RUN PH-4, FILE 7 OF CON6



X-SCALE=1.00E-01 UNITS INCH.

Y-SCALE=2.00E+01 UNITS INCH.

POWER SPECTRUM LEVEL (DB) X-AM, Z-AM

RUN PH-4, FILE 7 OF CON6

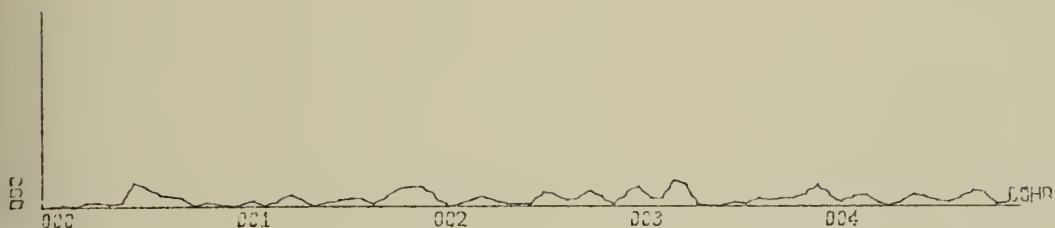


X-SCALE=1.00E+00 UNITS INCH.

Y-SCALE=1.00E-01 UNITS INCH.

CROSS-CORRELATION FN, X-AM, Z-AM

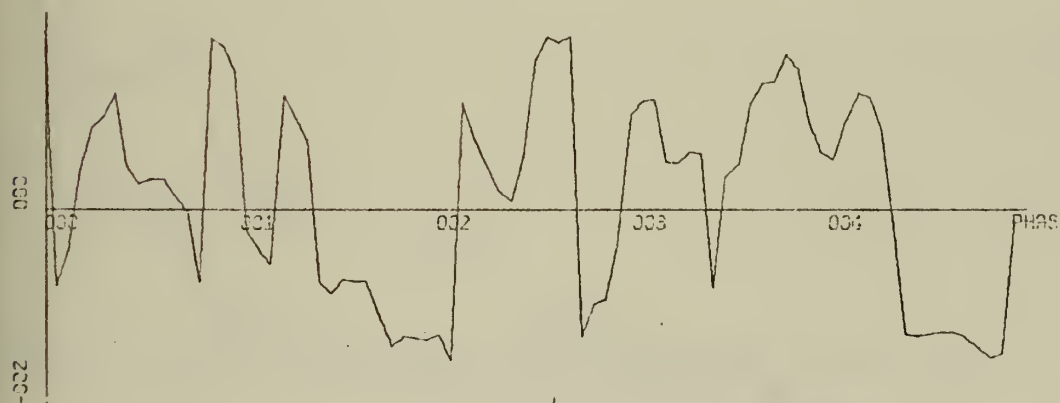
RUN PH-4, FILE 7 OF CON6



X-SCALE=1.00E-01 UNITS INCH.

Y-SCALE=1.00E+00 UNITS INCH.

COHERENCE FUNCTION, X-AM, Z-AM

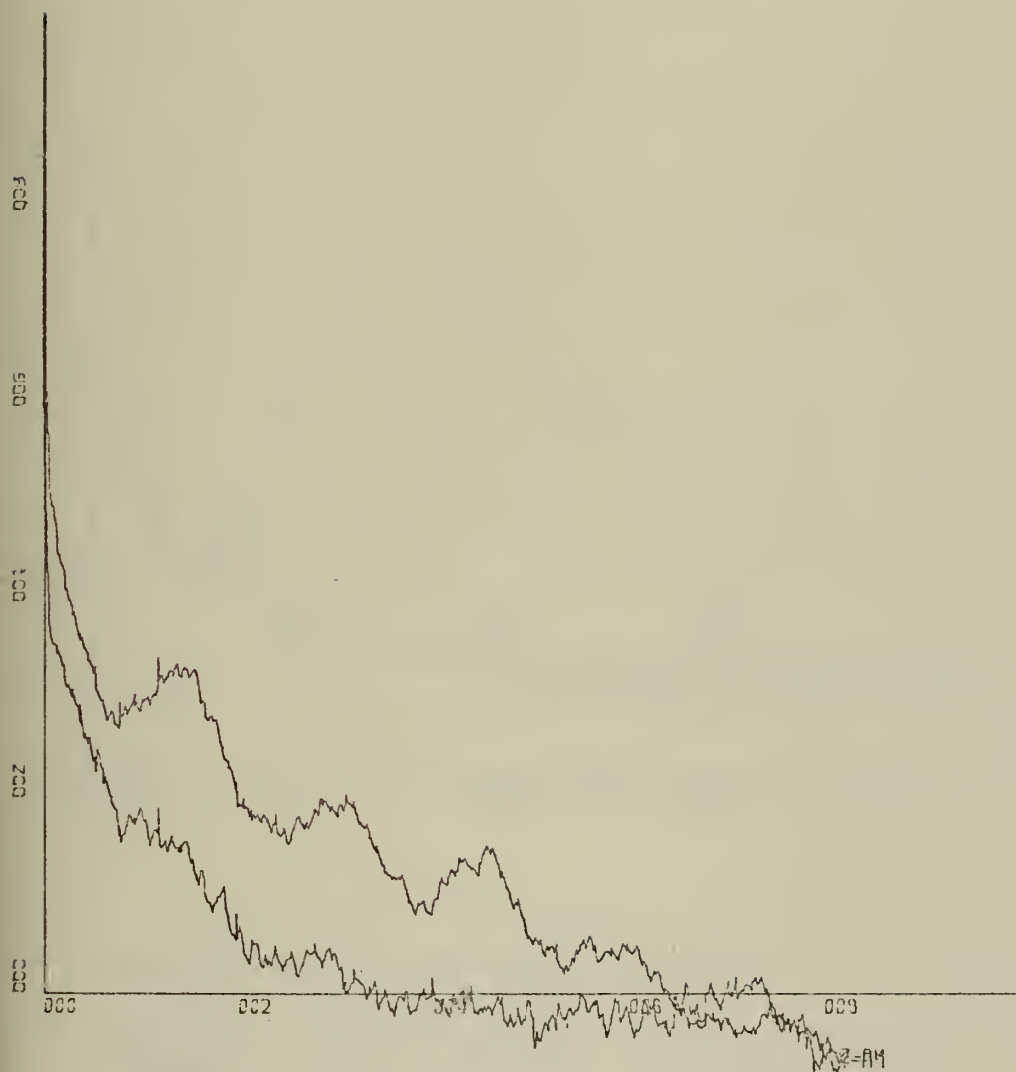


X-SCALE=1.00E-01 UNITS INCH.

Y-SCALE=2.00E+02 UNITS INCH.

CROSS SPECTRAL PHASE ANGLE, X-AM, Z-AM

RUN PH-4



X-SCALE=2.00E+01 UNITS INCH.

Y-SCALE=2.00E-01 UNITS INCH.

TEMPORAL AUTOCORRELATION FN, Y-AM, Z-AM
RUN PH-4, FILE 7 OF CON6

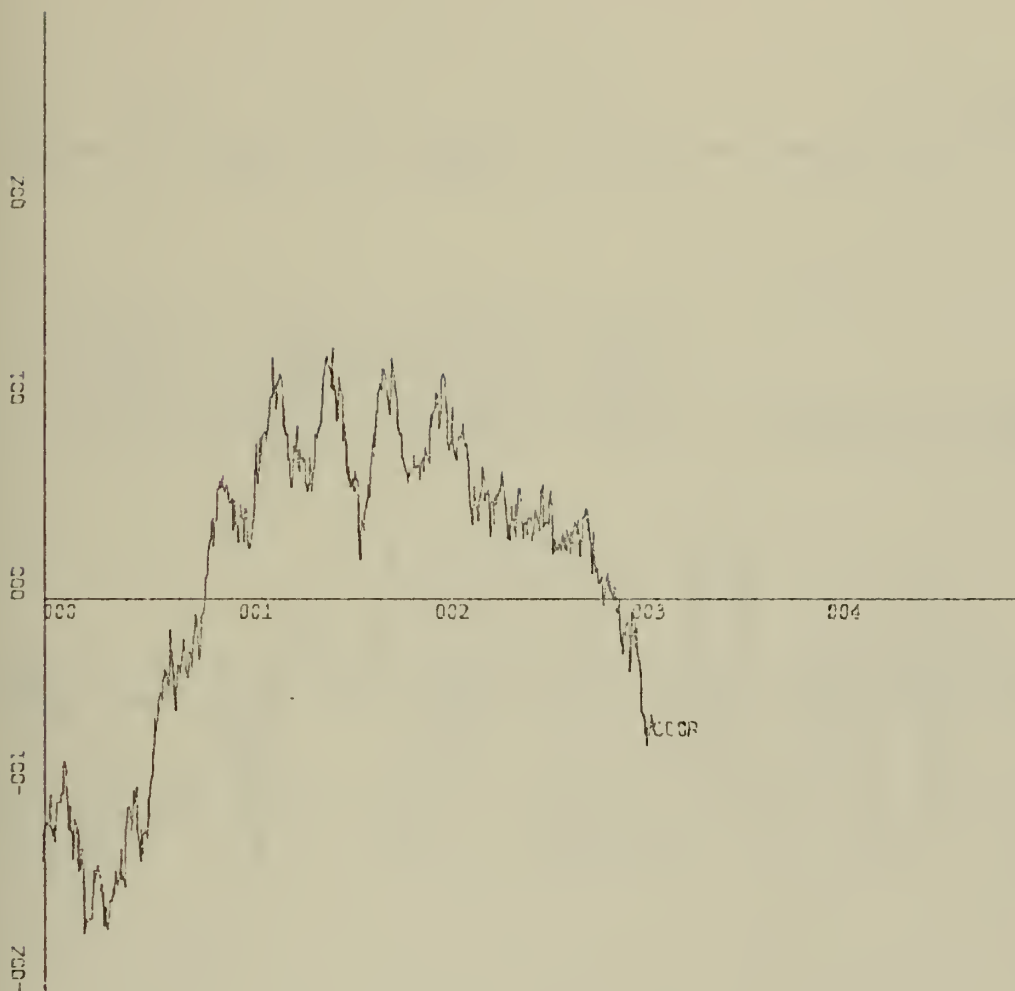


X-SCALE:-1.00E-01 UNITS INCH.

Y-SCALE:-1.00E+01 UNITS INCH.

POWER SPECTRUM LEVEL (DB) Y-AM, Z-AM

RUN PH-4, FILE 7 OF CON6

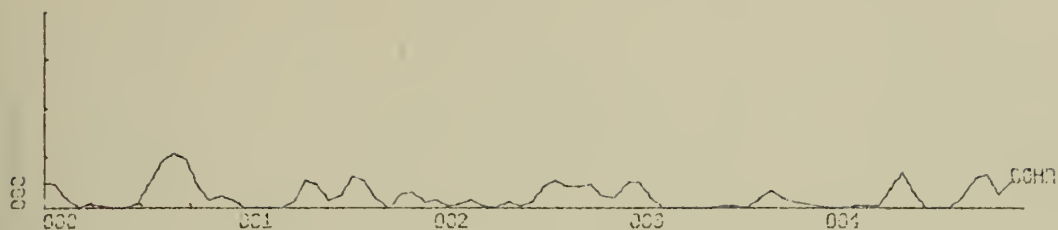


X-SCALE=1.00E+00 UNITS INCH.

Y-SCALE=1.00E-01 UNITS INCH.

CROSS-CORRELATION FN, Y-AM, Z-AM

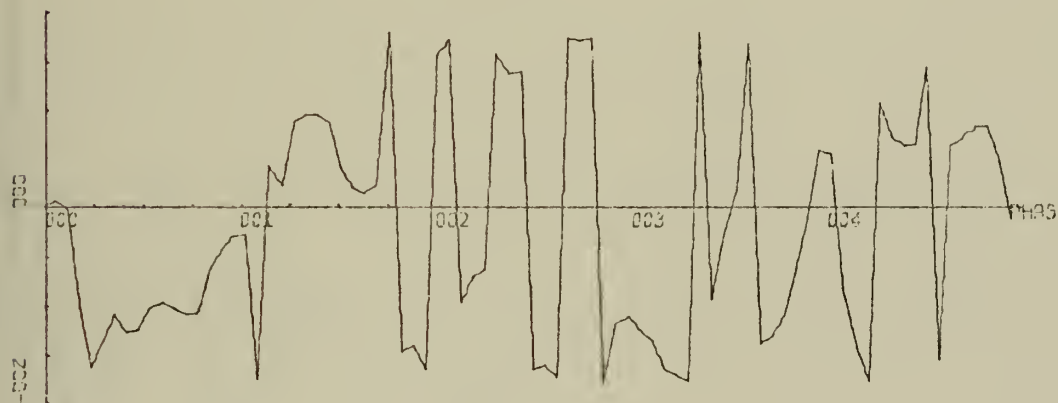
RUN PH-4, FILE 7 OF CON6



X-SCALE=1.00E-01 UNITS INCH.

Y-SCALE=1.00E+00 UNITS INCH.

COHERENCE FUNCTION Y-AM, Z-AM

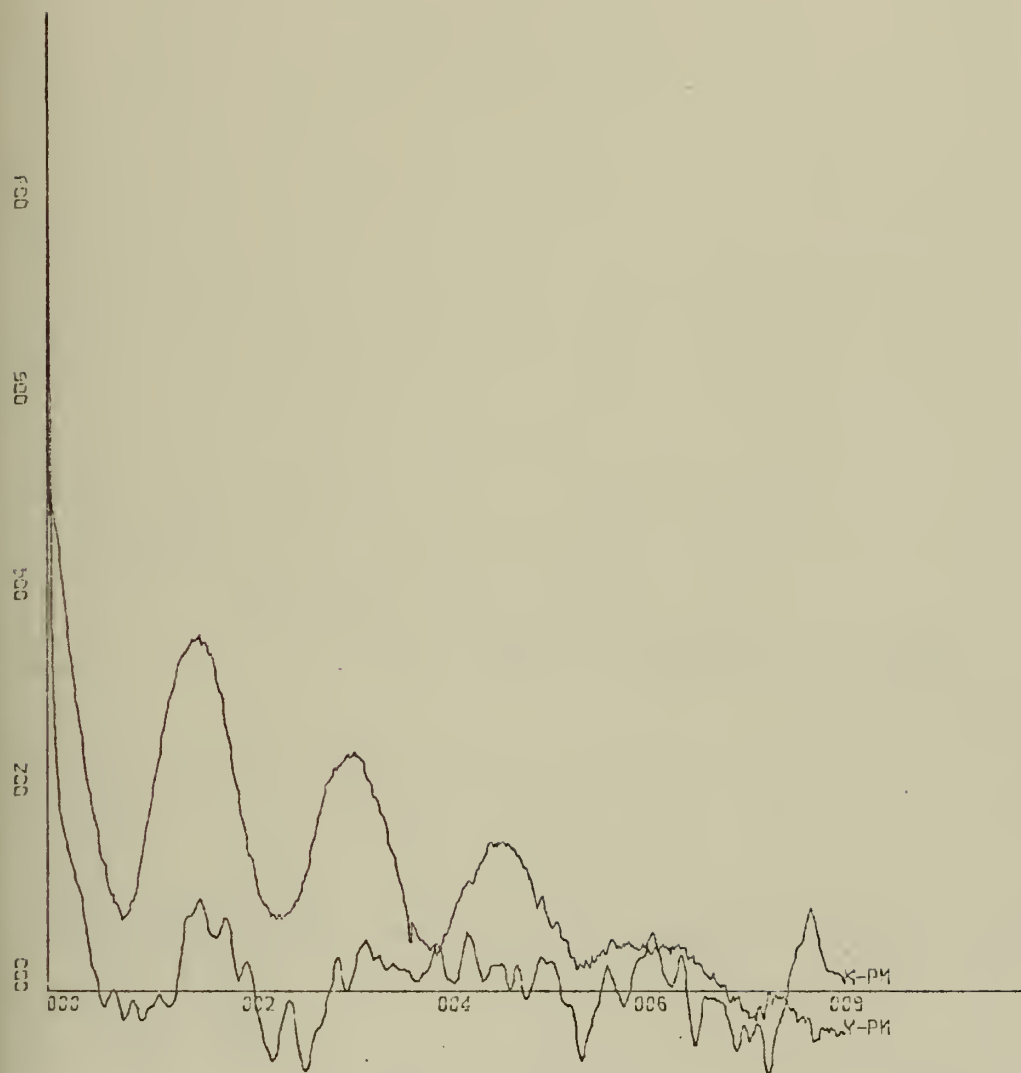


X-SCALE=1.00E-01 UNITS INCH.

Y-SCALE=2.00E+02 UNITS INCH.

CROSS SPECTRAL PHASE ANGLE, Y-AM, Z-AM

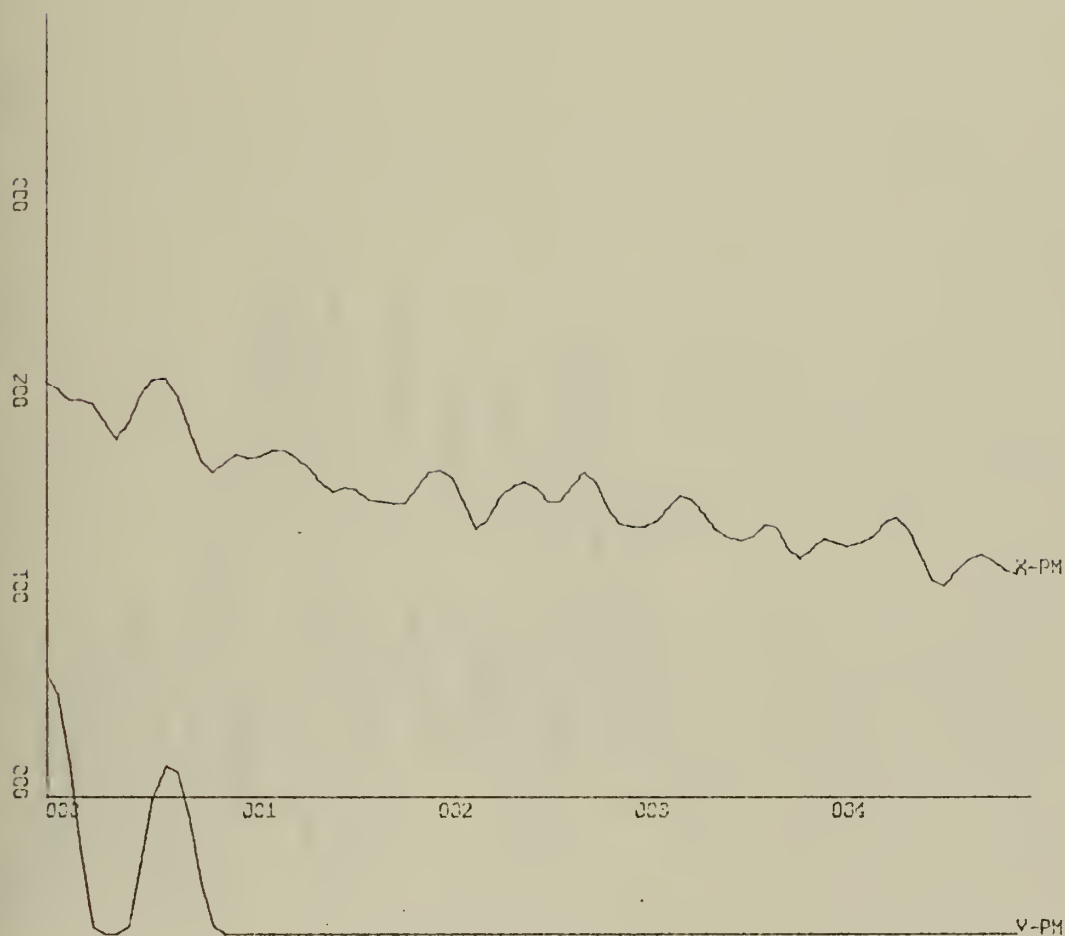
RUN PH-4



X-SCALE=2.00E+01 UNITS INCH.

Y-SCALE=2.00E-01 UNITS INCH.

TEMPORAL AUTOCORRELATION FN, X-PM, Y-PM
RUN PH-4, FILE 7 OF CON6

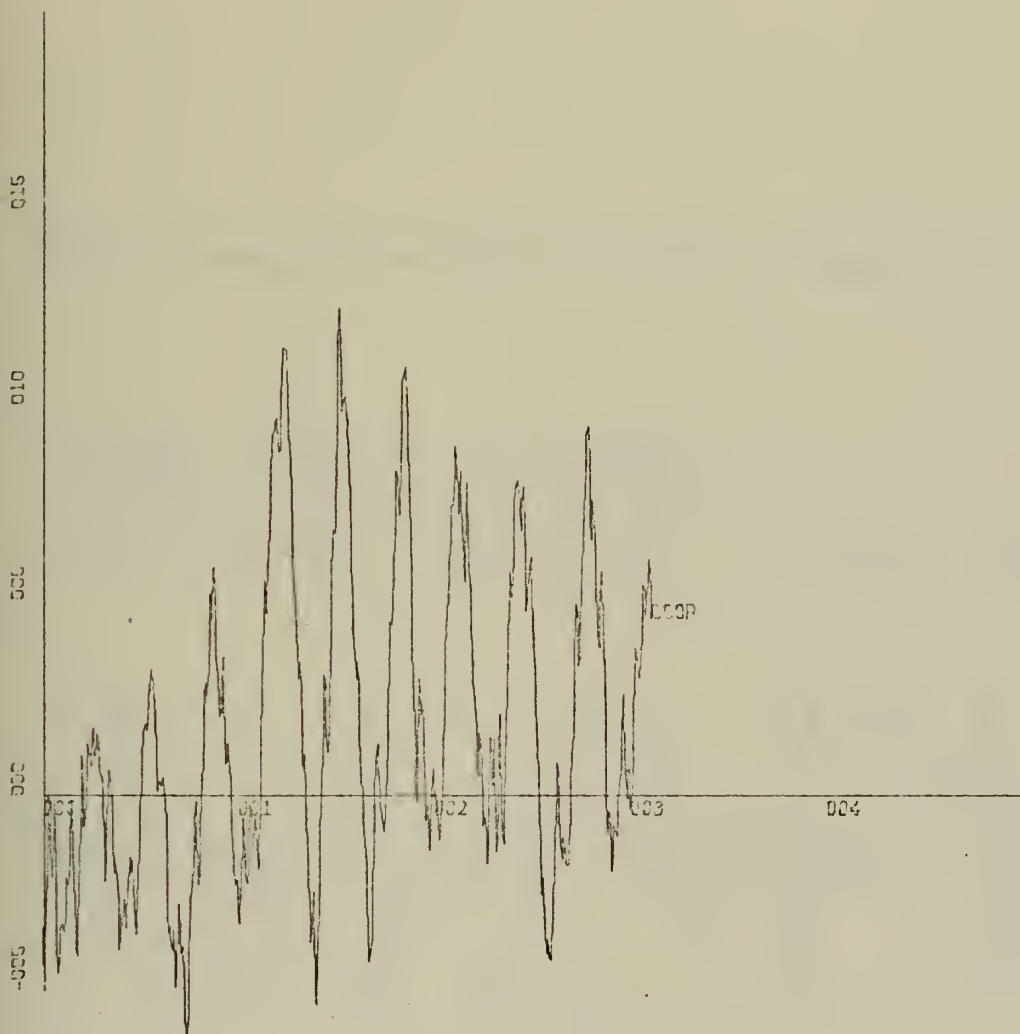


X-SCALE=-1.00E-01 UNITS INCH.

Y-SCALE=-1.00E+01 UNITS INCH.

POWER SPECTRUM LEVEL (DB) X-PM, Y-PM

RUN PH-4, FILE 7 OF CON6

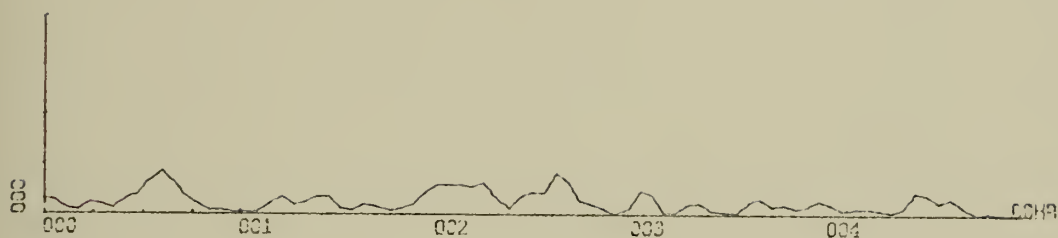


X-SCALE=1.00E+00 UNITS INCH.

Y-SCALE=5.00E-02 UNITS INCH.

CROSS-CORRELATION FN, X-PM, Y-PM

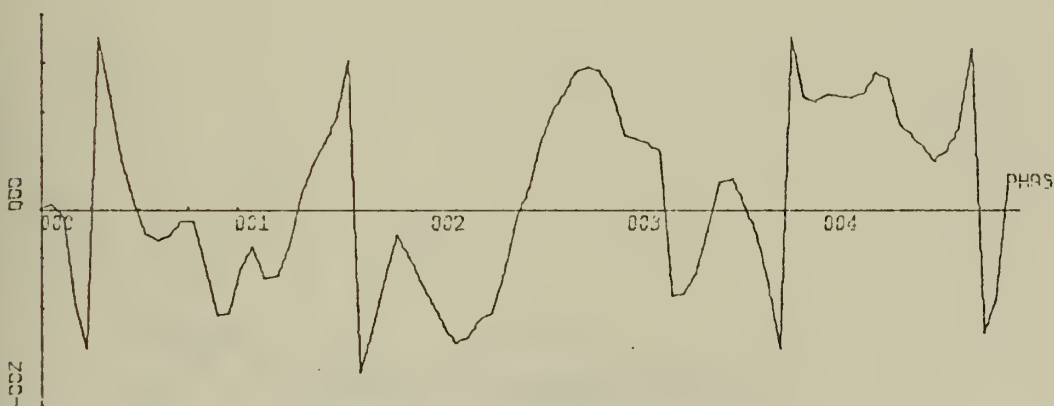
RUN PH-4, FILE 7 OF CON6



X-SCALE=1.00E-01 UNITS INCH.

Y-SCALE=1.00E+00 UNITS INCH.

COHERENCE FUNCTION X-PM, Y-PM

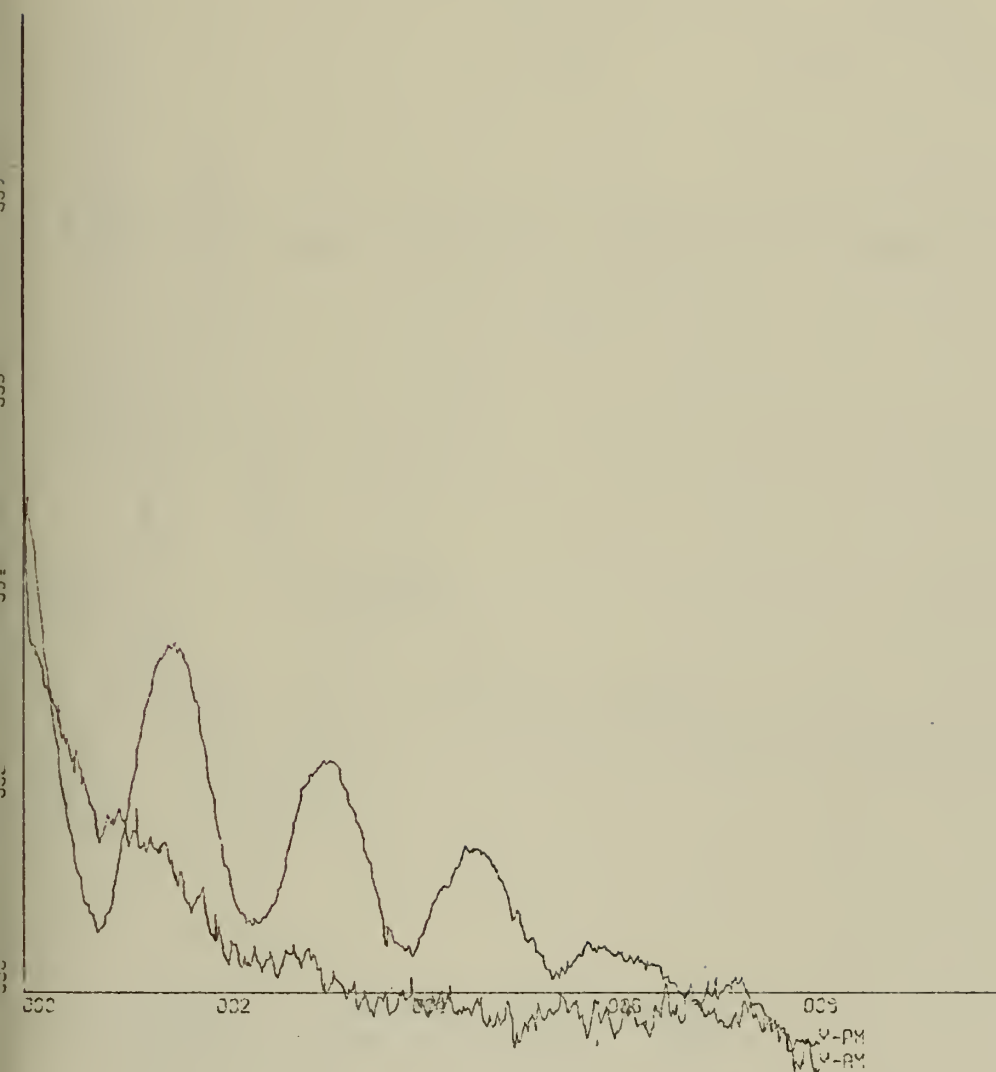


X-SCALE=1.00E-01 UNITS INCH.

Y-SCALE=2.00E+02 UNITS INCH.

CROSS SPECTRAL PHASE ANGLE, X-PM, Y-PM

RUN PH-4

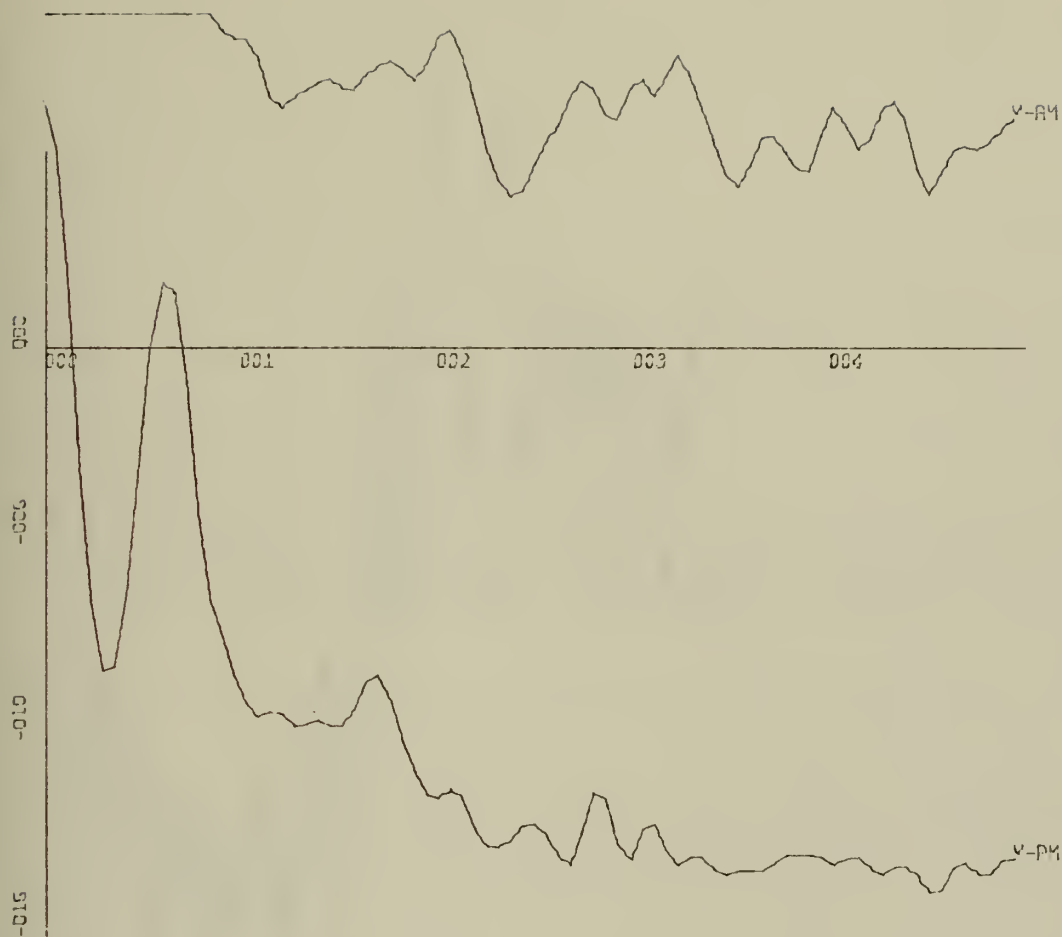


X-SCALE:-2.00E+01 UNITS INCH.

Y-SCALE:-2.00E-01 UNITS INCH.

TEMPORAL AUTOCORRELATION FN, Y-PM, Y-AM

RUN PH-4, FILE 7 OF CON6

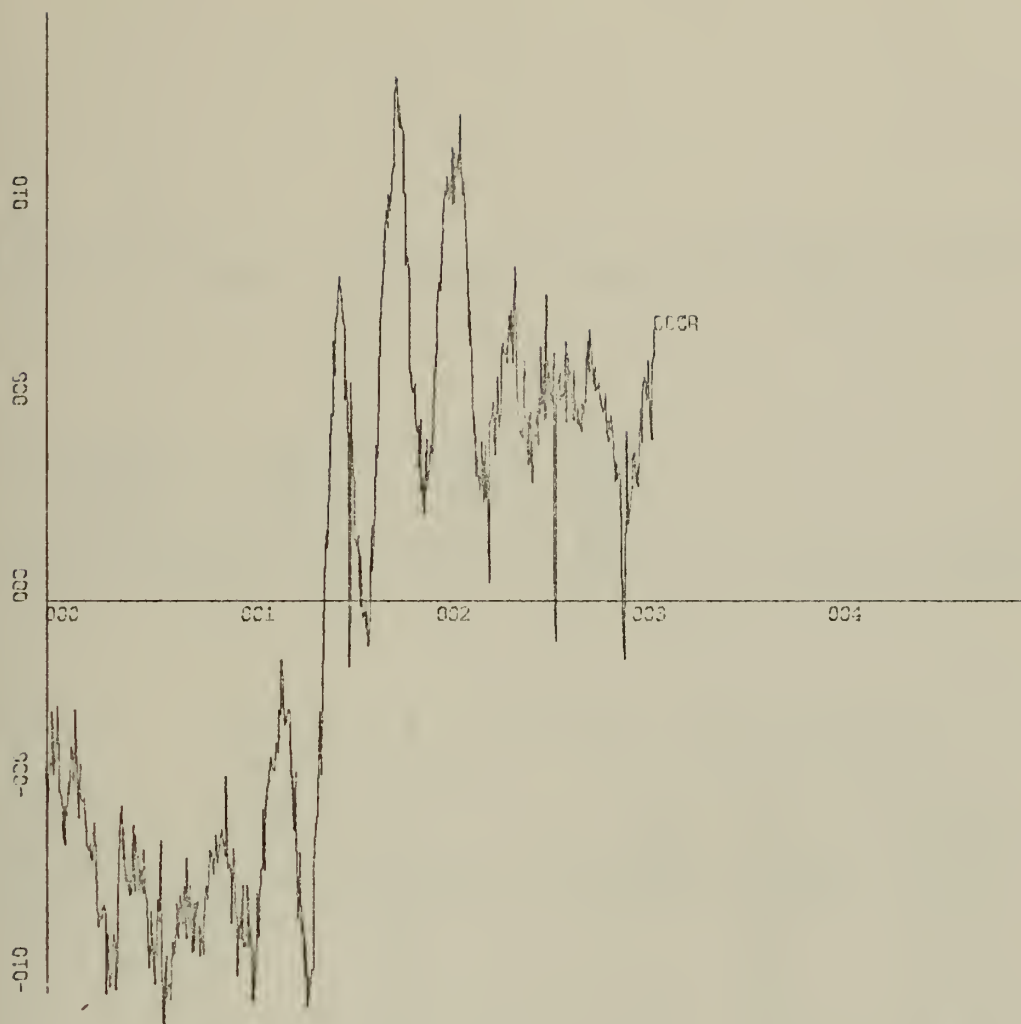


X-SCALE=1.00E-01 UNITS INCH.

Y-SCALE=5.00E+00 UNITS INCH.

POWER SPECTRUM LEVEL (DB) Y-PM, Y-AM

RUN PH-4, FILE 7 OF CON6

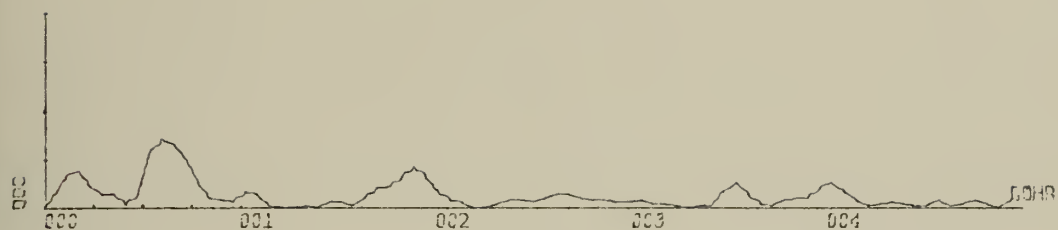


X-SCALE=-1.00E+00 UNITS INCH.

Y-SCALE=-5.00E-02 UNITS INCH.

CROSS-CORRELATION FN, Y-PM, Y-AM

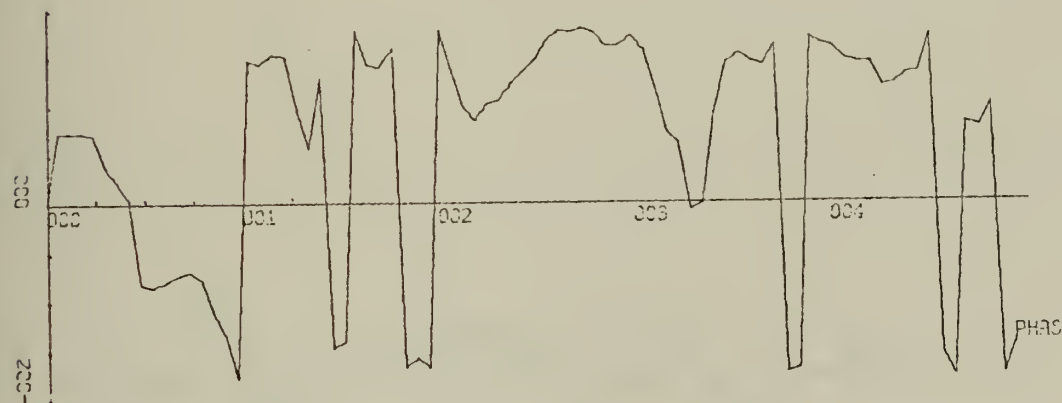
RUN PH-4, FILE 7 OF CON6



X-SCALE=1.00E-01 UNITS INCH.

Y-SCALE=1.00E+00 UNITS INCH.

COHERENCE FUNCTION Y-PM, Y-AM

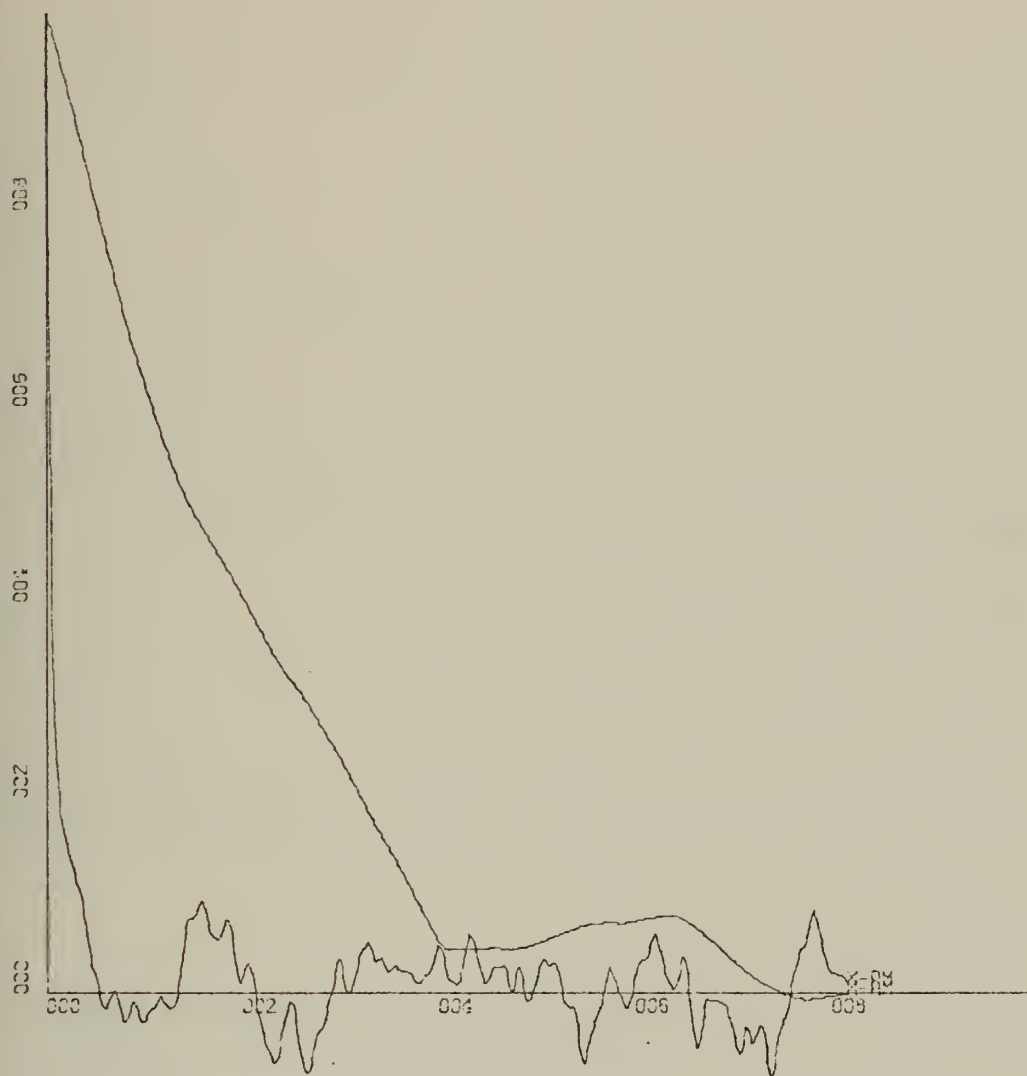


X-SCALE=1.00E-01 UNITS INCH.

Y-SCALE=2.00E+02 UNITS INCH.

CROSS SPECTRAL PHASE ANGLE, Y-PM, Y-AM

RUN PH-4



X-SCALE=2.00E+01 UNITS INCH.

Y-SCALE=2.00E-01 UNITS INCH.

TEMPORAL AUTOCORRELATION FN, X-PM, X-AM

RUN PH-4, FILE 7 OF CON6

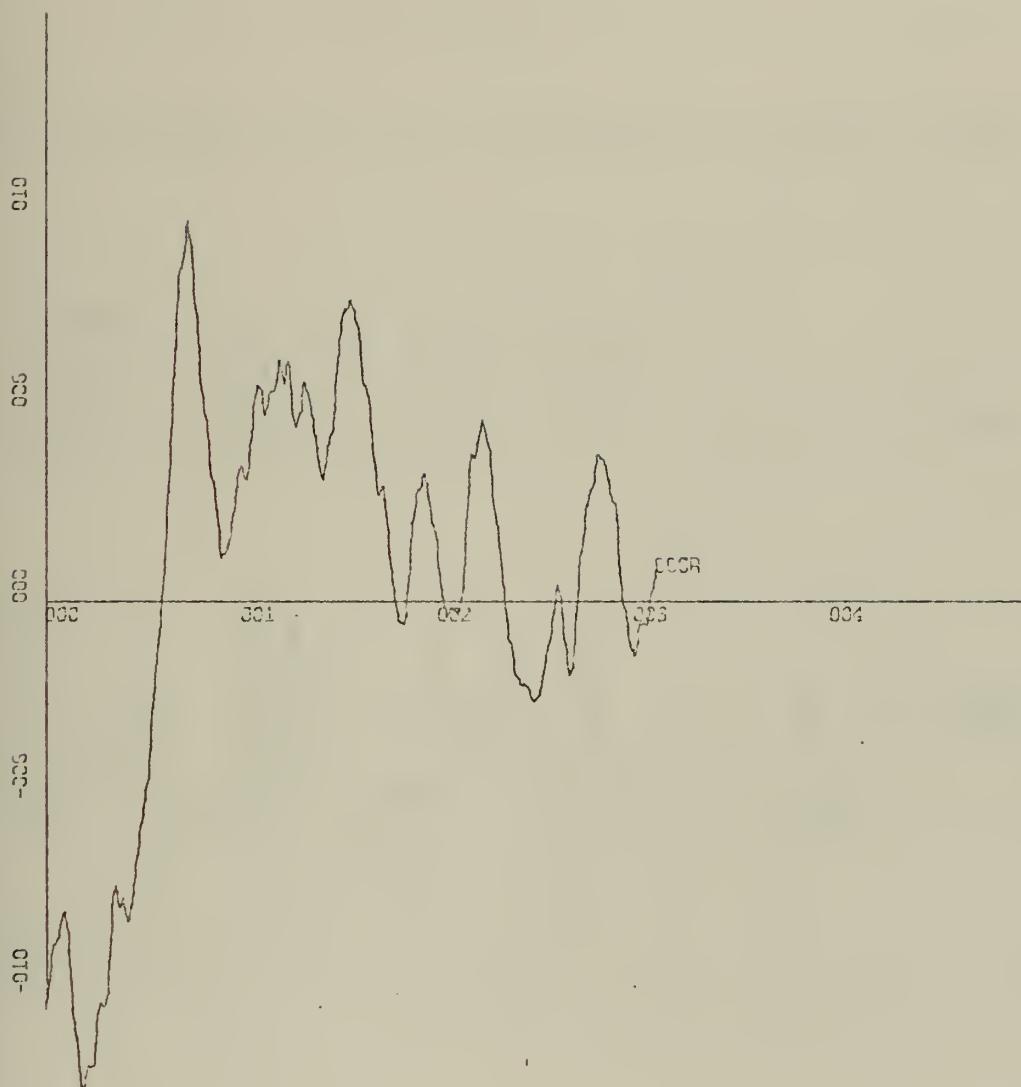


X-SCALE=1.00E-01 UNITS INCH.

Y-SCALE=1.00E+01 UNITS INCH.

POWER SPECTRUM LEVEL (DB) X-PM, X-AM

RUN PH-4, FILE 7 OF CON6

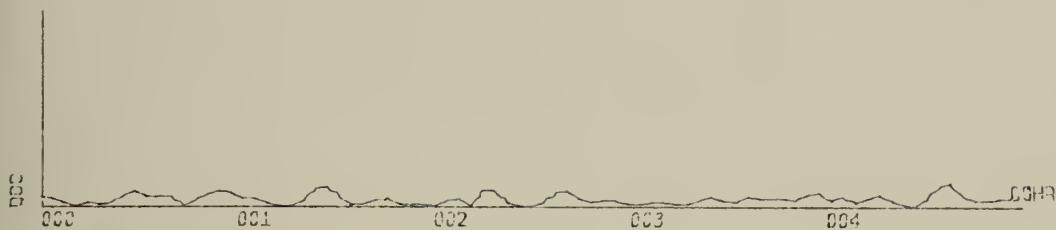


X-SCALE=1.00E+00 UNITS INCH.

Y-SCALE=5.00E-02 UNITS INCH.

CROSS-CORRELATION FN, X-PM, X-AM

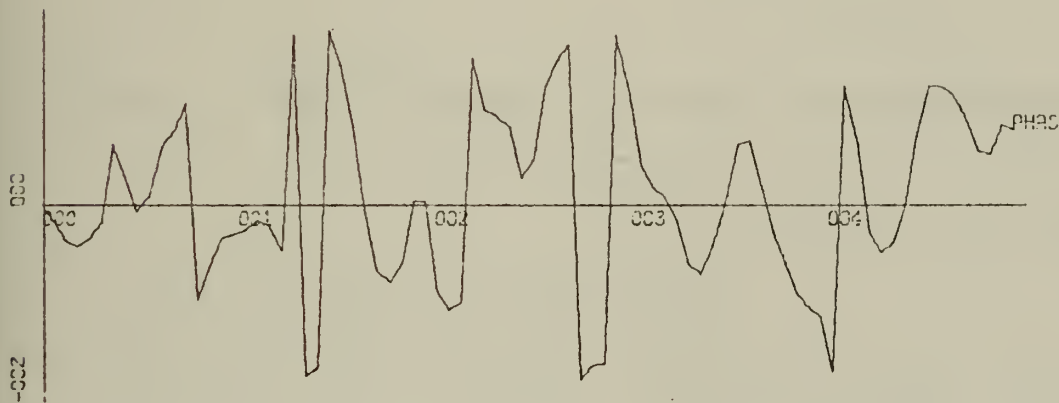
RUN PH-4, FILE 7 OF CON6



X-SCALE=1.00E-01 UNITS INCH.

Y-SCALE=1.00E+00 UNITS INCH.

COHERENCE FUNCTION X-PM, X-AM

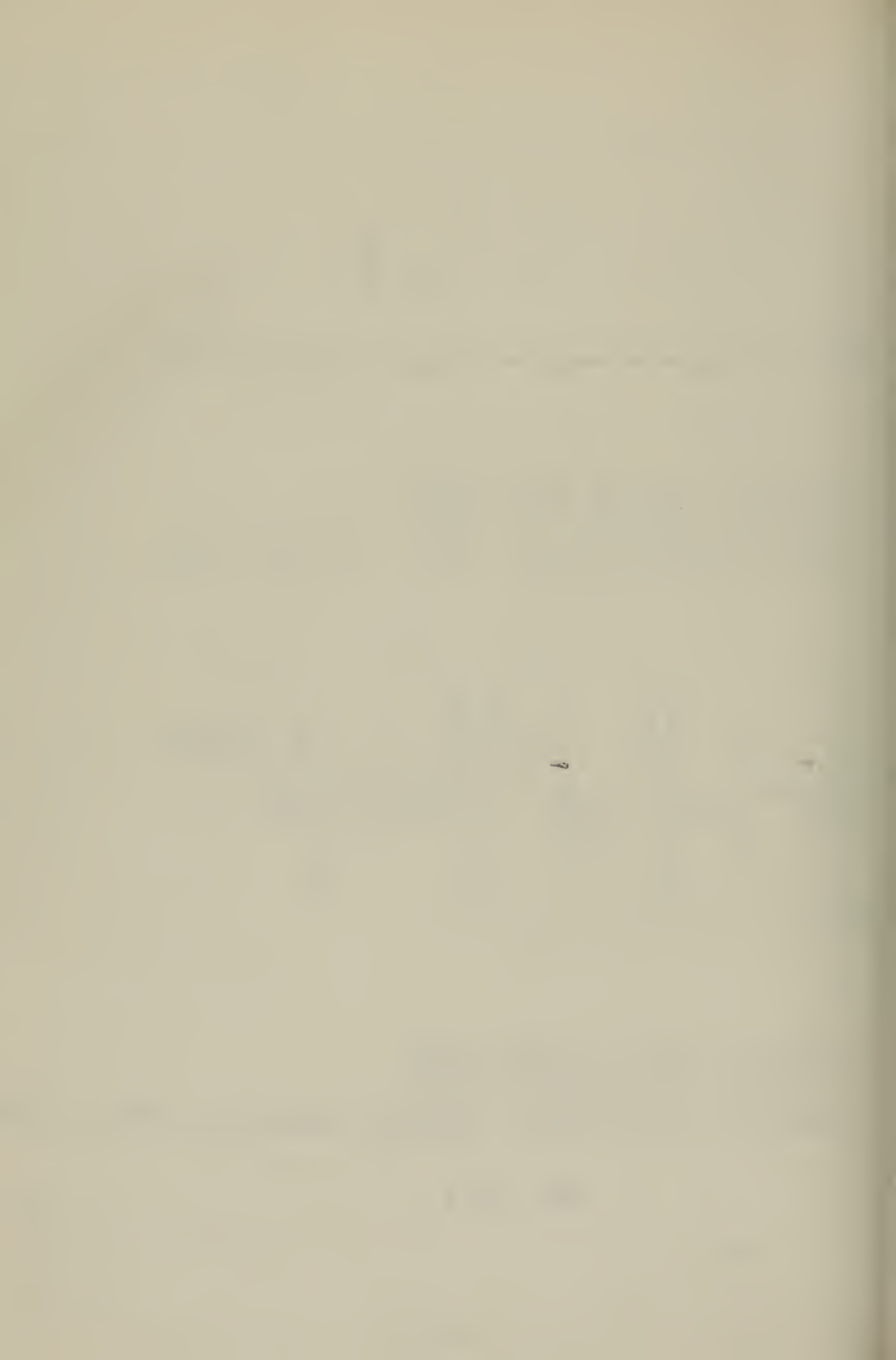


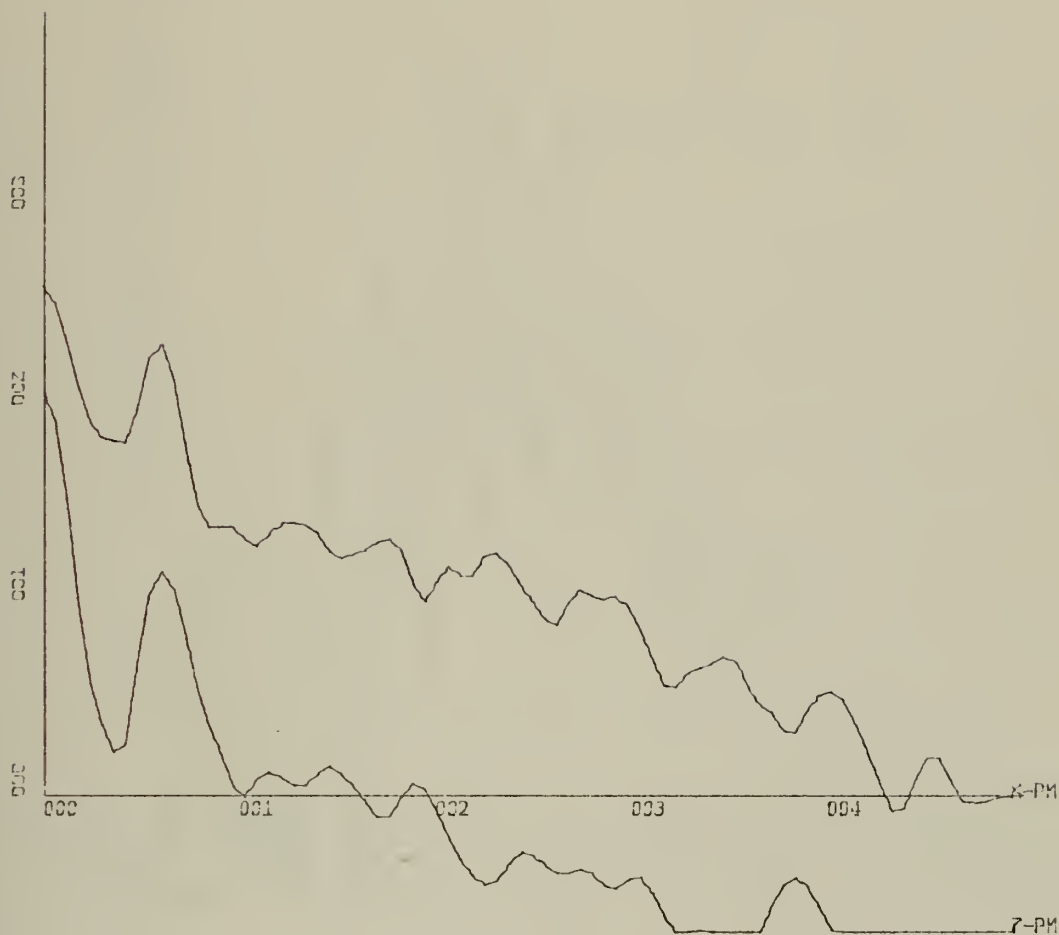
X-SCALE=1.00E-01 UNITS INCH.

Y-SCALE=2.00E+02 UNITS INCH.

CROSS SPECTRAL PHASE ANGLE, X-PM, X-AM

RUN PH-4



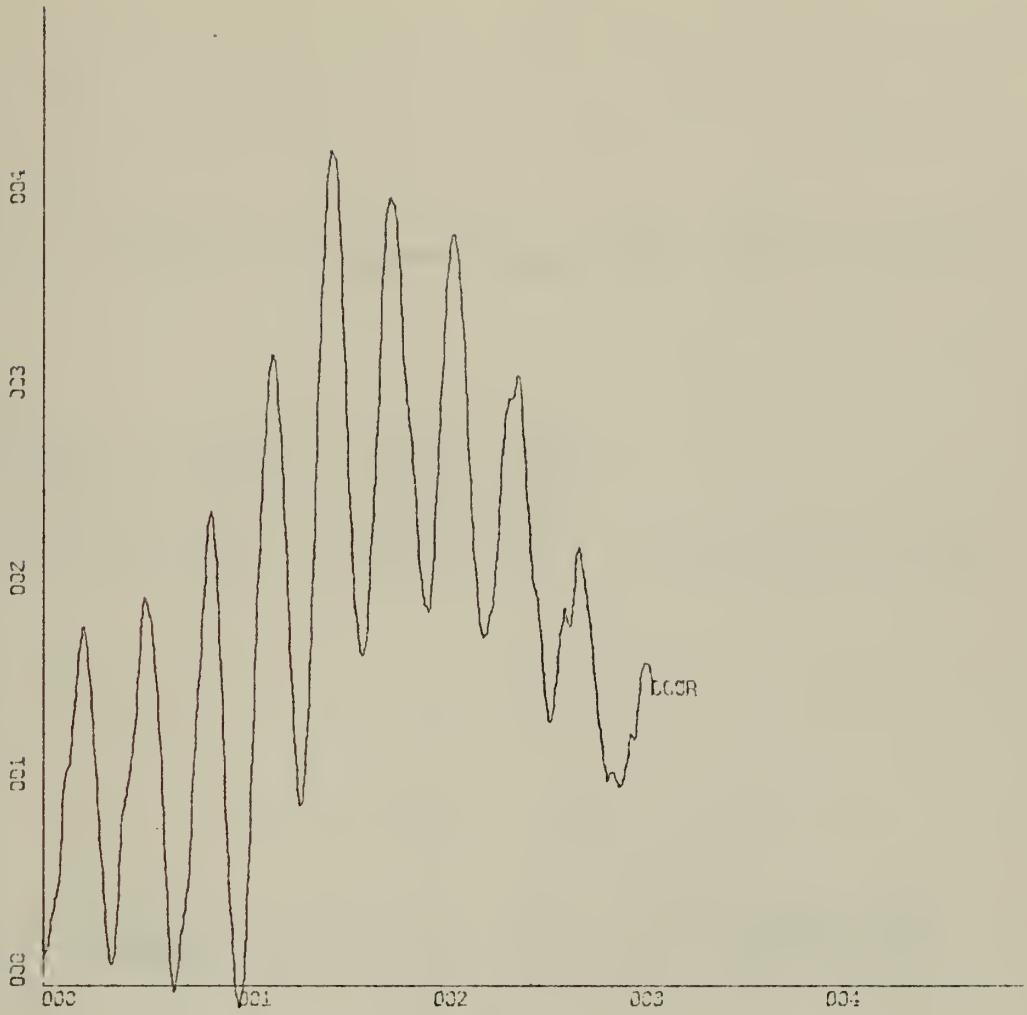


X-SCALE=1.00E-01 UNITS INCH.

Y-SCALE=1.00E+01 UNITS INCH.

POWER SPECTRUM LEVEL (DB) X-PM, Z-PM

RUN PH-5, FILE 8 OF C0N6



X-SCALE:-1.00E+00 UNITS INCH.

Y-SCALE:-1.00E-01 UNITS INCH.

CROSS-CORRELATION FN, X-PM, Z-PM

RUN PH-5, FILE 8 OF CON6

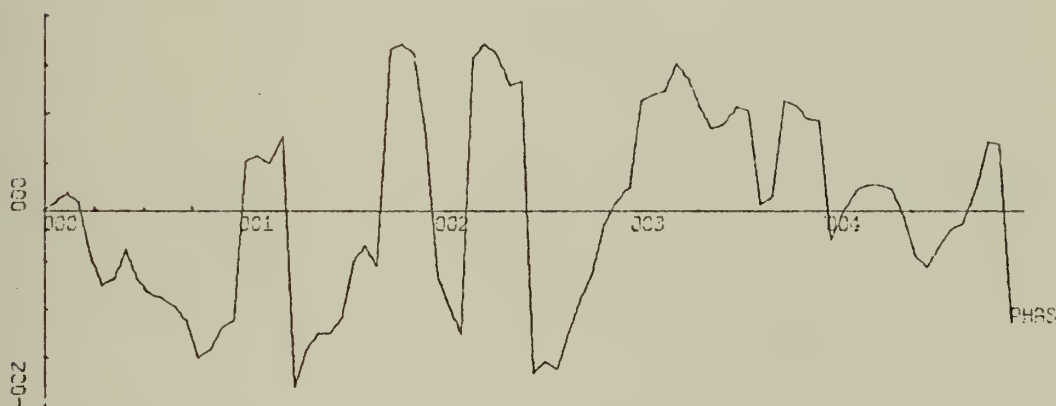


X-SCALE=1.00E-01 UNITS INCH.

Y-SCALE=1.00E+00 UNITS INCH.

COHERENCE FUNCTION X-PM, Z-PM

CH ALEXANDER



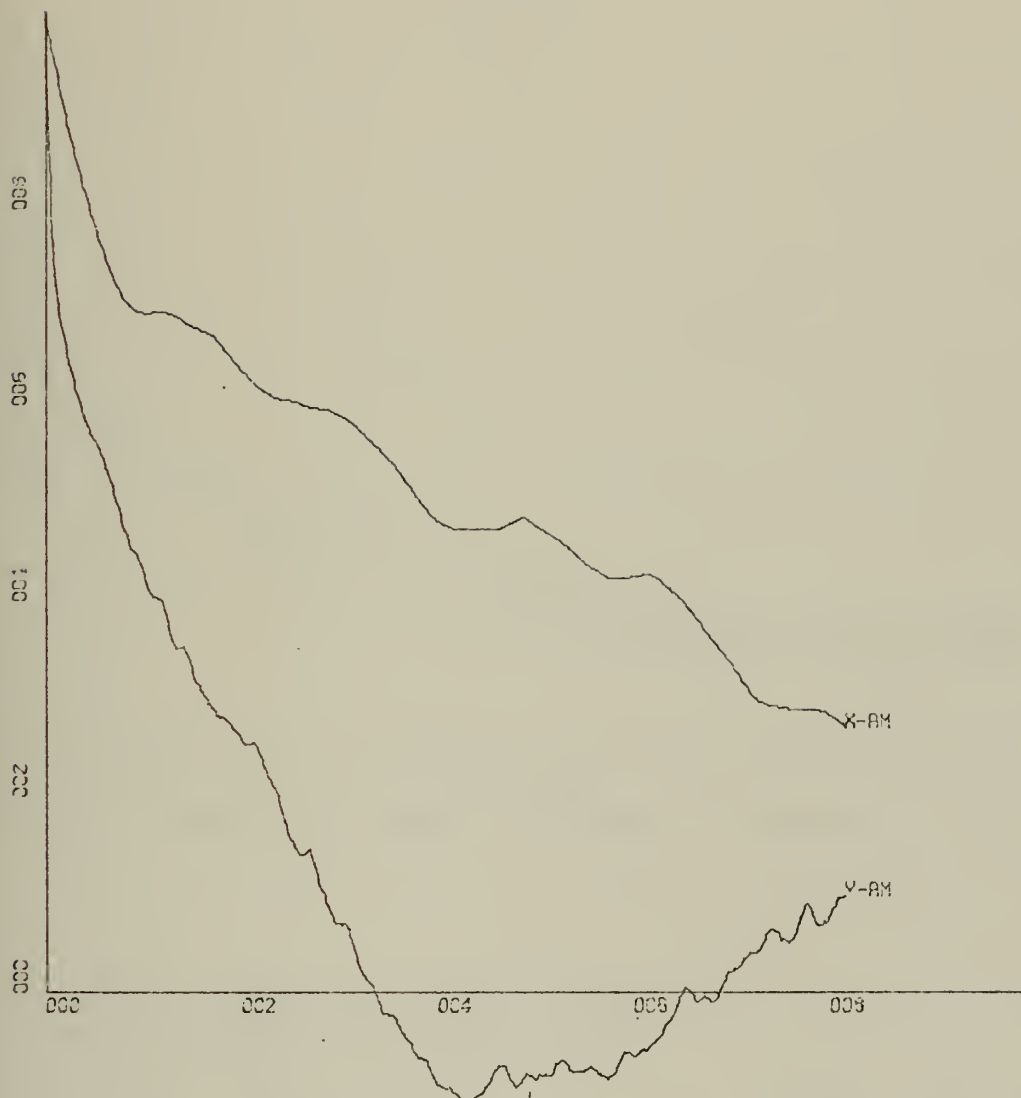
X-SCALE=1.00E-01 UNITS INCH.

Y-SCALE=2.00E+02 UNITS INCH.

CROSS SPECTRAL PHASE ANGLE, X-PM, Z-PM

CH ALEXANDER

RUN PH-5

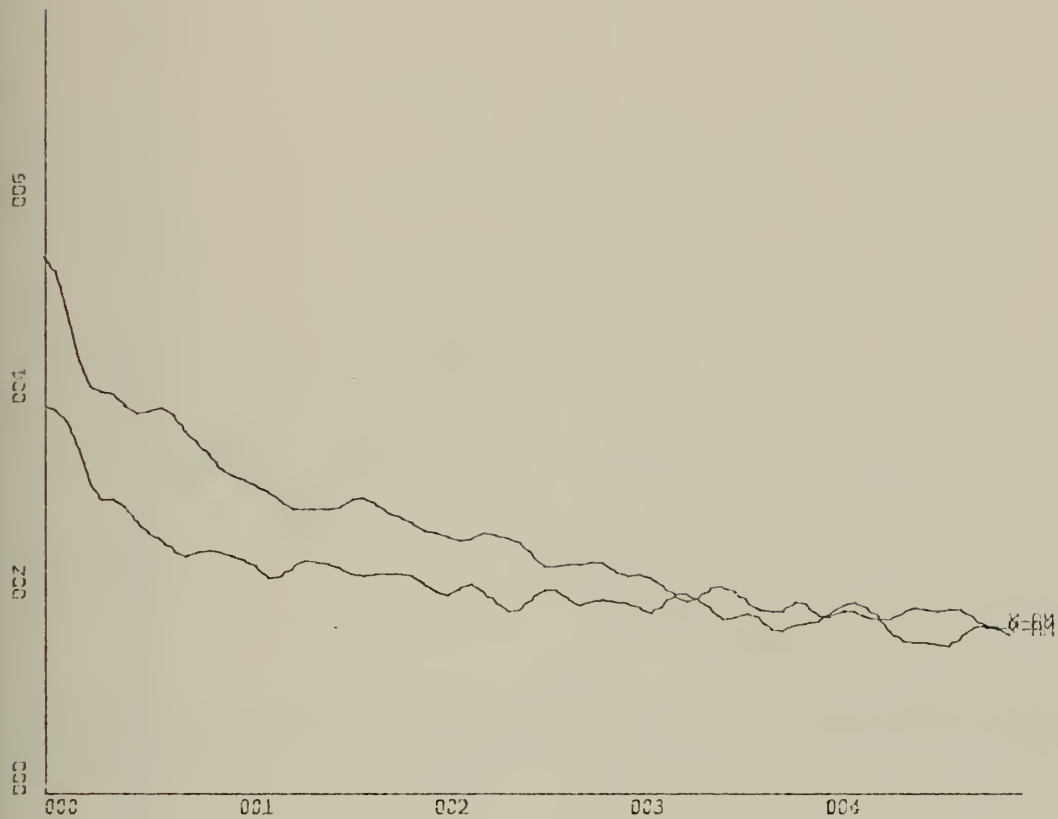


X-SCALE= $2.00E+01$ UNITS INCH.

Y-SCALE= $2.00E-01$ UNITS INCH.

TEMPORAL AUTOCORRELATION FN, X-AM, Y-AM

RUN PH-5, FILE 8 OF CON6

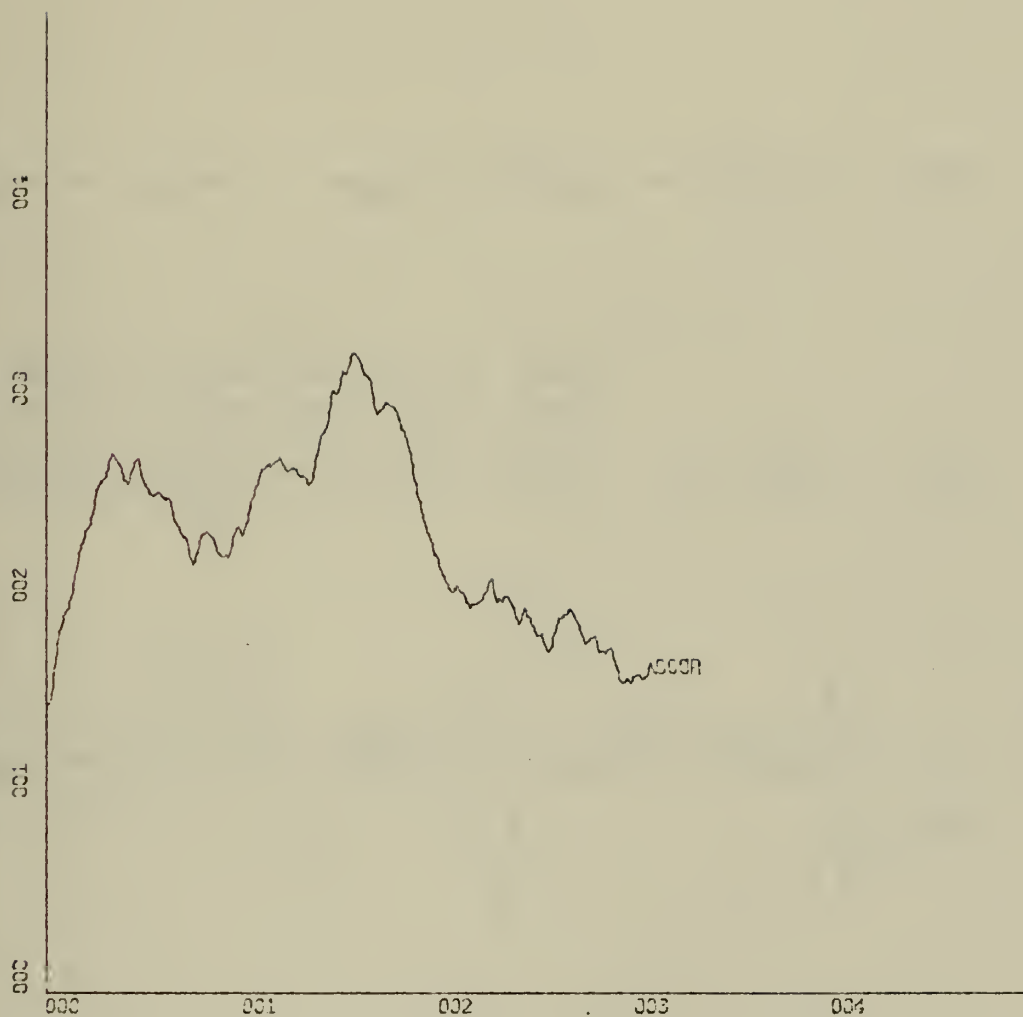


X-SCALE=1.00E-01 UNITS INCH.

Y-SCALE=2.00E+01 UNITS INCH.

POWER SPECTRUM LEVEL (DB) X-AM, Y-AM

RUN PH-5, FILE 8 OF CON6

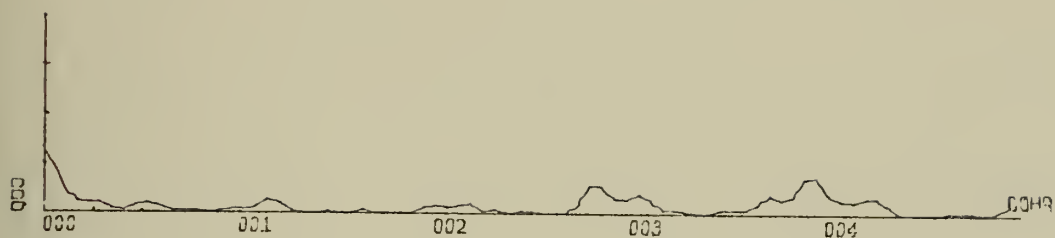


X-SCALE=1.00E+00 UNITS INCH.

Y-SCALE=1.00E-01 UNITS INCH.

CROSS-CORRELATION FN, X-AM, Y-AM

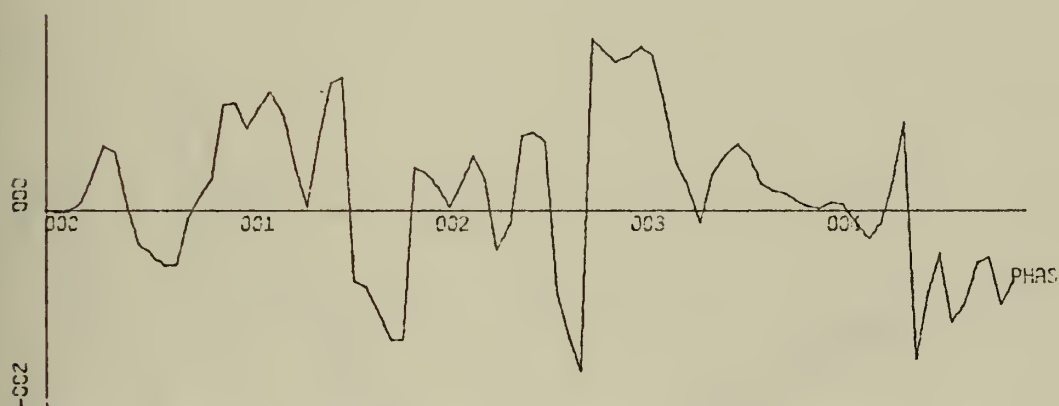
RUN PH-5, FILE 8 OF CON6



X-SCALE=1.00E-01 UNITS INCH.

Y-SCALE=1.00E+00 UNITS INCH.

COHERENCE FUNCTION X-AM, Y-AM
 ALL DIMENSIONS

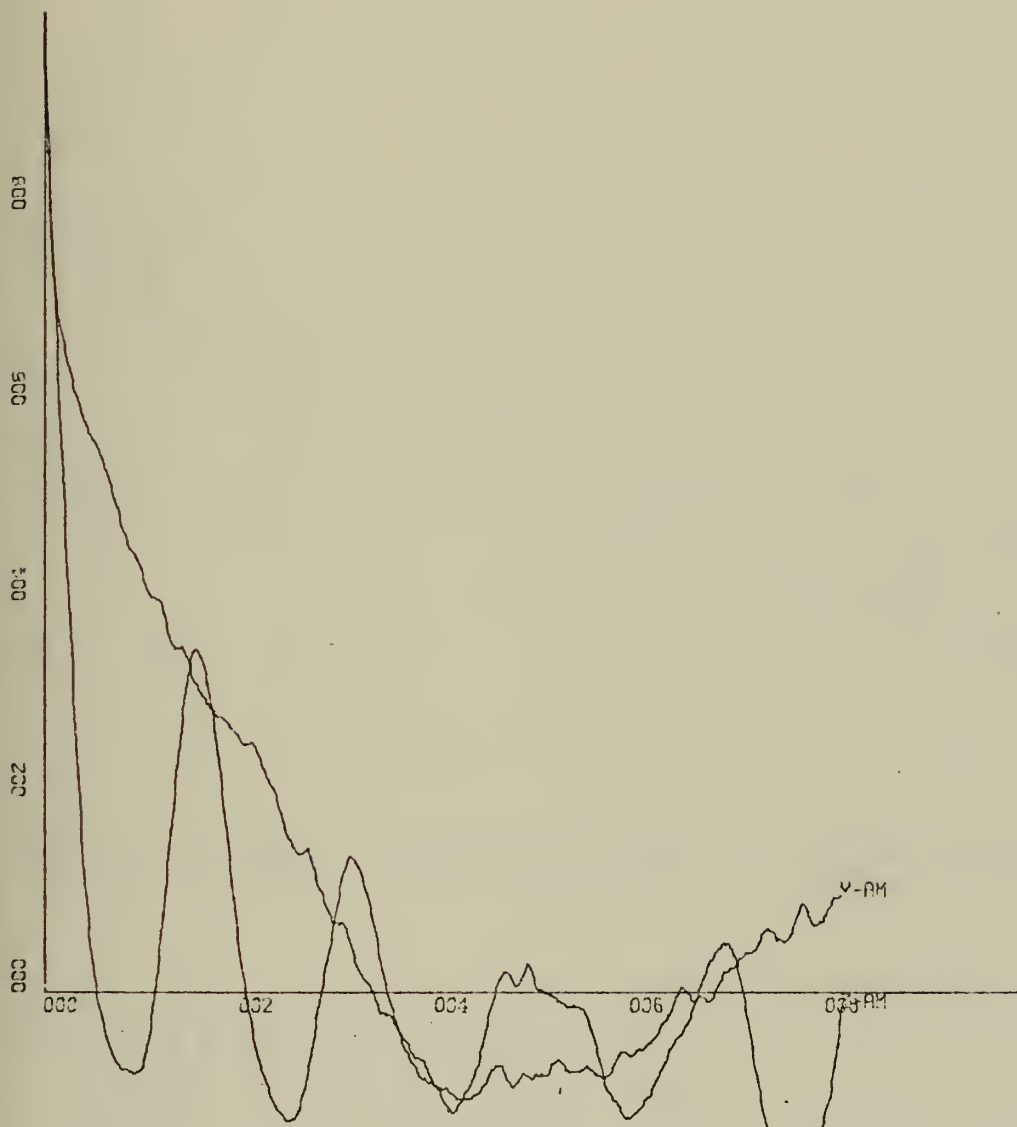


X-SCALE=1.00E-01 UNITS INCH.

Y-SCALE=2.00E+02 UNITS INCH.

CROSS SPECTRAL PHASE ANGLE, X-AM, Y-AM
 ALL DIMENSIONS

RUN PH-5

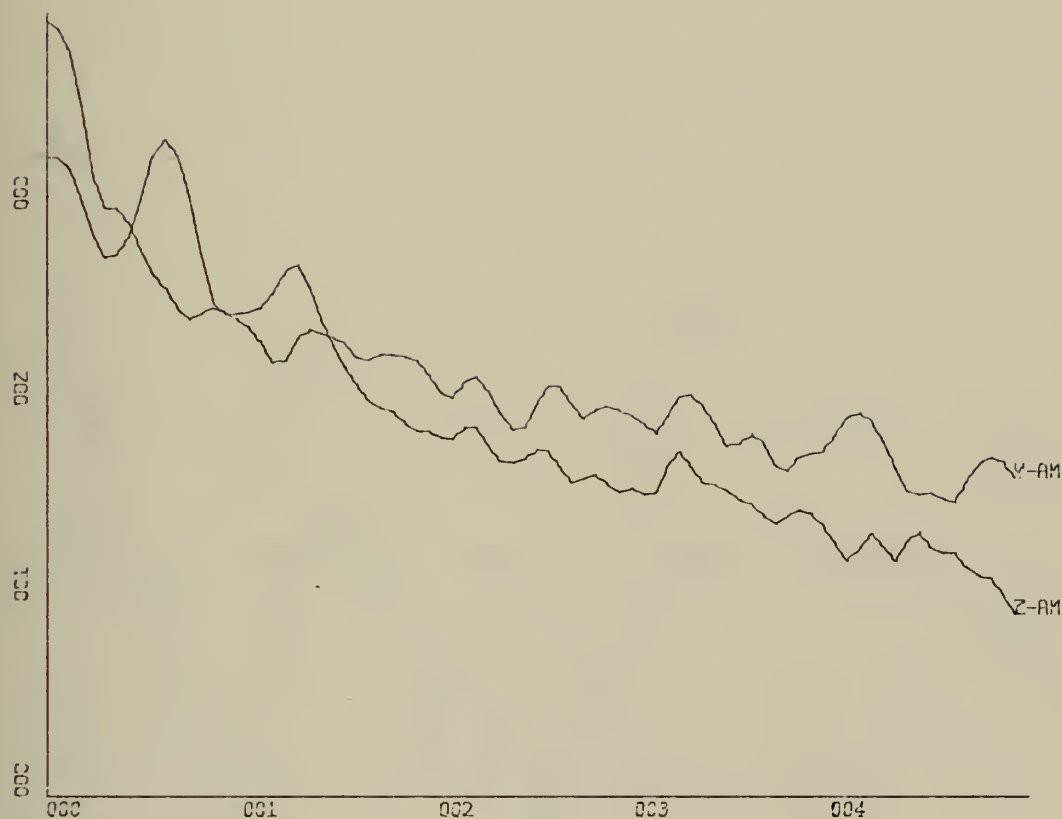


X-SCALE=2.00E+01 UNITS INCH.

Y-SCALE=2.00E-01 UNITS INCH.

TEMPORAL AUTOCORRELATION FN, Y-AM, Z-AM

RUN PH-5, FILE 8 OF CON6

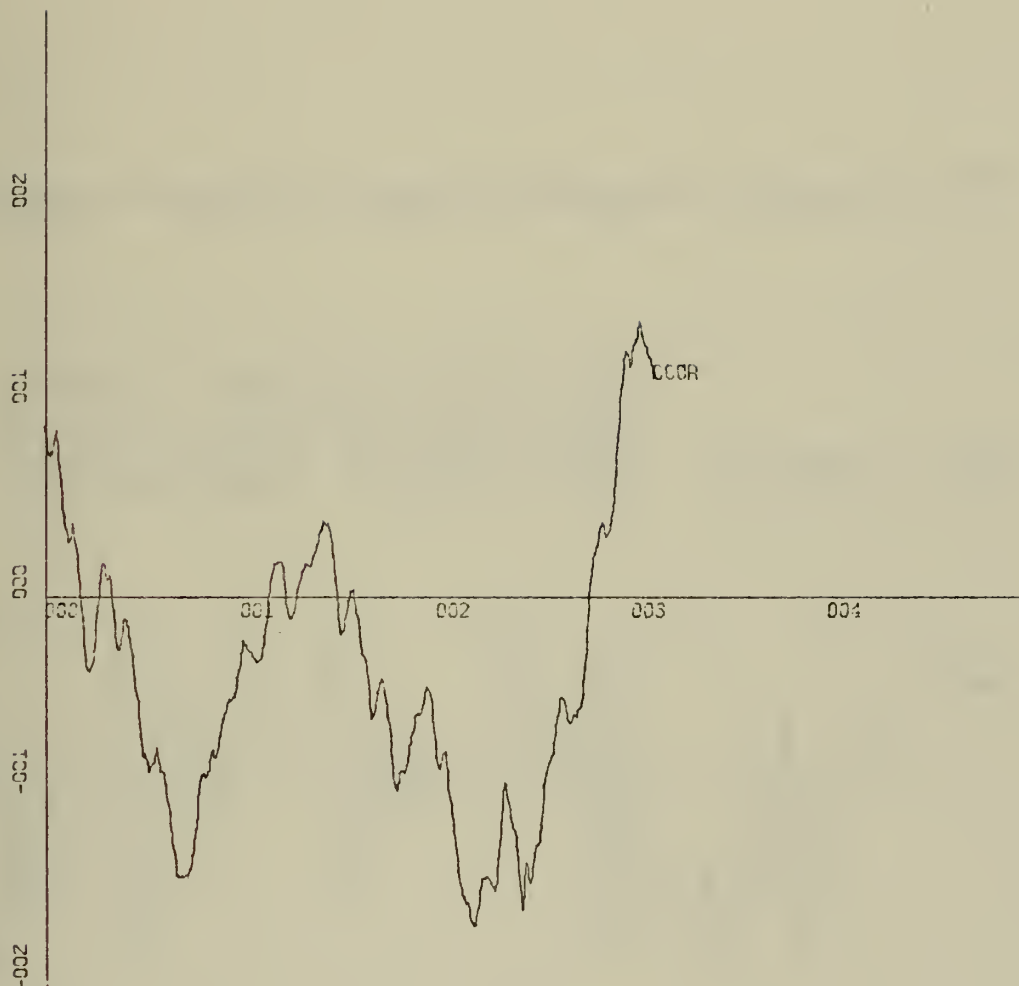


X-SCALE=1.00E-01 UNITS INCH.

Y-SCALE=1.00E+01 UNITS INCH.

POWER SPECTRUM LEVEL (DB) Y-AM, Z-AM

RUN PH-5, FILE 8 OF CON6

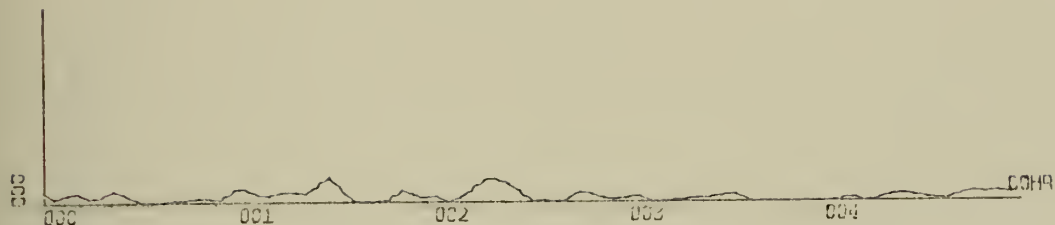


X-SCALE::1.00E+00 UNITS INCH.

Y-SCALE::1.00E-01 UNITS INCH.

CROSS-CORRELATION FN, Y-AM, Z-AM

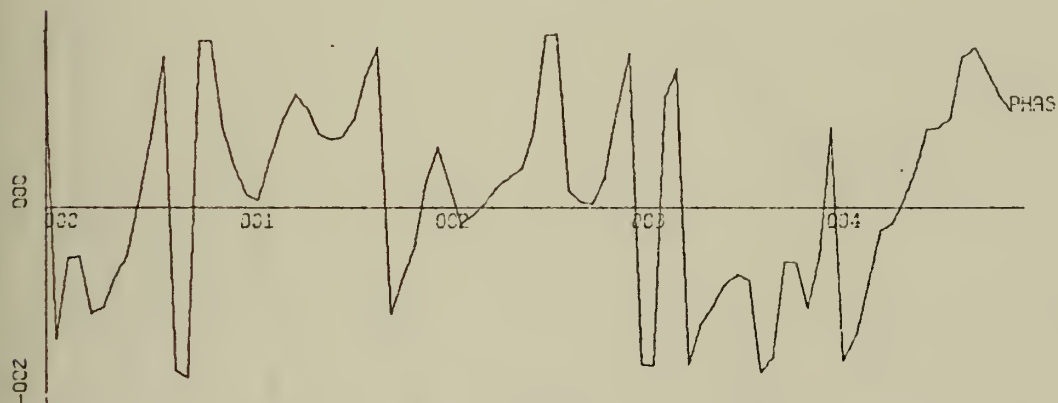
RUN PH-5, FILE 8 OF CON6



X-SCALE=1.00E-01 UNITS INCH.

Y-SCALE=1.00E+00 UNITS INCH.

COHERENCE FUNCTION Y-AM, Z-AM

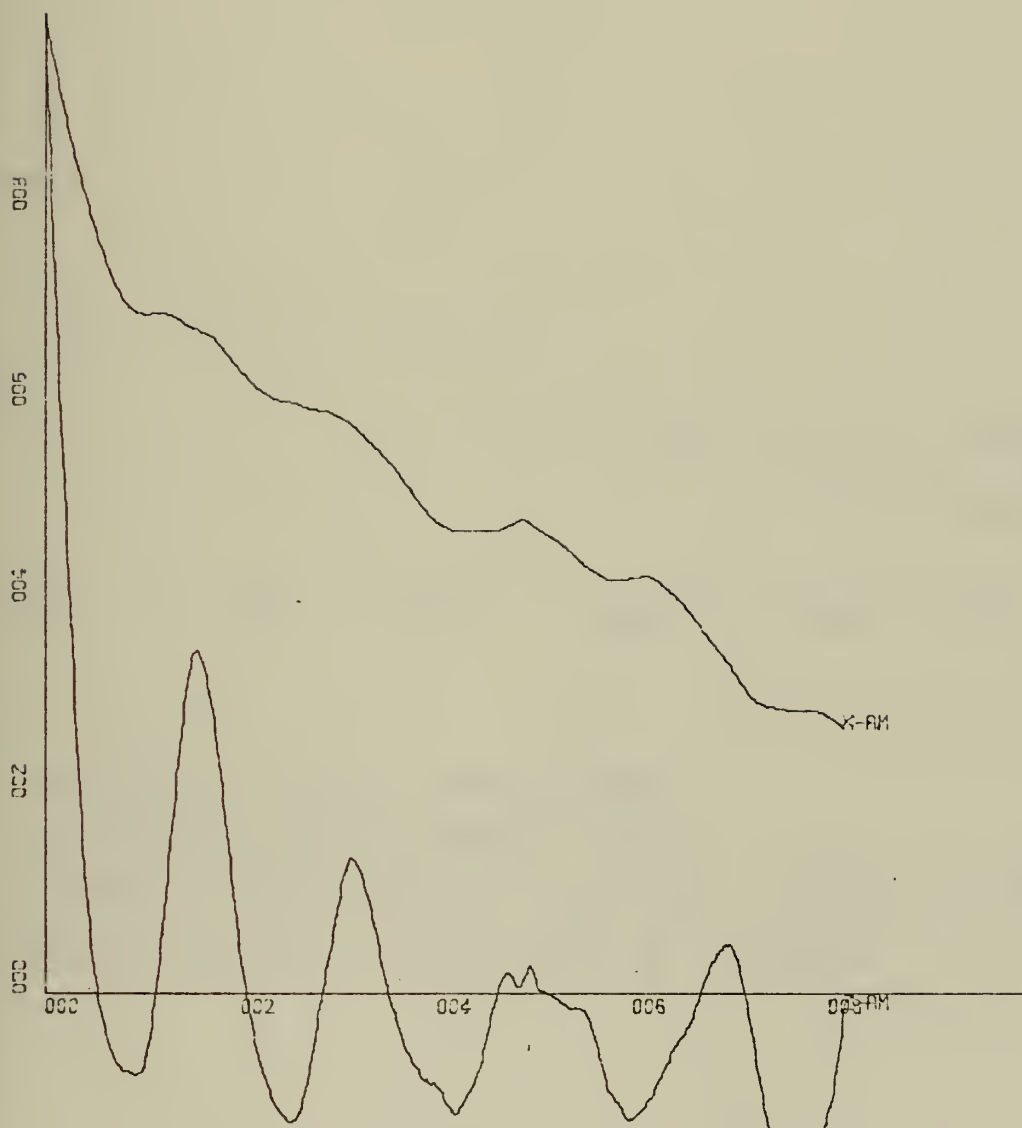


X-SCALE=1.00E-01 UNITS INCH.

Y-SCALE=2.00E+02 UNITS INCH.

CROSS SPECTRAL PHASE ANGLE, Y-AM, Z-AM

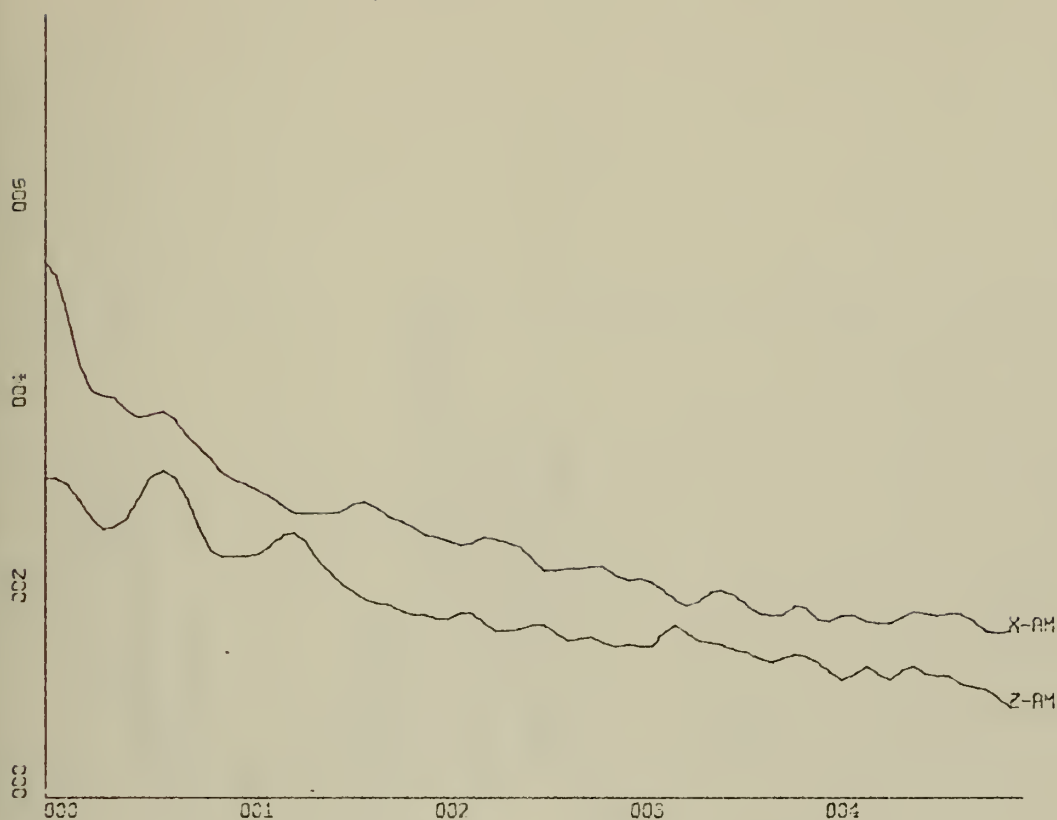
RUN PH-5



X-SCALE=2.00E+01 UNITS INCH.

Y-SCALE=2.00E-01 UNITS INCH.

TEMPORAL AUTOCORRELATION FN, X-AM, Z-AM
 RUN PH-5, FILE 8 OF CON6

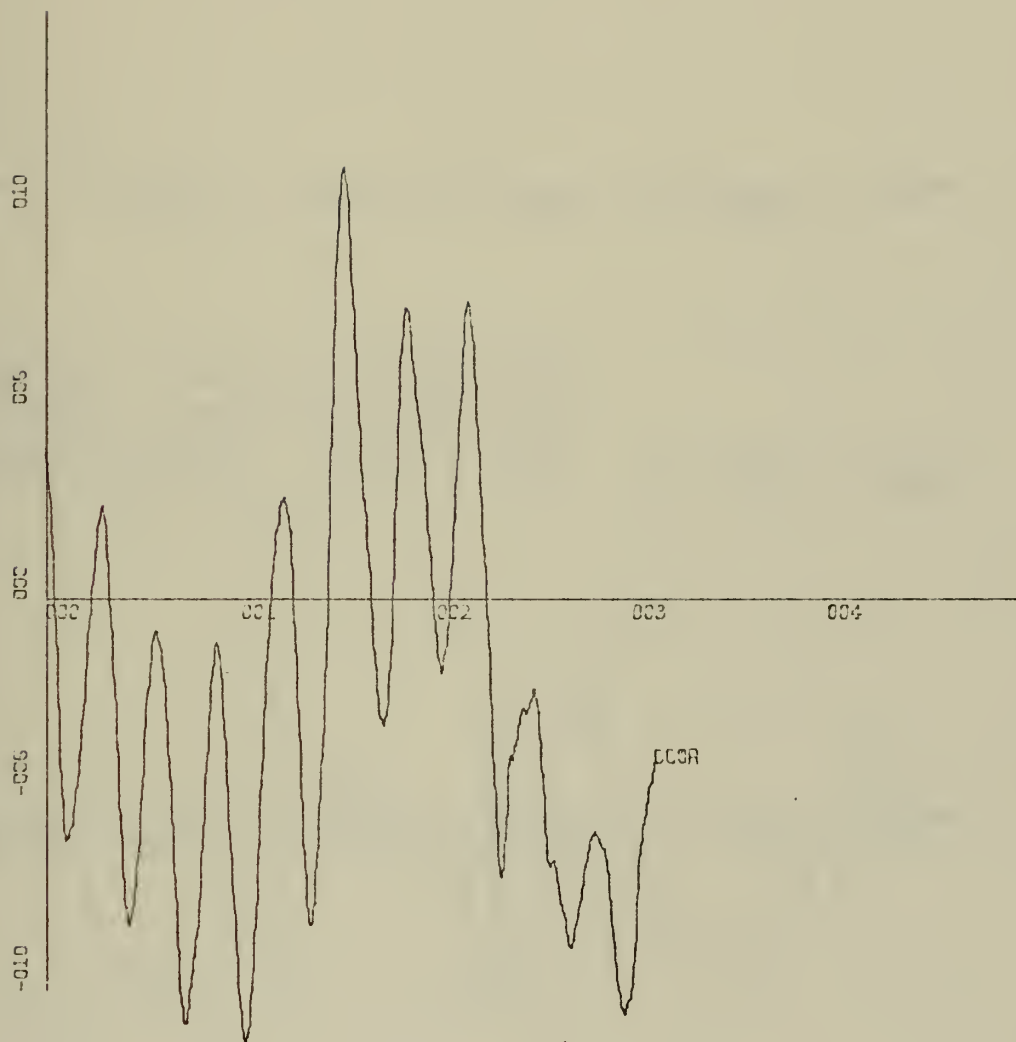


X-SCALE=1.00E-01 UNITS INCH.

Y-SCALE=2.00E+01 UNITS INCH.

POWER SPECTRUM LEVEL (DB) X-AM, Z-AM

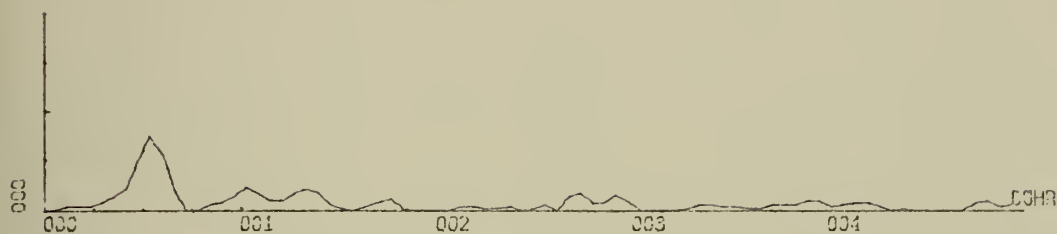
RUN PH-5, FILE 8 OF CON6



X-SCALE=1.00E+00 UNITS INCH.

Y-SCALE=5.00E-02 UNITS INCH.

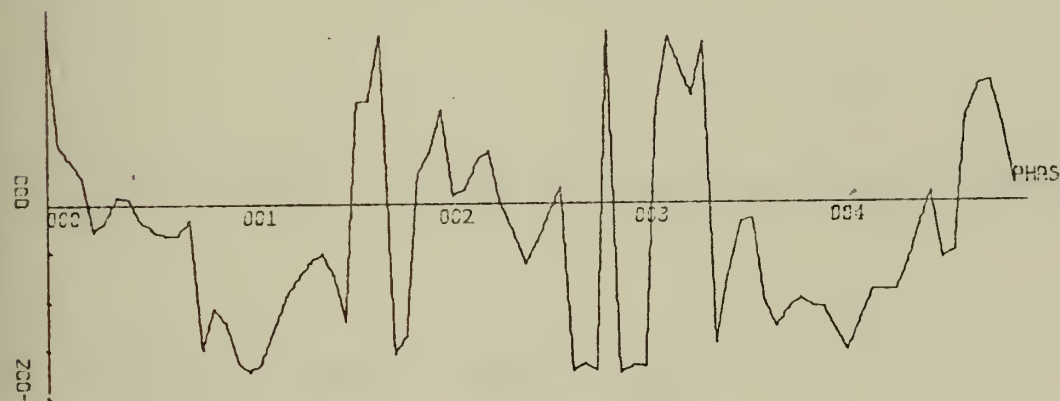
CROSS-CORRELATION FN, X-AM, Z-AM
 RUN PH-5, FILE 8 OF CON6



X-SCALE=1.00E-01 UNITS INCH.

Y-SCALE=1.00E+00 UNITS INCH.

COHERENCE FUNCTION X-AM, Z-AM

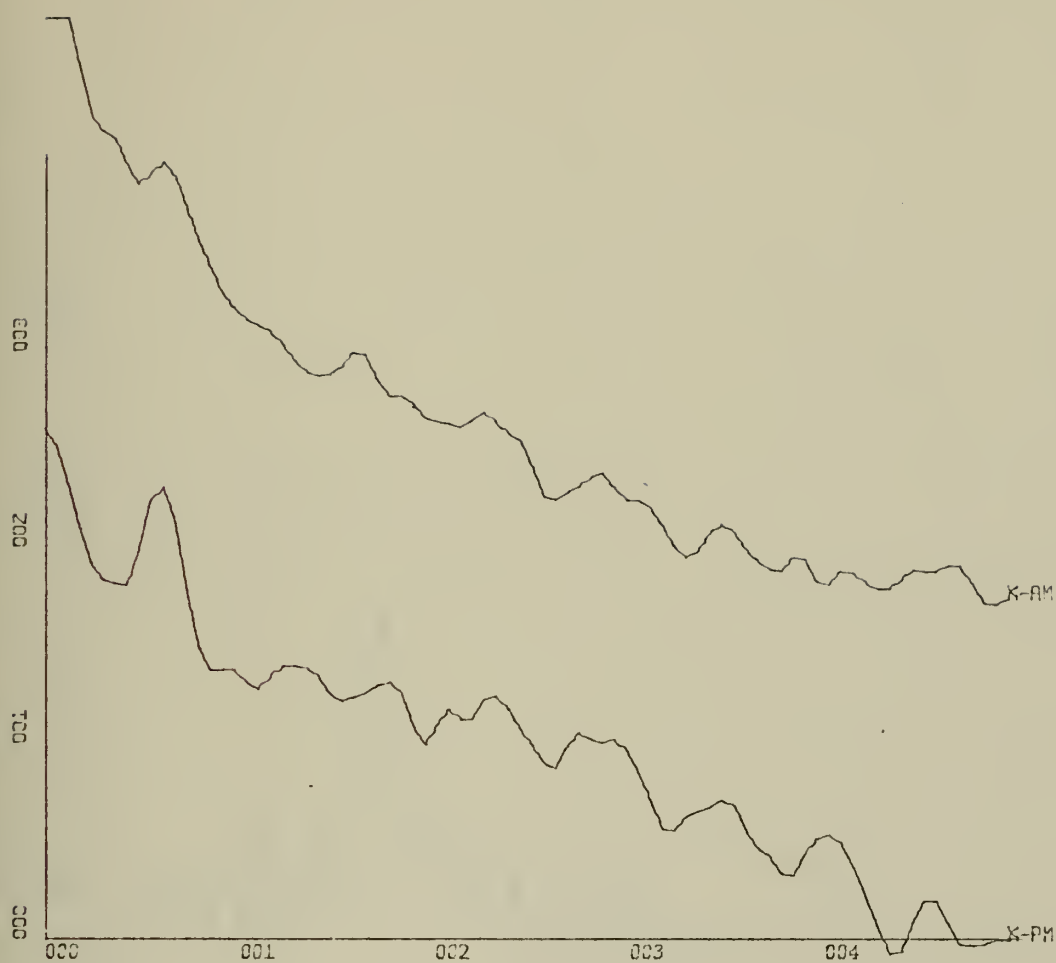


X-SCALE=1.00E-01 UNITS INCH.

Y-SCALE=2.00E+02 UNITS INCH.

CROSS SPECTRAL PHASE ANGLE, X-AM, Z-AM

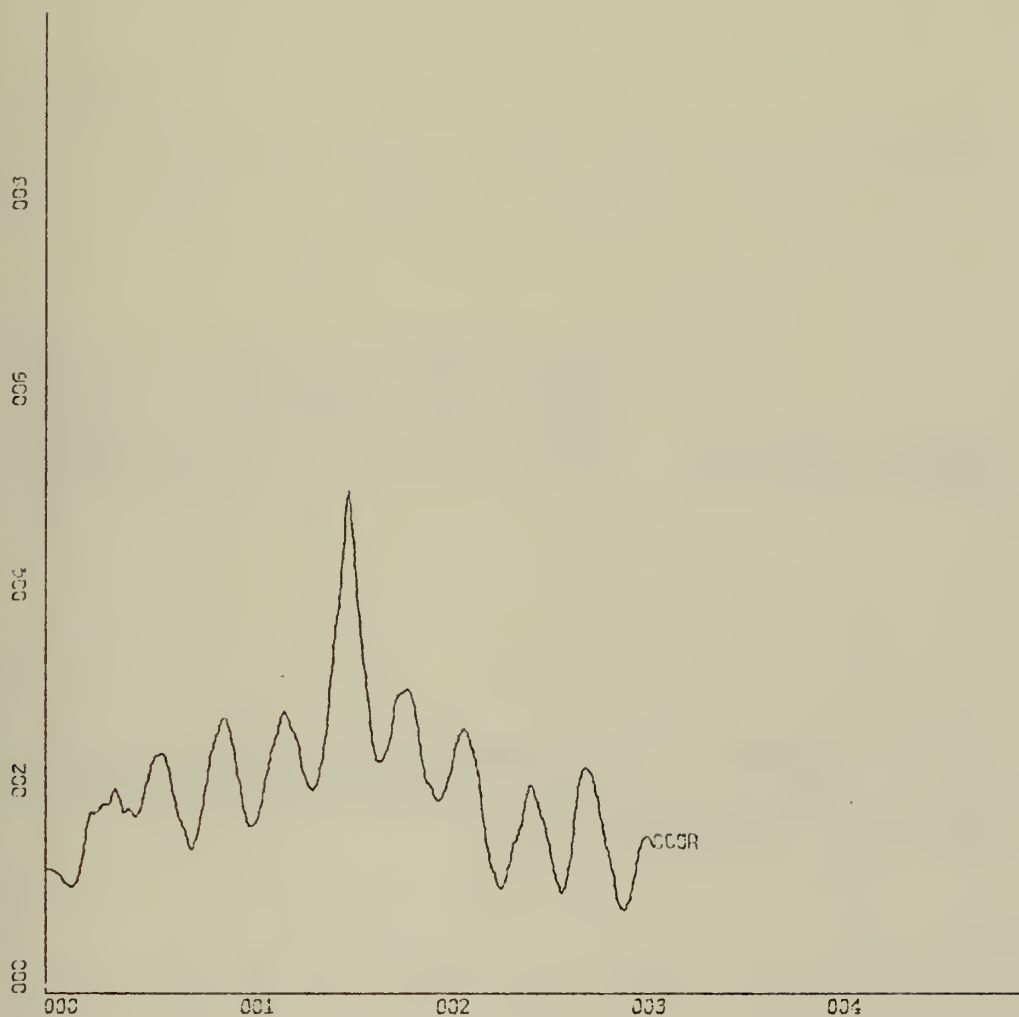
RUN PH-5



X-SCALE=1.00E-01 UNITS INCH.

Y-SCALE=1.00E+01 UNITS INCH.

POWER SPECTRUM, LEVEL (DB) X-PM, X-AM
 RUN PH-5, FILE 8 OF CON6



X-SCALE=1.00E+00 UNITS INCH.

Y-SCALE=2.00E-01 UNITS INCH.

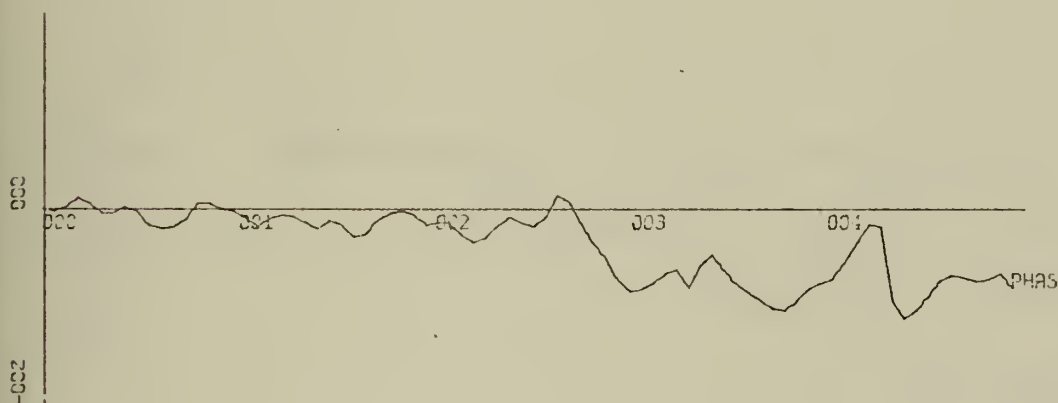
CROSS-CORRELATION FN, X-PM, X-AM
RUN PH-5, FILE 8 OF CON6



X-SCALE=1.00E-01 UNITS INCH.

Y-SCALE=1.00E+00 UNITS INCH.

COHERENCE FUNCTION X-PM, X-AM

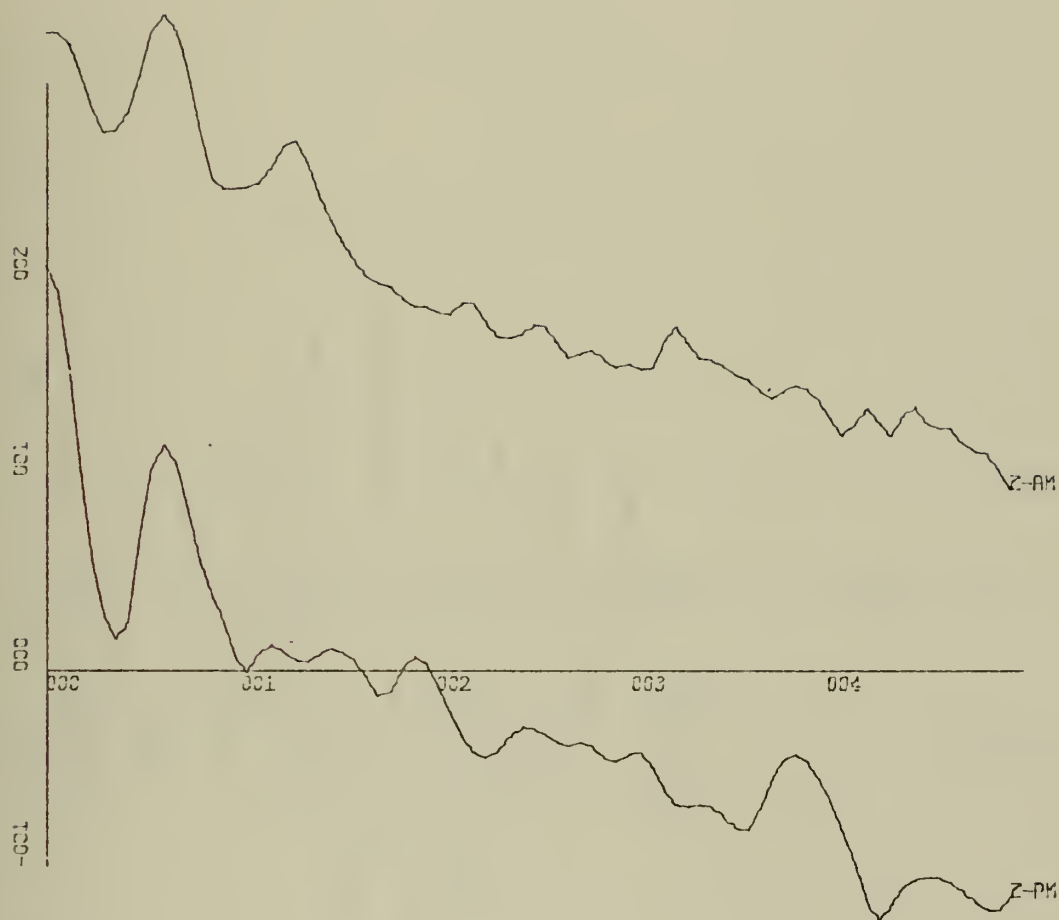


X-SCALE=1.00E-01 UNITS INCH.

Y-SCALE=2.00E+02 UNITS INCH.

CROSS SPECTRAL PHASE ANGLE, X-PM, X-AM

RUN PH-5

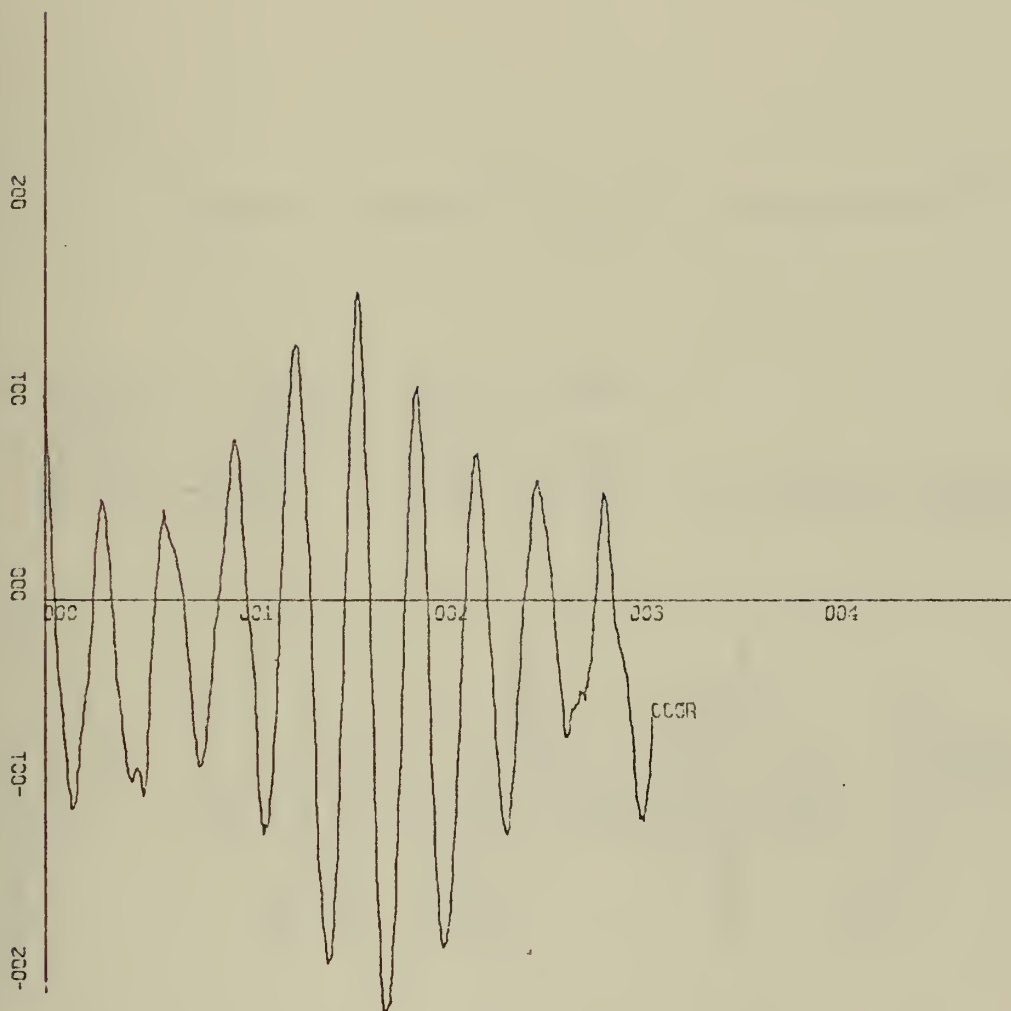


X-SCALE=1.00E-01 UNITS INCH.

Y-SCALE=1.00E+01 UNITS INCH.

POWER SPECTRUM LEVEL (DB) Z-PM, Z-AM

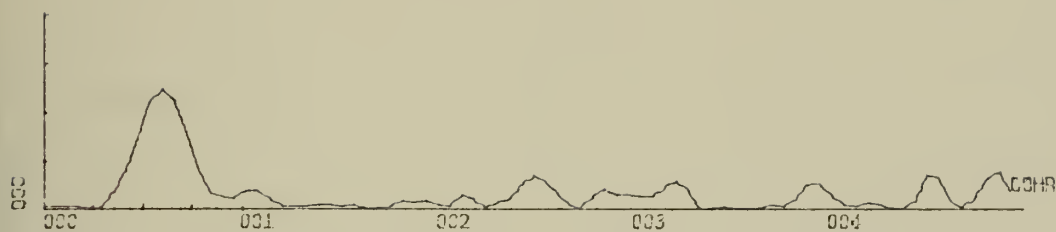
RUN PH-5, FILE 8 OF CON6



X-SCALE=1.00E+00 UNITS INCH.

Y-SCALE=1.00E-01 UNITS INCH.

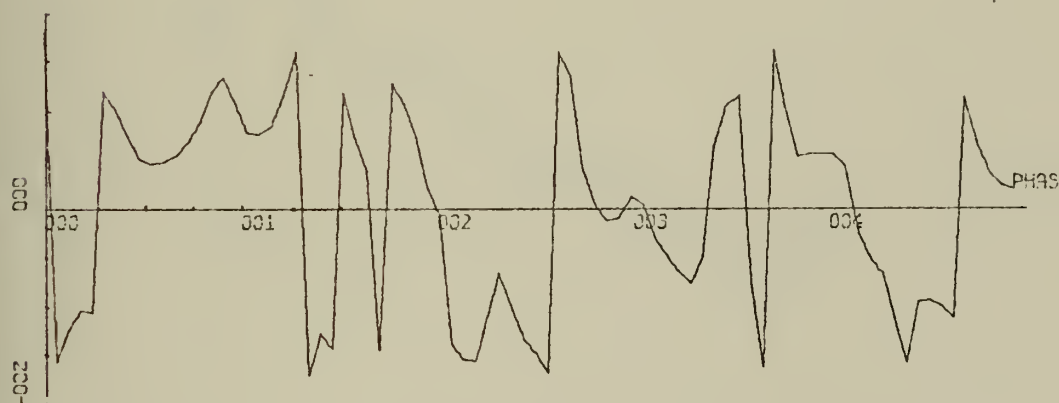
CROSS-CORRELATION FN, Z-PM, Z-AM
RUN PH-5, FILE 8 OF CON6



X-SCALE=1.00E-01 UNITS INCH.

Y-SCALE=1.00E+00 UNITS INCH.

COHERENCE FUNCTION Z-PM, Z-AM

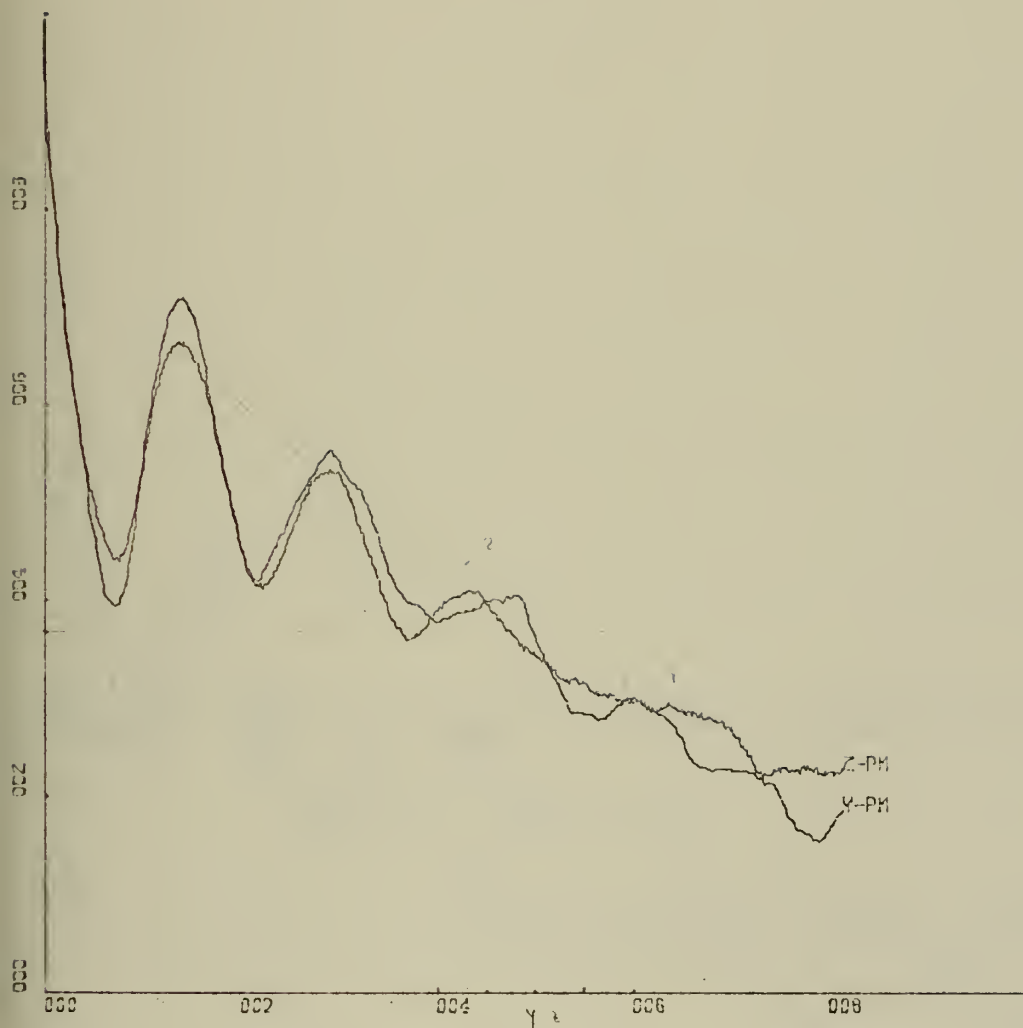


X-SCALE=1.00E-01 UNITS INCH.

Y-SCALE=2.00E+02 UNITS INCH.

CROSS SPECTRAL PHASE ANGLE, Z-PM, Z-AM

RUN PH-5



X-SCALE=2.00E+01 UNITS INCH.

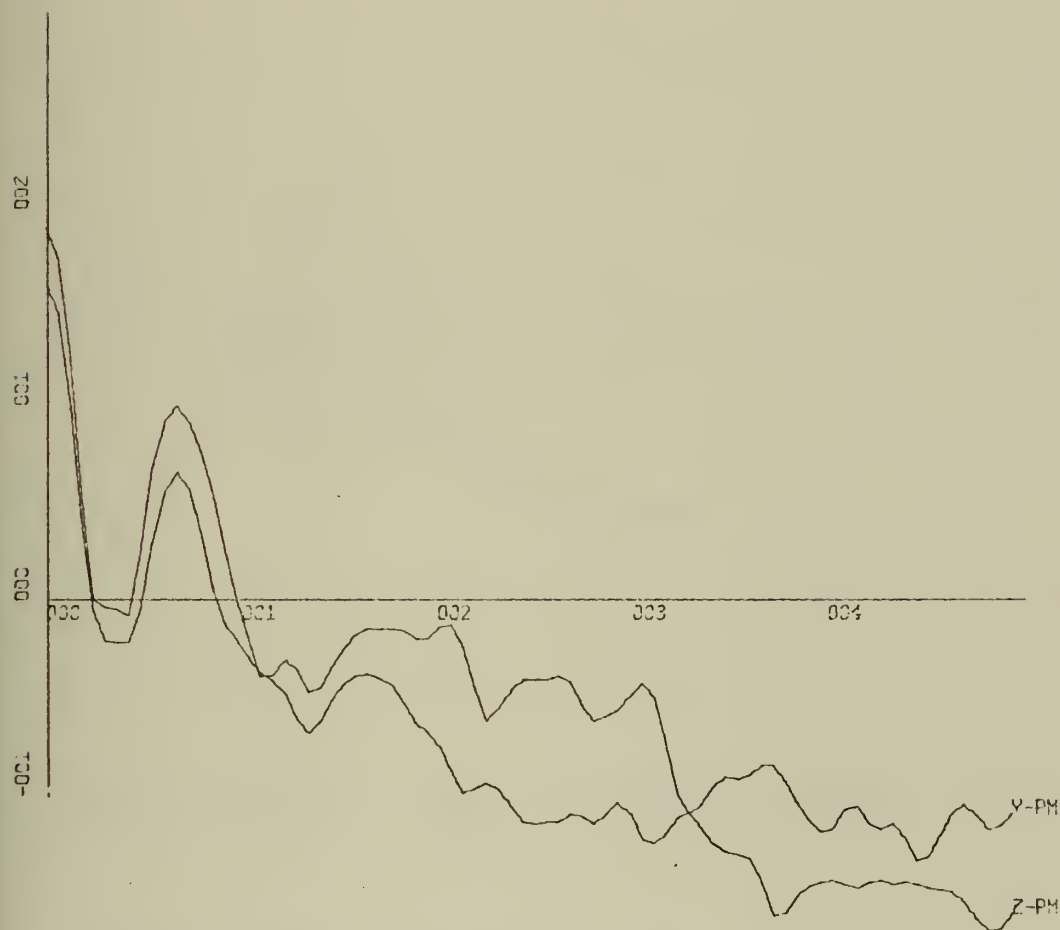
Y-SCALE=2.00E-01 UNITS INCH.

TEMPORAL AUTOCORRELATION FN, Y-PM, Z-PM

RUN PH-6, FILE 9 OF CON6

Y- 5.000

Z- 5.124000

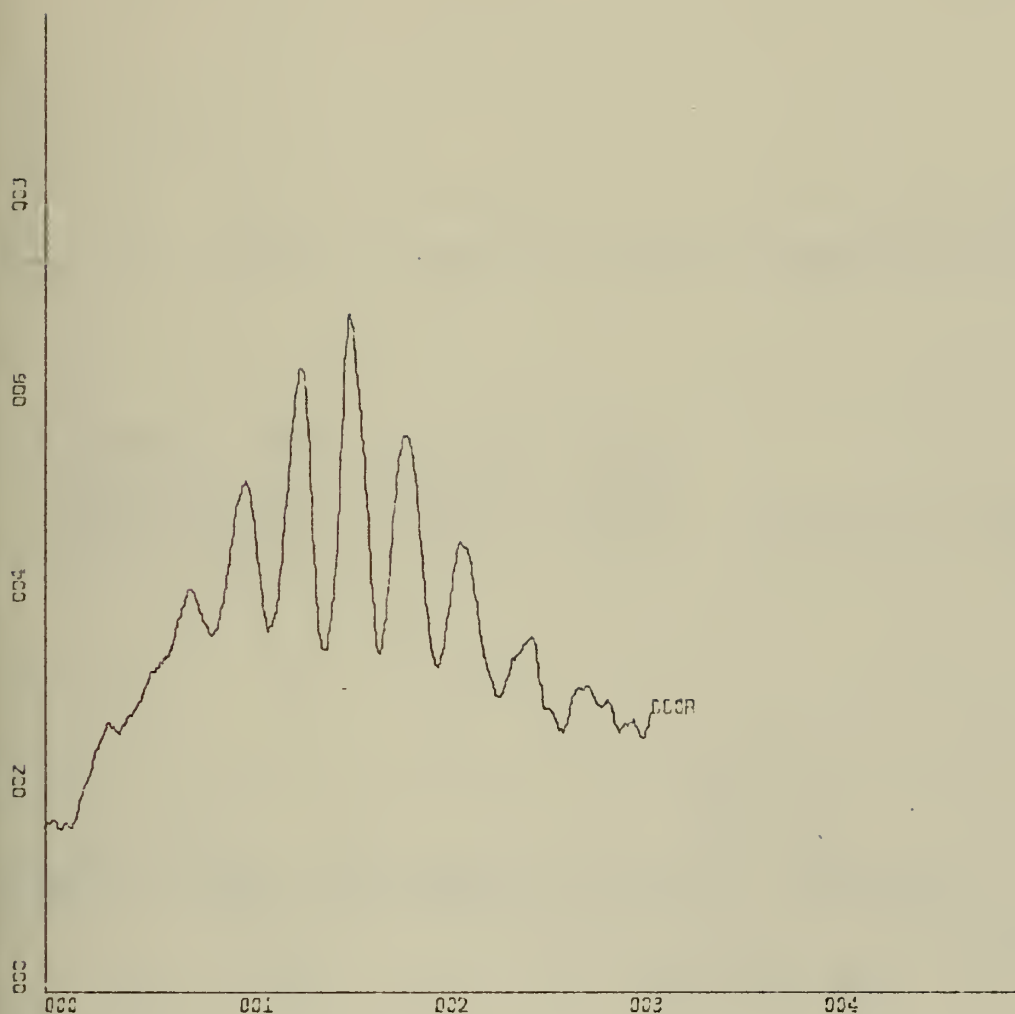


X-SCALE=1.00E-01 UNITS INCH.

Y-SCALE=1.00E+01 UNITS INCH.

POWER SPECTRUM LEVEL (DB) Y-PM, Z-PM

RUN PH-6, FILE 9 OF CON6



X-SCALE=1.00E+00 UNITS INCH.

Y-SCALE=2.00E-01 UNITS INCH.

CROSS-CORRELATION FN, Y-PM, Z-PM

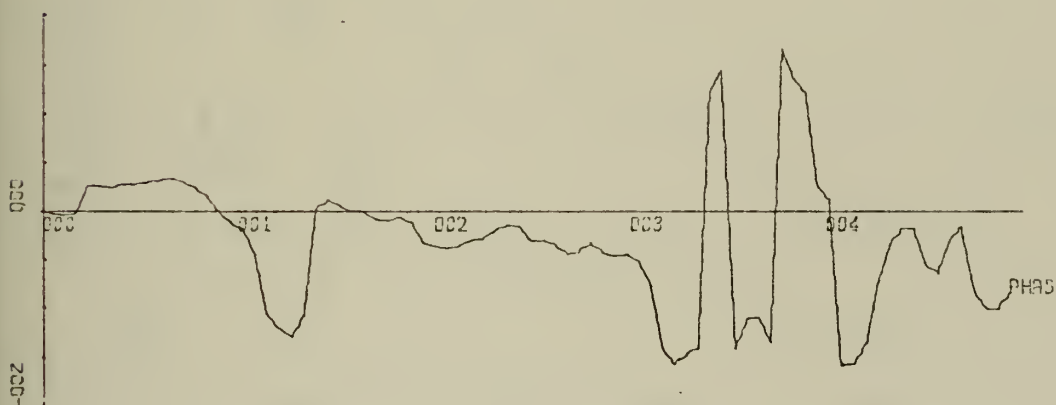
RUN PH-6, FILE 9 OF CON6



X-SCALE=1.00E-01 UNITS INCH.

Y-SCALE=1.00E+00 UNITS INCH.

COHERENCE FUNCTION Y-PM, Z-PM

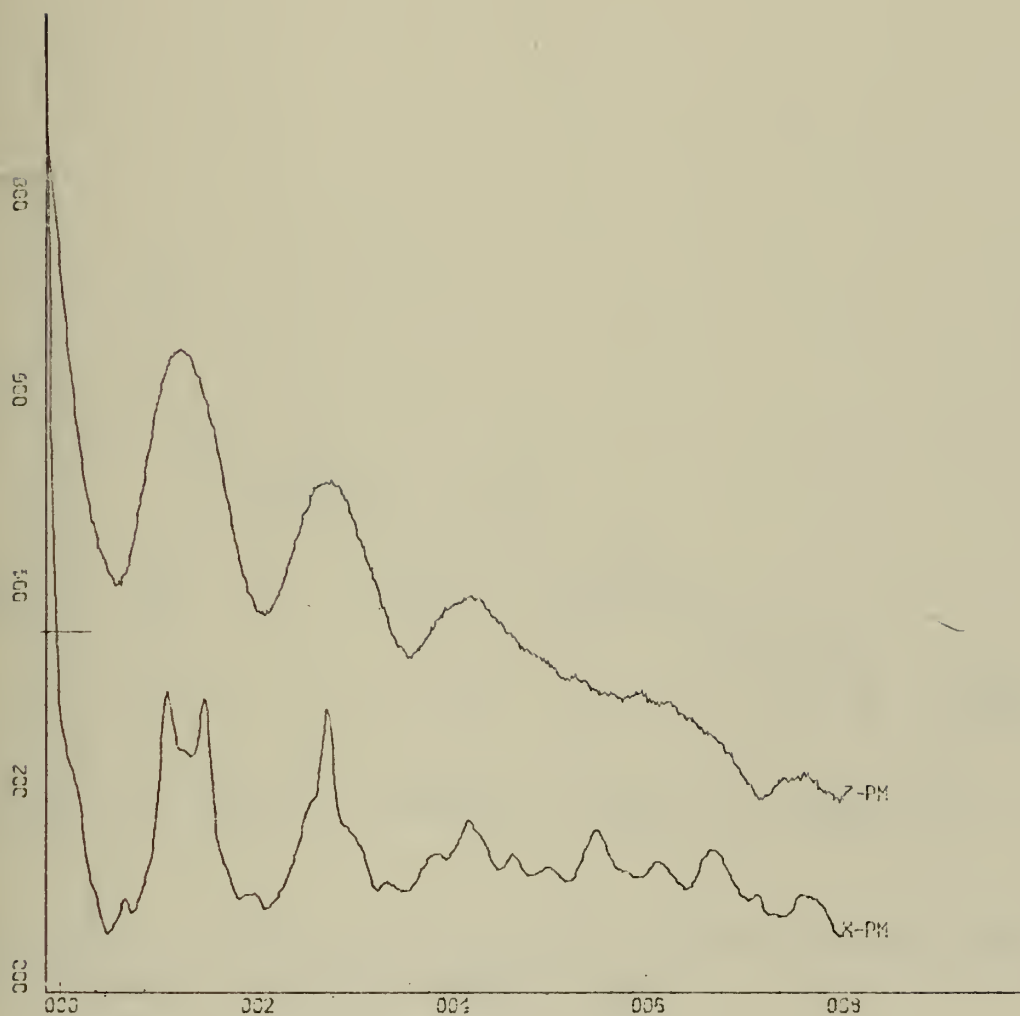


X-SCALE=1.00E-01 UNITS INCH.

Y-SCALE=2.00E+02 UNITS INCH.

CROSS SPECTRAL PHASE ANGLE, Y-PM, Z-PM

RUN PH-6

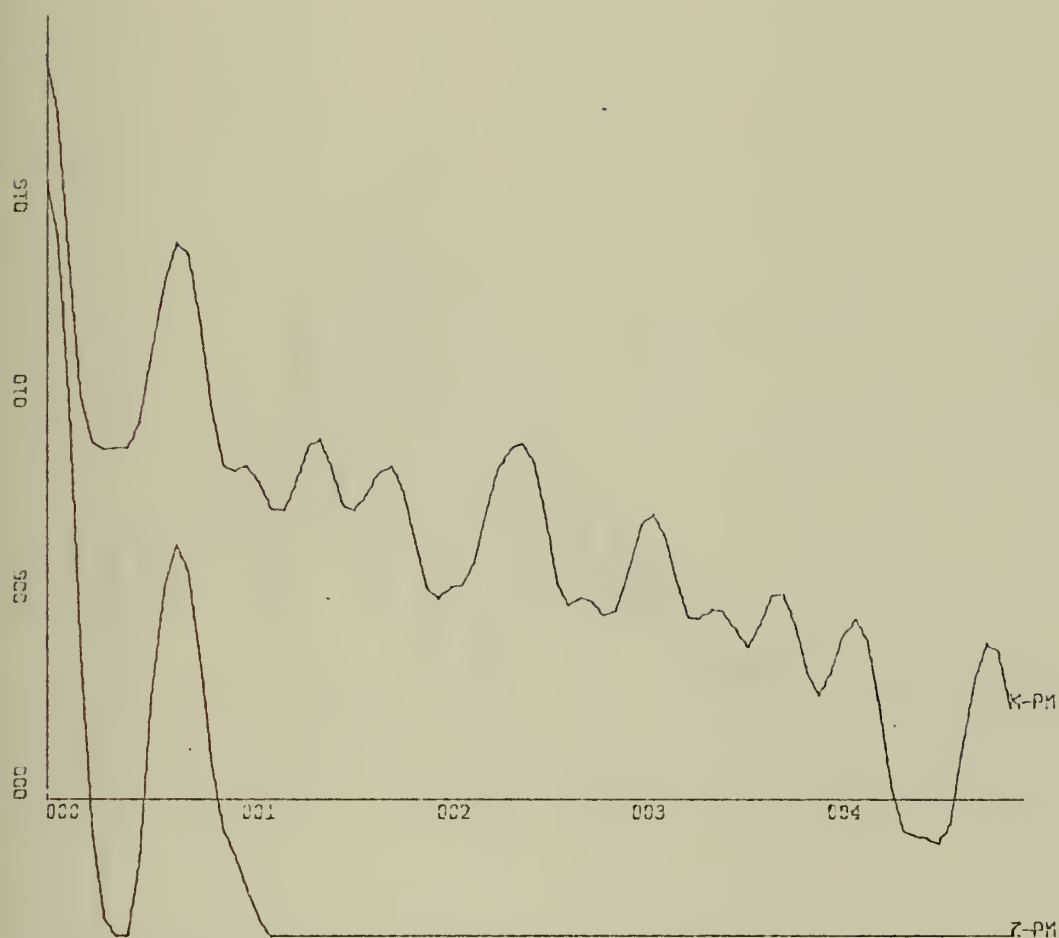


X-SCALE=2.00E+01 UNITS INCH.

Y-SCALE=2.00E-01 UNITS INCH.

TEMPORAL AUTOCORRELATION FN, X-PM, Z-PM

RUN PH-6, FILE 9 OF CON6

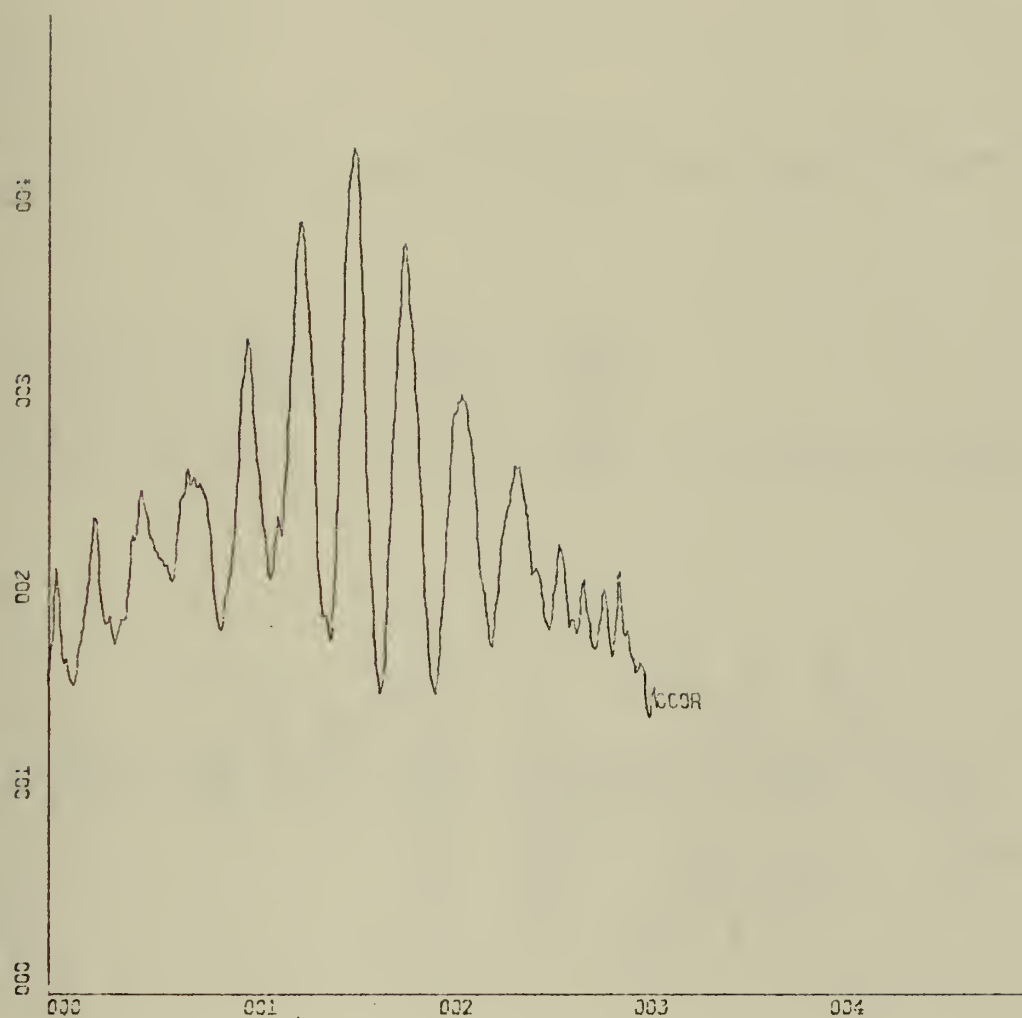


X-SCALE=1.00E-01 UNITS INCH.

Y-SCALE=5.00E+00 UNITS, INCH.

POWER SPECTRUM LEVEL (DB) X-PM, Z-PM

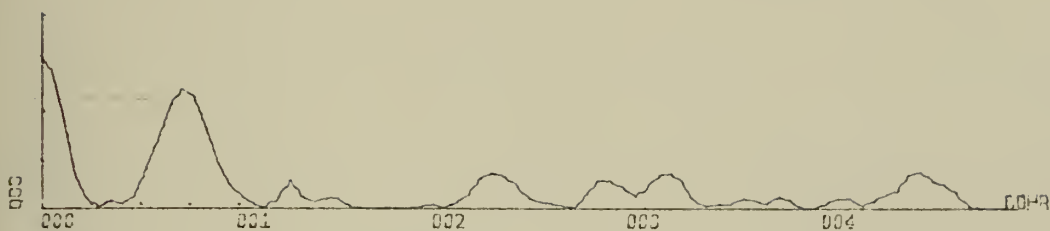
RUN PH-6, FILE 9 OF CON6



X-SCALE=1.00E+00 UNITS INCH.

Y-SCALE=1.00E-01 UNITS INCH.

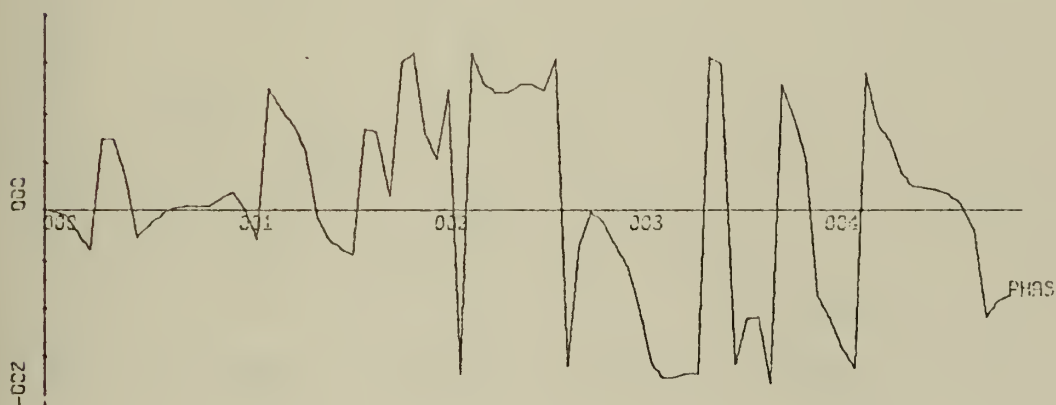
CROSS-CORRELATION FN, X-PM, Z-PM
RUN PH-6, FILE 9 OF CON6



X-SCALE=1.00E-01 UNITS INCH.

Y-SCALE=1.00E+00 UNITS INCH.

COHERENCE FUNCTION X-PM, Z-PM

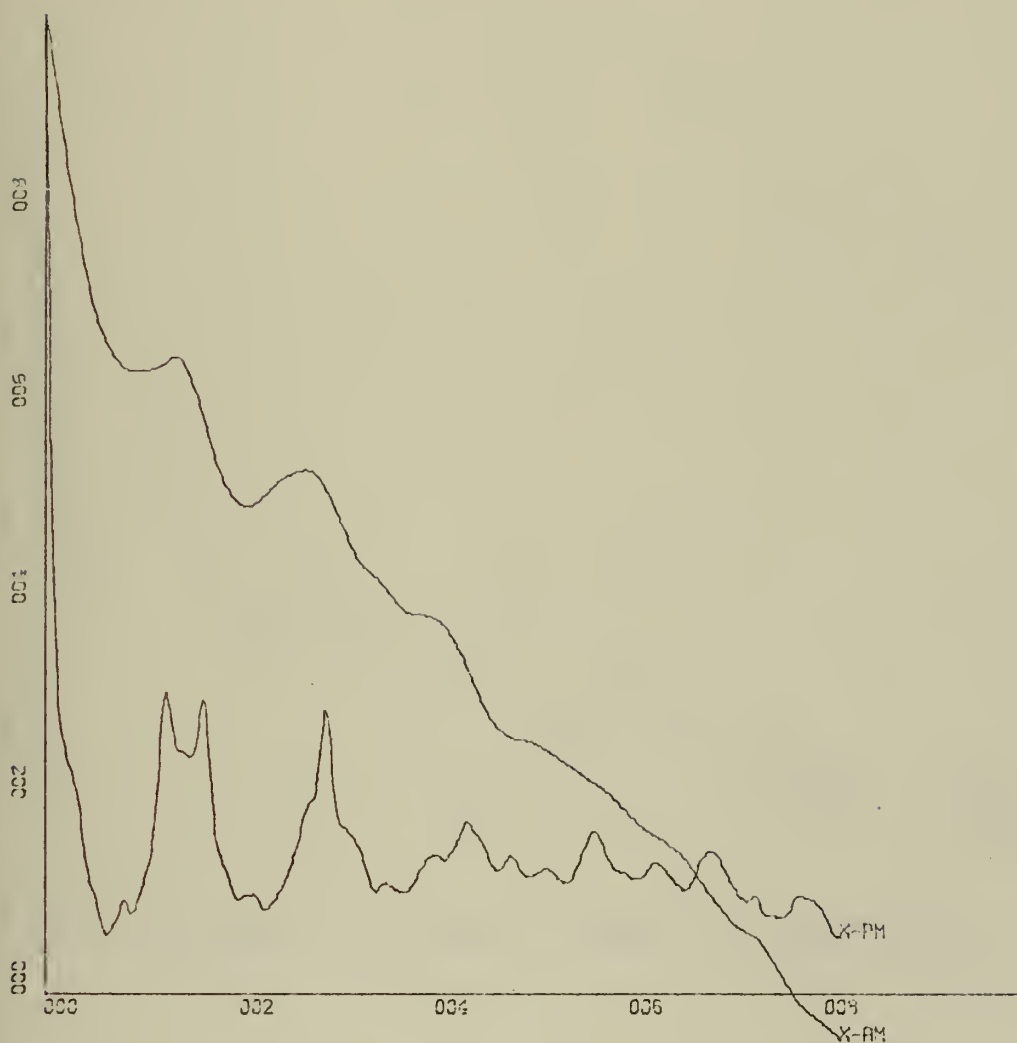


X-SCALE=1.00E-01 UNITS INCH.

Y-SCALE=2.00E+02 UNITS INCH.

CROSS SPECTRAL PHASE ANGLE, X-PM, Z-PM

RUN PH-6

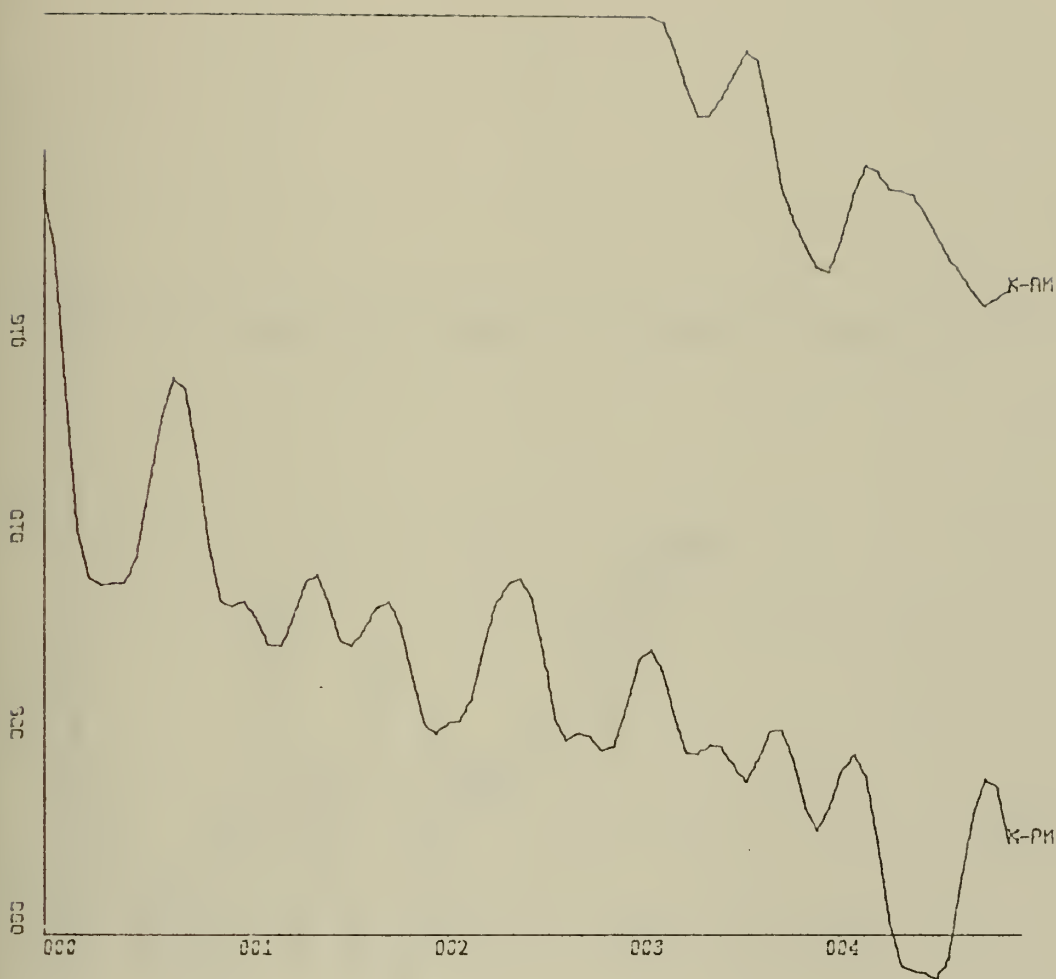


X-SCALE::2.00E+01 UNITS INCH.

Y-SCALE::2.00E-01 UNITS INCH.

TEMPORAL AUTOCORRELATION FN, X-PM, X-AM

RUN PH-6, FILE 9 OF CON6

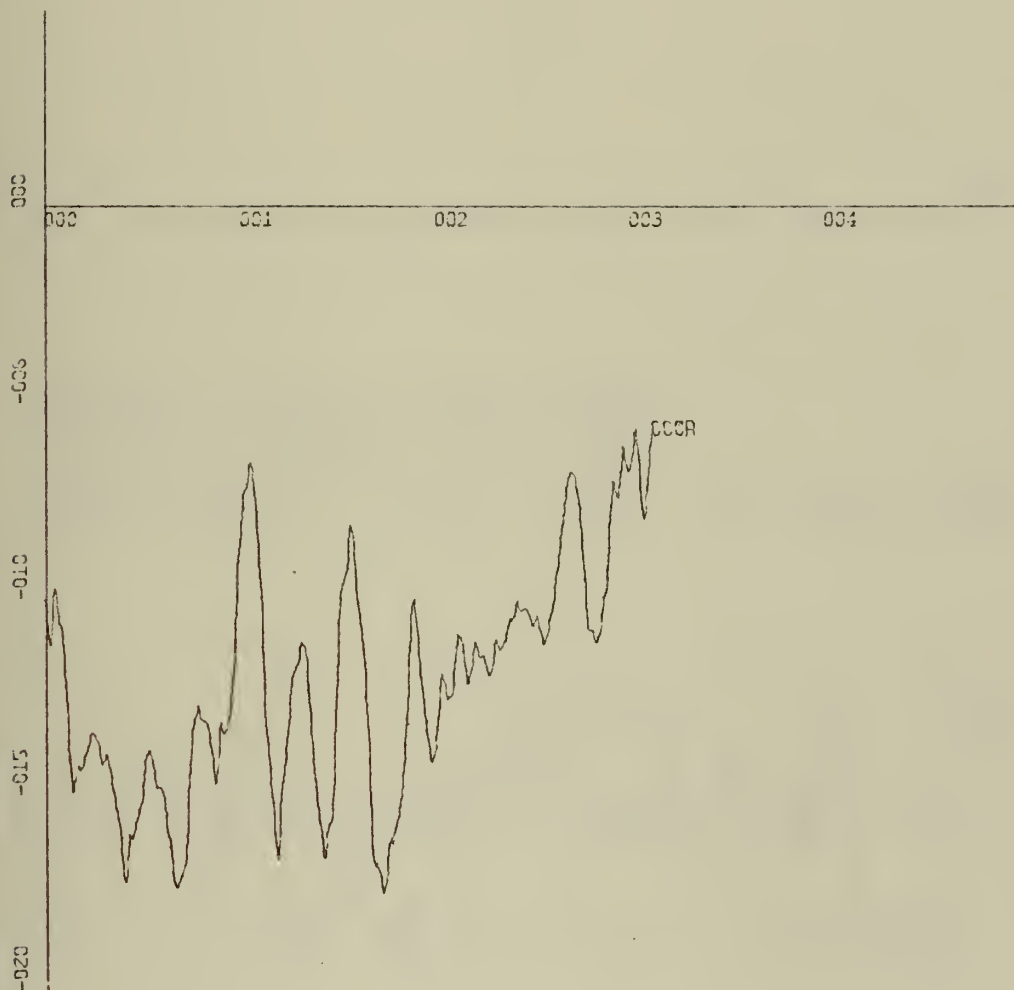


X-SCALE=1.00E-01 UNITS INCH.

Y-SCALE=5.00E+00 UNITS INCH.

POWER SPECTRUM LEVEL (DB) X-PM, X-AM

RUN PH-6, FILE 9 OF CON6

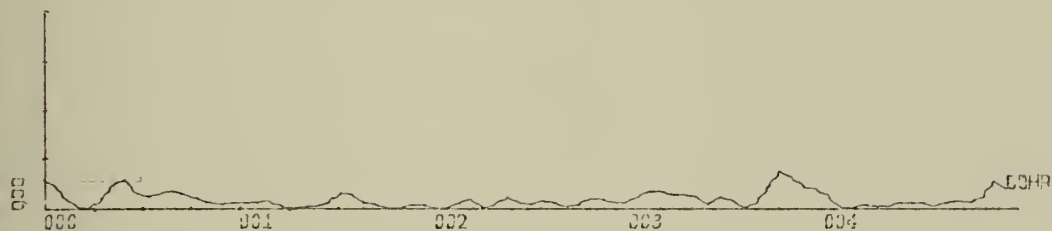


X-SCALE=1.00E+00 UNITS INCH.

Y-SCALE=5.00E-02 UNITS INCH.

CROSS-CORRELATION FN, X-PM, X-AM

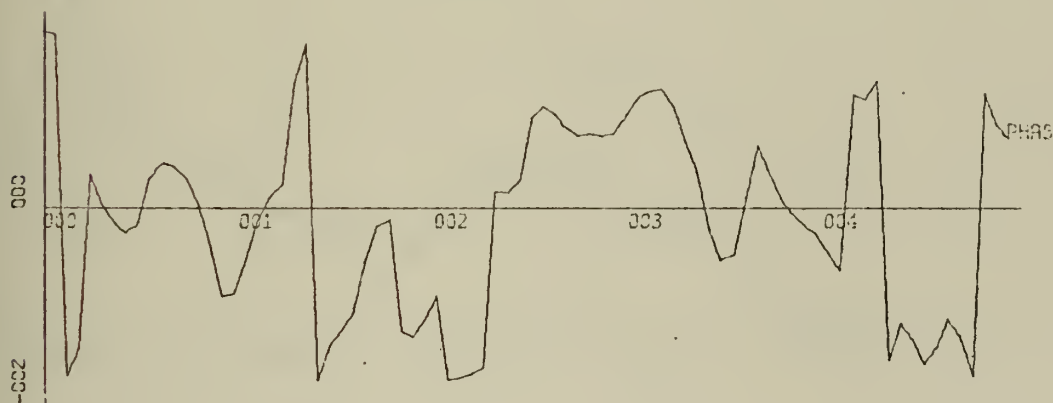
RUN PH-6, FILE 9 OF CON6



X-SCALE=1.00E-01 UNITS INCH.

Y-SCALE=1.00E+00 UNITS INCH.

COHERENCE FUNCTION X-PM, X-AM

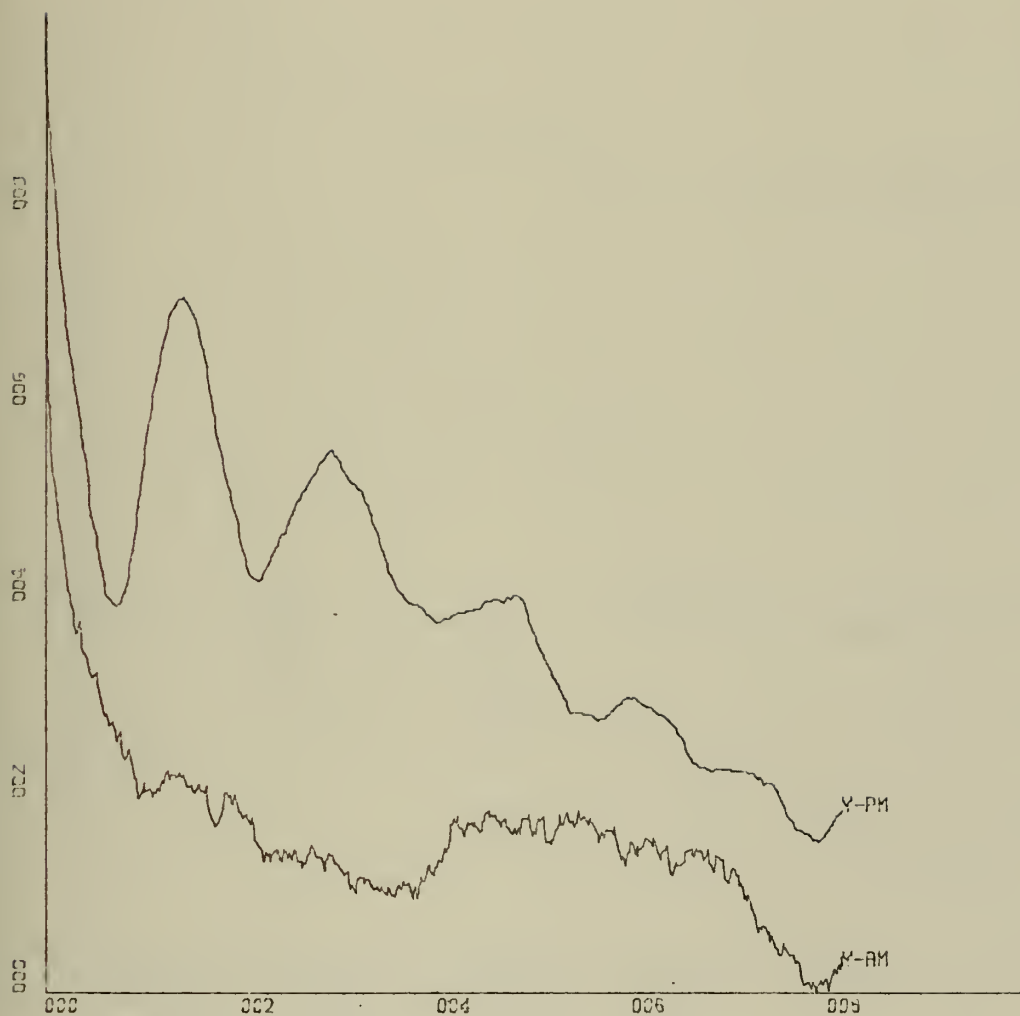


X-SCALE=1.00E-01 UNITS INCH.

Y-SCALE=2.00E+02 UNITS INCH.

CROSS SPECTRAL PHASE ANGLE, X-PM, X-AM

RUN PH-6

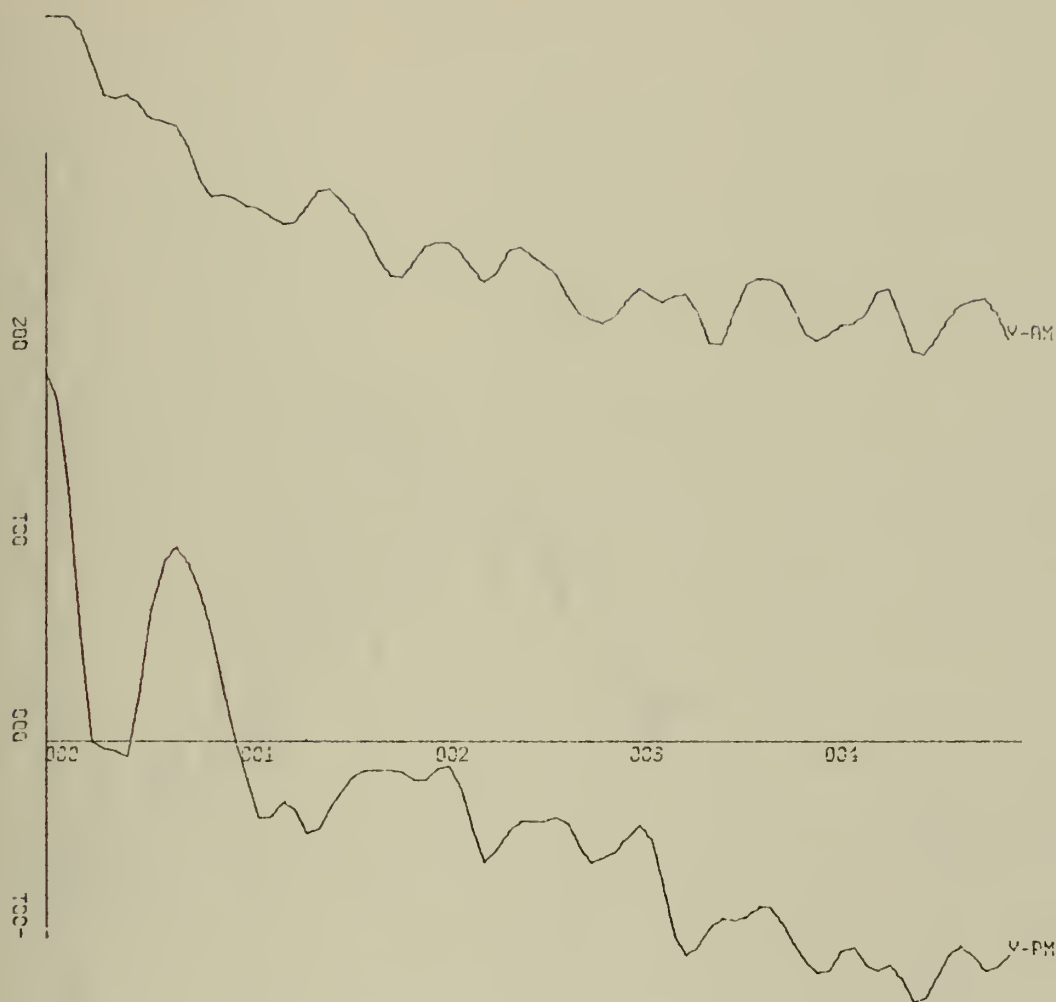


X-SCALE=2.00E+01 UNITS INCH.

Y-SCALE=2.00E-01 UNITS INCH.

TEMPORAL AUTOCORRELATION FN, Y-PM, Y-AM

RUN PH-6, FILE 9 OF CON6

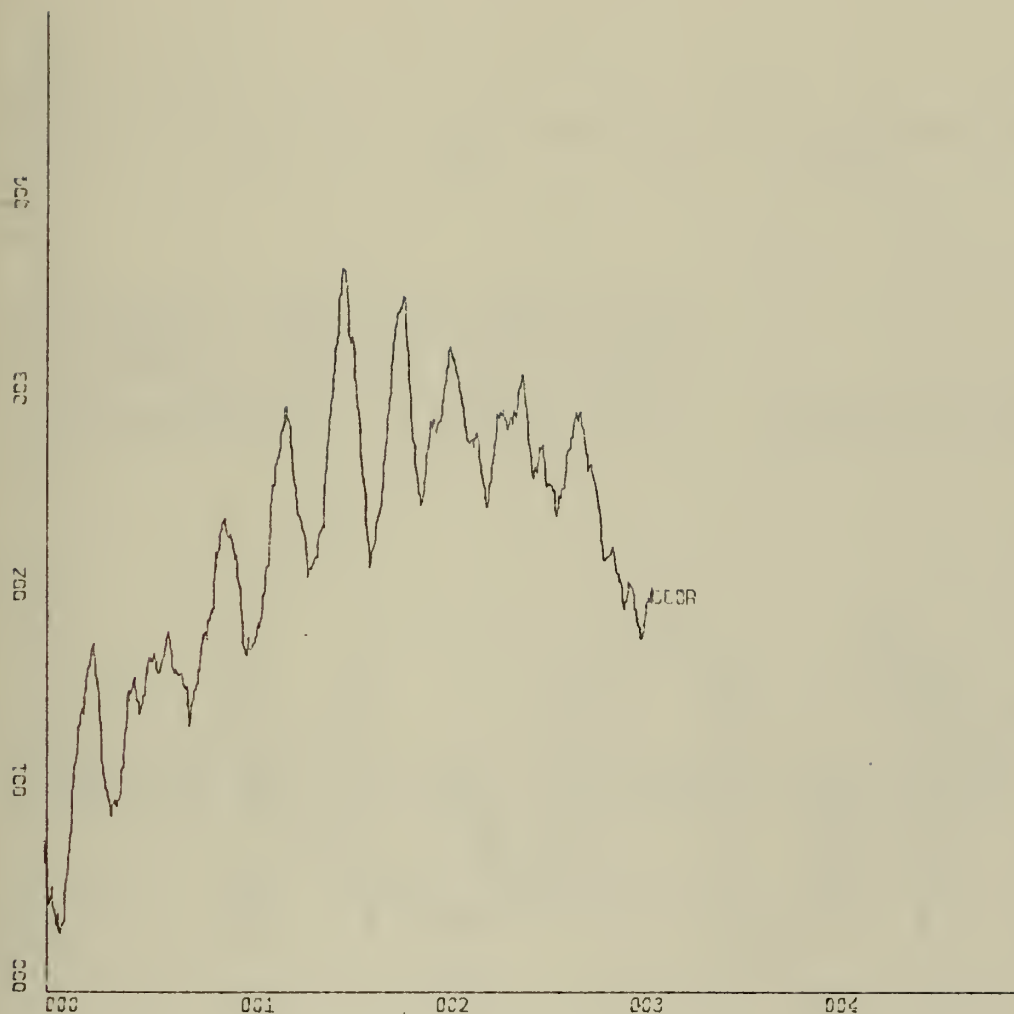


X-SCALE:=1.00E-01 UNITS INCH.

Y-SCALE:=1.00E+01 UNITS INCH.

POWER SPECTRUM LEVEL (DB) Y-PM, Y-AM

RUN PH-6, FILE 9 OF CON6

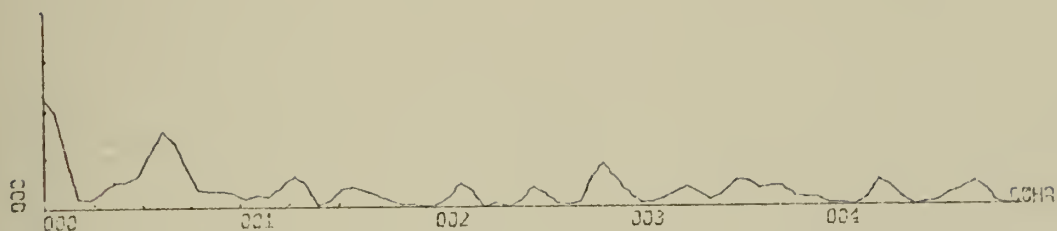


X-SCALE=1.00E+00 UNITS INCH.

Y-SCALE=1.00E-01 UNITS INCH.

CROSS-CORRELATION FN, Y-PM, Y-AM

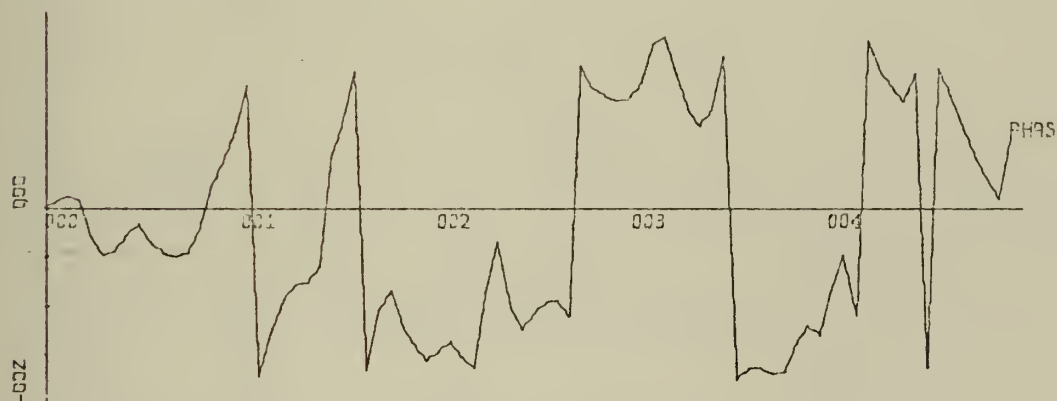
RUN PH-6, FILE 9 OF CON6



X-SCALE=1.00E-01 UNITS INCH.

Y-SCALE=1.00E+00 UNITS INCH.

COHERENCE FUNCTION Y-PM, Y-AM

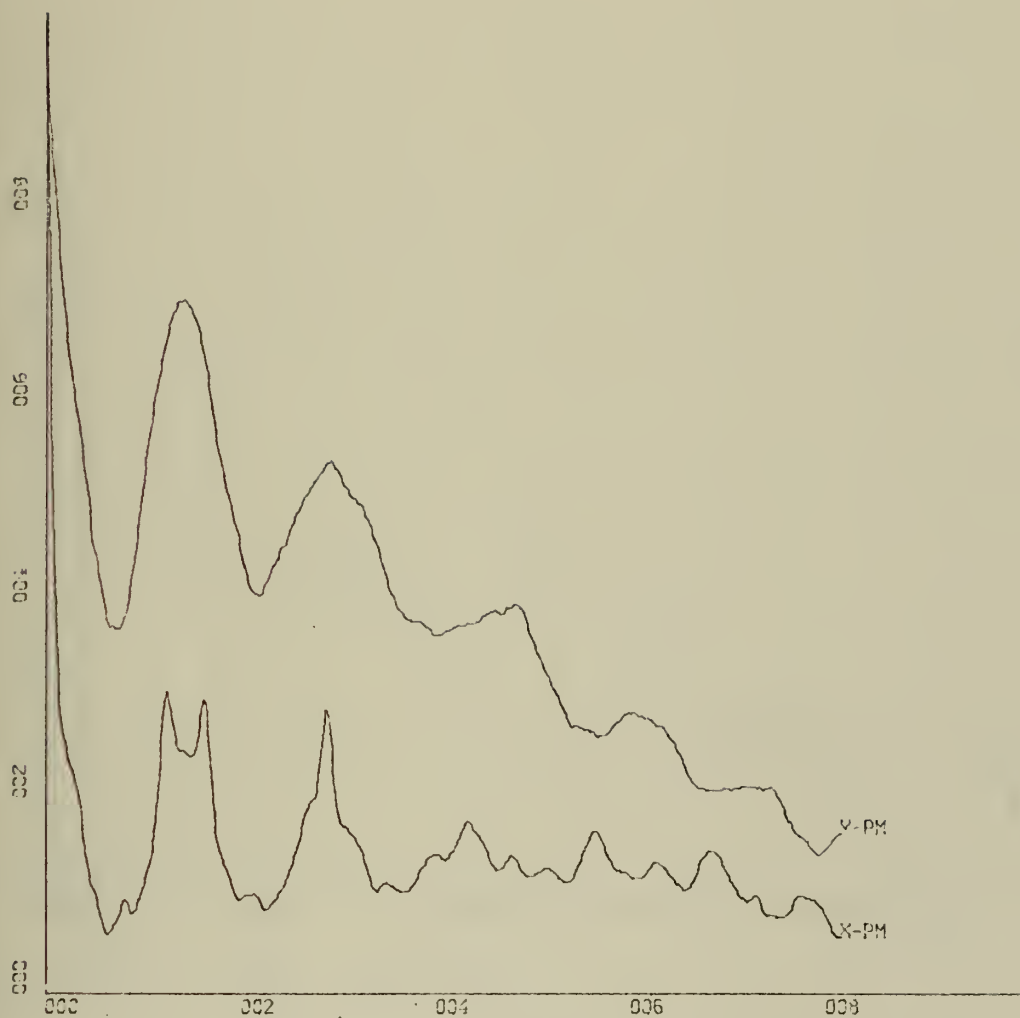


X-SCALE=1.00E-01 UNITS INCH.

Y-SCALE=2.00E+02 UNITS INCH.

CROSS SPECTRAL PHASE ANGLE, Y-PM, Y-AM

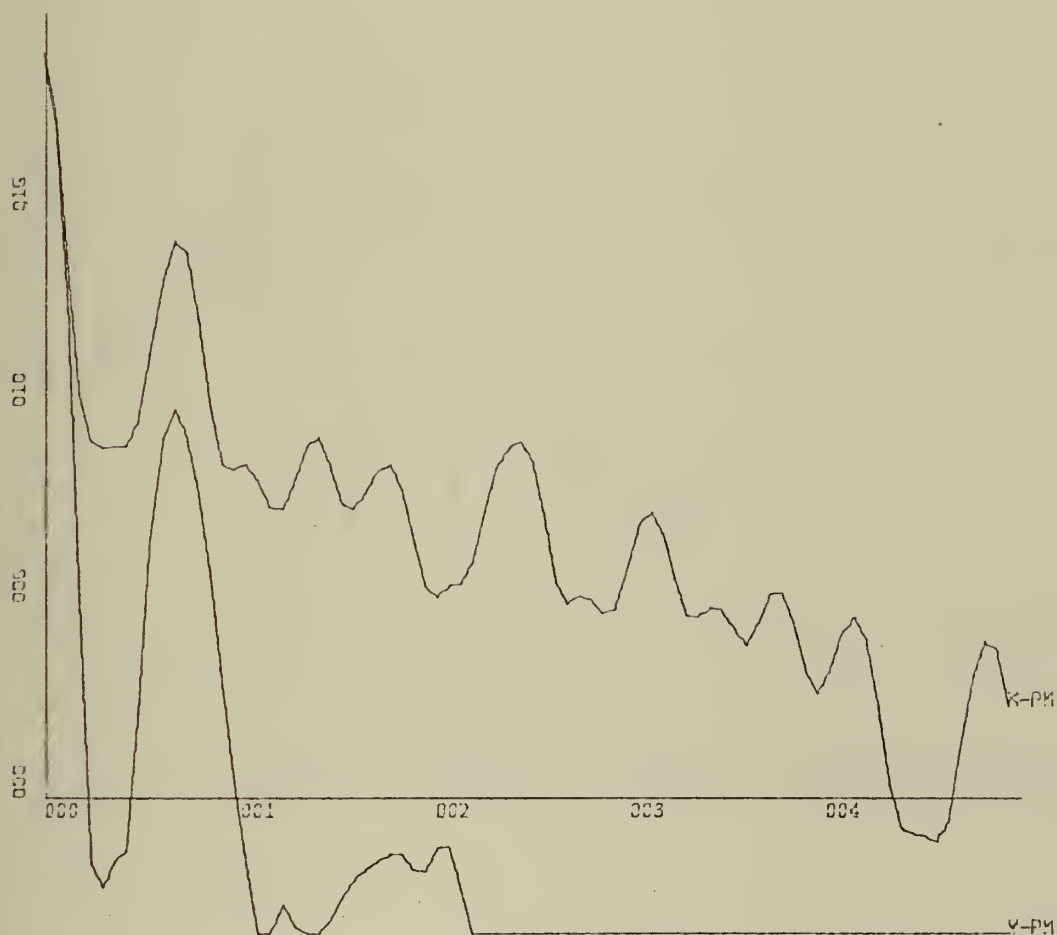
RUN PH-6



X-SCALE=2.00E+01 UNITS INCH.

Y-SCALE=2.00E-01 UNITS INCH.

TEMPORAL AUTOCORRELATION FN, X-PM, Y-PM
 RUN PH-6, FILE 9 OF CON6

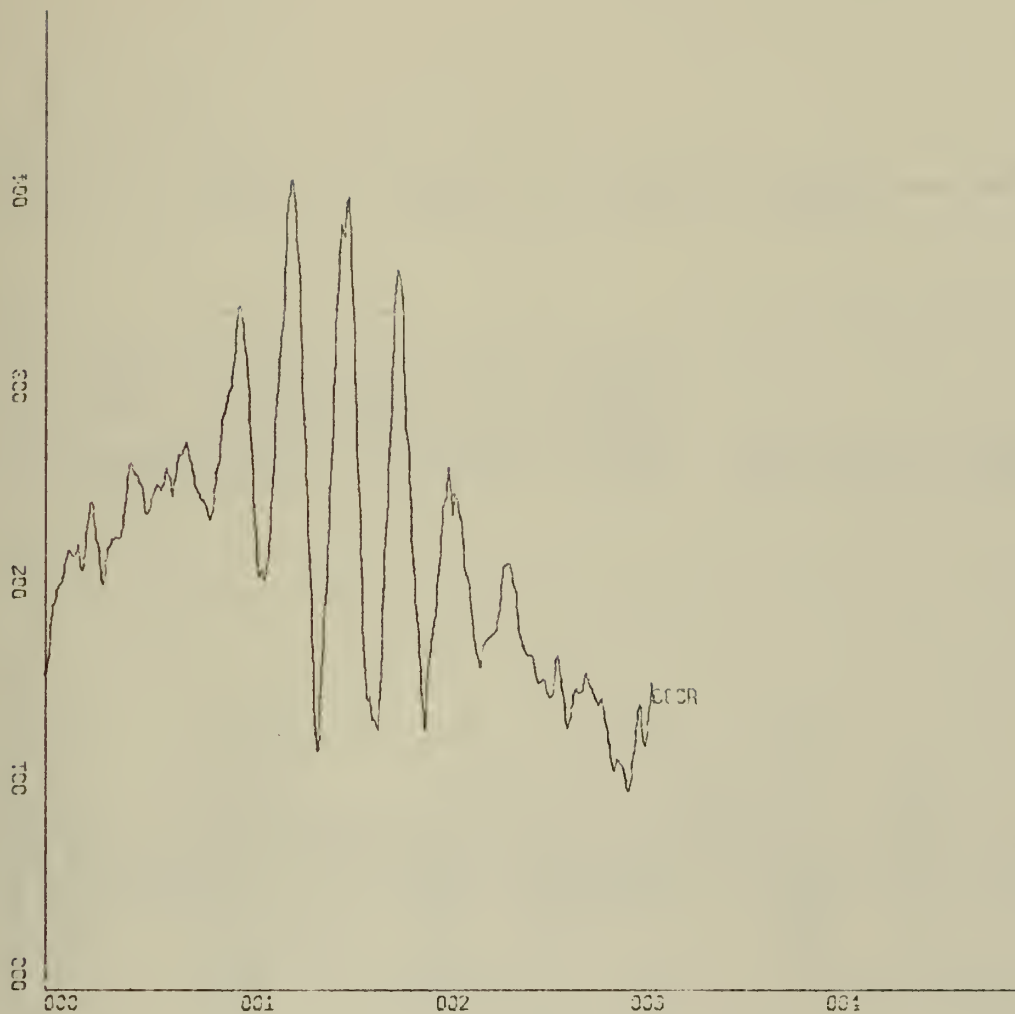


X-SCALE=1.00E-01 UNITS INCH.

Y-SCALE=5.00E+00 UNITS INCH.

POWER SPECTRUM LEVEL (DB) X-PM, Y-PM

RUN PH-6, FILE 9 OF CON6

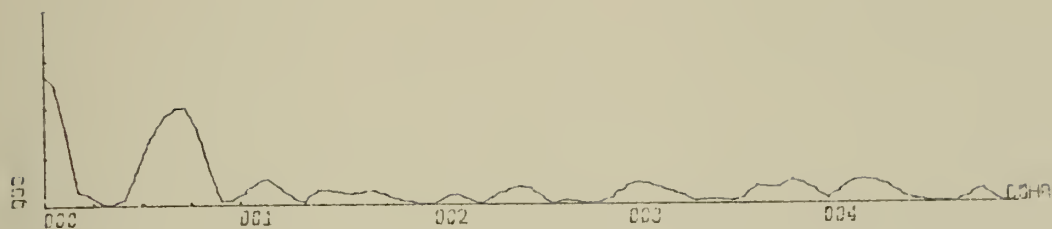


X-SCALE=1.00E+00 UNITS INCH.

Y-SCALE=1.00E-01 UNITS INCH.

CROSS-CORRELATION FN, X-PM, Y-PM

RUN PH-6, FILE 9 OF CON6



X-SCALE=1.00E-01 UNITS INCH.

Y-SCALE=1.00E+00 UNITS INCH.

COHERENCE FUNCTION X-PM, Y-PM

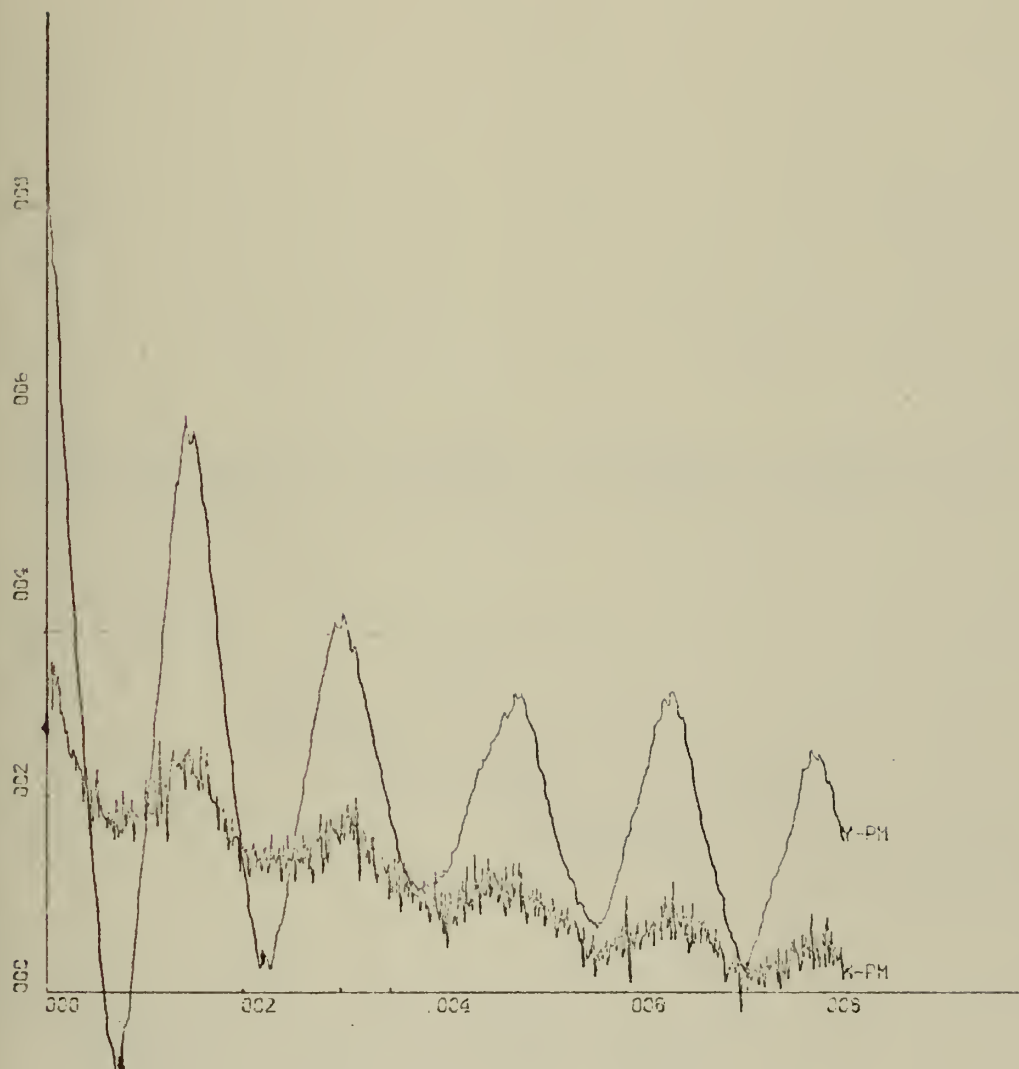


X-SCALE=1.00E-01 UNITS INCH.

Y-SCALE=2.00E+02 UNITS INCH.

CROSS SPECTRAL PHASE ANGLE, X-PM, Y-PM

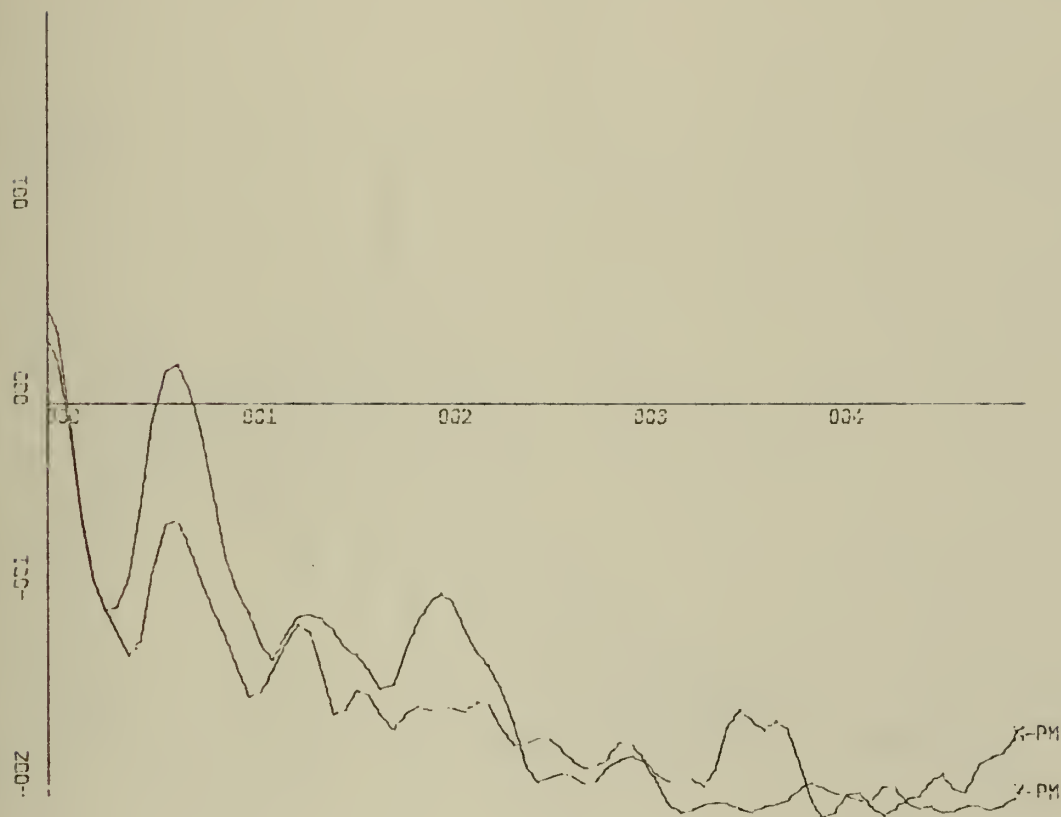
RUN PH-6



X-SCALE=2.00E+01 UNITS INCH.

Y-SCALE=2.00E-01 UNITS INCH.

TEMPORAL AUTOCORRELATION FN, X-PH Y-PH
 RUN PH-7, FILE 10 OF CON 6

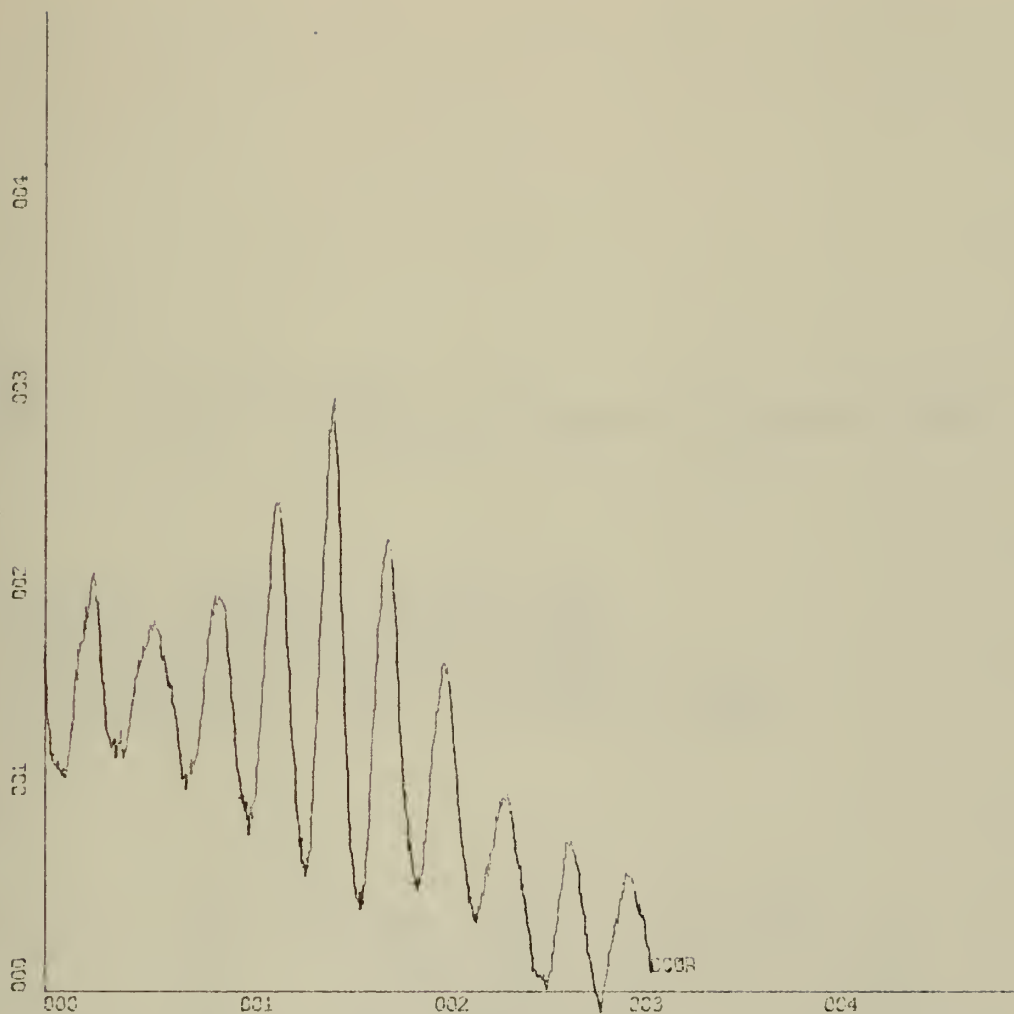


X-SCALE=1.00E-01 UNITS INCH.

Y-SCALE=1.00E+01 UNITS INCH.

POWER SPECTRUM LEVEL (DB) X-PM Y-PM

RUN PH-7, FILE 10 OF CON 6



X-SCALE=-1.00E+00 UNITS INCH.

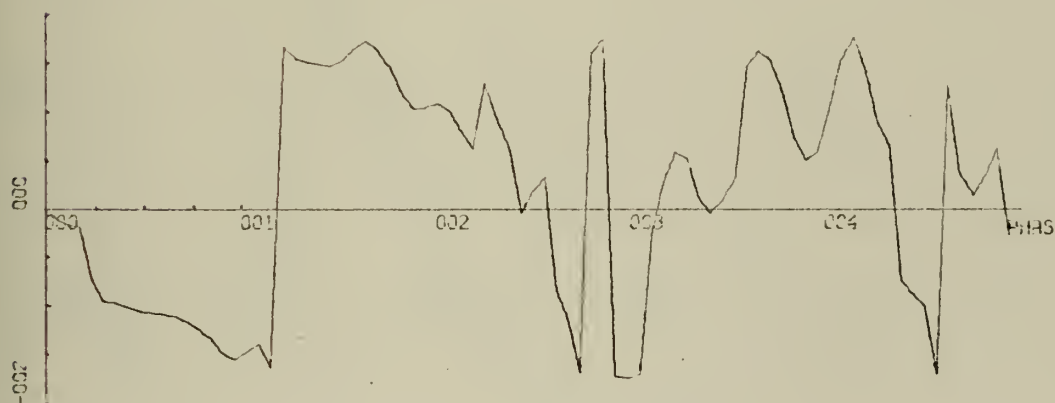
Y-SCALE=-1.00E-01 UNITS INCH.

CROSS-CORRELATION FN, X-PM, Y-PM

RUN PH-7, FILE 10 OF CON 6

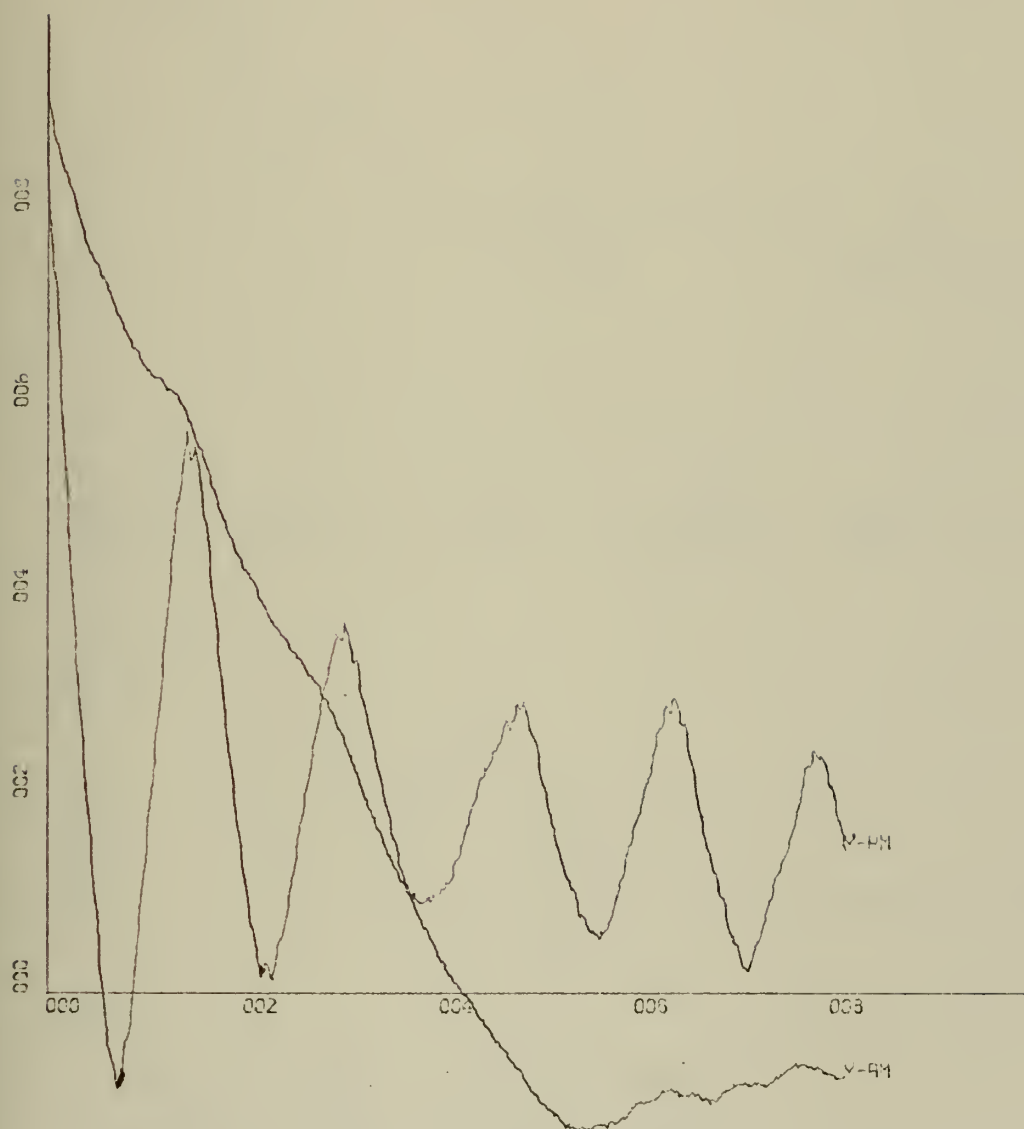


X-SCALE= $1.00E-01$ UNITS INCH.
 Y-SCALE= $1.00E+00$ UNITS INCH.
 COHERENCE FN. X-PM, Y-PM



X-SCALE= $1.00E-01$ UNITS INCH.
 Y-SCALE= $2.00E+02$ UNITS INCH.
 CROSS SPECTRAL PHASE ANGLE, X-PM Y-PM

RUN PH-7

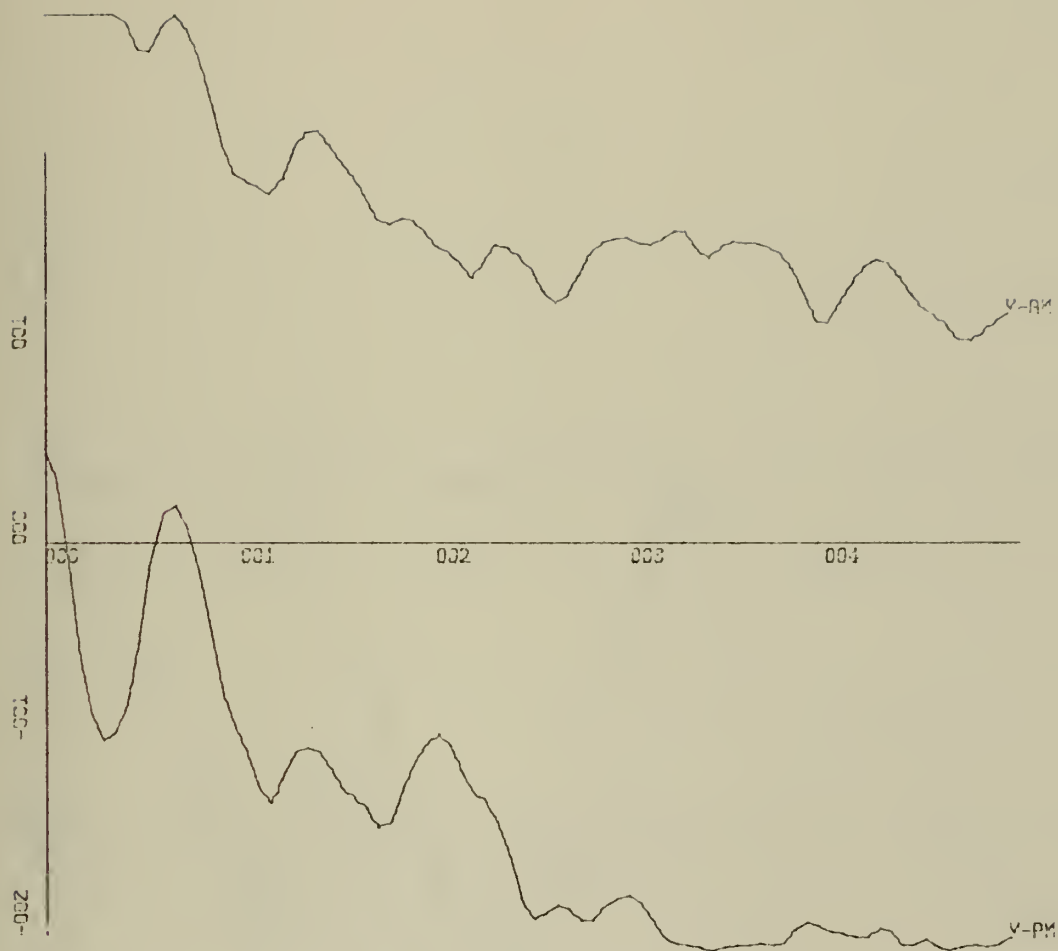


Y-SCALE=2.00E-01 UNITS INCH.

Y-SCALE=2.00E-01 UNITS INCH.

TEMPORAL AUTOCORRELATION FN, Y-PM, Y-AM

RUN PH-7, FILE 10 OF CON 6

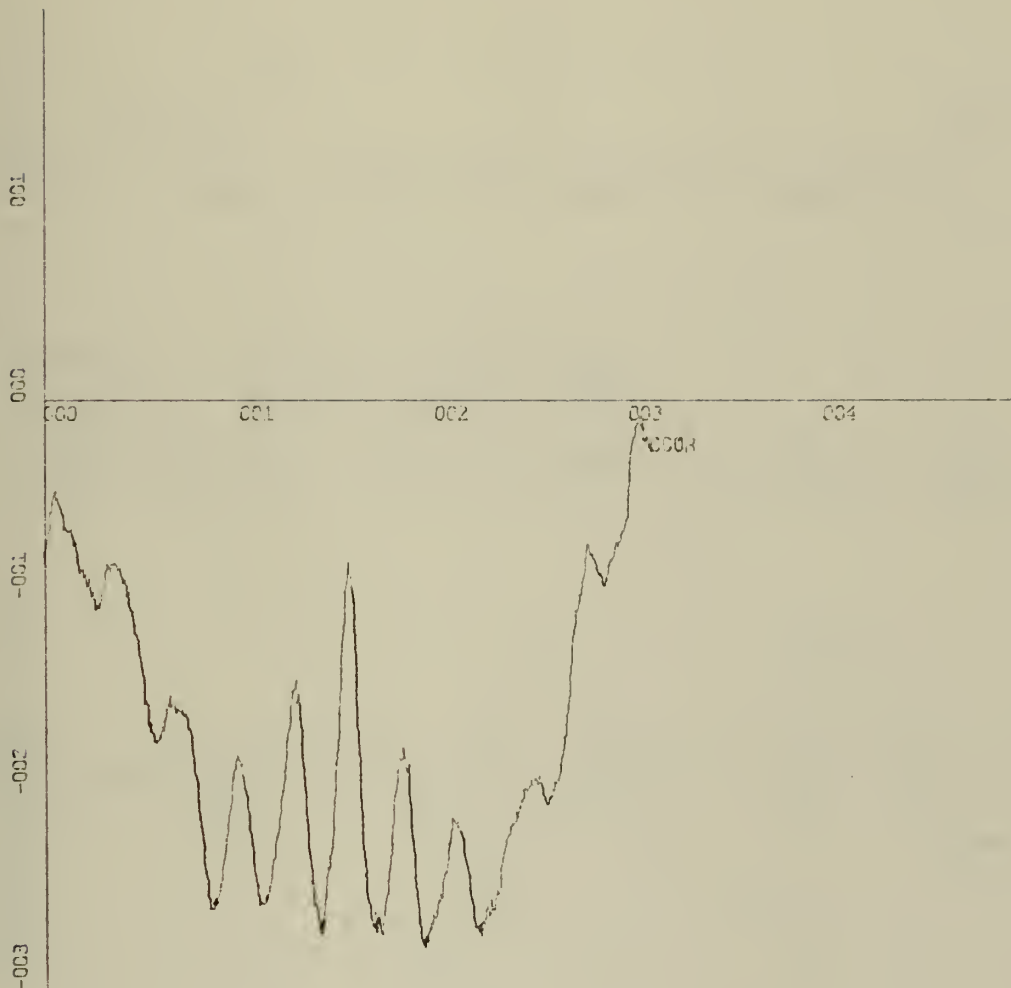


Y-SCALE=1.00E-01 UNITS INCH.

Y-SCALE=1.00E+01 UNITS INCH.

POWER SPECTRUM LEVEL (DB) Y-PM, Y-AM

RUN PH-7, FILE 10 OF CON 6

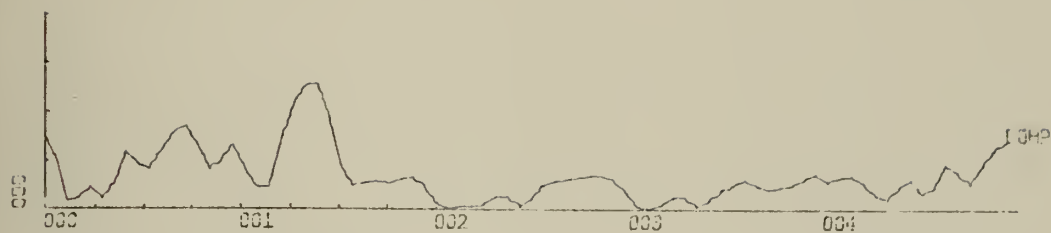


X-SCALE=-1.00E+00 UNITS INCH.

Y-SCALE=-1.00E-01 UNITS INCH.

CROSS-CORRELATION FN, Y-PM, Y-AM

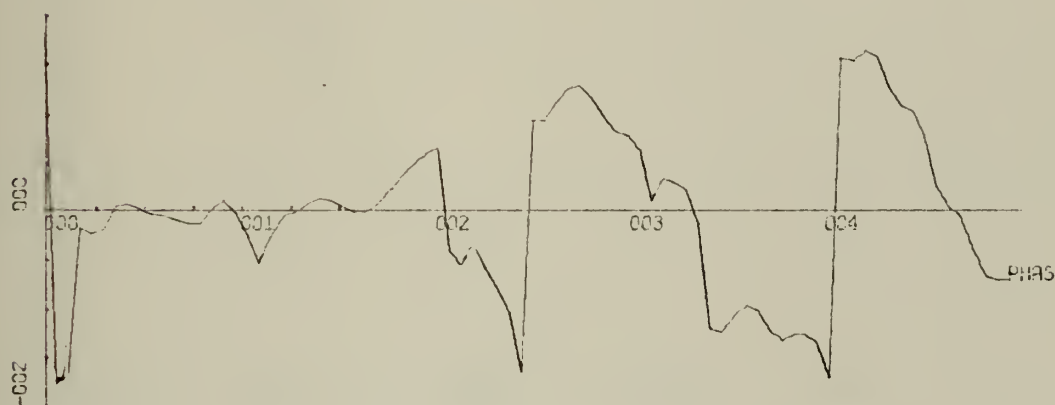
RUN PH-7, FILE 10 OF CON 6



X-SCALE=1.00E-01 UNITS INCH.

Y-SCALE=1.00E+00 UNITS INCH.

COHERENCE FUNCTION Y-PM, Y-AM



X-SCALE=1.00E-01 UNITS INCH.

Y-SCALE=2.00E+02 UNITS INCH.

CROSS SPECTRAL PHASE ANGLE, Y-PM, Y-AM

RUN PH-7

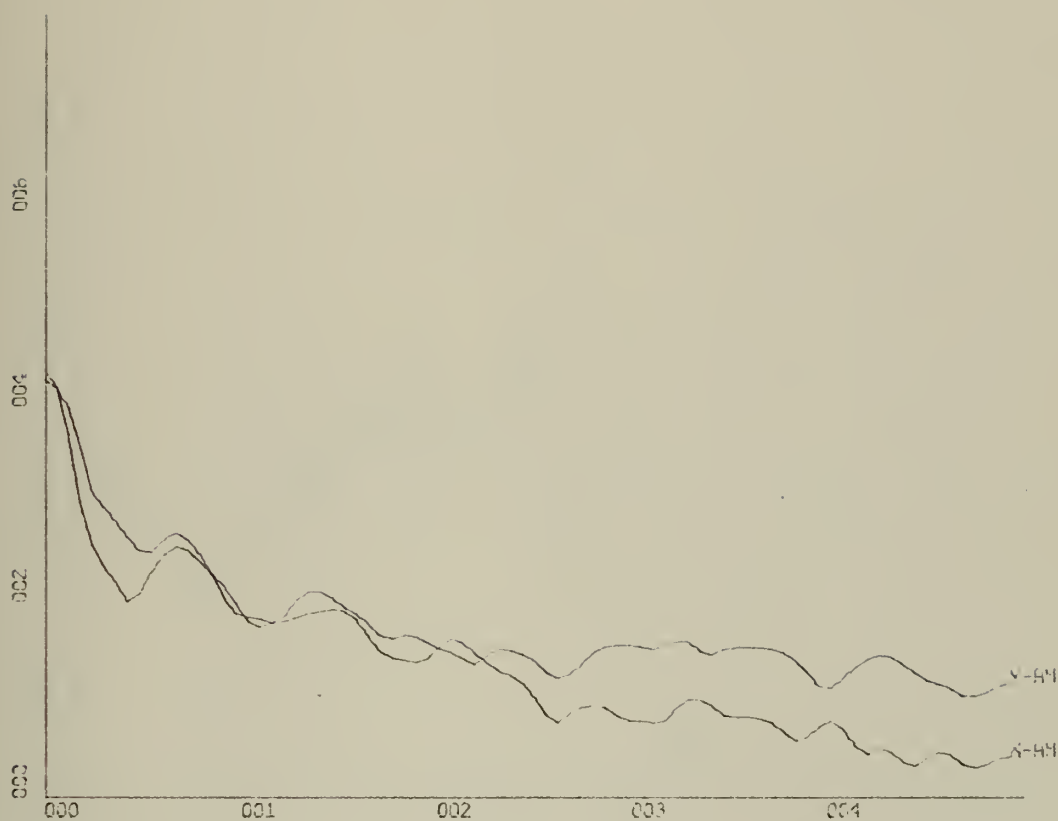


X-SCALE=2.00E+01 UNITS INCH.

Y-SCALE=2.00E-01 UNITS INCH.

TEMPORAL AUTOCORRELATION FN. X-AM, Y-AM

RUN PH-7, FILE 10 OF CON 6

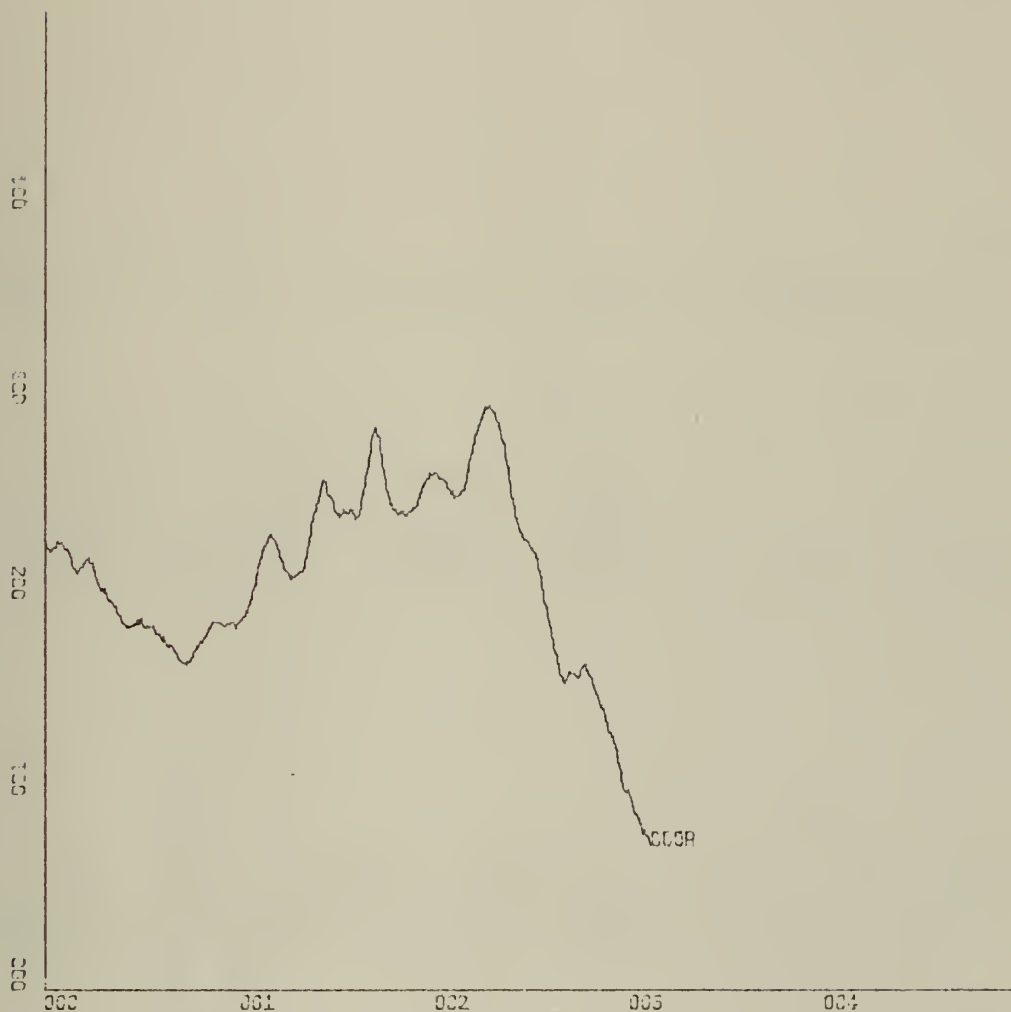


X-SCALE=1.00E-01 UNITS INCH.

Y-SCALE=2.00E+01 UNITS INCH.

POWER SPECTRUM LEVEL (DB) X-AM, Y-AM

RUN PH-7, FILE 10 OF CON 6

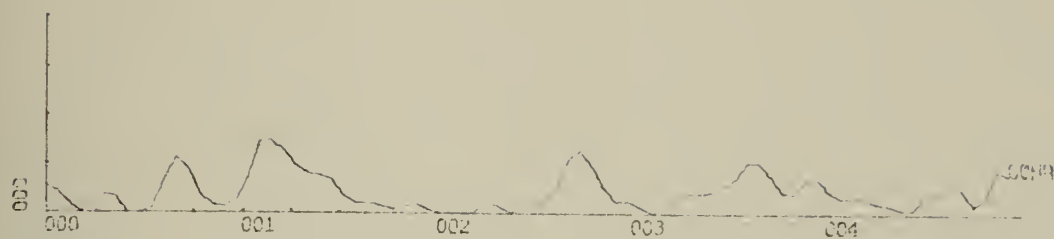


X-SCALE=1.00E+00 UNITS INCH.

Y-SCALE=1.00E-01 UNITS INCH.

CROSS-CORRELATION FN, X-AM, Y-AM

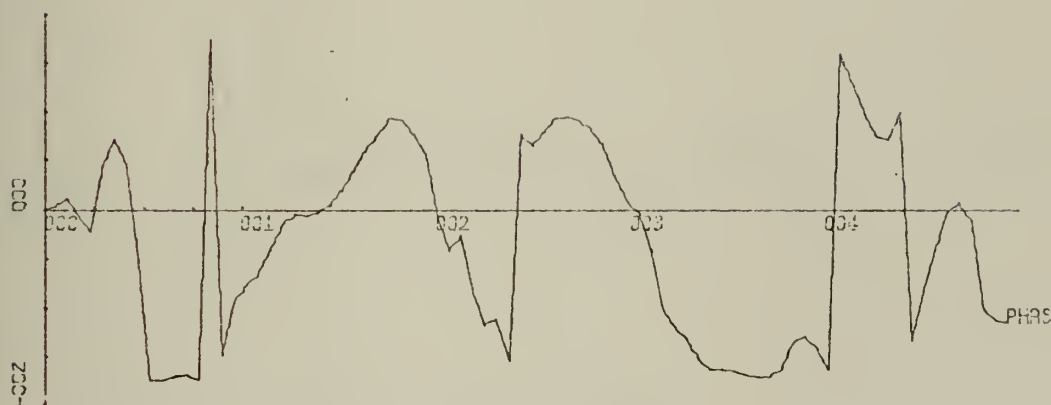
RUN PH-7, FILE 10 OF CON 6



X-SCALE= $1.00E-01$ UNITS INCH.

Y-SCALE= $1.00E+00$ UNITS INCH.

COHERENCE FUNCTION X-AM, Y-AM



X-SCALE= $1.00E-01$ UNITS INCH.

Y-SCALE= $2.00E+02$ UNITS INCH.

CROSS SPECTRAL PHASE ANGLE, X-AM, Y-AM

RUN PH-7

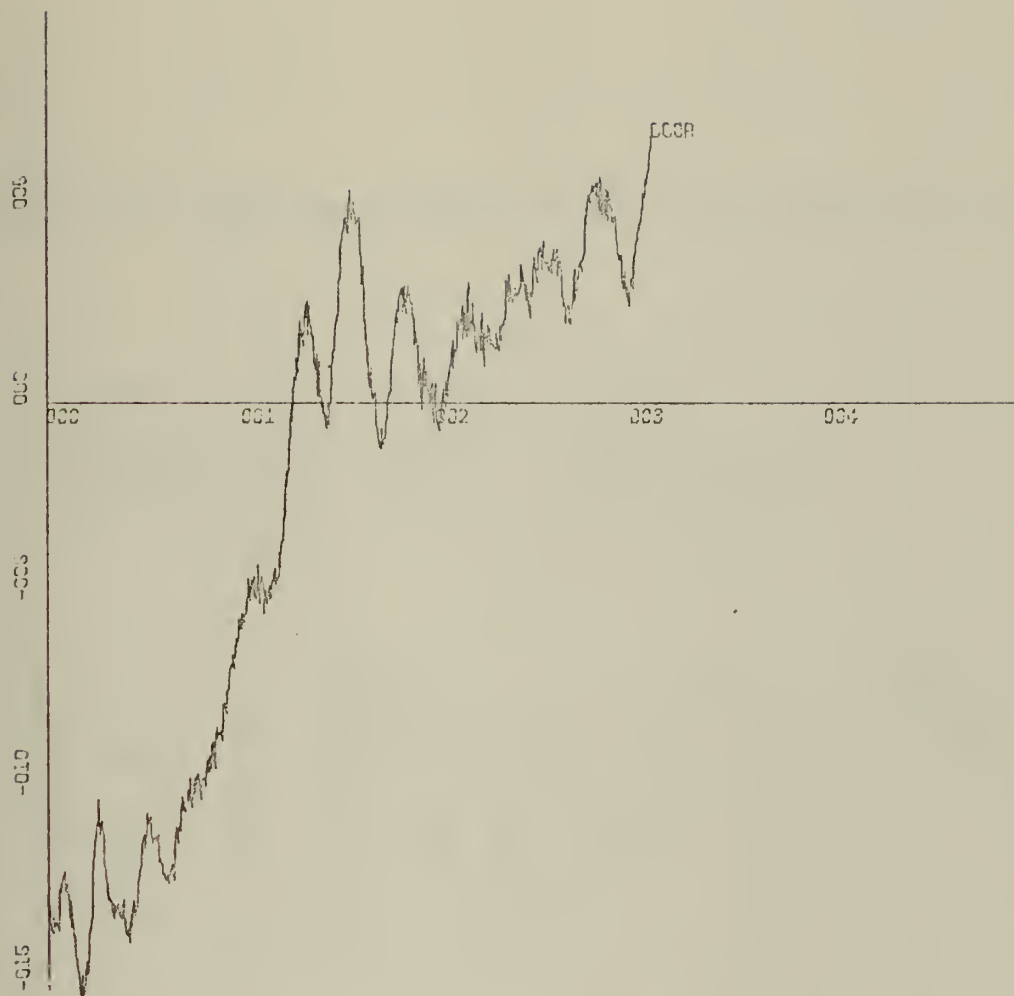


X-SCALE=1.00E-01 UNITS INCH.

Y-SCALE=1.00E+01 UNITS INCH.

POWER SPECTRUM LEVEL (DB) X-PM, X-AM

RUN PH-7, FILE 10 OF CON 6

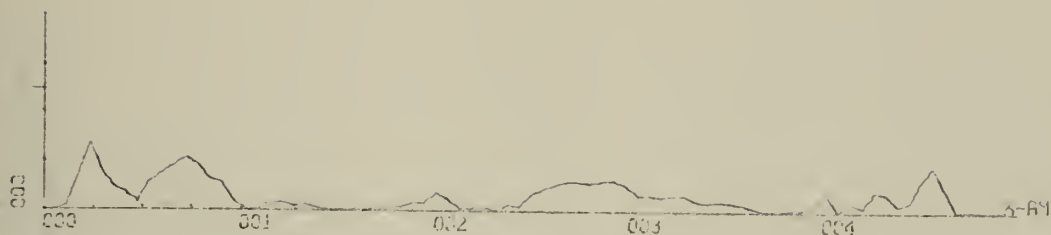


X-SCALE=1.00E+00 UNITS INCH.

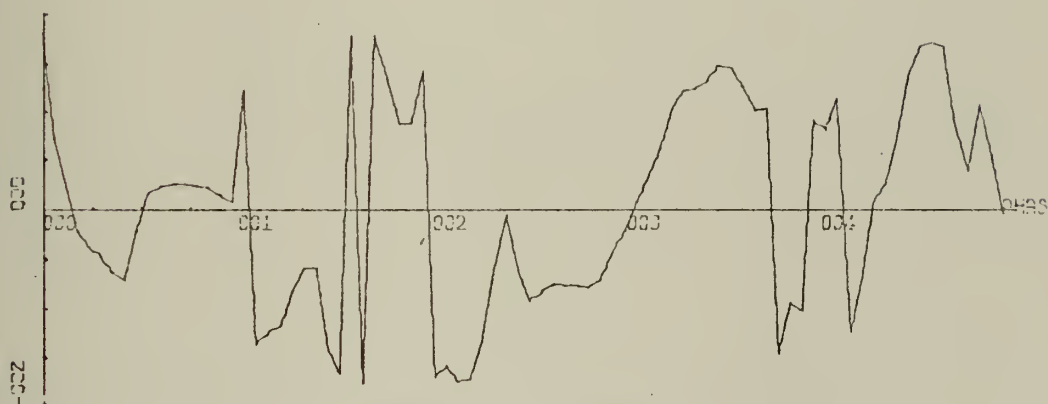
Y-SCALE=5.00E-02 UNITS INCH.

CROSS-CORRELATION FN, X-PM, X-AM

RUN PH-7, FILE 10 OF CON 6

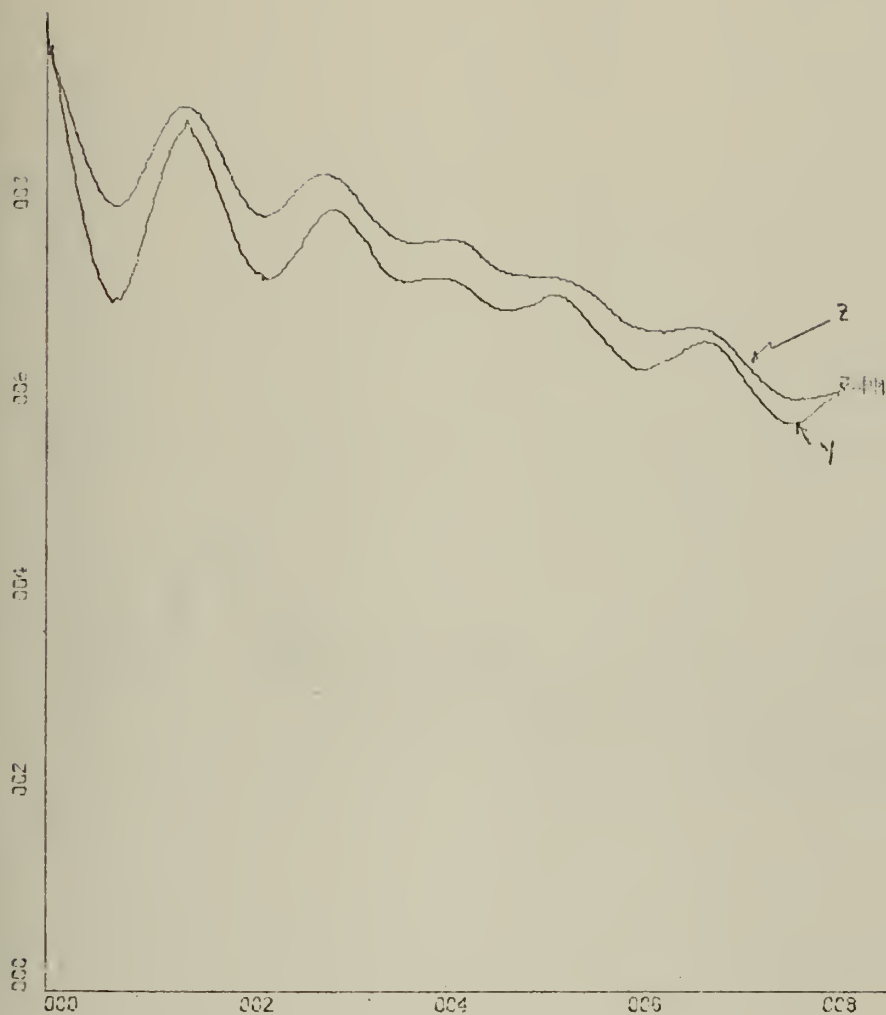


X-SCALE= $1.00E-01$ UNITS INCH.
 Y-SCALE= $1.00E+00$ UNITS INCH.
 COHERENCE FN. X-PM, X-AM



X-SCALE= $1.00E-01$ UNITS INCH.
 Y-SCALE= $2.00E+02$ UNITS INCH.
 CROSS SPECTRAL PHASE ANGLE, X-PM, X-AM

RUN PH-7

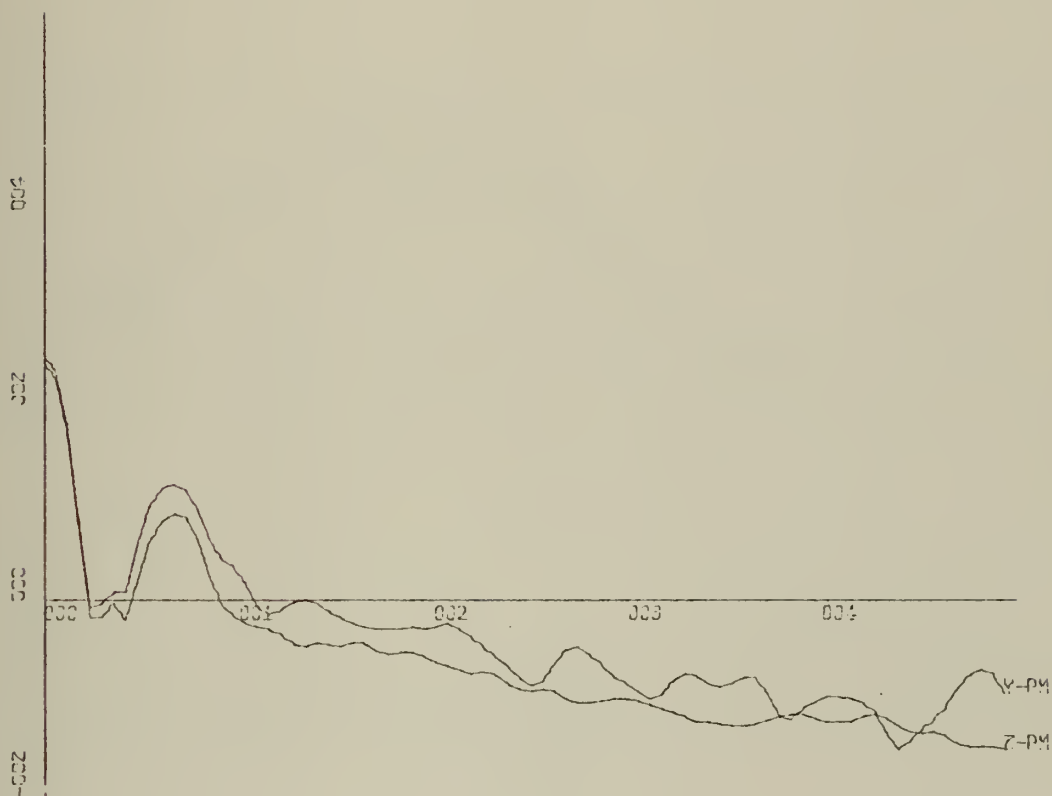


X-SCALE=2.00E+01 UNITS INCH.

Y-SCALE=2.00E-01 UNITS INCH.

TEMPORAL AUTOCORRELATION FN, Y-PH Z-PH

RUN PH-3 FILE 11 OF CON 6



X-SCALE=1.00E-01 UNITS INCH.

Y-SCALE=2.00E+01 UNITS INCH.

POWER SPECTRUM LEVEL (DB) Y-PM Z-PM

RUN PH-8, FILE 11 OF CON 6

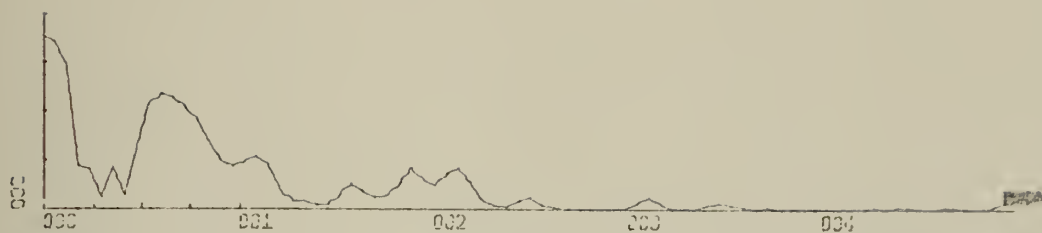


X-SCALE=1.00E+00 UNITS INCH.

Y-SCALE=2.00E-01 UNITS INCH.

CROSS-CORRELATION FN, Y-PM, Z-PM

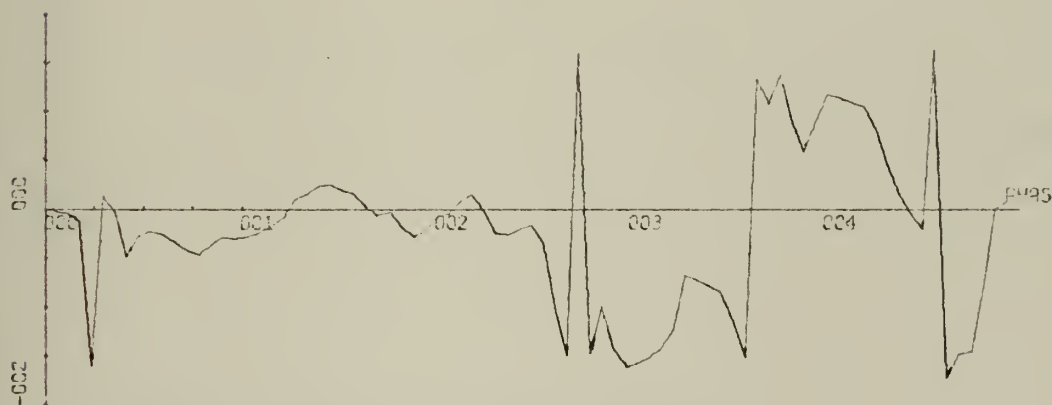
RUN PH-8. FILE 11 OF CON 6



X-SCALE= $1.00E-01$ UNITS INCH.

Y-SCALE= $1.00E+00$ UNITS INCH.

COHERENCE FUNCTION Y-PM AND Z-PM

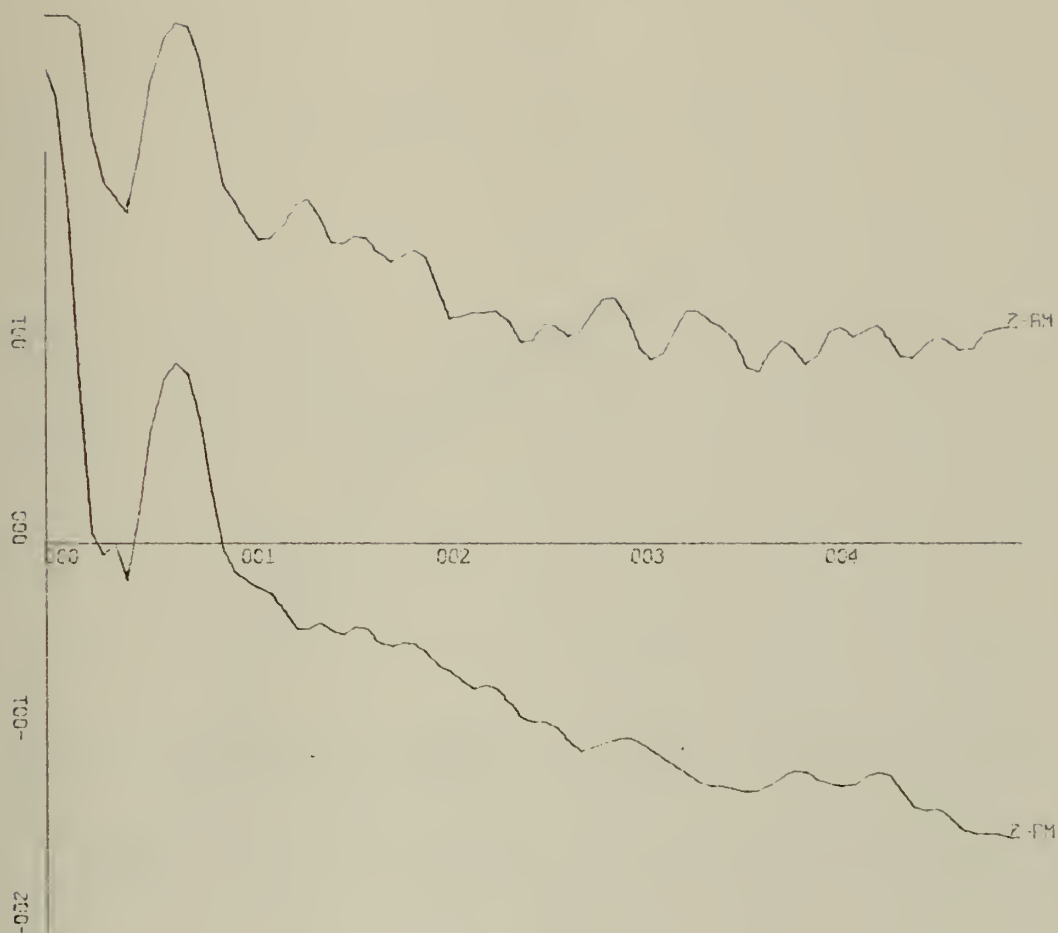


X-SCALE= $1.00E-01$ UNITS INCH.

Y-SCALE= $2.00E+02$ UNITS INCH.

CROSS SPECTRAL PHASE ANGLE, Y-PM Z-PM

RUN PH-8

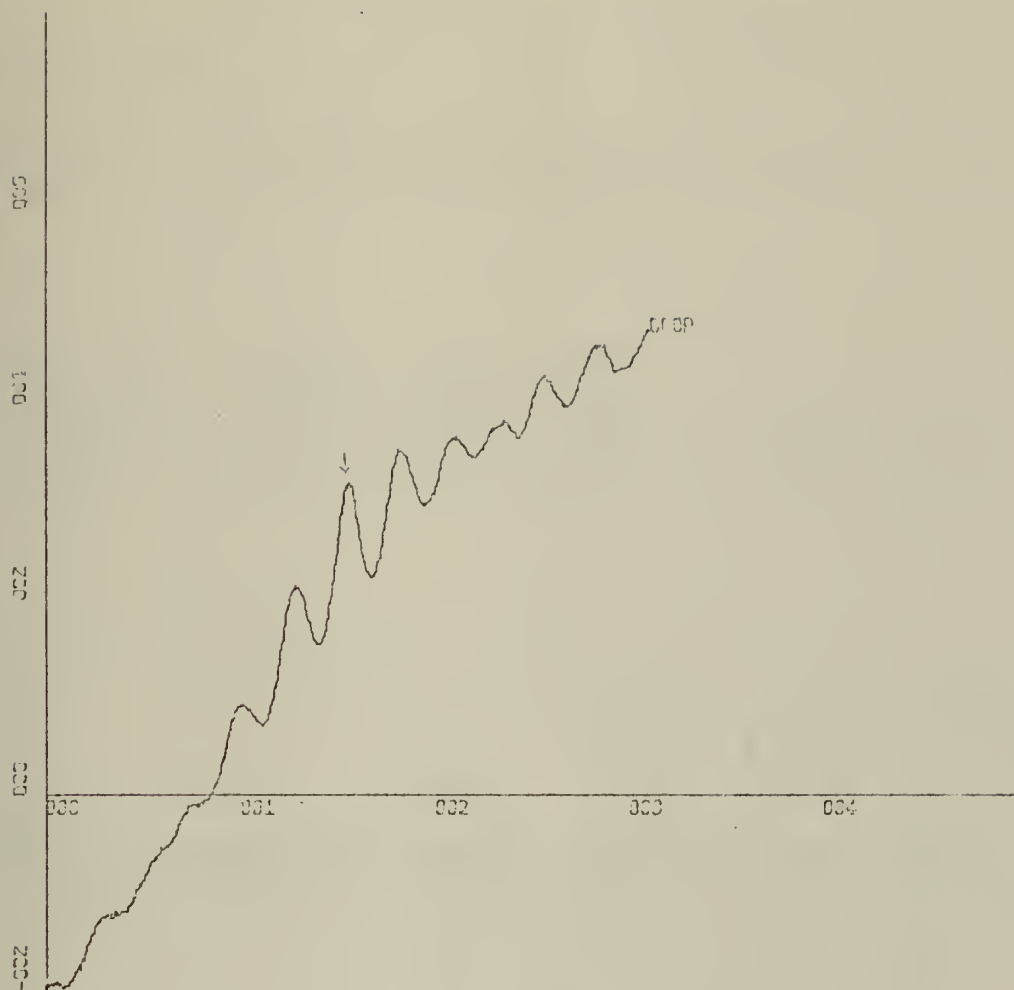


X-SCALE=1.00E-01 UNITS INCH.

Y-SCALE=1.00E+01 UNITS INCH.

POWER SPECTRUM LEVEL (DB) Z-PM, Z-AM

RUN PH-8. FILE 11 OF CON 6

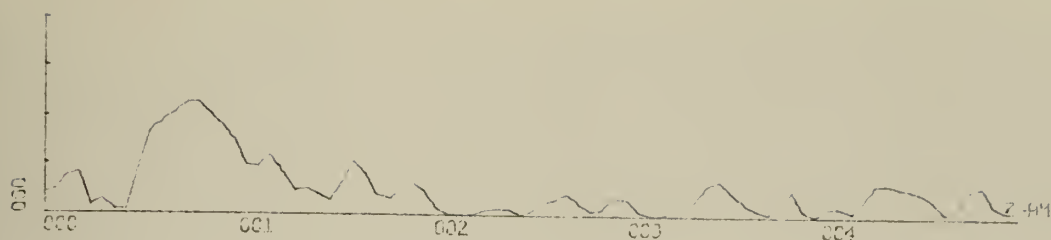


X-SCALE=-1.00E+00 UNITS INCH.

Y-SCALE=2.00E-01 UNITS INCH.

CROSS-CORRELATION FN, Z-PH, Z-AM

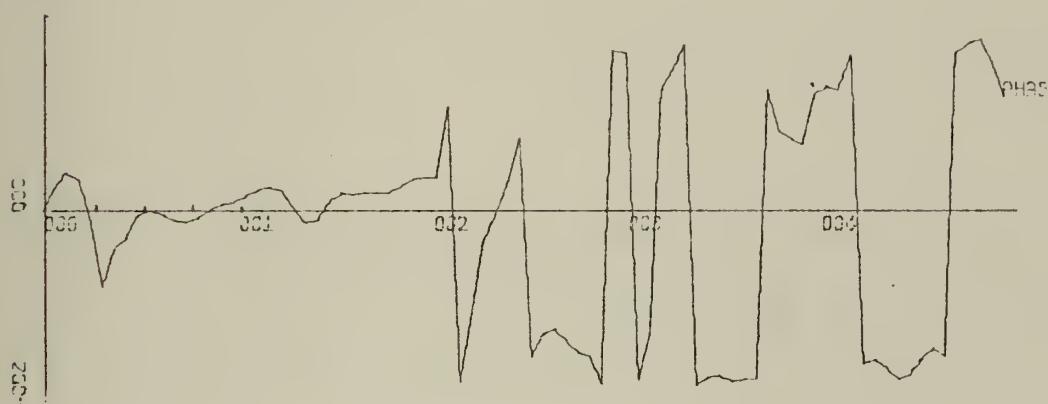
RUN PH-11 FILE 11 OF CON 6



X-SCALE= $1.00E-01$ UNITS INCH.

Y-SCALE= $1.00E+00$ UNITS INCH.

COHERENCE FUNCTION Z-PM AND Z-AM

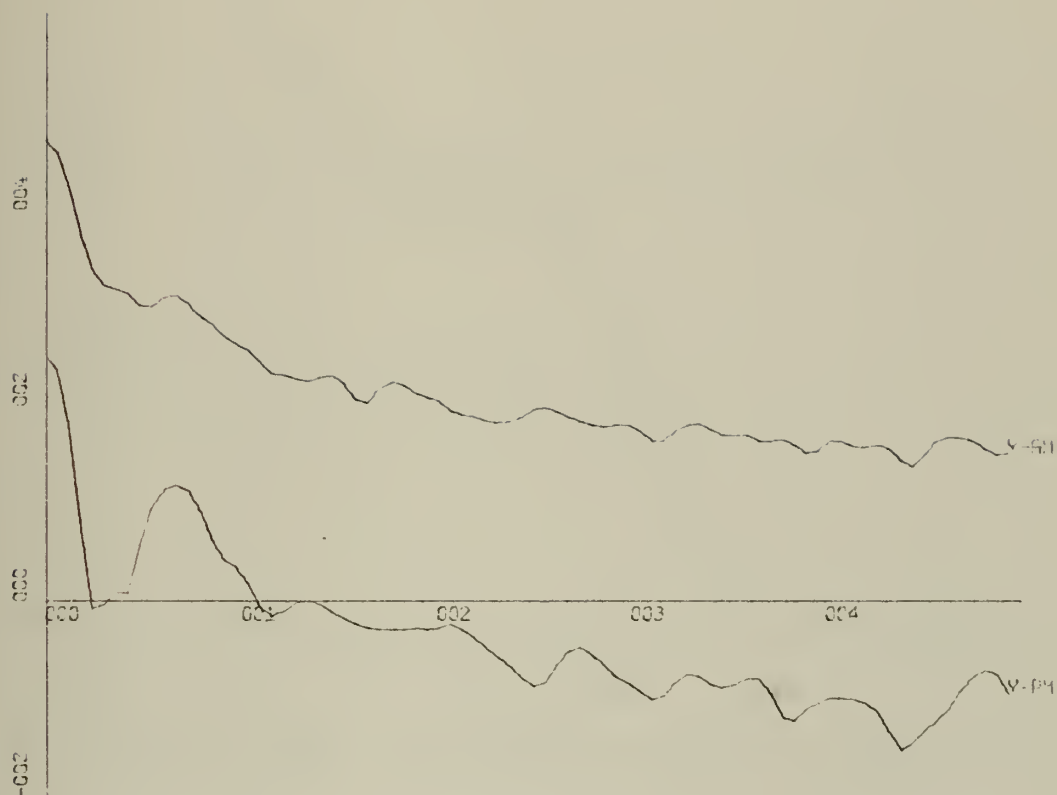


X-SCALE= $1.00E-01$ UNITS, INCH.

Y-SCALE= $2.00E+02$ UNITS INCH.

CROSS SPECTRAL PHASE ANGLE, Z-PM, Z-AM

RUN PH-8



X-SCALE=1.00E-01 UNITS INCH.

Y-SCALE=2.00E+01 UNITS INCH.

POWER SPECTRUM LEVEL (DB) Y-PM, Y-AM

RUN PH-8, FILE 11 OF CON 6

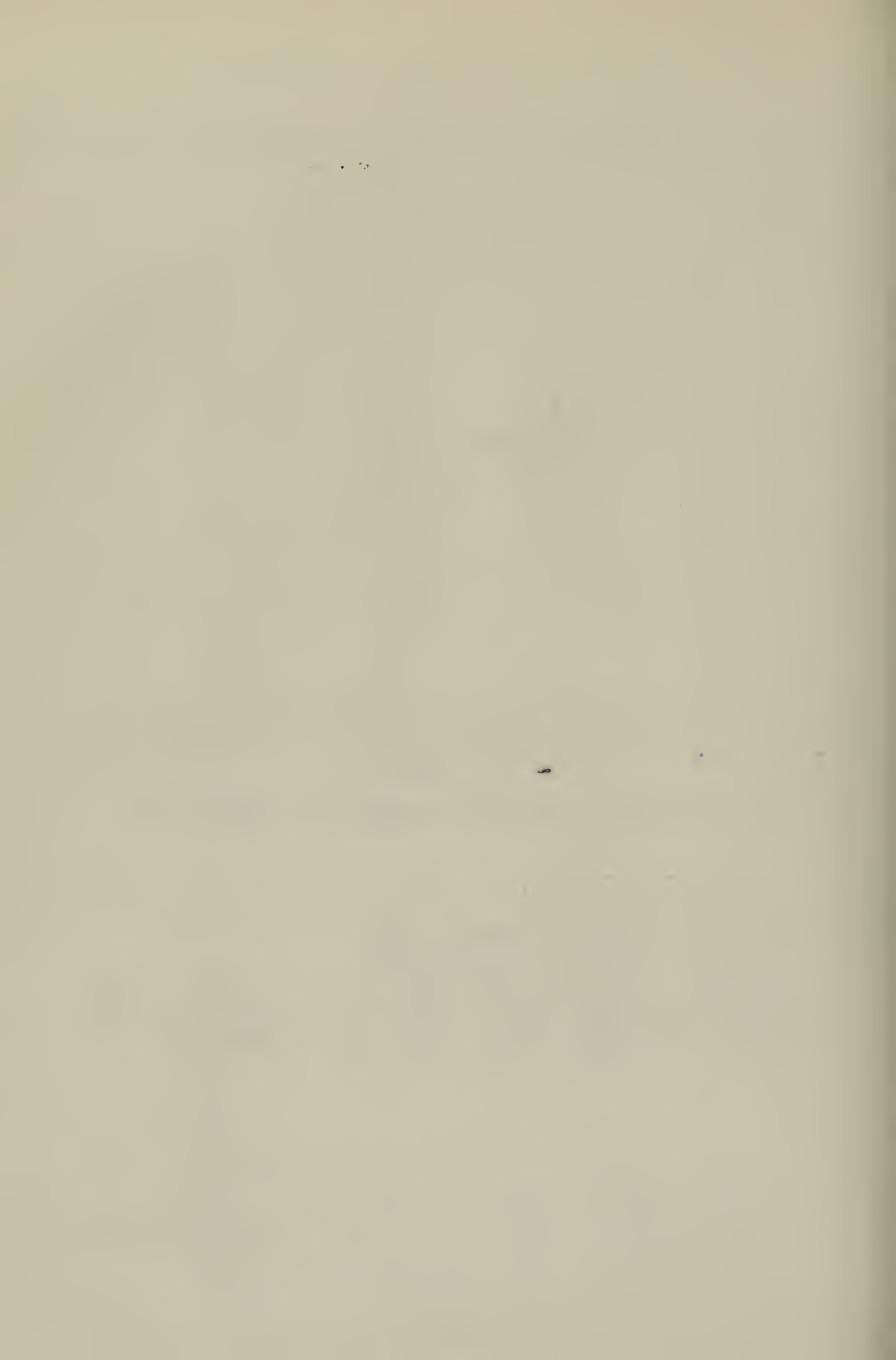


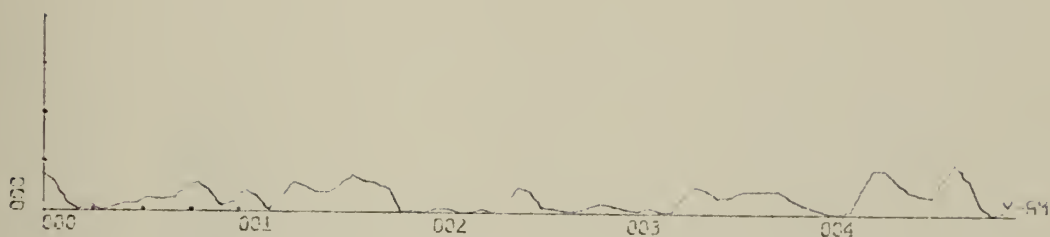
X-SCALE=1.00E+00 UNITS INCH.

Y-SCALE=1.00E-01 UNITS INCH.

CROSS-CORRELATION FN, Y-PM, Y-AM

RUN PH-8 FILE 11 OF CON 6

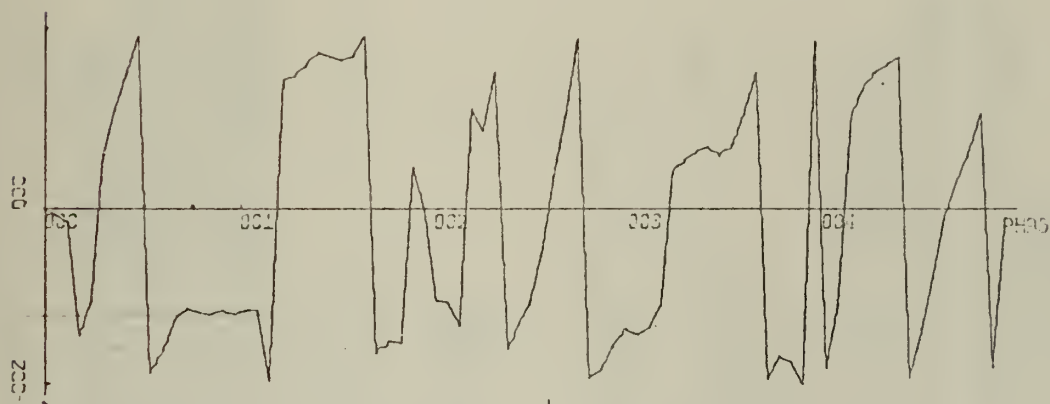




X-SCALE=1.00E-01 UNITS INCH.

Y-SCALE=1.00E+00 UNITS INCH.

COHERENCE FUNCTION Y-PM AND Y-AM



X-SCALE=-1.00E-01 UNITS INCH.

Y-SCALE=-2.00E+02 UNITS INCH.

CROSS SPECTRAL PHASE ANGLE, Y-PM Y-AM

RUN PH-8

CONVERT, SCALE, CLIP

```

C THIS PROGRAM CONVERTS FROM 9-TRACK TO 7-TRACK HEXI-DECIMAL FORMAT TAPE. THE PROGRAM IS
C DESIGNED TO HANDLE SIX CHANNELS OF DATA. THE PROGRAM
C SCALES EACH CHANNEL, AND APPLIES A SIMPLE CLIPPING
C OPERATION TO ELIMINATE SPURIOUS NOISE SPIKES.
C DIMENSION DAT(3072),DAT1(512),DAT2(512),DAT3(512),DAT4(512),
  1 DAT5(512),DAT6(512),X1PLOT(5120),Y1PLOT(5120),Y2PLOT(5120),
  1 Y3PLOT(5120),Y4PLOT(5120),IDAT(3072),GAR(512)
  REAL*4 Y1,'RAW',/
  REAL*4 Y2,'CLIP',/
  REAL*4 Y3,'RAW',/
  REAL*4 Y4,'CLIP',/
  FACTOR=100.0/(2**23)
  SCALE1=10.0
  SCALE4=10.0**3.967
  SCALE5=10.0**3.085
  SCALE6=10.0**2.926
  REWIND 2
  REWIND 4
  LRECL=3072
11 J=0
10 READ(2,15,END=50,ERR=60)IDAT
15 FORMAT(24(128A4))
  J=J+1
70 WRITE(6,70)J
  FORMAT('0',I0X,'RECORD NO.=',I4)
  DO 22 I=1,LRECL
22 DAT(I)=IDAT(I)*FACTOR
23 DO199 I=6,LRECL,6
  M=I/6
  DAT1=X-DIRECTION PHASE FLUCTUATION
  DAT2=Y-DIRECTION PHASE FLUCTUATION
  DAT3=Z-DIRECTION PHASE FLUCTUATION
  DAT4=X-DIRECTION AMPLITUDE FLUCTUATION
  DAT5=Y-DIRECTION AMPLITUDE FLUCTUATION
  DAT6=Z-DIRECTION AMPLITUDE FLUCTUATION
  SCALING OF X,Y,AND Z DIRECTIONS PHASE FLUCTUATION
  DAT1(M)=DAT(I-5)*SCALE1
  DAT2(M)=DAT(I-4)*SCALE1
  DAT3(M)=DAT(I-3)*SCALE1
  DAT4(M)=DAT(I-2)
  DAT5(M)=DAT(I-1)
  199 DAT6(M)=DAT(I)

```



```

16 FORMAT(4(128A4))
DO299 I=1,512
  DAT4(I)=(DAT4(I)/100.0)+.514
  DAT4(I)=6.321*DAT4(I)-11.012*(DAT4(I)**2)+19.827*(DAT4(I)**3)
  I-14.933*(DAT4(I)**4)+3.732*(DAT4(I)**5)
C SCALING X,Y,AND Z DIRECTIONS AMPLITUDE FLUCTUATION
  DAT4(I)=DAT4(I)*SCALE4
  DAT5(I)=DAT5(I)/100.+184
  DAT5(I)=8.595*DAT5(I)-51.441*(DAT5(I)**2)+253.087*(DAT5(I)**3)
  I-554.28*(DAT5(I)**4)+436.84*(DAT5(I)**5)
  DAT5(I)=DAT5(I)*SCALE5
  DAT6(I)=DAT6(I)/100.+309
  DAT6(I)=7.1067*DAT6(I)-23.2006*(DAT6(I)**2)+83.1730*(DAT6(I)**3)
  I-149.476*(DAT6(I)**4)+104.6540*(DAT6(I)**5)
299 DAT6(I)=DAT6(I)*SCALE6
  WRITE(8,16) DAT1
  WRITE(9,16) DAT2
  WRITE(10,16) DAT3
  WRITE(11,16) DAT4
  WRITE(12,16) DAT5
  WRITE(13,16) DAT6
DO 499 LL=1,512
  IF(LL.EQ.1) GO TO 480
  DIFF1=250.0
  DELTA1=ABS(DAT1(LL)-DAT1(LL-1))
  DELTA2=ABS(DAT2(LL)-DAT2(LL-1))
  DELTA3=ABS(DAT3(LL)-DAT3(LL-1))
C APPLY CLIPPING ROUTINE TO THE TIME SIGNAL
  IF(DIFF1.LT.DELTA1) GO TO 450
  IF(DIFF1.LT.DELTA2) GO TO 460
  IF(DIFF1.LT.DELTA3) GO TO 470
  GO TO 499
  DAT1(LL)=DAT1(LL-1)
  GO TO 461
  DAT2(LL)=DAT2(LL-1)
  GO TO 462
  DAT3(LL)=DAT3(LL-1)
  GO TO 499
  IF(J.EQ.1) GO TO 499
  DEL1=ABS(SAVE1-DAT1(1))
  DEL2=ABS(SAVE2-DAT2(1))
  DEL3=ABS(SAVE3-DAT3(1))
  IF(DIFF.LT.DEL1) GO TO 451
  IF(DIFF.LT.DEL2) GO TO 465
  IF(DIFF.LT.DEL3) GO TO 471
  GO TO 499
  DAT1(1)=SAVE1
  GO TO 463

```



```

465 DAT2(1)=SAVE2
GO TO 464
471 DAT3(1)=SAVE3
GO TO 499
499 CONTINUE
SAVE1=DAT1(512)
SAVE2=DAT2(512)
SAVE3=DAT3(512)
DO 399 JJ=1,512
IF(JJ.EQ.1) GO TO 380
DIFF2=200
DELTA4=ABS(DAT4(JJ)-DAT4(JJ-1))
DELTA5=ABS(DAT5(JJ)-DAT5(JJ-1))
DELTA6=ABS(DAT6(JJ)-DAT6(JJ-1))
IF(DIFF2.LT.DELTA4) GO TO 350
IF(DIFF2.LT.DELTA5) GO TO 360
IF(DIFF2.LT.DELTA6) GO TO 370
GO TO 399
350 DAT4(JJ)=DAT4(JJ-1)
GO TO 361
360 DAT5(JJ)=DAT5(JJ-1)
GO TO 362
370 DAT6(JJ)=DAT6(JJ-1)
GO TO 399
380 IF(JJ.EQ.1) GO TO 399
390 DEL4=ABS(SAVE4-DAT4(1))
DEL5=ABS(SAVE5-DAT5(1))
DEL6=ABS(SAVE6-DAT6(1))
IF(DIFF.LT.DEL4) GO TO 351
IF(DIFF.LT.DEL5) GO TO 365
IF(DIFF.LT.DEL6) GO TO 371
GO TO 399
351 DAT4(1)=SAVE4
GO TO 363
365 DAT5(1)=SAVE5
GO TO 364
371 DAT6(1)=SAVE6
GO TO 399
399 CONTINUE
SAVE4=DAT4(512)
SAVE5=DAT5(512)
SAVE6=DAT6(512)
WRITE(14,16) DAT1
WRITE(15,16) DAT2
WRITE(16,16) DAT3
WRITE(17,16) DAT4
WRITE(18,16) DAT5
WRITE(19,16) DAT6

```



```

60 GO TO 10
61 WRITE(6,61) J
61 FORMAT('0',5X,'READ ERROR,RECORD NO.=' ,I3)
50 WRITE(6,51) N,J
51 FORMAT('0',5X,'END OF FILE',I2,'RECORD NO.=' ,I3)
REWIND 8
REWIND 9
REWIND 10
REWIND 11
REWIND 12
REWIND 13
REWIND 14
REWIND 15
REWIND 16
REWIND 17
REWIND 18
REWIND 19
101 READ(8,16,END=102) DAT1
WRITE(4,16) DAT1
GO TO 101
102 READ(9,16,END=103) DAT2
WRITE(4,16) DAT2
GO TO 102
103 READ(10,16,END=104) DAT3
WRITE(4,16) DAT3
GO TO 103
104 READ(11,16,END=105) DAT4
WRITE(4,16) DAT4
GO TO 104
105 READ(12,16,END=106) DAT5
WRITE(4,16) DAT5
GO TO 105
106 READ(13,16,END=107) DAT6
WRITE(4,16) DAT6
GO TO 106
END FILE4
301 READ(14,16,END=302) DAT1
WRITE(4,16) DAT1
GO TO 301
302 READ(15,16,END=303) DAT2
WRITE(4,16) DAT2
GO TO 302
303 READ(16,16,END=304) DAT3
WRITE(4,16) DAT3
GO TO 303
304 READ(17,16,END=305) DAT4
WRITE(4,16) DAT4
GO TO 304

```



```

305 READ(18,16,END=306) DAT5
   WRITE(4,16) DAT5
   GO TO 305
306 READ(19,16,END=307) DAT6
   WRITE(4,16) DAT6
   GO TO 306
307 END FILE 4
   REWIND 8
   REWIND 9
   REWIND 10
   REWIND 11
   REWIND 12
   REWIND 13
   REWIND 14
   REWIND 15
   REWIND 16
   REWIND 17
   REWIND 18
   REWIND 19
DO 220 I1=1,5120
X1PLOT(I1)=.02*(I1-1)
220 CONTINUE
   I5=8
   I6=14
   I7=9
   I8=15
79 READ(I5,16)(Y1PLOT(J),J=1,5120)
   READ(I6,16)(Y2PLOT(J),J=1,5120)
   READ(I7,16)(Y3PLOT(J),J=1,5120)
   READ(I8,16)(Y4PLOT(J),J=1,5120)
   WRITE(6,20)
20 FORMAT(1H1,8X,'TIME',9X,'CLIP',9X,'RAW',9X,'CLIP',
15120)
   WRITE(6,19)(X1PLOT(I),Y1PLOT(I),Y2PLOT(I),Y3PLOT(I),Y4PLOT(I),I=1,
19)
19 FORMAT(5(F9.4,5X))
DO 500 J1=1,2560
TEMP=Y1PLOT(5121-J1)
Y1PLOT(5121-J1)=Y1PLOT(J1)
Y1PLOT(J1)=TEMP
TEMP=Y2PLOT(5121-J1)
Y2PLOT(5121-J1)=Y2PLOT(J1)
Y2PLOT(J1)=TEMP
TEMP=Y3PLOT(5121-J1)
Y3PLOT(5121-J1)=Y3PLOT(J1)
Y3PLOT(J1)=TEMP
TEMP=Y4PLOT(5121-J1)
Y4PLOT(5121-J1)=Y4PLOT(J1)
Y4PLOT(J1)=TEMP
500

```



```

CALL SCALE(X1PLOT,5120,1,8.0,0.50,XMIN,DX)
CALL SCALE(Y1PLOT,5120,1,2.0,0.5,Y1MIN,DY1)
CALL SCALE(Y2PLOT,5120,1,2.0,0.5,Y2MIN,DY2)
CALL SCALE(Y3PLOT,5120,1,2.0,0.5,Y3MIN,DY3)
CALL SCALE(Y4PLOT,5120,1,2.0,0.5,Y4MIN,DY4)
CALL PLOTS
CALL PLOT(0.0,0.0,-3)
CALL AXIS(3.0,20.5,Y1,+4,2.0,0.0,Y1MIN,DY1)
CALL AXIS(5.0,20.5,Y2,+4,2.0,0.0,Y2MIN,DY2)
CALL PLOT(0.0,0.0,-3)
CALL LINE(Y1PLOT,X1PLOT,5120,1,1)
CALL PLOT(5.0,0.0,-3)
CALL LINE(Y2PLOT,X1PLOT,5120,1,1)
CALL SYMBOL(-6.0,22.0,0.49,'ALEXANDER C.H.',0.0,14)
CALL PLOT(-6.0,25.0,-3)
CALL PLOTS
CALL PLOT(0.0,0.0,-3)
CALL AXIS(0.0,20.5,Y3,+4,2.0,0.0,Y3MIN,DY3)
CALL AXIS(5.0,20.5,Y4,+4,2.0,0.0,Y4MIN,DY4)
CALL PLOT(0.0,0.0,-3)
CALL LINE(Y3PLOT,X1PLOT,5120,1,1)
CALL PLOT(5.0,0.0,-3)
CALL LINE(Y4PLOT,X1PLOT,5120,1,1)
CALL SYMBOL(-6.0,22.0,0.49,'ALEXANDER C.H.',0.0,14)
CALL PLOT(-6.0,25.0,-3)
I5=I5+2
I6=I6+2
I7=I7+2
I8=I8+2
IF(I5.LT.14) GO TO 79
RETURN
END
//GO.FT06F001 DD SYSOUT=A,SPACE=(CYL,(50,1))
//GO.SYSF001 DD SYSOUT=C,SPACE=(CYL,(25,2))
//GO.FT02F001 DD JNIT=2400-1,VOL=SER=CON6,LABEL=(1,NL),
//DISP=OLD,DCB=(DEN=1,RECFM=F,BLKSIZE=12288)
//GO.FT04F001 DD UNIT=2400,VOL=SER=NPS388,DSNAME=RUF2SR2,LABEL=(5,SL),
//DISP=(OLD,KEEP),DCB=(DEN=2,RECFM=FB,LRECL=2048,BLKSIZE=2048)
//GO.FT04F002 DD UNIT=2400,VOL=SER=NPS388,DSNAME=RUF2SR2,LABEL=(6,SL),
//DISP=(OLD,KEEP),DCB=(DEN=2,RECFM=FB,LRECL=2048,BLKSIZE=2048)
//GO.FT08F001 DD JNIT=SYSDA,DSNAME=F2614.CHAN1A,
//DCB=(RECFM=FB,LRECL=2048,BLKSIZE=2048),DISP=(NEW,DELETE),
//SPACE=(CYL,(4,1))
//GO.FT09F001 DD JNIT=SYSDA,DSNAME=F2614.CHAN2A,
//DCB=(RECFM=FB,LRECL=2048,BLKSIZE=2048),DISP=(NEW,DELETE),
//SPACE=(CYL,(4,1))

```



```

//GO.FT10F001 DD UNIT=SYSDA,DSNAME=F2614.CHAN3A,
// DCB=(RECFM=FB,LRECL=2048,BLKSIZE=2048),DISP=(NEW,DELETE),
// SPACE=(CYL,(4,1))
//GO.FT11F001 DD JNIT=SYSDA,DSNAME=F2614.CHAN4A,
// DCB=(RECFM=FB,LRECL=2048,BLKSIZE=2048),DISP=(NEW,DELETE),
// SPACE=(CYL,(4,1))
//GO.FT12F001 DD JNIT=SYSDA,DSNAME=F2614.CHAN5A,
// DCB=(RECFM=FB,LRECL=2048,BLKSIZE=2048),DISP=(NEW,DELETE),
// SPACE=(CYL,(4,1))
//GO.FT13F001 DD JNIT=SYSDA,DSNAME=F2614.CHAN6A,
// DCB=(RECFM=FB,LRECL=2048,BLKSIZE=2048),DISP=(NEW,DELETE),
// SPACE=(CYL,(4,1))
//GO.FT14F001 DD JNIT=SYSDA,DSNAME=F2614.CHAN7A,
// DCB=(RECFM=FB,LRECL=2048,BLKSIZE=2048),DISP=(NEW,DELETE),
// SPACE=(CYL,(4,1))
//GO.FT15F001 DD JNIT=SYSDA,DSNAME=F2614.CHAN8A,
// DCB=(RECFM=FB,LRECL=2048,BLKSIZE=2048),DISP=(NEW,DELETE),
// SPACE=(CYL,(4,1))
//GO.FT16F001 DD JNIT=SYSDA,DSNAME=F2614.CHAN9A,
// DCB=(RECFM=FB,LRECL=2048,BLKSIZE=2048),DISP=(NEW,DELETE),
// SPACE=(CYL,(4,1))
//GO.FT17F001 DD JNIT=SYSDA,DSNAME=F2614.CHAN10A,
// DCB=(RECFM=FB,LRECL=2048,BLKSIZE=2048),DISP=(NEW,DELETE),
// SPACE=(CYL,(4,1))
//GO.FT18F001 DD JNIT=SYSDA,DSNAME=F2614.CHAN11A,
// DCB=(RECFM=FB,LRECL=2048,BLKSIZE=2048),DISP=(NEW,DELETE),
// SPACE=(CYL,(4,1))
//GO.FT19F001 DD JNIT=SYSDA,DSNAME=F2614.CHAN12A,
// DCB=(RECFM=FB,LRECL=2048,BLKSIZE=2048),DISP=(NEW,DELETE),
// SPACE=(CYL,(4,1))

```


ANALYSIS PACKAGE

THIS PROGRAM IS AN ANALYSIS PACKAGE FOR PERFORMING SPECTRAL ANALYSIS OF TIME RECORDS. TWO TIME RECORDS TO BE CONSIDERED ARE FIRST READ INTO COMPUTER STORAGE FROM MAGNETIC TAPE. THE AUTOCOVARIANCE FUNCTION IS THEN COMPUTED FOR EACH TIME RECORD. THE AUTOCOVARIANCES ARE THEN FOURIER TRANSFORMED TO OBTAIN THE POWER SPECTRUM OF EACH OF THE TIME RECORDS. THE TWO TIME RECORDS ARE THEN CROSS-CORRELATED, AND THE CROSS-CORRELATION FUNCTION IS TRANSFORMED TO YIELD THE CO-SPECTRUM AND THE QUAD-SPECTRUM.

THE CO-SPECTRUM

AND THE QUAD-SPECTRUM ARE COMBINED TO YIELD THE COHERENCE FUNCTION AND THE CROSS-SPECTRAL PHASE ANGLE OF THE TWO TIME RECORDS.

NTS= NUMBER OF TIME SAMPLES

MLAG = NUMBER OF TIME LAGS

DT = TIME INCREMENT

DHZ = FREQUENCY SPACING

DHZ = $1/(2*TM)$

TM = DT*MLAG

FBHZ = LOWEST FREQUENCY (HZ)

FBHZ = $1/(2*TM)$

FEHZ = HIGHEST FREQUENCY OF INTEREST (HZ)

FEHZ = $1/(2*DT)$

CALX1 = CALIBRATION FACTOR FOR TIME SERIES F1

CALX2 = CALIBRATION FACTOR FOR TIME SERIES F2

H = WATER DEPTH (METERS)

X2 = DEPTH OF WAVE PRESSURE TRANSDUCER BELOW SURFACE

DIMENSION F1(7000), F2(7000), GAR(512), AX(2048), A(256), BX(2048)

DIMENSION PHI(1023), TAU(1023), SPHI(512), APHI(512), PHN(512)

DIMENSION PHN2(1023), PHN1(512), B(256)


```

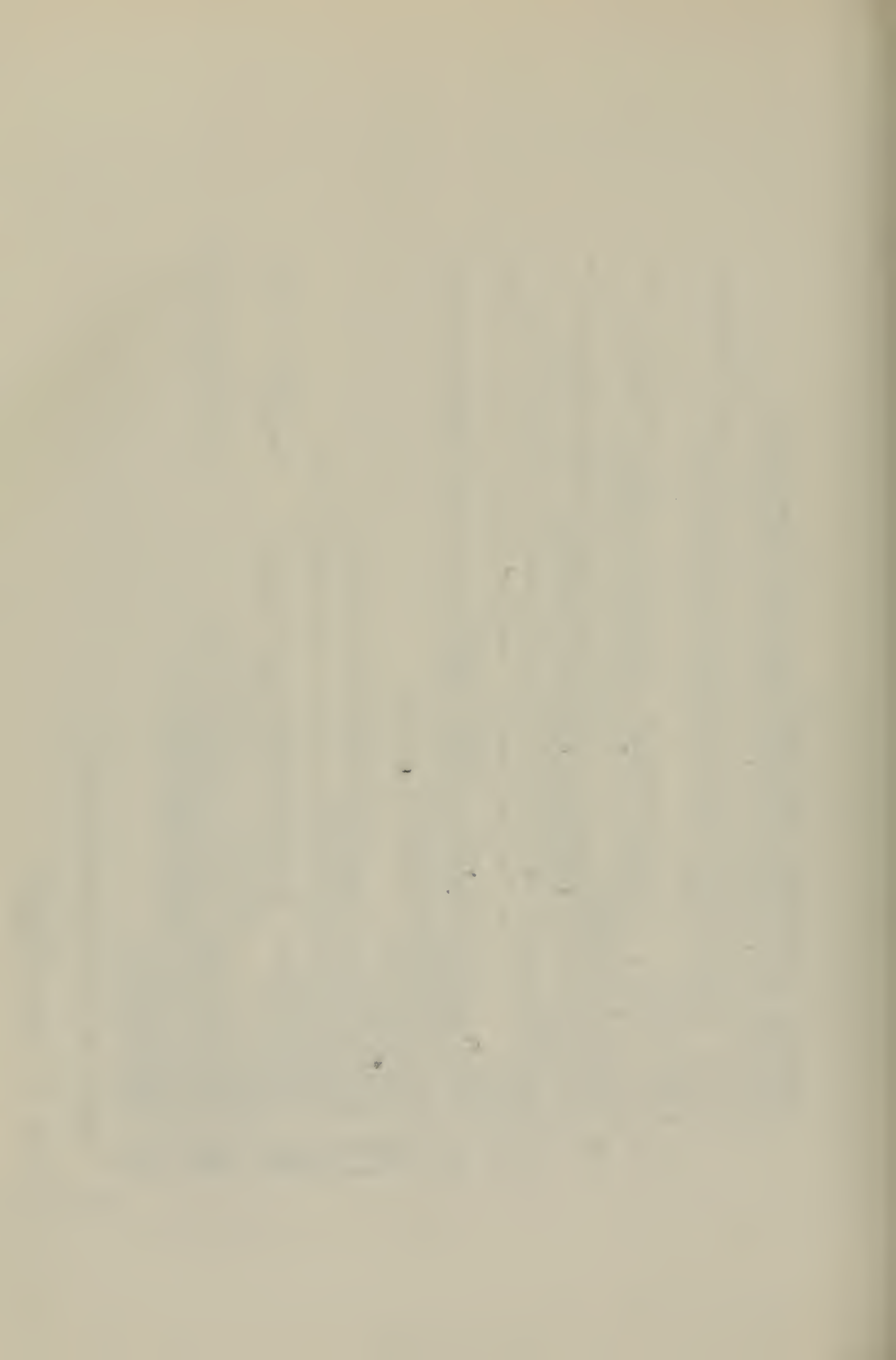
DIMENSION CSPEC(1025), QSPEC(1025)
DIMENSION RESPF(1025), PER(1025), PHASE(1025), COHER(1025)
DIMENSION FREQ(1025), CYCL(1025), SPEC(1025), SPE2(1025)
REAL*8 ITITLE(12), ITITEL(12), ITITLI(12), ITITLA(12),
1 ITITAL(12), ITITLC(12)
REAL*4 LABEL/4HY-PM/, LABEL2/4HY-PM/, LABEL3/4HCOHR/
REAL*4 LABEL1/4H XX/, LABEL5/5HPHASE/, LABEL4/4HZ-PM/
REAL*4 LABEL6/4HCCOR/
96 FORMAT(2I6)
98 FORMAT(7H NTS = ,I6//,8H MLAG = ,I6//,6H DT = ,F9.5//,6H DHZ= ,F10
1.8//,6H FBHZ = ,F10.8//,6H FEHZ = ,F12.8//,6H CALX1 = ,F10.8//,
2. CALX2 = ,F10.8//,6H H = ,F10.3//,6H X2 = ,F10.3//)
99 FORMAT(2I6,3F10.8)
101 FORMAT(4X,10H FREQUENCY,4X,15H AUTO-SPECTRUM1,3X,15H AUTO-SPECTRUM
12,3X,12H CO-SPECTRUM,2X,14H QUAD-SPECTRUM,3X,15H WAVE PERIOD ,
2. PHASE ,6H COHERENCE',//)
102 FORMAT(4X,F8.5,7X,E13.7,5X,E13.6,5X,E13.6,3X,F10.5,3X,
1F10.5,3X,F10.5)
103 FORMAT(9X,49H SMOOTHED(PARZEN WINDOW) ENERGY SPECTRAL DENSITY
1//)
104 FORMAT(3X,10H (CYC/SEC), 6X,7H M2/HZ)
105 FURMAT(10X,24H ENERGY SPECTRAL DENSITY//,5X,10H FREQUENCY,5X,13H
1SPECTRUM)
106 FORMAT(5X,F10.5,6X,E12.6)
107 FORMAT(5X,F10.6,6X,F10.6,6X,F10.6)
108 FORMAT(2F10.8)
109 FORMAT(16)
110 FORMAT(1X,6H LAG TIME CROSS CORRELATION FN',//)
111 FORMAT(5X,F10.6,6X,F10.6)
112 FORMAT(10,7X,6H LAG TIME',8X,'AUTO 1',11X,'AUTO 2',//)
200 FORMAT(6A8)
201 FORMAT(13,2(1X, 6H F3,1),6(1X,11))
651 FORMAT(25H VARIANCE OF SPECTRUM//,3X,16H VARIANCE = ,F12.
13,10H M2//)
798 FORMAT(16H PHI(0) = ,F12.3//)
801 FORMAT(4F10.5)
803 FORMAT(40H UPPER OCEAN TURBULENCE STUDY
14,10H HOUR ,2A4//,5X,10A4//)
806 FORMAT(10,18H WAVE RECORD NO. 2//)
811 FORMAT(1H1)
900 FORMAT(14F5.2)
901 FORMAT(14F9.3)

```

READING IN TITLE CARDS FOR PLOTS

READ IN TITLES FOR PLOTS
(TWO CARDS)

CCCCC



```

C   READ(5,200) (ITITEL(I),I=1,12)
C   TITLE FOR AUTO-COVARIANCE FUNCTION PLOT(TWO CARDS)
C   READ(5,200) (ITITLA(I),I=1,12)
C   TITLE FOR ENERGY DENSITY SPECTRA (TWO CARDS)
C   READ(5,200) (ITITEL(I),I=1,12)
C   TITLE FOR PHASE SPECTRUM PLOT (TWO CARDS)
C   READ(5,200) (ITITIL(I),I=1,12)
C   TITLE FOR COHERENCE SPECTRUM PLOT (TWO CARDS)
C   READ(5,200) (ITITLI(I),I=1,12)
C   TITLE FOR CROSS-CORRELATION FN. PLOT (TWO CARDS)
C   READ(5,200) (ITITLC(I),I=1,12)
C
C   READ IN CONTROL AND DATA CARDS
C
C   READ(5,99) NTS,MLAG,DT,FBHZ,FEHZ
C   READ(5,801) CALX1,CALX2,H,X2
C   DHZ=1.0/(2.0*DT*MLAG)
C   WRITE(6,811)
C   WRITE(6,200) (ITITEL(I),I=1,12)
C   BAND WIDTH FREQUENCIES OF TOTAL ENERGY FLUX- CMIN,CMAX
C   CMIN = 0.0
C   CMAX = 2.5
C   PI=3.14159265
C   FB = FBHZ*2.0*PI
C   FE = FEHZ*2.0*PI
C   DF = DHZ *2.0*PI
C   FMIN = 2.0*PI*CMIN
C   FMAX = 2.0*PI*CMAX
C   CALCULATING PERIOD AND FREQUENCY ARRAYS
C   NFREQ=(FE-FB)/DF+0.1
C   DO 14 N=1,NFREQ
C   XN=N
C   FREQ(N)=(XN-1.0)*DF+FB
14  CYCL(N) = FREQ(N)/(2.0*PI)
C   PER(1) = 0.0
15  DO 15 N = 2,NFREQ
C   PER(N) = 1.0/CYCL(N)
C
C   COMPUTING POWER SPECTRUM FIRST TIME SERIES.
C
C   READING IN FIRST TIME SERIES F1 AND DETRENDING
C   REWIND 4
C   NREAD=26
C   IDREC1=115
C   IDREC2=11
523  DO 4322 IM=1,IDREC1
4322  READ(4,16) (GAR(K),K=1,512)

```



```

524 CONTINUE
DO 3000 IN=1,NREAD
  READ(4,16) (AX(K),K=1,2048)
  J=0
DO 100 I=1,2048,8
  J=J+1
  A(J)=AX(I)
CONTINUE
100 WRITE(8,18) (A(L),L=1,256)
CONTINUE
3000 DO 5432 IN=1,IDREC2
525 READ(4,16) (GAR(K),K=1,512)
5432 CONTINUE
DO 3001 JN=1,NREAD
  READ(4,16) (BX(K),K=1,2048)
  J=0
DO 308 I=1,2048,8
  J=J+1
  B(J)=BX(I)
308 WRITE(9,18) (B(L),L=1,256)
3001 REWIND 8
      REWIND 9
18 FORMAT(2(128A4))
16 FORMAT(4(128A4))
INT=1
DO 19 JJ=1,NREAD
  MINT=INT+255
  READ(8,18) (F1(I),I=INT,MINT)
19 INT=INT+256
  CALL TREND(F1,NTS,DT,CALX1)
  CALL AVER(F1,NTS,DT)
  WRITE(6,901) (F1(I),I=1,NTS)
C CALCULATING AUTO-CORRELATION FUNCTION
21 DO 10 M=1,MLAG
  SUM=0.0
  NMAX=NTS-M+1
DO 8 I=1,NMAX
  NN=M+I-1
  SUM=SUM+F1(I)*F1(NN)
8 XNMAX=NMAX
  XX=M-1
  TAU(M)=XX*DT
  PHI(M)=SUM/XNMAX
  PHN(M)=PHI(M)/PHI(1)
10 CONTINUE
  ANORM=PHI(1)
C APPLYING LAG WINDOW
  CALL PARZ(MLAG,PHI)

```



```

C FOURIER INTEGRAL TRANSFORMING AUTO-CORRELATION FUNCTION
  MLAGM1=MLAG-1
  XMLAG=MLAG
46  DO 50 N=1,NFREQ
    SUM=0.5*(PHI(1)+PHI(MLAG)*COS(FREQ(N)*TAU(MLAG)))
    C1=COS(FREQ(N)*DT)
    S1=SIN(FREQ(N)*DT)
    CC=1.0
    SC=0.0
    DO 49 M=2,MLAGM1
      CT=CC*C1-SC*S1
      ST=SC*C1+CC*S1
      CC=CT
      SC=ST
49  SUM=SUM+PHI(M)*CC
50  SPECTRAL VALUES -- A*A/DHZ*DHZ ( AMPLITUDE SQUARED/HZ)
C ROUTINE TO CALCULATE THE VARIANCE BY SUMMING THE AREA UNDER THE SPECTRUM
C UNDER THE SPECTRUM
  SUM = 0.0
  DO 650 N=1,NFREQ
    SUM = SUM + SPEC(N)
    WRITE(6,651) SUM
    WRITE(6,798) PHI(1)
    IF(NFLAG1) 743,743,744
744 CONTINUE

C COMPUTING POWER SPECTRUM SECOND TIME SERIES.
C
C
C READ 2ND TIME SERIES F2 AND DETRENDING
  READ(9,18) (F2(I),I=1,NTS)
  WRITE(6,901)(F2(I),I=1,NTS)
  CALL TREND(F2,NTS,DT,CALX2)
  CALL AVER(F2,NTS,DT)
  WRITE(6,806)
C CALCULATING AUTO-CORRELATION FUNCTION
  DO 70 M=1,MLAG
    SUM=0.0
    NMAX=NTS-M+1
    DO 7 I=1,NMAX
      NN=M+I-1
7  SUM=SUM+F2(I)*F2(NN)
      XNMAX=NMAX
      XX=M-1
      TAU(M)=XX*DT
      PHI(M)=SUM/XNMAX
      PHN1(M) = PHI(M)/PHI(1)
73 CONTINUE

```



```

BNORM=PHI(1)
ABNORM=ANORM*BNORM
C APPLYING LAG WINDOW
CALL PARZ(MLAG,PHI)
C WRITE AND DRAW AUTO-CORRELATION FUNCTIONS
WRITE(6,112)
WRITE(6,107)(TAU(M),PHN(M),PHN1(M),M=1,MLAG)
CALL DRAW(512,TAU,PHN,1,0,LABEL,ITITLA,0.0,0.0,0.0,2,0,5,5,0,
1 LAST)
CALL DRAW(512,TAU,PHN1,3,0,LABEL4,ITITLA,0.0,0.0,0.0,2,0,4,6,0,
1 LAST)
C FOURIER INTEGRAL TRANSFORMING AUTO-CORRELATION FUNCTION
DO 71 N=1,NFREQ
SUM=0.5*(PHI(1)+PHI(MLAG)*COS(FREQ(N)*TAU(MLAG)))
SI=COS(FREQ(N)*DT)
SI=SIN(FREQ(N)*DT)
CC=1.0
SC=0.0
DO 79 M=2,MLAGM1
CT=CC*CI-SC*SI
ST=SC*CI+CC*SI
CC=CT
SC=ST
79 SUM=SUM+PHI(M)*CC
71 SPE2(N)=SUM*2.0/XMLAG
C ROUTINE TO CALCULATE THE VARIANCE BY SUMMING THE AREA UNDER THE SPECTRUM
C UNDER THE SPECTRUM
SUM=0.0
DO 660 N=1,NFREQ
SUM=SUM+SPE2(N)
WRITE(6,651) SUM
WRITE(6,798) PHI(1)
C
C
C
C COMPUTING CROSS-CORRELATION FUNCTION.
20 MMT=2*MLAG-1
DO 5 M=1,MMT
AB=M-MLAG
MAB=ABS(AB)
IT=NTS-MAB
IF(M-MLAG) 1,1,2
1 IB1=MLAG-M+I
IB2=1
GO TO 3
2 IB1=1
IB2=M-MLAG+1

```



```

3 SUM=0.0
  DO 4 I=1,IT
    I1=IB1+I-1
    I2=IB2+I-1
    SUM=SUM+F1(I1)*F2(I2)
4  XIT=IT
    PHI(M)=SUM/XIT
    PHN2(M)=PHI(M)/SQRT(ABNORM)
5  TAU(M)=M-MLAG
    TAU(M)=TAU(M)*DT
    PARZEN FILTER APPLIED TO CORRELATION FUNCTION
    XMLAG = MLAG
    MLAGH1 = XMLAG/2.0-0.1
    DO 31 M=1,MLAGH
      MM = M-1
      R = MM
      RM = R/XMLAG
      MA = MLAG+MM
      MB = MLAG-MM
      UM = 1.0-6.0*RM*RM*(1.0-RM)
      PHI(MA) = PHI(MA)*UM
      PHI(MB) = PHI(MB)*UM
31  CONTINUE
      DO 32 M = MLAGH,MLAG
        MM = M-1
        R = MM
        RM = R/XMLAG
        RM1 = (1.0-RM)
        MA = MLAG+MM
        MB = MLAG-MM
        UM = 2.0*RM1*RM1*RM1
        PHI(MA) = PHI(MA)*UM
        PHI(MB) = PHI(MB)*UM
32  CONTINUE
      MFREQ=2*NFREQ
      FOURIER INTEGRAL TRANSFORMING THE CROSS-CORRELATION
      C FUNCTION TO OBTAIN THE CROSS-SPECTRUM
28  DO 30 M=1,MLAG
      MM=M-1
      MA=MLAG+MM
      MB=MLAG-MM
30  SPHI(M)=PHI(MA)+PHI(MB)
      APSHI(M)=PHI(MA)-PHI(MB)
      DO 40 N=1,NFREQ
        SUM1=0.5*(SPHI(1)+SPHI(MLAG)*COS(FREQ(N)*TAU(MLAG)))
        SUM2=0.5*(APSHI(1)+APSHI(MLAG)*SIN(FREQ(N)*TAU(MLAG)))
        C1=COS(FREQ(N)*DT)

```



```

*0, LAST) ANGLE AS A FUNCTION OF FREQUENCY.
C PLOT PHASE DRAW(82,CYCL,PHASE,0,0,LABEL5,ITITL,0.1,180.0,1,0,2,0,5,2,
*0, LAST)
C PLOT COHERENCE AS A FUNCTION OF FREQUENCY.
CALL DRAW(82,CYCL,COHER,0,0,LABEL3,ITITL,0.1,1.0,0,0,0,0,5,1,0,
*LAST)
C PLOT CROSS-CORRELATION AS A FUNCTION OF FREQUENCY
CALL DRAW(512,CYCL,PHN2,0,0,LABEL6,ITITLC,0.0,0.0,0,0,0,0,5,5,
*0, LAST)
11 CONTINUE
743 CONTINUE
999 STOP
END

```

```

SUBROUTINE TREND(FX,NTS,DT,CALXX)
DIMENSION FX(NTS)
C COMPUTING THE LINEAR TREND
FNTS = NTS
SUMF = 0.0
DO 101 I=1,NTS
SUMF = SUMF + FX(I)
101 SUMF1 = 0.0
DO 102 I=1,NTS
XI = I
SUMF1 = SUMF1 + XI*FX(I)
102 XNM1 = NTS-1
XNP1 = NTS+1
XM = (1.0/DT)*(12.0*SUMF1/(FNTS*XNM1*XNP1)-6.0*SUMF/(XNM1*FNTS))
B = SUMF/FNTS-XM*XNP1*DT/2.0
FMEAN = SUMF/FNTS
WRITE(6,9) FMEAN,XM,B
9 FORMAT(3X,8H MEAN = ,F10.5,3X,9H SLOPE = ,F10.5,3X,13H INTERCEPT
1= ,F10.5//)
DO 103 I=1,NTS
XI = I
FX(I) = FX(I) - (B+XM*XI*DT)
103 RETURN
END

SUBROUTINE SMD(MD,X1,X2,NFREQ)
DIMENSION X1(MD),X2(MD)
DO 1 N=1,MD
NA=N+MD
NN=NFREQ-N+1
NB=NN-MD

```



```

      X2(N) = 0.25*(X1(1)+X1(NA))+0.5*X1(N)
1  X2(NN)=0.5*(X1(NN)+X1(NB))
3  MB=MD+1
   ME=NN-1
5  DO 2 N=MB, ME
      NA=N+MD
      NB=N-MD
2  X2(N)=0.25*(X1(NA)+X1(NB))+0.5*X1(N)
   RETURN
   END

```

```

C  SUBROUTINE HAMM(MLAG, PHI)
   HAMM SUBROUTINE HAMMING LAG WINDOWS THE AUTO-CORRELATION FUNCTION
   DIMENSION PHI(MLAG)
   PI = 3.14159265
   XMLAG = MLAG
   DO 31 M=1, MLAG
      R = M
      UM = 0.54 + 0.46*COS(PI*R/XMLAG)
      PHI(M) = PHI(M)*UM
31  CONTINUE
   RETURN
   END

```

```

SUBROUTINE AVER (FX, NTS, DT)

```

C

```

   DIMENSION FX(NTS)
   U2 = 0.0
   SUMU2 = 0.0
   DO 151 I=1, NTS
      U2 = FX(I)*FX(I)
      SUMU2 = SUMU2 + U2
151 CONTINUE
   FNTS = NTS
   U2 = SUMU2/FNTS
   URMS = SORT(U2)
   WRITE(6,152) U2, URMS
152 FORMAT(3X,6H H2 = ,F10.5,3X,8H HRMS = ,F10.5,5H M )
   COMPUTING AVERAGE PERIOD, T
   COUNTS THE TOTAL ZERO UP-CROSSINGS
   USUM = 0.0
   K = 1
68  N = K
69  IF(FX(N)) 73,69,69

```



```

73 K=N
71 K = K+1
  IF(FX(K)) 71,71,80
80 USUM = USUM + 1.0
  IF(NTS-K) 83,83,68
83 T = FNTS*DT/USUM
  WRITE(6,82) T
82 FORMAT (3X,18H AVERAGE PERIOD = ,F10.5,4H SEC//)
  RETURN
END

C
SUBROUTINE PARZ(MLAG,PHI)
PARZ SUBROUTINE PARZEN FILTERS AUTO-CORRELATION FUNCTION
DIMENSION PHI(MLAG)
XMLAG = MLAG
MLAGH = XMLAG/2.0-0.1
MLAGH1 = MLAGH + 1
DO 31 M=1,MLAGH
  MM = M-1
  RM = MM
  UM = R/XMLAG
  UM = 1.0-6.0*RM*RM*(1.0-RM)
  PHI(M) = PHI(M)*UM
31 CONTINUE
DO 32 M = MLAGH1,MLAG
  MM = M-1
  RM = MM
  UM = R/XMLAG
  RM1 = (1.0-RM)
  UM = 2.0*RM1*RM1*RM1
  PHI(M) = PHI(M)*UM
32 CONTINUE
RETURN
END

//GO.FT06F001 DD SYSOUT=A,SPACE=(CYL,(6,1))
//GO.FT04F001 DD UNIT=2400,VOL=SER=NPS361,DSNAME=RUF2SR2,
// LABEL=(16,SL,IN),DISP=(OLD,KEEP),
// DCB=(DEN=2,RECFM=FB,LRECL=2048,BLKSIZE=2048)
//GO.FT08F001 DD UNIT=SYSDA,DSNAME=F2614.CHAN1A,
// DCB=(RECFM=FB,LRECL=2048,BLKSIZE=2048),DISP=(NEW,PASS),
// SPACE=(CYL,(4,1))
//GO.FT09F001 DD UNIT=SYSDA,DSNAME=F2614.CHAN2A,
// DCB=(RECFM=FB,LRECL=2048,BLKSIZE=2048),DISP=(NEW,PASS),
// SPACE=(CYL,(4,1))
//GO.SYSIN DD *
RUN PH-3, FILE 6 OF CON6

```


TEMPORAL AUTOCORRELATION FN, Y-PM, Z-PM
 RUN PH-3, FILE 6 OF CON6
 POWER SPECTRUM LEVEL (DB) Y-PM, Z-PM
 RUN PH-3, FILE 6 OF CON6
 CROSS SPECTRAL PHASE ANGLE Y-PM, Z-PM
 CH ALEXANDER
 COHERENCE FUNCTION, Y-PM, Z-PM
 CH ALEXANDER
 CROSS-CORRELATION FN, Y-PM, Z-PM
 RUN PH-3, FILE 6 OF CON6
 6656 512 0.16 0.0 3.125
 1.0 1.0 1.0

LIST OF REFERENCES

1. Chernov, Lev A., Wave Propagation in a Random Medium, p. 85-124, Dover Press, 1967.
2. Medwin, H., "In-Situ Acoustic Measurement of Bubble Population in Coastal Ocean Waters", Journal of Geophysical Research, v. 75, no. 3, p. 599-611, January 1970.
3. Rautmann, J., Sound Dispersion and Phase Fluctuations in the Upper Ocean, MS Thesis, United States Naval Postgraduate School, Monterey, 1971.
4. Skudrzyk, E.J., "Thermal Microstructure in the Sea and Its Contribution to Sound Level Fluctuations", Chapter 12, Underwater Acoustics, V.M. Albers, ed., p. 199-233, Plenum Press, New York, 1963.
5. Woods, J.D., 1968: "Wave-induced shear instability in the summer thermocline." Journal of Fluid Mechanics, 32, p. 791-800.
6. Fitzgerald, J.R., Statistical Study of Sound Speed in the Inhomogeneous Upper Ocean, MS Thesis, United States Naval Postgraduate School, Monterey, 1972.

INITIAL DISTRIBUTION LIST

	No. Copies
1. Defense Documentation Center Cameron Station Alexandria, Virginia 22314	2
2. Library, Code 0212 Naval Postgraduate School Monterey, California 93940	2
3. Commander, Naval Ship Systems Command Attn: Mr. Woodie L. Thompson Department of the Navy, Code PMS 302 Washington, D.C. 20360	1
4. Commander, Naval Ship Systems Command Attn: Mr. Alfred P. Franceschetti Department of the Navy, Code PMS 302-4 Washington, D.C. 20360	2
5. Professor H. Medwin, Code 6lMd Department of Physics Naval Postgraduate School Monterey, California 93940	7
6. Dean of Research Administration Naval Postgraduate School Monterey, California 93940	1
7. Assoc. Professor W.W. Denner, Code 58Dw Department of Oceanography Naval Postgraduate School Monterey, California 93940	1
8. Asst. Professor E.B. Thornton, Code 58Tm Department of Oceanography Naval Postgraduate School Monterey, California 93940	1
9. Assoc. Professor N.E. Boston, Code 58Bd Department of Oceanography Naval Postgraduate School Monterey, California 93940	1

10. Mr. William Smith 1
Department of Physics
Naval Postgraduate School
Monterey, California 93940
11. Commander, U.S. Naval Oceanographic Office 1
Attn: Code 037-B
Washington, D.C. 20390
12. Director of Acoustic programs (Code 468) 1
Office of Naval Research
Department of the Navy
Arlington, Virginia 22217
13. LT C.H. Alexander 1
USS Point Defiance (LSD - 31)
FPO San Francisco, California
96601
14. Mr. Ben Saltzer 1
Ocean Technology Department
Systems Development
Code 6513
Naval Undersea Research and Development Center
San Diego, California 92132

DOCUMENT CONTROL DATA - R & D

(Security classification of title, body of abstract and indexing annotation must be entered when the overall report is classified)

ORIGINATING ACTIVITY (Corporate author)

Naval Postgraduate School
Monterey, California 93940

2a. REPORT SECURITY CLASSIFICATION

2b. GROUP

REPORT TITLE

Sound Phase and Amplitude Fluctuations in an Anisotropic Ocean

DESCRIPTIVE NOTES (Type of report and, inclusive dates)

Master's Thesis; December 1972

AUTHOR(S) (First name, middle initial, last name)

Charles Homer Alexander

REPORT DATE

December 1972

7a. TOTAL NO. OF PAGES

257

7b. NO. OF REFS

6

CONTRACT OR GRANT NO.

PROJECT NO.

9a. ORIGINATOR'S REPORT NUMBER(S)

9b. OTHER REPORT NO(S) (Any other numbers that may be assigned this report)

DISTRIBUTION STATEMENT

Approved for public release; distribution unlimited.

SUPPLEMENTARY NOTES

12. SPONSORING MILITARY ACTIVITY

Naval Postgraduate School
Monterey, California 93940

ABSTRACT

Sound of constant amplitude and frequency was transmitted simultaneously in three orthogonal beams over a distance of 1.5 meters in the upper ocean. Time records of the resulting phase and amplitude fluctuations of the sound beams were studied by means of auto and cross spectral analysis and correlation. The time lag between corresponding peaks of the phase fluctuation autocorrelation functions of vertical and horizontal beams indicate movement of inhomogeneities between the sound fields due to water particle motion caused by surface wave action. Envelope correlation times of the phase fluctuations are found to be approximately one-half as great in the mixed layer as in the thermocline, and are greater in the vertical than in the horizontal direction in the thermocline. Anisotropy in the thermocline is also indicated by the variance of phase fluctuation being greater for sound paths in the horizontal than in the vertical direction. The autocorrelation functions of amplitude and phase fluctuations in any one direction are similar.

KEY WORDS	LINK A		LINK B		LINK C	
	ROLE	WT	ROLE	WT	ROLE	WT
Underwater Acoustics						
Sound Amplitude, Phase Fluctuation						
Spectral Analysis						
Upper Ocean Microstructure						

141207

Thesis
A3703
c.1

Alexander
Sound phase and am-
plitude fluctuations in
an anisotropic ocean.

SEP 23 85

29686

141207

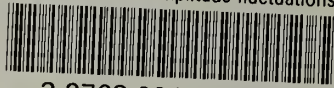
Thesis
A3703
c.1

Alexander

Sound phase and am-
plitude fluctuations in
an anisotropic ocean.

thesA3703

Sound phase and amplitude fluctuations i



3 2768 001 90982 3

DUDLEY KNOX LIBRARY